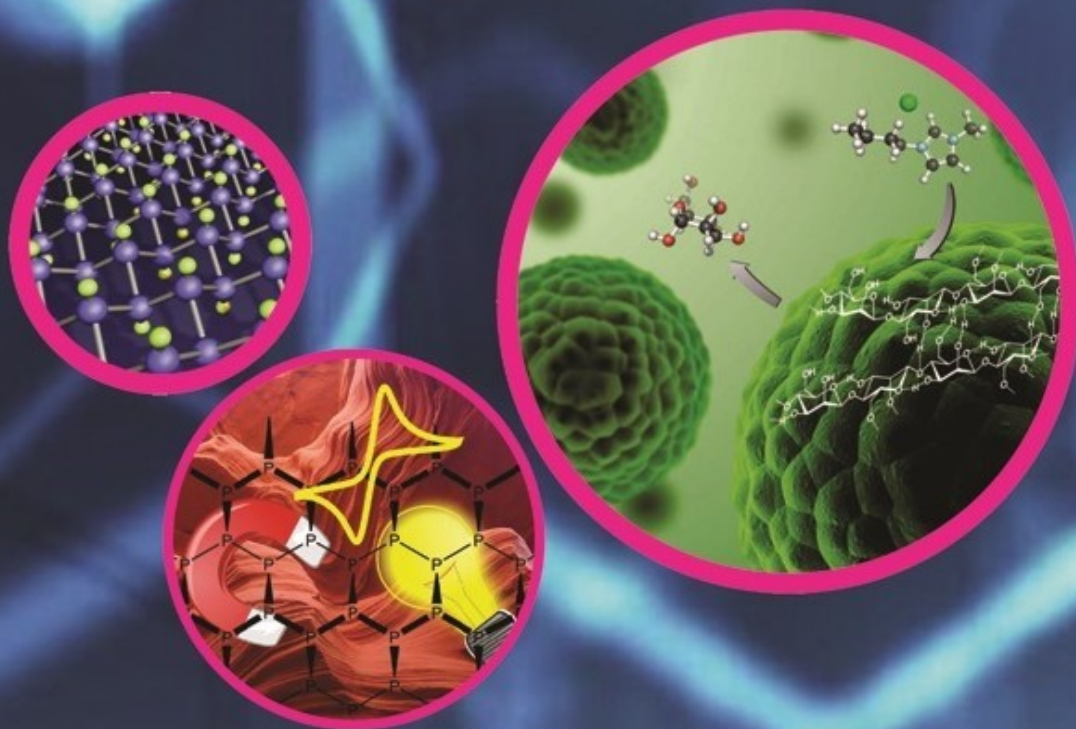


Frontier Areas in Chemical Technologies

Volume - II



Editors

H. GURUMALLESH PRAPHU

G. GOPU

S. VISWANATHAN



ALAGAPPA UNIVERSITY

[Accredited with A+ Grade by NAAC (CGPA: 3.64) in the Third Cycle]

Karaikudi-630 003, Tamil Nadu, India.



Padma bhushan
Vaital Dr. RM. ALAGAPPA CHETTIAR

Frontier Areas in Chemical Technologies

Volume - II

Editors

H. Gurumallesh Prabu

G. Gopu

S. Viswanathan



ALAGAPPA UNIVERSITY

[Accredited with A+ Grade by NAAC (CGPA: 3.64) in the Third Cycle]

Karaikudi - 630 003

Second Impression: 2017

© Alagappa University, Tamil Nadu

Frontier Areas in Chemical Technologies – Volume II

**A Compendium of Research Papers presented in the International Conference
FACTs 2017, July 06-08, 2017**

**Conference Organised by:
Department of Industrial Chemistry
Alagappa University, Karaikudi**

ISBN: 978-81-928690-7-0

No part this publication may be reproduced or transmitted in any form by any means, electronic or mechanical, including photocopy, recording, or any information storage and retrieval system, without permission in writing from the copyright owners.

DISCLAIMER

The authors are solely responsible for the contents of the papers compiled in this volume. The publishers or editors do not take any responsibility for the same in any manner. Errors, if any, are purely unintentional and readers are requested to communicate such errors to the editors or publishers to avoid discrepancies in future.

Published by
Alagappa University
Karaikudi

Typeset by:
Department of Industrial Chemistry
Alagappa University, Karaikudi – 630 003

Printed by:
Poocharam Printers,
Karaikudi – 2.

Preface

Chemical technologies involving Green Chemistry, Material Chemistry, Electrochemistry, Sensor Chemistry, Nanoscience, Computational Chemistry, etc., are the challenging as well as promising frontiers of advanced technologies and they find applications in almost all areas of modern technology. It is important for the researchers, educators and developers from academic institutions and industries to know the research and recent developments that have been made on the frontiers of Chemical and Electrochemical Sciences and Technologies. The present conference **International Conference on Chemical Technologies (FACTS-2017)** is the First International Conference organized by the Departments of Industrial Chemistry, Bioelectronics & Biosensors and Nanoscience & Technology to focus on the update of recent advancements in different areas of chemical science and technologies. The aim of this international conference is to provide a forum for the chemists, physicists, biologists and material scientists and technologists and researchers to discuss their recent findings and information and to promote cooperation both nationally and internationally. The invited talks and papers focus mainly on various advanced aspects of Chemical Technologies such as Electrochemical Technologies, Nanoscience and Technology, Sensor Technologies, Supramolecular and Photochemical Technologies, Green Chemical Technologies and other allied technologies.

It is indeed a matter of great pleasure and satisfaction to the Editors to present this volume-II containing collection of extended abstracts of the presented in the International FACTS 2017 held at Alagappa University, Karaikudi during 06-08 July 2017. There are about 16 Invited Talks, 28 Oral Presentations and 170 Poster Presentations. In addition, the programme includes open forum discussions. About 250 delegates from various Research Institutes, Universities, Colleges and industries in India including four Invited Speakers from overseas participate in the conference.

The editors are thankful to **Prof. S. Subbiah**, Vice-Chancellor, Alagappa University, Karaikudi for supporting all the activities of this International Conference and advising in promoting the research culture among the young researchers. Our sincere thanks are to all the **Syndicate Members**, **Prof. V. Balachandran**, Registrar and Authorities of Alagappa University, Karaikudi for their constant support and encouragement. The editors are pleased to acknowledge all the sponsors particularly DST-SERB. Sincere thanks are due to the Organizing Committee Members of the conference, Faculty Members, Research Scholars and Students of the Department of Industrial Chemistry. We also thank all the authors for submitting their extended abstracts in time.

We hope all the delegates had a pleasant stay in Karaikudi and stimulating discussions during the International Conference on FACTS 2017.

Editors

CONTENTS

1. ELECTROCHEMICAL TECHNOLOGIES

- | | | |
|------|--|----|
| 1.1 | Recent Trends in Electronic Industry: Intermetallic Aluminides
T. Joseph Sahaya Anand | 1 |
| 1.2 | Significance and development of the advanced energy storage devices
Ravikumar Raman, David Aradilla and Gopukumar Sukumaran | 1 |
| 1.3 | Ethylenediamine based Covalent Triazine Framework and its carbon composite as an Oxygen Evolution Reaction Catalyst
Sivalingam Gopi and Murugavel Kathiresan | 2 |
| 1.4 | Electrocatalysis of mediated oxygen reduction at Glassy carbon electrode modified with Riboflavin and anthraquinone derivatives
P. Manisankar and S. Valarselvan | 3 |
| 1.5 | Electrocatalytic Reduction of Oxygen on Copper Nanoparticle Modified Glassy Carbon Electrode with 1,4-Naphthoquinone
J. Antony Rajam, A. Gomathi and C. Vedhi | 5 |
| 1.6 | Studies on Oxygen reduction with 2- amino anthraquinone at poly (aniline) modified electrode
G. Amala Jothi Grace, A. Gomathi, C. Vedhi and M. Abdul Kadir | 5 |
| 1.7 | High rate performing N-rich spherical carbon particles for Li/Na ion cells
V.Selvamani S. Gopi, V. Rajagopal, M. Kathiresan, V. Suryanarayanan, D. Velayutham and S. Gopukumar | 7 |
| 1.8 | Fabrication of g-C ₃ N ₄ /NiO heterostructural nanocomposite modified glassy carbon electrode for quercetin biosensor
S. Selvarajan, A. Suganthi and M. Rajarajan | 8 |
| 1.9 | Studies on the electrochemical oxidation of Styrene
V. M. Shanmugam, K. Kanmani, T. Raju, and D. Velayutham. | 9 |
| 1.10 | Effects of Alumina Nanofiller Incorporated Polymer Blend Electrolytes for Lithium Batteries
R. Sasikumar, M. Ramesh Prabhu and K. Selva Kumar | 10 |
| 1.11 | Inhibitive effect of 1-(3-aminopropyl imidazole) on copper corrosion in 3.0% sodium chloride solution
P. Durainatarajan, M. Prabakaran, S. Ramesh and V. Periasamy | 12 |
| 1.12 | Electrochemical process for the Synthesis of Diacetone -2-keto-L-gulonic acid(Vitamin-C-intermediate) from L-Sorbose.
S. Sangeetha, K. Kulangiappar and T. Vijayarathi | 14 |
| 1.13 | Performance Comparison of Nafion 117 and Speek membrane in Microbial fuel cell system for Power Generation and Wastewater Treatment
Vidhyeswari.D and S. Bhuvaneshwari | 15 |
| 1.14 | Enhancement of Thermal Properties in Oleic Acid Phase Change Material using Graphene Oxide Nanosheets for Thermal Energy Storage Applications
S. Imran Hussain, And S. Kalaiselvam | 16 |
| 1.15 | Modified Electrode Surface as a Sensitive Sensors of Heavy metals in Seaweed of Gracilaria Corticata
A.Vimalaand C.Vedhi | 16 |

1.16	Corrosion of mild steel in sulphuric acid medium inhibited by benzimidazole G. Kavitha, P. Karpagavinayagam and C. Vedhi	17
1.17	Trichromic behaviour of co-polymer of substituted thiophenes P. Authidevi, D. Kanagavel, V. Sreeja and C. Vedhi	18
1.18	In-situ spectroelectrochemical behavior of Reactive Blue 19 in sodium hydroxide solution V. Sreeja P. Authidevi and C. Vedhi	19
1.19	Design, synthesis and characterization of novel acceptor materials for polymer solar cell applications Bharatraj Kasi and Vajjiravel Murugesan	21
1.20	Ionic Liquid-Assisted One-Step Synthesis of rGO/MnCO ₃ Composite for High- Performance Supercapacitor Electrodes S. Jegatheeswaran, M. Balaji, J. Anandha Raj, P. Boomi, J. Jeyakanthan, J. Joseph Sahayarayan, M. Sundrarajan and S. Selvam	22
1.21	Physical and Electrochemical characterization of Direct current electrodeposited Ni-ZrO ₂ nanocomposite coatings S. Kasturibai and G. ParuthimalKalaigan	23
1.22	A High Performance Electrochemical Sensor for Paracetamol Based on N-CeO ₂ doped rGO Modified Glassy Carbon Electrode Sathish Kumar Ponnaiah and Prakash Periakaruppan	24
1.23	Electrochemical determination of metals on GCE/ Graphene in well water of Neyveli at Cuddalore district in Tamil Nadu T. Rani, P. Karpagavinayagam, D. Kanagavel and C. Vedhi	25
1.24	Corrosion behaviour of mild steel using an aqueous seed extract of Citrullus Lanatus K Anuradha, C Sugapriya and K Velmanirajan	26
1.25	Synthesis and characterization of Chitosan-Co ₂ O ₃ /graphene oxide for energy storage application R. Karthik and S. Thambidurai	27
1.26	Preparation and Characterization of activated Carbon from Peanut shells by Chemical activation method C.Kalaiselvi, M. Sivakumar and R. Subadevi	28
1.27	Influence of composition on ionic conductivity of P(S-co-MMA)/PVC blend polymer electrolyte M.Shanthi, M. Sivakumar and R. Subadevi	29
1.28	Effect of BaTiO ₃ filler in P(VDC-co-AN) based gel polymer electrolytes employed in Lithium secondary batteries M.Shanthi, M. Sivakumar and R. Subadevi	29
1.29	Stable nanofibrous poly (aryl sulfone ether benzimidazole) membrane with high conductivity for high temperature PEM fuel cells P. Muthuraja, S. Prakash, V. Sethuraman and P. Manisankar	30
1.30	Corrosion behavior of Zn/Graphene composite in aqueous electrolyte system K. Saminathan, M. Selvam, R. Sathiyamoorthi and P. Saha	31

1.31	Enhancement of Discharge Capacity of Mg/MnO ₂ Primary Cell with Nano α -MnO ₂ -Graphene as Cathode K. Saminathan, M. Selvam, R. Sathiyamoorthi and P. Saha	31
1.32	Enhanced capacitance behaviour CuS@Cu(OH) ₂ Binary nanocomposite for Supercapacitors Applications P. Naveenkumar and G. ParuthimalKalaigan	32
1.33	Synthesis of Mn ₂ O ₃ nanomaterials for high-performance asymmetric supercapacitor applications Srinivasan Alagar, Rajesh Madhuvilakku and Shakkthivel Piraman	33
1.34	Nanostructured Zr substituted LiNi _{1/3} Mn _{1/3} Co _{1/3} O ₂ as a cathode material for high- Energy lithium-ion battery K. Kalaiselvi and G. ParuthimalKalaigan	33
1.35	Preparation and Analysis of thermoelectric thin films at different coating cycles A. Amali Roselin, N. Anandhan, R. Priyatharshinin and M. Karthikeyan	34
1.36	A case study on Sol-gel Spin coated Rare Earth Doped ZnO thin films S. Fathima Thaslin, N. Anandhan, A. Amali Roselin and M. Karthikeyan	35
1.37	Synthesis of Nanostructured NiCo ₂ O ₄ by Hydrothermal Route for Supercapacitor Applications K. Uma Maheswari, R. Dhilip Kumar, C. Karthikeyan and S. Karuppuchamy	36
1.38	Development of inorganic hole conductor for highly efficient perovskite solar cells R. Dhilip Kumar, Vibha Saxena, G. Murugadoss, R. Thangamuthu and S. Karuppuchamy	36
1.39	Electrochemical Determination of 3-Nitro – 1, 4-Dihydro-1,2,4-Triazol-5-one using Glassy Carbon Electrode B. Kavitha, N. Senthil Kumar and H. Gurumalles Prabu	37
1.40	<i>In-situ</i> generation of Pt based nanocatalysts on conducting polymer support by Galvanic Displacement Reaction route and its electro-(chemical) catalytic applications C. Mathi and C. Sivakumar	38
1.41	Nanostructural modified glassy carbon electrode utilized for voltammetric determination of ibuprofen E. Suresh, K. Sundaram, B. Kavitha and N. Senthil Kumar	39
1.42	Microbial Fuel Cell Assisted Disposal of Phosphate Sorbed Rice Husk Biochar D. Krishnaveni, M. Jayalakshmi and A.N. Senthilkumar	40
1.43	Studies on Synthesis, Structure and Characterization of Nd ₂ Mo _{2-x} In _x O ₉ Oxide Ion Conductor for Solid Oxide Fuel Cell Application N. Kalaivani and M. Rajasekhar	41
1.44	Label Free Microfluidic Electrochemical Biosensor for Aflatoxin B1 in Rice S. Viswanathana, Cristina Delerue-Matos, C. Rani	42
1.45	Label Free Electrochemical detection of exosomes derived from ovarian cancer cells S. Viswanathan, Cristin Delerue-Matos, C. Rani	42

1.46	Electrochemical Biosensor for Organophosphorus Insecticides- Chlorpyrifos K. Divya, T. Ponmuthuselvi, C. Rani, P. Manisankar, S. Viswanathan	43
1.47	Determination of Heavy metals in fish liver oil extracts using Bismuth electrode R. Logeswari, T. Ponmuthuselvi, C. Rani, P. Manisankar, S. Viswanathan	44
1.48	Label-Free Detection of Myoglobin- a Cardiovascular Disease Biomarker S. Viswanathan, M. Sangeetha, C. Rani	44
1.49	Single Drop Micro-Extraction of Methyl Parathion and Electrochemical Determination D. Suganthi, T. Ponmuthuselvi, C. Rani, P. Manisankar, S. Viswanathan	45
1.50	Structure and Electrochemical performance of $\text{LiV}_x\text{Mn}_{2-x}\text{O}_4$ ($0 \leq x \leq 0.20$) cathode materials for rechargeable lithium ion batteries P. Mohana and G. Paruthimal Kalaignan	46
1.51	Studies on Pani/Zno Nanocomposite Polymer Electrolyte for PEMFC J. Marimuthu, M. Rajasekhar	46

2. NANOSCIENCE AND TECHNOLOGIES

2.1	Effect of metal incorporation in tungsten oxide / zinc sulphide nanostructures V P Mahadavan Pillai	47
2.2	Graphene based metal chalcogenide nanocomposite catalysts for effective degradation of organic pollutants E. Murugan	47
2.3	The Development of Silica Nanoparticle from Top Down & Bottom Up Approach for Using in Nanocomposites Toemsak Sriksirin	48
2.4	AIE Nanodots Ensued from Pyrene Schiff Base and Its Indispensable Applications Venkatesan Srinivasan, Mariadoss Asha Jhonsi and Arunkumar Kathiravan	49
2.5	Green Synthesis and Characterization of Nano bound Terpolymer Resin Neela, G.R. Priya Dharsini and V. Rama	50
2.6	CuO Nanoparticles Catalyzed Synthesis of 1,2,3-Triazoles under Solvent-Free Condition J. Paul Raj, D. Gangaprasad, M. Vajjiravel and J. Elangovan	51
2.7	Nano Al_2O_3 Impregnated Cellulose acetate - Polystyrene Membrane for Dye Removal A. Rajeswari and Anitha Pius	52
2.8	Nano scale zero valent Iron (n ZVI) - montmorillonite (MMT) composite for dye adsorption K. Jayaraj, G. Aruna Devi and Anitha Pius	53
2.9	Silver nanoparticles mediated reduction of 2-nitro to 2-amino-5-(4-phenylquinolin-2-yl) phenols; molecular rationale of these small molecules as Topoisomerase-II inhibitors and anticancer therapeutics Manikandan Aand Sivakumar A	54

2.10	Design and development of a novel poly(melamine) entrapped gold nanoparticles composite for sensitive and low-level detection of catechol S. Sonadevi, R. HemaKalyani, S. Josphine Sarahand and R. Sayee Kannan	55
2.11	Preparation, characterization and photocatalytic activity of MgO nanoparticles for the degradation of Rose Bengal dye P. Vasantha Kumar, V. Vasanthi and K. Anitha	55
2.12	Fabrication of Copper Oxide/ Poly Vinyl Alcohol nanocomposite for Electrocatalytic and Photocatalytic Applications Karthika, S. Selvarajan, A. Suganthi and M. Rajarajan	56
2.13	Electron beam irradiated Polypyrrole nanospheres in selective determination of L-Tyrosine D. Nathiya and J. Wilson	57
2.14	Synthesis, Characterization and Photocatalytic Activities of Co_3O_4 - MnO_2 - ZnO Ternary Nanoparticles S. Alwin David and C. Vedhi	59
2.15	Synthesis and Characterization of N-doped ZnO Nanoparticles for Glucose sensor Tamilselvan Ganesan, M. Chinnadurai and Gurunathan Karuppasamy	60
2.16	Synthesis and Characterization of Rgo-Zno Nanocomposite S. Muthumariappan and C. Vedhi	60
2.17	A Bio-Derived Carbon Quantum Dots functionalized with conducting Organic Polymers for energy storage Applications A. Gowrisankar and T. Selvaraju	62
2.18	Studies on Nanocomposites of Rice Husk with Palmitic Acid and Their Application Jessica Fernando and V. Rajeshwari	63
2.19	Non-enzymatic based on β -NiS@rGO/Au nanocomposites for simultaneous determination of epinephrine and uric acid in presence of ascorbic acid P. Muthukumaran and J. Wilson	64
2.20	Optical and conductivity properties of 2,5-dimethoxy-polyaniline / tin oxide nanocomposites M. Senthil Kumar and P. Manisankar	65
2.21	Development of TiO_2 Nanofiber and nanoparticle composite photo-anode for planar structure form amidinium lead iodide perovskite solar cell K. Sakthi Velu, B. Suganya Bharathi, P. Manisankar And T. Stalin	65
2.22	Facile synthesis and physical analyses of Sulfur/Carbon nanofibre composite via Solid State Reaction P. Rajkumar, S. Sasikala, K. Diwakar, R. Subadevi and M. Sivakumar	66
2.23	Anticancer potential of green synthesized Zinc oxide nanoparticle using Red seaweed Gracilaria edulis M. Kavitha and N. Suganthy	67
2.24	Antibacterial treatment of Textile Effluent by Immobilized MgO NPs in a Column Reactor KavithaManoharan and ArumugamAyyakannu	68
2.25	One-step hydrothermal synthesis of iron oxide nanoparticles for photocatalytic and antimicrobial applications PR. Kaleeswarran and A. Arumugam	68

2.26	Synthesis of chitosan nanoparticles using <i>Penaeus semisulcatus</i> shells and their growth impact on <i>Sphaeranthus indicus</i> medicinal plant C. Balalakshmi, K. Gopinath, S. Abinaya, A. Arumugam and K. Gurunathan	69
2.27	Biotemplate-ZnO/graphene nanocomposite for better photocatalytic performance M.Karpuraranjith and S. Thambidurai	69
2.28	Interaction of chitosan-ZnO nanocomposite for better antibacterial activity T. Revathi and S. Thambidurai	70
2.29	One-step hydrothermal synthesis of Palladium nanoparticles and reduced graphene oxide nanocomposite for enhanced antibacterial activities R. Rajeswari, and H. Gurumallesh Prabu	71
2.30	Ionic liquid mediated green synthesis of CeO ₂ -ZrO ₂ core metal oxide nanoparticles and its Antioxidant activity P. Nithya, M. Balaji, S. Jegatheeswaran, S. Selvam and M. Sundrarajan	72
2.31	Morphology Improved Synthesis of Yttrium doped Hydroxyapatite Nanocrystals in Ionic Liquid medium R. Sumathi, S. Jegatheeswaran, S. Selvam, and M. Sundrarajan	73
2.32	Nano polymer bio composites for electronic application Boopalan. M	74
2.33	Synthesis and characterization of silver nanoparticles conjugate with antibiotics and its enhanced antibacterial activity P. Boomi, H. Gurumallesh Prabu, J. Jeyakanthan, S. Ramuthai and M. Karunakaran	75

3. SENSOR TECHNOLOGIES

3.1	Electrochemical Immunosensors –Universal Tools for Rapid Detection of Antigens and Antibodies Hanna Radecka, Jerzy Radecki	77
3.2	Electrochemical anions recognition in water using gold electrodes modified with dipodal or di-peptide anion receptor attached to dipyrromethene-Me(II) complex Jerzy Radecki, Balvider Kaur, Piotr Gołębiewski	78
3.3	Aggregation Induced Emission of Novel Pyrene based Polyaminal Networks and Selective Sensing of a Polyaromatic Hydrocarbon, Tetracene Thanasekaran Nandhini, Murugesan Shunmughanathan and Kasi Pitchumani	78
3.4	A study of Lpg Sensor using Nano-Structured Polypyrrole Composite as a Sensing Material A.J. Heiner and K. Gurunathan	79
3.5	Microwave-Assisted Synthesis of Carbon Quantum Dots and its Sensing Evaluation of Ammonia Rajendiran Nagappan and Rajendran Kalimuthu	81
3.6	Au-Pd bimetallic nanoparticles anchored on α -Fe ₂ O ₃ non-enzymatic catalyst for simultaneous electrochemical detection of dopamine and uric acid R. Ramya and J. Wilson	82

3.7	Synthesis and Fabrication of Au-Nanoparticles decorated Go-Pani Nanocomposites and their Electrochemical Sensing of Hydroquinone N. Radha And K. Rajeshwari	83
3.8	Electrochemical Sensing of Carbendazim Using Metal Organic Framework Modified Electrode Y. Jekapar Nisha, S. Prakash, P. Muthuraja and P. Manisankar	84
3.9	Preparation and characterization of polypyrrole decorated graphene/ β -cyclodextrin composite for electrochemical detection of mercury (II) in water Kasi Viswanathan, M. Velammal and R. Sayee Kannan	84
3.10	Zinc oxide - multiwalled carbon nanotube-poly (vinyl chloride) film for Biocompatible glucose sensing Palinci Nagarajan Manikandan, Habibulla Imran and Venkataraman Dharuman	85
3.11	Stabilization of Graphene Oxide Film on Gold Electrode with Influence of Volatile Solvents for Electrochemical Sensing of Acetaminophen Habibulla Imran and Venkataraman Dharuman	85
3.12	Fabrication of Co-Ni alloy nanostructures on 3D Copper foam for highly sensitive amperometric sensing of acetaminophen S. Premlatha and G.N.K. Ramesh Babu	86
3.13	Fabrication of 2-Nitrophenol sensor based on green synthesized hydroxyapatite N. Sudhan and C. Sekar	87
3.14	Binary liposome (DOTAP-DOPE) vesicle-gold nanoparticle for enhanced label free DNA and protein sensing Karutha Pandian Divya and Venkataraman Dharuman	88
3.15	Synthesis and Fabrication of Au-Nanoparticles decorated GO-PANI Nanocomposites and their Electrochemical Sensing of Phenols S. Michelraj, K. Rajeswari and C. Sivakumar	88
3.16	Electrochemical Hydrocarbon Sensing Performances of YSZ-based sensor attached with Nano-NiO K. Mahendraprabhu, V. Dharuman, P. Elumalai and E.R. Nagarajan	89
3.17	Development of newer Poly (Aniline-co-ethyl-4-amino benzoate)-Laccase based Biosensor for Catechol by One-Pot Method V. Sethuraman, P. Manisankar	90
3.18	Synthesis and live cell imaging studies of rhodamine based organic nanorods: a new strategy in cation and anion sensing applications M. Maniyazagan, R. Mariadass, M. Nachiappan, J. Jeyakanthan, N. K. Lokanath, S. Naveen, G. Sivaraman, P. Muthuraja, P. Manisankar, T. Stalin	91

4. SUPRAMOLECULAR AND PHOTOCHEMICAL TECHNOLOGIES

4.1	Reversible 2D Supramolecular Organic Frameworks encompassing Viologen Cation Radicals and CB[8] Kanagaraj Madasamy, David Velayutham and Murugavel Kathiresan	92
4.2	Novel Pyrimidine Tagged Silver Nanoparticle Based Fluorescent Immunoassay for the Detection of Pseudomonas aeruginosa Sundaram Ellairaja and Vairathevar Sivasamy Vasantha	92

4.3	Discovery of novel pyrazolo[3,4- <i>h</i>] quinolone-3-carbonitriles as efficient ‘turn-off’ fluorescence sensors for Fe ³⁺ ions Adaikalam Shylaja, Gopi Kalaiyarasan, James Joseph and Raju Ranjith Kumar	94
4.4	Anthracene based highly sensitive fluorescent sensor for Al(iii) ions Ganesan Jeyashree and Duraisamy Chellappa	95
4.5	Synthesis and scavenging applications of polyurethane dendritic nitroxide radical dendrimers B. Mohamad Ali and A. Sultan Nasar	96
4.6	Development of a Novel Bimetallic Au-FeNPS Decorated on g-C ₃ N ₄ with Enhanced Photocatalytic Performance for the Degradation of Organic Dyes Baishnisha Amanulla and Sayee Kannan Ramaraj	97
4.7	Novel NiO/Ag ₃ VO ₄ composite for efficient degradation of organic pollutants under visible-light V. Ramasamy Raja, D. Rani Rosaline, A. Suganthi and M. Rajarajan	98
4.8	Visible light induced photocatalytic degradation of Celestine Blue using ZrO ₂ /CeO ₂ D.Rani Rosaline, V. Ramasamy Raja, A. Suganthi and M. Rajarajan	99
4.9	Novel magnetically separable visible-light-driven ThO ₂ /Fe ₃ O ₄ photocatalyst with enhanced activity in degradation of Malachite Green Ramya Arumugam and Prakash Periakaruppan	99
4.10	Host-guest chemistry of Coumarin-460 with <i>p</i> -Sulfonatocalix[4]arene B. M. Ashwin, A. Herculin Arun Baby, P. Muthu Mareeswaran	100
4.11	Investigation on molecular recognition of 4-nitro-o-phenylenediamine with <i>para</i> -sulfonatocalix[4]arene C. Saravanan, G. Vignesh Kumar and P. Muthu Mareeswaran	101
4.12	Encapsulation of Triphenylpyrylium cation with <i>p</i> -Sulfonatocalix [4] arene M. Senthilkumaran, G. Vignesh kumar, K. Maruthanayagam and P. Muthu Mareeswaran	103
4.13	Morphology controlled synthesis of Carbon Quantum Dot/Cu ₂ O Hybrid Material for Visible Light Photocatalyst G. Muthusankar, S. Revathi, S. Dhanalakshmi and G. Gopu	105
4.14	PVA/β-CD Functionalized Electrospun Silver Nanofibers For In Vitro Biological Evaluation B. Suganya Bharathi and T. Stalin	106
4.15	Synthesis and Characterization of Polythiophene- Graphene Oxide-Zinc Selenite Nanocomposite for Photocatalytic hydrogen production S. Senthilnathan, S. Sivasakthi, K. Gurunathan	107

5. GREEN CHEMICAL TECHNOLOGIES

5.1	Chitosan - A Natural Biopolymer: Applications in Biosorption and Pervaporation Krishnaiah Abburi	109
5.2	Green Chemistry through Process Research & Development S. Srinivasan	110

5.3	Antimicrobial silver nanoparticles green synthesized using aqueous extracts of red seaweeds against plant pathogens: A potential source for nanopesticide formulation T. Antony Roseline and K. Arunkumar	110
5.4	Facile and eco-friendly synthesis of ruin functionalized silver nanoparticles (rAg NPs) and their biocompatible interaction with Bovine Haemoglobin (BHb) M. Karuppuraja and S. Murugesan	112
5.5	Dodonaea viscosa extract mediated synthesis of AuNPs and its anticancer potential against A549 NSCLC cancer cells M. Anandan and H. Gurumallesh Prabu	113
5.6	Green Synthesis of Some Piperidin-4-one Derivatives Using Sugar Based Deep Eutectic Solvent D. Ilangeswaran and K. Hemalatha	113
5.7	Development of Newer Ethylene Glycol Based Deep Eutectic Solvents and Their Applications for the Synthesis of Some Piperidin-4-one Derivatives D. Ilangeswaran, P. Sukanya, R. Periyanyaki, R. Ranjitha and P.G. Ramesh	115
5.8	Synthesis, Characterization, Anti-Microbial and Anti-Oxidant screening of novel Sulfonamide Schiff's bases Swathi.S, Umarani.G and Abdul hasan sathali. A	116
5.9	Subsurface Oxygen and its effect on catalytic process towards application in Environmental pollution. Nagarajan Sankaranarayanan	119
5.10	Extraction and characterization of Carrageenan from some red algae (Fresh and Defatted algae) along the Pamban coast, Tamilnadu, India C. Poonamand C. Pothiraj	120
5.11	Adsorptive removal of Orange G using activated carbon obtained from most abundant cashew nut shell and karuvelai leaves: Equilibrium, thermodynamics and kinetic studies Govindan Ramathilagam and Kanakkan Ananthakumar	121
5.12	Green synthesis of novel benzimidazole derivatives, characterization and screening of anti-inflammatory activity. Abdul hassan sathali.A , Umarani.G, Tamilarasi.G and Rajasekaran.K	123
5.13	Green synthesis of Ce doped CdO nanoparticles by the peel extract of <i>citrus sinensis</i> and its photocatalytic activity R.R. Muthuchudarkodi and G. Murugeswari	123
5.14	Green synthesis of nano-size graphene and characterization D.Carolin Jeniba Rachel and C. Vedhi	125
5.15	Biosynthesis of cobalt nanoparticles using morus indica and application R. Kirupagaran and C. Vedhi	126
5.16	Eco- friendly synthesis of zinc oxide nanoparticles for biomedical applications Arjun Kumar Bojarajan, Gurunathan Karuppasamy	127
5.17	Green synthesis of silver nanoparticles and their antimicrobial activity against gram positive and negative bacteria Prakashkumar Nallasamy and Gurunathan Karuppasamy	127

5.18	A Green approach: Silver/manganese oxide nanocomposite supported on bentonite by thermal decomposition method and their biological activities K. Bama and M. Sundrarajan	128
5.19	Green synthesis and characterisation of MnO ₂ nanoparticles using croton superciliosus morong leaves extract and their antibacterial study N. Latha, J. Anuradha and M. Gowri	129
5.20	Validation of Anti-inflammatory Phytocompounds from Methanolic Leaf Extract of <i>Crateva adansonii</i> DC by Using Molecular Docking Study Subramanian Ammashi and Thirumalaisamy Rathinavel.	131
5.21	Synthesis and characterization of TiO ₂ Nanoparticles by <i>Nigrospora oryzae</i> for biomedical applications S. Gowri and A. Arumugam	134
5.22	Biosynthesis of cobalt oxide nanoparticles and their evaluation of antimicrobial, hemolytic and cytotoxicity studies Viswanathan Karthika and Ayyakannu Arumugam	134
5.23	A microwave mediated solvent-free Biginelli reaction towards the synthesis of highly functionalized novel tetrahydropyrimidines J. Shanmugapriya, K. Rajaguru and S. Muthusubramanian	135
5.24	Biofabrication of copper nanoparticle using <i>Enicostema axillare</i> extract and antibacterial and antimicrobial activity S. Saravanan S. Pari, D. Madankumar, K. Praveen, V. Balachandran and G. Govindarajan	135
5.25	Bio synthesis of copper silver nanoparticles using <i>Scoparia dulcis</i> extract and antibacterial activity S. Saravanan S. Pari, R. G. Kanagan, G. Sathiskumar, V. Balachandran and N. Kathirvel	136

6. INORGANIC CHEMISTRY

6.1	The usefulness of d-d transitions in designing new Inorganic Pigments Srinivasan Natarajan	137
6.2	DNA binding studies of novel bioactive benzimidazole derived mixed ligand metal complexes Ganesan Kumaravel and Natarajan Raman	138
6.3	DNA interaction and enhanced DNA cleavage investigation of transition metal(II) mixed ligand complexes having 2-naphthylamine derived Schiff Base Natarajan Raman and Ganesan Kumaravel	139
6.4	Synthesis, structural studies, chemical nuclease activity and antimicrobial evaluation of tridentate (nos) schiff base ligand: 2-(4-(thiophen-2-yl) but-3-en-2-ylideneamino) phenol and their metal-organic hybrids G.R. Priya Dharsini, A. Neela, T. Clarina and V. Rama	139
6.5	Synthesis, Structural characterization, Electrochemical and biological behavior of Some transition metal complexes A. Kulandaisamy, A. Palanimurugan and M. Kalaiselvi	141
6.6	Synthesis, spectral, redox and antimicrobial activities of mixed ligand complexes derived from salicylidene-4-iminoantipyrinyl-2-iminophenol A. Kulandaisamy, A. Palanimurugan and S. Valarmathi	142

6.7	Thin-Layer Chromatographic Separation and Identification of certain Inorganic toxic anions in soil, ground water and sewage sludge samples from Fireworks and Safety Matches manufacturing areas in Sivakasi, Virudhunagar District, Tamil Nadu, India S. Thangadurai and B. Karthik prabu	144
6.8	Investigation on biomolecular interactions with nickel(II) complexes A. Jayamani, M. Sethupathi and N. Sengottuvelan	145
6.9	Synthesis, spectral, electrochemical and DNA binding studies of symmetric oxamidato–bridged binuclear cobalt(II) complexes C. Chitra, N. Kavitha and N. Sengottuvelan	146

7. MISCELLANEOUS

7.1	Podophyllotoxin Mimics: Synthesis and Biological Activity H. Surya Prakash Rao	148
7.2	Oxidative Cyclization of Carbanion: Cascade Synthesis of Biologically Relevant Molecules Sundarababu Baskaran	149
7.3	Metal Catalysed Coupling Reactions in Modifying Heterocycles S. Muthusubramanian	150
7.4	Efficient and safer synthesis of value-added organic molecules adopting continuous flow technologies Balamurugan Ramalingam	150
7.5	Crystal Structure of Glutaminyl-tRNA synthetase from <i>Thermus thermophilus</i> HB8 and its complexes Nachappan Mutharasappan, Vitul Jain, Amit Sharma, Yogavel Manickam and Jeyakanthan Jeyaraman	151
7.6	Wastewater Treatment for Removal of Solvents - Degradation of Octanol using Hydrodynamic Cavitation Pravin B. Patil, Jyotsnarani Jena, Vinay M. Bhandari, and Laxmi Gayatri Sorokhaibam	152
7.7	Coagulation-Flocculation treatment of dyes removal through chemical and natural coagulants Sweety Badalia, Laxmi Gayatri Sorokhaibam, Vinay and M. Bhandari	152
7.8	Biologically important of curcumin derivatives: DFT calculations and molecular docking studies Govindharasu Banuppriyaand VEDIAPPEN PADMINI	153
7.9	A facile one-pot four-component domino protocol for the synthesis of novel cycloocta/cyclododeca–pyridine-3-carbonitrile–indole hybrids Muthumani Muthu and Raju Ranjith Kumar	154
7.10	Computational Study on Molecular-based Non-linear Optical property of Wittig based Schiff-Base ligands Bathula Rajasekhar and Toka Swu	155
7.11	A facile synthesis of thiazole–pyridine hybrid heterocycles through a one-pot four-component domino protocol Rathinavel Mariammal, Muthumani Muthu and Raju Ranjith Kumar	157

7.12	One pot synthesis of 2-amino-4-arylpyridine-3-carbonitrile tethered phenothiazines Somi Santharam Roja and Raju Ranjith Kumar	158
7.13	Synthesis, Spectroscopic and DFT Studies of 4-(5-Chlorothiophen-2-Yl)-1,2,3-Selenadiazole Sankari S and Saranya K	158
7.14	Atom Transfer Radical polymerization of Poly(methylmethacrylate)s from a multifunctional initiator Gopinath A and A Sultan Nasar	160
7.15	Development of Simple Methodology for <i>ipso</i> -Hydroxylation of Aryl Boronic acids to Phenols using Graphene Oxide as Green Carbocatalyst Murugan Karthik and Palaniswamy Suresh	161
7.16	Synthesis and Characterization of Newer Sugar Based Deep Eutectic Solvents D. Ilangeswaran and K. Sarjuna	162
7.17	The stereodivergent formation of substituted tetrahydro-2 <i>H</i> -pyran by memory of chirality R. Chithiravel and S. Muthusubramanian	163
7.18	TEMPO-Promoted Oxidative Azide–Olefin Cycloaddition for the Synthesis of 1,2,3-Triazoles in Water D. Gangaprasad, J. Paul Raj, K. Karthikeyan and J. Elangovan	164
7.19	IRMOF-3 as an Efficient Heterogeneous Solid Base Catalyst for the Synthesis of 3-Cyanoacetyl-Indole-Acrylonitriles Murugesan Kanagaraj and Palaniswamy Suresh	166
7.20	Catalysis of cure reaction of ϵ -caprolactam-blocked poly-isocyanate with diol using non-tin catalysts G. Libni and A. Sultan Nasar	167
7.21	MIL-53(Fe) as an Efficient Heterogeneous Catalyst for the Synthesis and Characterization of Substituted Xanthenes and Pyrans Ganesapandian Latha, Nainamalai Devarajan, and Palaniswamy Suresh	168
7.22	Effect of diluents on extraction of chromium (VI) from aqueous solution Using Pickering Emulsion liquid membrane P. Murugan T.V. Nihal, and S. Bhuvaneshwari	168
7.23	Triaminopyrimidine derived Polymeric Network Gels: Synthesis, Influence of Molar Ratio of Reactants and its Catalytic Applications Murugesan Shunmughanatha, Pillaiyar Puthiaraj, and Kasi Pitchumani	170
7.24	One-pot synthesis of β -enaminones from β -nitrostyrenes, β -dicarbonyl compounds and amines using organic polyaminal networks (OPN) as heterogeneous catalysts Natarajan Madankumar, Murugesan Shunmughanathan and Kasi Pitchumani	171
7.25	TEMPO-Promoted organo catalyzed synthesis of 2-nitro-3- arylimidazo [1,2-a] pyridines under solvent free conditions M. Vadivelu, S. Sugirtha, K. Karthikeyan	172

7.26	Synthesis of new polyurethane bearing azomethine moieties for sequestration of Ni(II) and Cd(II) from wastewater: Parameter optimization, equilibrium, kinetics and thermodynamic predictions Manickam Sornalatha, Rangaraj Arunkumar, Kuzhandaivel Hemalatha, Selvaraj Dinesh Kirupha and Lingam Ravikumar	174
7.27	Investigation on the Development of Newer Glycerol Based Deep Eutectic Solvents and Their Applications for the Synthesis of Some Piperidin-4-one Compounds D. Ilangeswaran, R. Suganya, G. Vaitheshwari, K. Ramasundaram and I. Gnanasundaram	175
7.28	Quality Assessment of irrigation Water in Major Rice Growing Areas of Kilvelur Taluk in Nagapattinam District, Tamil Nadu – India A. Vincentraj, S. Kalyanasundharam, A. Arokiyaraj, S. Leo Arokiyaraj and D. Sathya	177
7.29	Performance of phase transfer catalysts on radical polymerization of alkyl methacrylate (RMA) in two phase system- a kinetic study. Elumalai Marimuthu and Vajjiravel Murugesan	179
7.30	Limestone: Heterogeneous and An Efficient Reusable Catalyst for Synthesis of Tetrahydrobenzo[<i>B</i>] Pyran and Its Derivatives T. Clarina, S. Amsaveni and V. Rama	180
7.31	Effect of Mechanical and Mechanochemical Shear Treatments on Cellulose in Solid State R. Lavanya and N. Natchimuthu	182
7.32	Synthesis of CPT releasing Poly (ϵ -caprolactone- <i>co</i> -citrate) by using Deep Eutectic Solvents Periyakaruppan Pradeepkumar and Mariappan Rajan	183
7.33	Summer affects calcification to organic matter production in coralline red alga <i>Amphiroa fragilissima</i> occurring along the Thondi coast (Palk Bay, Indian) J. Archanadevi and K. Arunkumar	185
7.34	Advanced Linear Integral Isoconversional Methods for Estimating Activation Energy: Thermal Degradation of Polypropylene Stephen Joel K, Vimalathithan PK and Vijayakumar CT	186
7.35	Aza-Baylis–Hillman Reaction of salicyl <i>N</i> -tosylimines with <i>N</i> -substituted maleimides under solvent free condition. S. Sugirdha, M. Vadivelu and K. Karthikeyan	188
7.36	Direct measurement of High pressure and High Temperature Dissolution of Supercritical CO ₂ in polymers using High Pressure NMR Technique S. Saravanakumar, Prof. J. Klankermayer, Prof. M. Liauw and Prof. W. Leitner	189
7.37	Biosorption of Arsenic (V) From Aqueous Solutions onto Chitin of Shrimp Shell: Kinetics and Isotherm Studies N. Vijayanand and G. Raja	189
7.38	Removal of Basic Dye from Aqueous solution using acid Activated Carbons Developed from the Various Tree Bark: Adsorption Equilibrium and Kinetics R. Pagutharivalan and N. Kannan	190

7.39	Removal of Rhodamine B from Aqueous Solution by Adsorption using acid Activated Adsorbents. A. Sivakumar, G. Ramachandran, R. Pagutharivalan and N. Kannan	191
7.40	Studies on Removal of Malachite Green from Aqueous Solution by Adsorption onto Acid Activated Carbons – Kinetic and Equilibrium Study R. Arunkumar, K. Sarathkumar, R. Saravanan, R. Pagutharivalan and N. Kannan	191
7.41	Adsorption of acidic Dye from Aqueous Solution Using Low Cost Adsorbents - A Comparative Study R. Saravanan, R. Arunkumar, K. Sarathkumar, R. Pagutharivalan and N. Kannan	192
7.42	A Comparative Study on Removal of Crystal Violet from Aqueous Medium with Activated Low Cost Adsorbents K. Sarathkumar, R. Arunkumar, R. Saravanan, R. Pagutharivalan and N. Kannan	192
7.43	Removal of Acidic Dye from Aqueous Solution by Adsorption Using Low Cost Acid Activated Adsorbents R. Muthlakshmi, M. Muthumani, R. Pagutharivalan and N. Kannan	193
7.44	Adsorption of Chromotope Dye from Aqueous Solution onto Acid Activated Low Cost Adsorbents M.Muthumani, R. Muthlakshmi, R. Pagutharivalan and N. Kannan	193
7.45	Convenient ytterbium triflate catalyzed one-pot multicomponent synthesis of spiro[indoline-3,4'-pyrano[2,3-c] pyrazole] Aishwarya Venkateswaran, Muthuraja Perumal, Prakash Sengodu, and Manisankar	194
7.46	Environmentally Benign Copper Triflate Mediated One Pot Multicomponent Synthesis of Benzo[g]chromenes Possessing Potent Anticancer Activity D.Umamaheswari, D. Nandhini, P. Muthuraja, S. Prakash, S. Chitra, and P. Manisankar	194
7.47	Bi-polymer based ZnO hybrid composite for better optical and thermal properties S. Rajaboopathi and S. Thambidurai	195
7.48	Synthesis and characterization of new ionic liquid crystals exhibiting chiral mesophases R. Mangaiyarjkarasi and S. Umadevi	195
7.49	Synthesis, NMR spectral and DFT studies of styryl imidazole derivatives- Nano SiO ₂ as efficient catalyst. P. Navamani and N. Srinivasan	197
7.50	Synthesis, Characterization of Benzimidazole (With Isoindoline) Derivatives by Leuckart Reaction and Their Antimicrobial Activity Ashokkumar. N, Umarani.G and Abdul Hassan sathali. A	198
7.51	Silver Microparticles Stabilized in A Lyotropic Liquid Crystal Medium K. Mohana, PR. Meyyathal and S. Umadevi	199
7.52	Fabrication of Graphene Oxide/ β -Cyclodextrin Composite and their application in the removal of Direct Red 7 dye G. Sumathi and H. Gurumallesh Prabu	200

7.53	Synthesis of Carbonate Doped TiO ₂ Submicrospheres for Fabrication of Photovoltaic Solar Cell. E. Murugan and S. Govindaraju	201
7.54	Photocatalytic degradation of methylene blue dye using TiO ₂ nanomaterials K. Santhi, S. Karuppuchamy and C. Rani	201
7.55	Bifunctional Biological Active Antibiofilm and Osteoblast Adhesion Efficacy from MWCNT/PPy/Pd nanocomposite Murugesan Balaji, Sonamuthu Jegatheeswaran, Pandiyan Nithya, and Mahalingam Sundrarajan	202
7.56	Silica-coated Magnetic Nanoparticles Supported Heteropoly Acid composites catalyzed an efficient conversion of nitrile from aldehyde A. Sangili, S. Jegatheeswaran, S. Ambika, K. Bama, M. Balaji, P. Nithiya, R. Sumathi, M. Abdul Kadir and M. Sundrarajan	203
7.57	Alignment of liquid crystal on a flexible polymer substrate B. Sivaranjani, V. Ganesh and S. Umadevi	204
7.58	<i>In silico</i> docking studies of anti-diabetic and breast cancer activity by N'-(1-benzylpiperidin-4-ylidene)-2-cyanoacetohydrazide K. Tharini, S. Umamatheswari and <u>K. Sundaresan</u>	205
7.59	Design, Synthesis and Anticancer Activity Evaluation of 2,6-diarylpiperidin-4-ones Containing Thiazolidin-4-one Moiety <u>P. Sangeetha</u> , R. Balaji, C. Sankar and K. Tharini	206
7.60	In silico Docking studies of α -amylase inhibitory activity of Glycoalkaloids Jannathul Firdhouse M, Nirmala Devie T, Hajara Banu TM, Christina Susan I, and Saxthi Vinmathi K	207
7.61	Theoretical Studies on Structural and Electronic Properties of Coumarin Derivative F. Kilirani, S. Stephysahayam, S. Karthick, R. Karkuzhali, M. Krishnan, G. Gopu	208
7.62	Structure and Electrochemical performance of LiV _x Mn _{2-x} O ₄ (0 ≤ x ≤ 0.20) cathode materials for rechargeable lithium ion batteries P. Mohana and G. Paruthimal Kalaignan	209
7.63	Synthesis of highly solar active Fe ₂ (MO ₄) ₃ nanocatalyst for the degradation of Rhodamine B S. Tamilarasi, K. Balakrishnan, I. Muthuvel, B. Muralidharan	210
7.64	Multistep synthesis of Newer 3'-(2-methoxyphenyl)-1'H-spiro[piperidine-4,2'-quinazolin]-4'(3'H)-one derivatives and their biological evaluation V. Veeramani, P. Sathyaseelan, P. Muthuraja, P. Manisankar	210
7.65	Understanding the fundamental concepts on Electrochemiluminescence (ECL) and its significance in applied aspects S. SenthilKumar	211
7.66	Probing the significance of cooperative and fluxional effects in clusters and phospholipids through Ab-initio molecular dynamical simulations Sailaja Krishnamurthy	211

1. Electrochemical Technologies

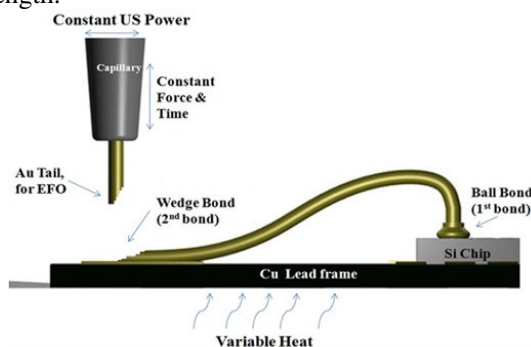
1.1 Recent Trends in Electronic Industry: Intermetallic Aluminides

Dr. T. Joseph Sahaya Anand

Faculty of Manufacturing Engineering, Universiti Teknikal, Malaysia Melaka (UTeM), 76100 Durian Tunggal, Malacca, Malaysia

Ph: 06 - 331 6489 (O) 016 - 412 7232 (M), Fax: 06 - 331 6431

The paper presents an overview of current and prospective applications of Aluminides based intermetallic alloys - modern engineering materials with special properties that are potentially useful for both structural and functional purposes. Intermetallics are a unique group of materials composed of two (or more) types of metal (or metal and non-metal) atoms, which exist as solid compounds and differ in a structure from that of the constituent components. Thermosonic bonding of the Cu wire on Al bond pad is a common technology used in the industry. Cu wire in the semiconductor interconnection technology has been extensively developed as replacement of Au wire. This is due to the cost advantages, superior material properties and better reliability performance. Despite the cost and material advantages of Cu wire, it has been reported that premature failure of voids formation occur at the Cu wire–Al pads interface. This is observed after certain duration of high temperature storage (HTS) at 175°C. This defect in turn causes the electrical failure to the device. The quality of wire bonds prepared at different conditions, specifically various bonding temperature (150°C, 280°C and 400°C) and annealed at different HTS durations (0 hours; i.e.: as-synthesized, 500 hours and 1000 hours) are determined by measurements of the strength of the interface between the bond wire and the bond pad. It was observed that the higher bonding temperature as well as the longer duration of HTS increased the quality of the bond strength.



Keywords : Wire bonding, Cu-Al intermetallic compound (IMC), High temperature storage (HTS), bulk materials, thin foils.

1.2 Significance and development of the advanced energy storage devices

¹Ravikumar Raman, ¹David Aradilla and ²Gopukumar Sukumaran

¹INAC-SPRAM/PCI, CEA, 17 Rue des martyrs, F-38000, Grenoble, France

²CSIR-Central Electrochemical Research Institute, Karaikudi, India, 630003

Lithium ion batteries (LIBs) currently dominate the field of electrochemical energy storage. The supply of lithium is finite and its availability and cost remain a concern, particularly in terms of larger scale storage applications. Considerable research effort is being expended to reduce the cost of the LIBs and to find viable alternatives. Sodium is one less expensive, more Earth-abundant alternative. With a standard reduction potential of -2.8 V and good compatibility with both current lithium processing techniques and selected electrode materials, it is particularly attractive as a lithium replacement. Recent work on sodium ion batteries (NIBs) has concentrated on all the possible cell components, but arguably most research has concerned the development of cathode materials [1-3], especially NaCoO₂ [2], Na₄Mn₉O₁₈ [4] and sodium manganese hexacyanoferrate [5].



Moreover, Solid-state lithium ion batteries are being more intensely being studied for the improvised safety features. Magnesium ion batteries are another important field of study because of its high safety and abundance, use of MgNWs are being studied and proved to be better anode for LIBs and MIBs [6, 7]. Stationary energy storage devices like flow battery concept is a well-established technology, example is Zn-Br flow battery.

Based on the power and energy density in accordance with the application battery designs varies with the various electrode materials. On the other hand, supercapacitors and micro capacitors also plays important role for the achievement of high power for specific devices. The materials like porous carbon with metal nano wires are showing very important role in super capacitors. Thus, more advances have been achieved to help the society to store energy efficiently.

References

- [1] J. Barker, M.Y. Saidi, J.L. Swoyer, A Sodium-Ion Cell Based on the Fluorophosphate Compound NaVPO_4F , *Electrochem. Solid-State Lett.* . 6 (2003) A1–A4.
- [2] M.M. Doeff, M.Y. Peng, Y. Ma, L.C. De Jonghe, Orthorhombic Na_xMnO_2 as a Cathode Material for Secondary Sodium and Lithium Polymer Batteries, *J. Electrochem. Soc.* . 141 (1994) L145–L147.
- [3] M.M. Doeff, T.J. Richardson, L. Kepley, Lithium Insertion Processes of Orthorhombic Na_xMnO_2 -Based Electrode Materials, *J. Electrochem. Soc.* . 143 (1996) 2507–2516.
- [4] Y. Cao, L. Xiao, W. Wang, D. Choi, Z. Nie, J. Yu, L. V Saraf, Z. Yang, J. Liu, Reversible sodium ion insertion in single crystalline manganese oxide nanowires with long cycle life., *Adv. Mater.* 23 (2011) 3155–60.
- [5] L. Wang, Y. Lu, J. Liu, M. Xu, J. Cheng, D. Zhang, J.B. Goodenough, A superior low-cost cathode for a Na-ion battery., *Angew. Chem. Int. Ed. Engl.* 52 (2013) 1964–7.
- [6] L. Viyannalage, V. Lee, R. V. Dennis, D. Kapoor, C. D. Haines and S. Banerjee, *Chem. Commun.*, 48 (2012), 5169–5171.
- [7] S. Brutti, G. Mulas, E. Piciollo, S. Panero and P. Reale, *J. Mater. Chem.*, 22 (2012) 14531–14537.

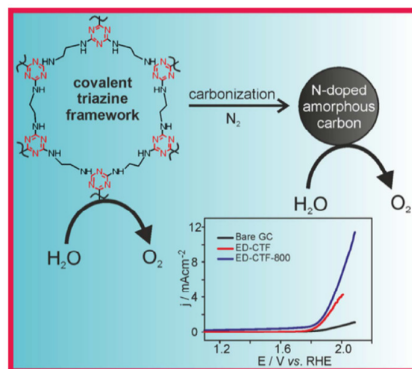
1.3 Ethylenediamine based Covalent Triazine Framework and its carbon composite as an Oxygen Evolution Reaction Catalyst

Sivalingam Gopi, Murugavel Kathiresan*

**Electro Organic Division, CSIR-Central Electrochemical Research Institute, Karaikudi-630003, TamilNadu, India*

Abstract

Herein, synthesized Ethylene diamine based covalent triazine framework and this carbonized material was electro chemically investigated. The porous materials were subjected to different characterization (FT-IR, ^{13}C and ^{15}N CP-MAS solid state NMR) to confirm the triazine network. The amorphous nature of the sample was defined by PXRD and Raman measurements. The PXRD 2θ value of the carbonized sample was very similar to amorphous nitrogen doped carbon^{[1],[2]}.



Electro chemical investigation of these materials using chronoamperometry and linear sweep voltammetry. These studies described that the OER activity and stability of the catalyst and excellent stability^[3] was observed for the catalysts after 1000 cycles and for 6 hrs. The current density and onset potential were compared between bare, carbonized and commercial GC, showed 10 times better current density than bare GC electrode and the onset potential also better than the commercial GC.

References

- [1] X. Wu, X. Yu, Z. Lin, J. Huang, L. Cao, B. Zhang, Y. Zhan, H. Meng, Y. Zhu and Y. Zhang, *Int. J. Hydrogen Energy*, 2016, 41, 14111-14122.
- [2] L. Hao, J. Ning, B. Luo, B. Wang, Y. Zhang, Z. Tang, J. Yang, A. Thomas and L. Zhi, *J. Am. Chem. Soc.*, 2015, 137, 219-225.
- [3] N.-T. Suen, S.-F. Hung, Q. Quan, N. Zhang, Y.-J. Xu and H. M. Chen, *Chem. Soc. Rev.*, 2017, 46, 337-365.

1.4 Electrocatalysis of mediated oxygen reduction at Glassy carbon electrode modified with Riboflavin and anthraquinone derivatives

P.Manisankar¹ and S.Valarselvan²

¹*Department of Industrial Chemistry, School of Chemistry, Alagappa University, Karaikudi-630003, Tamilnadu, India.*

²*Department of Chemistry, H.H. The Rajah's College(Autonomous), Pudukkottai-622001 Tamilnadu, India. email: svalarselvan@gmail.com*

Since riboflavin exhibits facile redox kinetics, it can be used as a good mediator of electrons [1]. Mediators are compounds of high electrochemical activity that undergo electron exchange readily with the analyte and again at the electrode surface and thus act as a shuttle to transport electrons between the analyte and electrode surface. The modification of flavins has been achieved by adsorption [2-4] and covalent linkage [5]. The catalytic effect of riboflavin and 1,4-naphthoquinone [6] and amino derivatives of anthraquinones [7] was already reported.

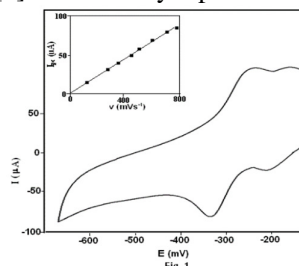


Fig. 1 Cyclic voltammogram for 1,5-DIHAQ/RB/GCE in phosphate buffer pH 7.0 at scan rate 40 mVs⁻¹. The inset shows the plot of cathodic peak current vs. scan rates.

In the present studies the electrochemical behavior of Riboflavin at glassy carbon electrode modified with hydroxyl derivatives of 9,10-anthraquinone was investigated by cyclic voltammetry, chronoamperometry and chronocoulometry techniques. The morphological character of AQ/RB/GCE was examined using scanning electron microscopy (SEM). The influence of pH on the shift in oxygen reduction potential and enhancement in peak current led to the selection of pH 7.0 as the optimum working pH. Combined mediation of 9,10-anthraquinones and riboflavin showed excellent electrocatalytic performance for the reduction of O₂ to H₂O₂. The involvement of two electrons in dioxygen reduction was confirmed from chronocoulometric and hydrodynamic voltammetric studies. The heterogeneous rate constants, mass specific current and the diffusion coefficients were determined by rotating disk voltammetry. The stability of the modified electrodes was ascertained in acidic and neutral media. Anthraquinones combined with riboflavin showed excellent electrocatalytic activities towards O₂ reduction in the neutral pH 7.0 with an over-potential of about 388 – 718 mV lower than the plain GCE. This oxygen reduction potential shift is more significant on comparison with the shift observed for GC electrodes modified with other anthraquinone derivatives.



The mechanism involved in the electrocatalytic oxygen reduction was studied by chronoamperometric techniques in various pH media. SEM analysis showed uniform dispersion of particles on GCE electrode. The modified electrode showed effective electron transfer with more stability and reproducibility.

AQ	Potential Shift ΔE (mV)		n_{O_2}
	AQ+RB	AQ	
1-HAQ	577	234	1.96
1,4-DIHAQ	718	298	2.01
1,5-DIHAQ	684	271	1.98
1,8-DIHAQ	655	245	1.95
2,6-DIHAQ	388	198	2.02

Table.1. Potential shift in O_2 reduction ΔE and number of electrons involved in O_2 reduction n_{O_2} .

References

- [1] S. Berchmans, R. Vijayavalli, Langmuir, 11 (1995) 286.
- [2] V.I Birss, H. Elzanowska, R.A. Purner, Can. J. Chem. 66 (1988) 86.
- [3] J. Xu, R.L. Birke, J.R. Lombardi, J. Am. Chem. Soc. 109 (1987) 5645.
- [4] M.M. Kamal, H. Elzanowska, M. Gaur, D. Kim, V.I. Birss, J. Electroanal. Chem. 244 (1988) 237.
- [5] C.N. Durfor, B.A. Yenser, M.I. Howers, J. Electroanal. Chem. 293 (1990) 125.
- [6] P. Manisankar, A. Mercy Pushpalatha, S. Vasanthakumar, A. Gomathi, S. Viswanathan, J. Electroanal. Chem. 571(2004) 43.
- [7] P. Manisankar, A. Gomathi, J. Power Sources 150 (2005) 240.

1.5 Electrocatalytic Reduction of Oxygen on Copper Nanoparticle Modified Glassy Carbon Electrode with 1,4-Naphthoquinone

J. Antony Rajam^a A. Gomathi^b and C. Vedhi^c

^aDepartment of Chemistry, St.Mary's College (Autonomous), Thoothukudi.

^bDepartment of Chemistry, Sri K.G.S Arts College, Srivaikuntam.

^cDepartment of Chemistry, V.O.Chidambaram College, Thoothukudi.

^aantonyrajam@ymail.com, ^bagomo66@yahoo.com & ^ccvedhi23@gmail.com

Abstract

The electrocatalytic reduction of oxygen was investigated on copper nanoparticle modified glassy carbon electrode (CuNP/GCE) with 1,4-naphthoquinone (NQNE) in different pH media 1.0 – 13.0. The electrochemical behaviour of CuNP/GCE with NQNE was studied in the absence and presence of oxygen by employing cyclic voltammetric technique. The stability of the modified electrode was also examined in acidic, neutral and basic media.

Voltammetric behaviour of NQNE at the modified GCE

Cyclic voltammogram of 1,4-naphthoquinone at CuNP/GCE exhibits a single redox couple under deaerated condition. On increasing the scan rate, the peak separation also increases (Figure A) which shows the quasi-reversibility of the electron transfer process at CuNP/GCE. The cathodic peak current (I_{pc}) increases linearly with square root of scan rate ($v^{1/2}$), indicating diffusion controlled mass transfer for NQNE reduction process at CuNP/GCE. The voltammetric peak potentials depend on pH for 1,4-naphthoquinone. Three distinct linear portions with different slope values were observed. The pH-potential diagram for NQNE at CuNP/GCE shows that at low pH (1 to 4) values, NQNE reduction involves two-electron three-proton process. In the intermediate pH range, it undergoes two-electron, two proton process and at pH above 10, the electrode surface reaction is a two electron, one proton process.



Catalytic Reduction of Oxygen at CuNP/GCE with NQNE

Under deaeration, 1,4-Naphthoquinone exhibited a single redox couple at the modified GCE whereas the cathodic peak reached its maximum current at the expense of anodic peak under aerated condition (Figure B), indicating the electrocatalytic reduction of oxygen. The influence of pH on the electrocatalytic behaviour of the modified electrode with NQNE was studied and pH 8.0 was chosen as the optimum working pH by comparing the shift in oxygen reduction potential (ΔE). The cathodic peak current I_{pc} is linearly proportional to square root of scan rate $v^{1/2}$ which clearly confirms the diffusion controlled process for oxygen reduction. The 1,4-naphthoquinone-adsorbed copper nanoparticle modified glassy carbon electrode possesses an excellent electrocatalytic abilities for oxygen reduction with overpotential 550 mV greater than that at a bare glassy carbon electrode.

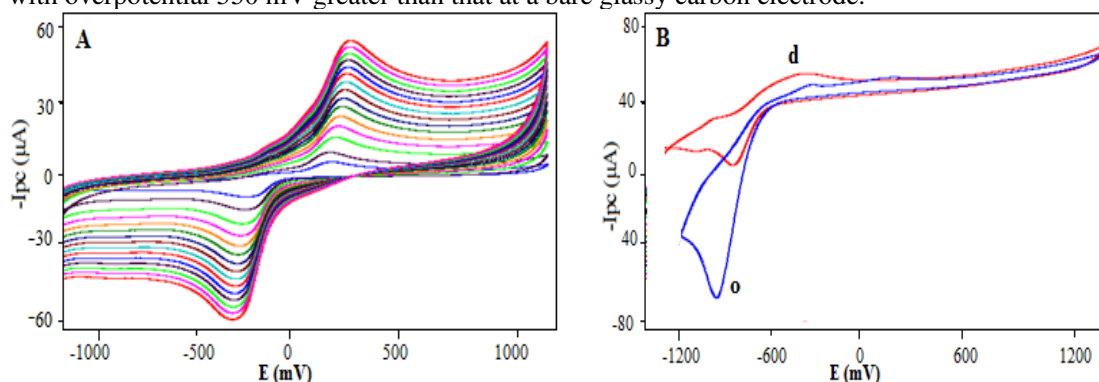


Figure: A. Cyclic voltammograms of NQNE at CuNP/GCE under de-aeration at scan rates 20, 50, 100, 200, 300, 400, 500, 600 and 700 mVs^{-1} . B. Cyclic voltammograms of NQNE at CuNP/GCE under aeration (o) and under de-aeration (d) at pH 8.0.

Keywords: Catalytic reduction, Voltammograms, Copper nanoparticle modified glassy carbon electrode, 1,4-Naphthoquinone, Oxygen reduction.

References:

- [1] M. Shamsipur, A. Salimi, S. M. Golabi, H. Sharghi, M. F. Mousayi, *Journal of Solid State Electrochemistry* 5 (1) (2001) 68-73.
- [2] Heechang Ye, Richard M. Crooks, *J. Am. Chem. Soc.* 127 (13) (2005) 4930-4934.
- [3] Lauri Tammeveski, Heiki Erikson, Ave Sarapuu, Jekaterina Kozlova, Peeter Titslaid, Vaino Sammelselg, Kaido Tammeveski, *Electrochemistry Communications* 20 (2012) 15-18.
- [4] Wei Yin, Han Zhou, Qi Li, Shihuan Lv, Xiaofei Liu, Huanbao Fa, Changguo Chen, *Asian Journal of Chemistry* 27 (7) (2015) 2457-2459.

1.6 Studies on Oxygen reduction with 2- amino anthraquinone at poly (aniline) modified electrode

G. Amala Jothi Grace^a A. Gomathi^{*b} C. Vedhi^c and M. Abdul Kadir^d

^aDepartment of Chemistry, St.Mary's College (Autonomous), Thoonthukudi.

^{*b}Department of Chemistry, Sri K.G.S Arts College, Srivaikuntam.

^cDepartment of Chemistry, V.O.Chidambaram college, Thoonthukudi.

^dDepartment of Chemistry, M.S.S. Wakf Board College, Madurai.

^aarsahana2010@gmail.com, ^bagomo66@yahoo.com & ^ccvedhi23@gmail.com

Abstract

Modified electrodes have proved their importance in the catalytic reduction of oxygen [1-4] due to its involvement in the energy conversion and storage.



The electrocatalytic reduction of oxygen with 2-amino anthraquinone (2-AMAQ) at the polyaniline modified glassy carbon electrode has been investigated by employing cyclic voltammetry, chronoamperometry and chronocoulometry techniques. The electrode was modified with polyaniline (PANI) by means of electrodeposition. The focus of electrode substrates is on carbon-based material since the oxygen reduction on these surfaces forms hydrogen peroxide as an end product. The electrochemical and electrocatalytic behaviour of 2- amino anthraquinone and PANI/GCE were investigated at different pH media. The stability of the polyaniline modified electrode was also studied in acidic, neutral and basic media.

A single redox couple for 2-AMAQ was obtained in the deaerated condition at PANI/GCE. Under aerated condition, there was an increase in cathodic peak current at the expense of anodic peak indicating electrocatalytic reduction of oxygen. The optimum working pH was found to be 7 by comparing the shift in oxygen reduction potential.

Figure 1 shows the cyclic voltammograms of 2-AMAQ at PANI/GCE in the presence (o) and absence (d) of oxygen at pH 7. The half peak potential $E_{P/2}$ vs pH (Figure 2) showed three distinct linear portions with different slopes of 90mV up to pH 4 (two electron three proton), 60mV at intermediate pH (two electron two proton) and 30mV at pH above 10 (two electron one proton) for 2- amino anthraquinone at the polymer modified electrode. The SEM photograph result in the figure 3 shows the strong adsorption of the 2-AMAQ on the modified electrode PANI/GCE. The Diffusion co-efficient value of 2-amino anthraquinone at the polyaniline modified electrode was found to be $7.75 \times 10^{-9} \text{ cm}^2/\text{s}$. The number of electrons involved in 2-amino anthraquinone reduction and oxygen reduction were determined by chronoamperometric and chronocoulometric studies and both were found to be 2.

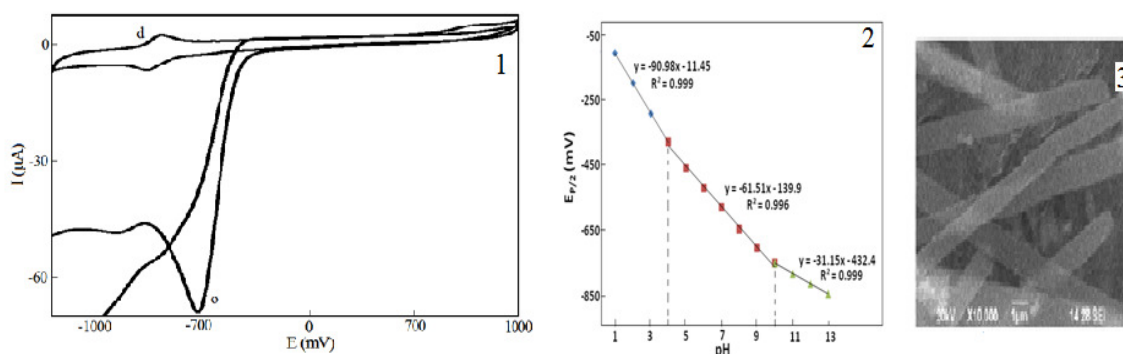


Fig.1 Cyclic voltammograms of 2-AMAQ at PANI/GCE in the presence (o) and absence (d) of oxygen at pH 7. **Fig.2** pH-potential diagram for 2-AMAQ. **Fig.3** SEM photograph of PANI/GCE with 2- AMAQ.

Keywords: Polymer, 2-amino anthraquinone, oxygen reduction, cyclic voltammetry, polyaniline.

References:

- [1] P. Manisnagar & A. Gomathi, *Electroanalysis*, 17 (12) (2005) 1051.
- [2] Yan Jiao, Yao Zheng, Mietek Jaroniec, and Shi Zhang Qiao, *J. Am Chem. Soc.*, 136 (2014) 4394.
- [3] J. Zhang, Z. Zhao, Z. Xia & L. Dai, *Nature Nanotechnology*, 10 (2015) 444.
- [4] Heiki Erikson, Ave Sarapuu, Jose Solla-Gullon & Kaido Tammeveski, *Journal of Electroanalytical Chemistry*, 780 (2016) 327.



References

- [1] C. Li, X. Yin, L. Chen, Q. Li and T. Wang, *J. Phys. Chem. C*, 113 (2009) 13438–13442.
- [2] Y. Cao, L. Xiao, M. L. Sushko, W. Wang, B. Schwenzer, J. Xiao, Z. Nie, L. V. Saraf, Z. Yang and J. Liu,
- [3] *Nano Lett.*, 12 (2012) 3783–3787.
- [4] F. Zheng, Y. Yang and Q. Chen, *Nat. Commun.*, 5 (2014) 5261–5270.
- [5] V. Selvamani, R. Ravikumar, V. Suryanarayanan, D. Velayutham and S. Gopukumar, *Electrochim. Acta*, 182 (2015) 1–10.

1.8 Fabrication of g-C₃N₄/NiO heterostructural nanocomposite modified glassy carbon electrode for quercetin biosensor

S. Selvarajan^a, A. Suganthi^{a**}, M. Rajarajan^{b*}

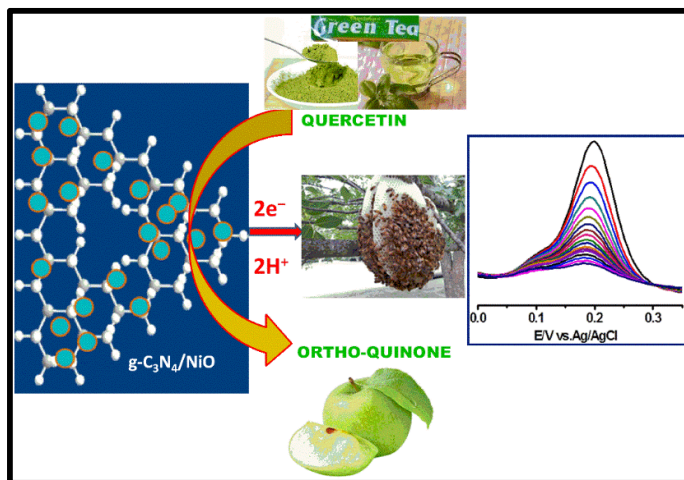
^a PG & Research Department of Chemistry, Thiagarajar College, Madurai - 625009, Tamilnadu, India.

^b PG & Research Department of Chemistry, Cardamom Planters' Association College, Bodinayakanur- 626513, Tamilnadu, India.

Corresponding author: suganthiphd09@gmail.com**, rajarajan_1962@yahoo.com*

Abstract

Herein, we report the one-pot route to synthesize structurally uniform and electrochemically active graphitic carbon nitride/nickel oxide (g-C₃N₄/NiO) nanocomposite and investigates the electrocatalytic activity toward the oxidation of quercetin (QR). The synthetic g-C₃N₄/NiO nanocomposite has a uniform surface distribution, which was characterized with scanning electron microscopy (SEM). Moreover, the composition of synthetic g-C₃N₄/NiO nanocomposite was characterized by UV-vis-spectroscopy, X-ray diffraction (XRD), fourier transform infrared spectroscopy (FT-IR spectra), BET, SEM and TEM. The peak current response increases linearly with quercetin concentration from 10 to 250 μM with a fast response time of less than 2s and a detection limit of 0.031 μM. The excellent performance of quercetin sensor, including long term stability, can be ascribed to the synergistic effects of the large surface area (resulting in high loading ability), dispersing ability and conductivity of g-C₃N₄ and the large surface-to-volume ratio and electrocatalytic activity of NiO nanoparticles. The proposed methodology was successfully used to quantify quercetin in green tea, green apple and honeysuckle.



Keywords: g-C₃N₄, NiO, glassy carbon electrode, cyclic voltammetry, differential pulse voltammetry.



References:

- [1] Tiago A. G. Duarte, Ana C. Estrada, Mário M. Q. Simões, Isabel C. M. S. Santos, Ana M. V. Cavaleiro, M. Graça P. M. S. Neves and José A. S. Cavaleiro, *Catalysis Science & Technology*, No.5, 351-363 (2015)
- [2] K. Rossen, R. P. Volante and P. J. Reider, *Tetrahedron Letters*, 38, No.5, 777-778. (1997)
- [3] Massuquinini Ines, Antonio J. Mendonca, Ana P. Esteves, Dina I. Mendonca, Maria J. Mendeiros. *Comptes Rendus Chimie*, 12, 841-849 (2009)
- [4] Nobuhiro Takano, Manabu Ogata, and Noboru Takeno. *Chemistry Letters*, 85-86 (1996)

1.10 EFFECTS OF ALUMINA NANOFILLER INCORPORATED POLYMER BLEND ELECTROLYTES FOR LITHIUM BATTERIES

R.Sasikumar^a, M. Ramesh Prabhu^b and K. Selva Kumar^b

^aDepartment of Physical Chemistry, University of Madras, Guindy Campus, Chennai 600 025, Tamil Nadu, India.

^bSchool of Physics, Alagappa University, Karaikudi 630 004 Tamil Nadu, India.
E-mail: skumaratr@gmail.com.

Abstract

Nano composite polymer electrolytes based on PEO/PVP with constant salt ratio of LiClO₄ and the plasticizer propylene carbonate (PC) were prepared for varies concentration of alumina. FTIR studies confirmed the complexation of LiClO₄ salt and filler alumina with the polymer matrix. The addition of plasticiser yields polymer electrolytes with enhanced ionic conductivity. It was found that 12 wt% of the filler added PEO (72) – PVP (8) - LiClO₄ (8) - PC (12) complex showed higher ionic conductivity has been found to be $7.31 \times 10^{-3} \text{ S cm}^{-1}$. The dispersion of nanoparticles in the plasticised polymer matrices is not only to improve the ionic conductivity but also to enhance the mechanical strength and stability of the polymer electrolytes. The morphology of thin films was examined by Atomic Force Microscopy (AFM). The electrical impedance spectroscopy technique was used to measure the ionic conductivity of polymer nanocomposite electrolyte. Hence this system can be used as for the fabrication of lithium battery.

Figure 1 shows the FTIR spectra of pure PEO, PVP, LiClO₄, PC with different concentrations of Al₂O₃, filler in the range of 4000 – 400 cm⁻¹. It has been observed that a very small intensity peak at 1799 cm⁻¹ corresponds to the ether oxygen group which is shifted to 1794, 1792, 1790, 1791 and 1798 cm⁻¹ respectively. It is observed that the small ether oxygen band at 1799 cm⁻¹ is found to smoothen gradually with the increase of LiClO₄ salt.

The mode responsible for the band at 845 cm⁻¹ is due to CH₂ rocking motion with little contribution from C-O stretching motion of PEO, while band at 947 cm⁻¹ originates primarily in the C-O stretching motion with some CH₂ rocking motion [1]. It is known that a vibrational band observed at 2900 cm⁻¹ is attributed to aliphatic C-H stretching of pure PVP is shifted to 2887, 2883, 2873, 2881 and 2890 cm⁻¹ respectively. The bands at 1651 and 1451 cm⁻¹ are attributed to C=O stretching and CH₂ wagging of pure PVP, which are shifted in all prepared composites. The intensity of the peak corresponding to C=O stretching at 1651 cm⁻¹ is decreased with the increase of filler concentration. The band at 630 cm⁻¹ corresponding to ClO₄⁻ anion which is present in the complexes. It is noted that the vibrational band is decreased with the increase of Al₂O content. Several new peaks have been observed in all the composition. The appearance of new peaks along with their changes in existing peaks and their disappearance in the IR spectra indicates the complexation of alumina with the polymers.

Polymer electrolytes with fixed ratios of polymers, salt and plasticizer (PEO (72)–PVP (8) – LiClO₄ (8)–PC (12) were prepared in order to find the appropriate nanofiller component for lithium battery applications. Fig.2. the ionic conductivity measurements have been carried out on these electrolytes by employing variable frequency range from 10 Hz to 1 MHz and temperature range from room temperature to 70°C. The thin films of the polymer complex were sandwiched between the two stainless steel electrodes attached to conductivity measurement setup.



The two stainless steel electrodes act as blocking electrodes for Li^+ ions under applied electric field. The semicircle may be due to the bulk effect of the electrolyte and the spike may be due to the effect of blocking electrodes [2].

The disappearance of semicircular portion in high frequency region of complex impedance plot indicates that the conduction is mainly due to the ions and the inclined line due to the effect of the blocking electrodes. The intercept of the semicircle or spike with the real impedance (z') axis gives the bulk electrical resistance (R_b) of the polymer electrolytes.

AFM image of PEO (72%) - PVP (8%) - LiClO_4 (8%) - PC (12%) – alumina (12%) is shown Fig.3. over the scanned area $2.5\mu\text{m} \times 2.5\mu\text{m}$. The topographic images clearly show the presence of alumina nanoparticles with polymer matrix which are responsible for maximum ionic conductivity. The alumina nanoparticles are clearly visible in these micrographs with data scale of 2~4cm and polymer matrix with scale of $\sim 0.25\mu\text{c}$.

Key words: Ionic conductivity, nanofiller, polymer blend electrolyte

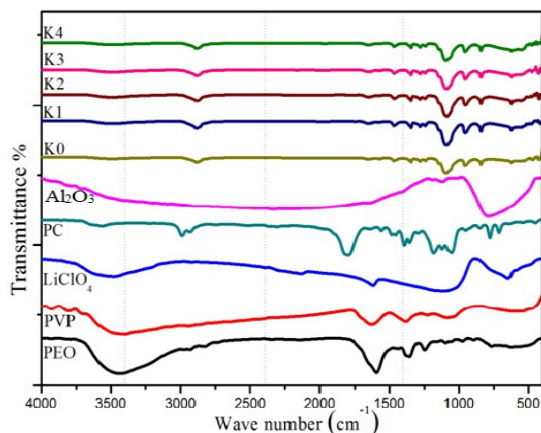


Figure. 1. FTIR spectra of prepared polymer electrolyte samples

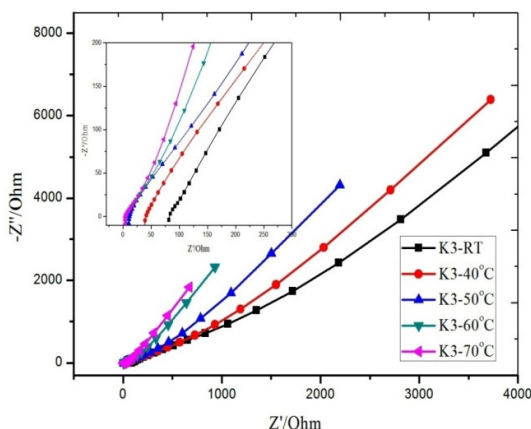


Figure.2. Different temperature complex impedance plot of the highest conductivity samples

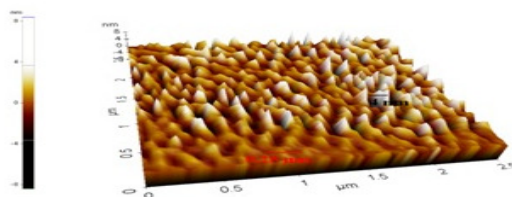


Figure.3. The topography image of the sample having maximum ionic conductivity in 3D image

References

- [1] S. Intarkamhang, Ionics, 393 (2003) 171
- [2] N. Vijaya, D. Vinoth Pandi, S. Selvasekarapandian, International Journal of Scientific Research 2(9) (2013)383.



1.11 Inhibitive effect of 1-(3-aminopropyl imidazole) on copper corrosion in 3.0% sodium chloride solution

P. Durainatarajan^a, M. Prabakaran^b, S. Ramesh^{a*} and V. Periasamy^a

^aDepartment of Chemistry, The Gandhigram Rural Institute – Deemed University,
Gandhigram 624 302, Dindigul, Tamil Nadu, India

^bDepartment of Chemistry, Gnanamani College of Technology,
Namakkal 637 018, Tamil Nadu, India

Abstract

This paper presents a study on 1-(3-aminopropyl) imidazole (API) on copper to investigate the inhibition effect of the API against copper corrosion in 3.0% NaCl solution. API films on copper were characterized by Fourier transform infrared spectroscopy (FT-IR), energy dispersive X-ray analysis (EDX). The presence of nitrogen in the FTIR analysis shows the formation of API film on the Cu surface. Corrosion resistance capability of the API on copper was assessed by the electrochemical impedance spectroscopy, potentiodynamic polarization studies, cyclic voltammetry and scanning electron microscopy. Results revealed that the API on copper showed good resistance against corrosion in 3.0% NaCl solution.

Introduction

Copper and alloys have been widely employed in various industrial and domestic applications due to its good mechanical, thermal and electrical properties. However, copper has poor corrosion resistance when exposed to chloride containing aqueous environments. Various techniques are widely utilized to protection of copper against corrosion in corrosive media. Corrosion inhibitor is a cost effective and practical choice to protect copper from corrosion. Many N-heterocyclic compounds and their derivatives are effective corrosion inhibitors for copper corrosion in corrosive media. Imidazole derivatives have exhibited excellent inhibitor properties against the corrosion of copper protection in neutral media and are also non-toxic inhibitors.

Film characterization

FT-IR spectroscopy studies were recorded to confirm the film formation on copper surface. In FT-IR spectrum of pure API (Fig 1a): the bands at 1568, 1391 and 3424 cm^{-1} are due to C=N, C-N and N-H stretching, respectively. In contrast, the spectrum of API Cu (Fig. 2b) displays the shifting of main characteristic C=N stretching band from 1568 to 1541 cm^{-1} , respectively which inferred that the formation of the API film on the copper by the N atoms.

Results and discussion

As can be seen from Table 1, compared to bare electrode, the values of R_{ct} , R_f and n increase in presence of API and this behavior are further enhanced by increasing their concentration, demonstrating that protective films are formed by the adsorption of API on copper surface. With an increase in concentration from 0.1 to 1.0 mM, the R_{ct} value increased from 6341 to 12060 cm^2 . It is also seen that inhibition efficiency increase from 84.30 to 92.08%. The capacitance value is decreased from 35.03 to 44.25 $\mu\text{F cm}^{-2}$ and the n value is increased from 0.57 to 0.63. The high R_{ct} , n values and lower capacitance value at 1.0 mM concentration reveal the dense and protective surface film formation on electrode surface.

Potentiodynamic polarization curves for API film copper electrode shifted to lower current densities compared to the bare electrode. In comparison with the bare copper, E_{corr} values in the presence of the API move to the anodic direction and the displacements are more than 85 mV. This suggests that the API inhibitor plays the anodic type role. i_{corr} value for bare copper is 7.515 $\mu\text{A cm}^{-2}$. By increasing the concentration of API from 0.1 mM to 1.0 mM in 3.0% NaCl solution, i_{corr} value is significantly shifted from 1.580 to 0.967 $\mu\text{A cm}^{-2}$ with maximum inhibition efficiency of 87.13%. Changes in b_a and b_c values indicate the inhibition of both cathodic and anodic corrosion. Therefore, the copper corrosion could be effectively protected by API inhibitor.



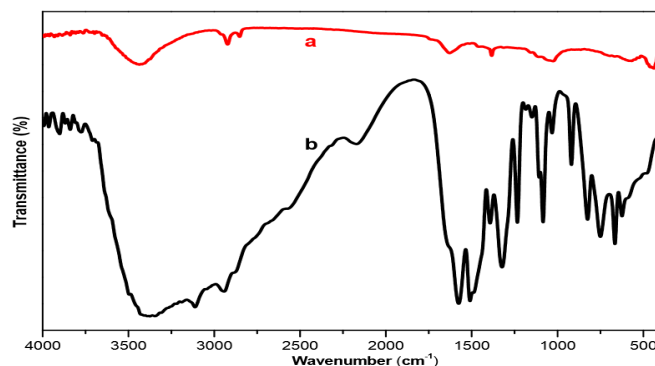


Figure. 1 FTIR spectra of (a) pure API and (b) presence of inhibitor.

Table 1. Impedance parameters obtained in 3.0% NaCl in the absence and presence of API inhibitor at various concentrations.

C (mM)	R_{ct} ($\Omega \text{ cm}^2$)	Q_{dl} ($\mu\text{F cm}^{-2}$)	n_1	R_f ($\Omega \text{ cm}^2$)	Q_f ($\mu\text{F cm}^{-2}$)	n_2	IE (%)
0	995	59.84	0.68	-	-	-	-
0.1	6341	35.03	0.57	1444	25.24	0.81	84.30
0.5	9482	42.33	0.62	6665	11.39	0.85	89.50
1.0	12060	44.25	0.63	8322	11.11	0.86	92.08

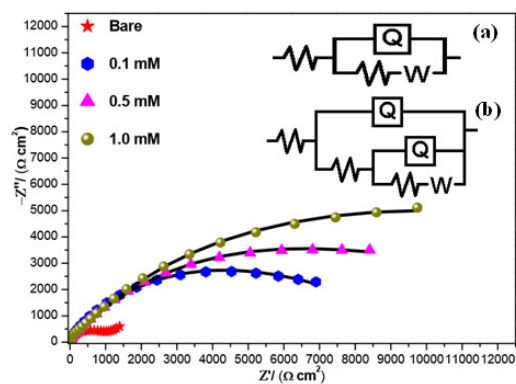


Figure 2. Nyquist plot recorded for Cu in 3.0% NaCl solution with and without API at different concentrations. (Inset Fig. a & b is circuits of bare and API film on Cu)

Acknowledgements

P. Durainatarajan is grateful to the UGC for a Research Fellowship in Sciences for Meritorious Students (RFSMS) for financial support and also the authorities of The Gandhigram Rural Institute for encouragement



1.12 Electrochemical process for the Synthesis of Diacetone -2-keto-L-gulonic acid (Vitamin-C-intermediate) from L-Sorbose.

S. Sangeetha, K. Kulangiappar and T. Vijayarathi*

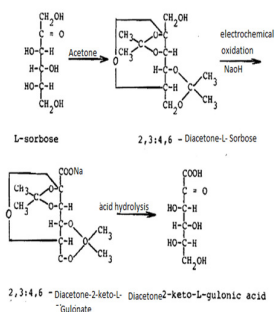
Electro organic division, Central Electrochemical Research Institute,
Karaikudi-630 006,India

* Email: vijimathi@cecri.res.in

Abstract:

Diacetone-2-keto-L-gulonic acid is an important intermediate in the synthesis of vitamin C (Ascorbic acid). Reichstein process of chemical synthesis is the main industrial route for producing ascorbic acid. The commercially available nickel hydroxide electrodes developed for Ni-Cd battery were employed as anodes in the present study for the electro oxidation of diacetone-L-sorbose (DAS) into diacetone -2-keto-L-gulonic acid (DAG). Diacetone -L-sorbose was prepared by the acetonation of the four hydroxyl groups of L-sorbose catalysed by sulphuric acid. Reaction conditions such as temperature, acetone -to-sorbose ratio and solvent for the isolation of diacetone-L-sorbose were optimized and the material yield obtained was found to be 85%.

The Electrochemical oxidation of diacetone - L-sorbose to diacetone-2-keto-L -gulonic acid was carried out galvanostatically in an undivided batch cell using porous nickel hydroxide electrode. The mediated or indirect electro oxidation of DAS was achieved by the Ni(OH)₂ / NiOOH redox couple



bound on the electrode surface in aqueous alkaline electrolyte media. The electro chemical process parameters such as current density, temperature and current required (F/mole) were optimized. Under optimum condition material yield of DAG was found to be 88.2% with a 44.1% faradaic yield. The reactions involved in the electrochemical process are outlined in the following scheme .

The isolated solid products of DAS and DAG were analysed and confirmed by melting point, by ¹H NMR, ¹³C NMR and FT-IR spectral data .

The stability and reusability of nickel hydroxide anode materials in batch processes were evaluated using SEM and XRD. Nickel hydroxide electrode exhibit excellent stability and reusability for the oxidation of DAS.

Key words: Sorbose, Diacetone-L-Sorbose, Electro oxidation , Nickel hydroxide anode, Diacetone-2-keto-L-gulonic acid.



1.14 Enhancement of Thermal Properties in Oleic acid Phase Change Material using Graphene Oxide Nanosheets for Thermal Energy Storage Applications

S. Imran Hussain, S. Kalaiselvam*

Department of Applied Science and Technology, AC Tech Campus, Anna University, Chennai, India.
E-mail: imran.usan@gmail.com, nanokalai@gmail.com

Abstract

Generally, organic PCMs has an extensive attention because of their higher latent heat density, suitable phase-transition temperature and stable physical and chemical properties. But, the pure organic PCMs possess some shortcomings that hinder their application in practice, including low thermal conductivity, high volume change and liquid seepage during phase transition. By the addition of high thermal conductivity materials in PCM can increase their various properties significantly. This present work investigates the effect of adding graphene oxide (GO) to oleic acid (OA) phase change material (PCM) in order to prepare nano enhanced PCM (NEPCM) with enhanced thermal conductivity and thermal stability. GO was synthesized via hummers method and characterization of structural, optical, morphological studies were taken. Structural studies analysed by x-ray diffraction (XRD) shows a 002 and 001 plane, raman spectroscopy have a D band at 1365 and G band at 1600 cm^{-1} , confirms the formation of GO. Sheet like morphology was confirmed by Field emission scanning electron microscopy (FESEM), which influence the shape stability of OA. The optical absorption peak at 230 nm observed with uv visible absorption spectroscopy. Fourier transform infrared spectroscopy (FTIR) was used to confirm the chemical composition and structure of GO nanosheets. NEPCMs were prepared by sonication followed with magnetic stirring and the thermo-physical properties were studied from melting and solidification, differential scanning calorimetry (DSC) analysis. DSC results show that, for pure OA melting and solidification temperature was 5.40 and 4.41 °C, corresponding latent heat values were 130.8 and 126.6 J/g. It also reveals that there was a slight decrease in the latent heat values for NEPCMs which is quashed by its improved heat transfer rate. Enhancement in thermal conductivity was observed with the help of the laser flash analyser (LFA). Thermogravimetric analysis (TGA) was used to analysis the as prepared NEPCM thermal reliability and stability. Outcome of these results concluded that shape stabilized OA NEPCM has acceptable thermal properties which are suitable for thermal energy storage.

Key words: Phase change materials, oleic acid, graphene oxide, thermal conductivity.

1.15 Modified electrode surface as a sensitive sensors of heavy metals In Seaweed Of *Gracilaria Corticata*

A.Vimala and C.Vedhi*

Department of Chemistry, V.O.Chidambaram College, Tuticorin – 628 008, Tamilnadu, India

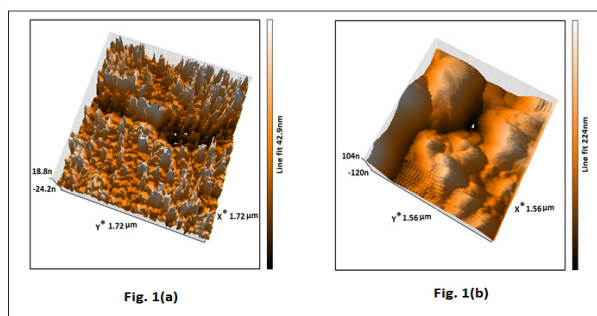
* correspondence: +91 4612310175, +91 9092368104, e-mail: cvedhi@rediffmail.com and vimjesusavn@gmail.com

Abstract

The electrochemical methods for heavy metals detection have been attracted considerable attention due to their simplicity, rapidity and high sensitivity. In particular, voltammetric methods are valid and very effective alternative for the simultaneous determination of heavy metals analysis. The electrochemical behaviour of heavy metals on multiwalled carbon nanotubes modified glassy carbon electrode (MWCNTs/GCE) were studied by cyclic voltammetry (CV), linear sweep anodic voltammetry (LSAV), square wave anodic voltammetry (SWAV) and differential pulse anodic voltammetry (DPAV). Under the optimized experimental conditions the differential pulse voltammogram shows four anodic peaks at 0.2842, 0.073, 0.185 and 0.6928 V representing the metals of Pb, Cu, Cr and As respectively in the seaweed *Gracilaria corticata*. Higher peak current values were obtained for all the four aforementioned peaks. This may be due to fast electron transfer rate and the presence of specific adsorption on MWCNTs/GCE.



FT-IR spectrum of *Gracilaria corticata* exhibits fourteen major bands in the range from 4000 - 400 cm^{-1} corresponding to secondary amines, ketones, alkanes, alcohols, halides, etc. Atomic absorption spectroscopic analysis concluded that although Cd, Zn, Ni, Pb and Cu concentrations in *Gracilaria corticata* were lower than those concentrations in the previous reports, *Gracilaria corticata* showed Fe concentration (315 ppm) higher than the permissible limit (15 ppm) set by World Health Organization (WHO). X-ray diffraction (XRD) pattern of *Gracilaria corticata* revealed the crystalline nature of the sample by the sharp peaks. The diffraction peaks at 31.2947° , 40.6137° , 45.9347° and 73.8567° suggests presence of Pb [1], Zn [2], Ag [3] and Cu [4] respectively. AFM images of thin film of *Gracilaria corticata* in acid and water are shown in Fig. 1(a) and 1(b). It could be seen from the Fig. 1(a) that the more uneven and rough surface with the frost structure exist in the 3-D image. Fig. 1(b)



revealed the snow structure. More agglomeration is seen on the picture of seaweed films.

Fig.1(a). Topographic image of thin film of *Gracilaria corticata* in acid

Fig.1(b). Topographic image of thin film of *Gracilaria corticata* in water

Difference in the structure of these adsorbents was mainly due to difference in their solvent medium. From the AFM analysis is observed that most of the pores in the seaweed were covered by heavy metals.

References

- [1] T. Theivasanthi, M. Alagar, Nano Biomedicine Engineering 5(1) (2013) 10-19.
- [2] D.I. Rusu, G.G. Rusu, D. Luca, Acta Physica Polonica A 119(6) (2011) 850-856.
- [3] M. YokeshBabu, V. JanakiDevi, C.M. Ramakritinan, R. Umarani, N. Nagarani, A.K. Kumaraguru, International Journal of Current Microbiology and Applied Sciences 2(8) (2013) 155-168.
- [4] R.P. Suresh Jeyakumar, V. Chandrasekaran, International Global Research Analysis 2(11) (2013) 10-13.

1.16 Corrosion of mild steel in sulphuric acid medium inhibited by benzimidazole

Dr. G. Kavitha^a, P. Karpagavinayagam^b and Dr. C. Vedhi^{*b}

^aDepartment of Chemistry, Rajalakshmi Institute of Technology, Chennai – 601206, Tamilnadu, India

^bDepartment of Chemistry, V.O Chidambaram College, Thoothukudi – 628008, Tamilnadu, India

* correspondence: Phone: +91 4612310175, +91 9092368104; Fax: +91 4612310275,

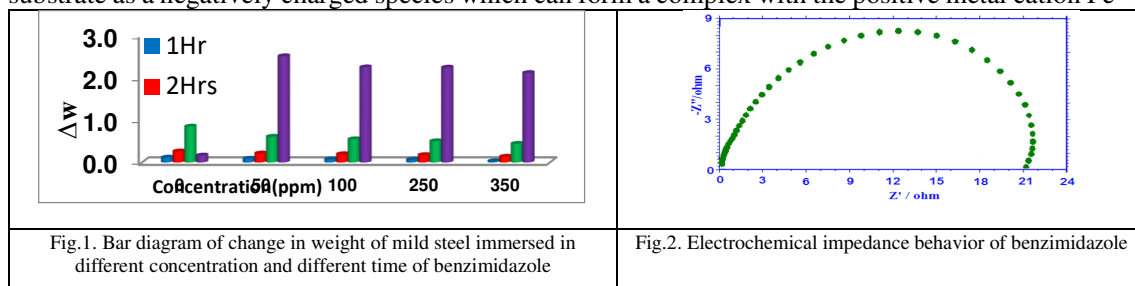
e-mail- cvedhi@rediffmail.com (or) cvedhi23@gmail.com

Investigate the effect of corrosion behaviour of mild steel specimens before and after addition of benzimidazole. All samples were prepared based on the testing specification requirement and the chemical compositions of the mild steel were obtained using spectrometer tester. Mild steel specimens of specified dimensions were immersed in aqueous solutions containing 2N H₂SO₄ with various concentrations of the studied inhibitors for a period of different time intervals. The mass of the specimens before and after immersion was determined using an analytical balance of 0.001 mg accuracy. To obtain corrosion rate, weight loss test was conducted and the samples were immersed in five different solutions which were distilled water, 2N H₂SO₄ acid.



Mild steel specimens were used for weight loss measurement. Each mild steel coupon was degreased by washing with ethanol followed by rinsing in acetone, allowed to dry and kept in a desiccator prior to use. The precleaned and weighed coupons were dipped in beakers containing 2N H₂SO₄ acid by choosing the inhibition concentrations in the range of 50 - 350 ppm of inhibitors (Fig 1). Double layer capacitance values (C_{dl}) and charge-transfer resistance values (R_{ct}) were obtained from impedance measurements. For Nyquist plots it is clear that the impedance diagrams contain semicircle (Fig 2) with centre under real axis. The size of the semicircle increases with the inhibitor concentration, indicating the charge transfer process as the main controlling factor of the corrosion of steel. It is apparent from the plot that the impedance of the inhibited solution has increased with the increase in the concentration of the inhibitors. The inhibition process is commonly related to adsorption of inhibitor molecules onto the metallic surface. In this study, the experimental data were tested with various isotherms including Langmuir, Temkin and Freundlich adsorption isotherms. The data best fit Langmuir adsorption isotherm. Langmuir theory allows the most basic presentation of adsorption on an ideal surface. The standard free energy of adsorption (ΔG_{ads}) and the equilibrium constant (K) are related by the following equation $\Delta G_{ads} = RT \ln (55.5K)$.

Potentiodynamic studies of the anodic dissolution of mild steel in acid medium in presence and absence of nitrones. From the polarization curves, it is evident that the inhibitors block the active sites for cathodic reaction to occur and prevent the metal dissolution process. Furthermore, it is observed that cathodic curves are more affected than anodic curves, indicating that the nitrones act as anodic inhibitors. Moreover, the nitrones possess electro-active nitrogen, oxygen atoms and an aromatic ring which favour the adsorption phenomena. The nitrone molecules tend to be adsorbed on to the mild steel substrate as a negatively charged species which can form a complex with the positive metal cation Fe²⁺.



1.17 Trichromic behavior of co-polymer of substituted thiophenes

P. Authidevi¹, Dr.D. Kanagavel², Dr.V. Sreeja³ and Dr. C. Vedhi¹

¹ Department of Chemistry, V.O. Chidambaram College, Thoothukudi-628008, Tamilnadu.

² Department of Chemistry, Kamaraj College, Thoothukudi-628002, Tamilnadu.

³ Department of Chemistry, Vellalar College for Women (Autonomous), Erode 12.

Abstract

Copolymer based on 3,4-ethylenedioxythiophene and 3-hexylthiophene are successfully electrodeposited on ITO electrodes in tertiary butyl ammonium perchlorate/acetonitrile as supporting electrolyte. Spectroelectrochemical properties of the co-polymer were studied through cyclic voltammetry with UV- visible spectroscopy. Spectroelectrochemical study reveals that this co-polymer film exhibits a wonderful multichromic behavior (sky blue-cement grey-wine red) under different potentials. This electrochromic properties of this co-polymer motivate for the future application in optical devices.

The in-situ UV-vis absorption spectra of Poly(2HT-co-EDOT) in pH 4.0 under various applied potentials ranging from -0.6 to 1.4V was shown in Fig 1. The maximum absorption band was obtained at 414nm due to the $\Pi-\Pi^*$ transition of the neutral state of the copolymer and it decreased with the increase of potential. Appearance of charge carrier bands at around 650nm >800nm confirmed the presence of polaron and bipolaron bands are confirmed by the appearance of charge carrier bands at around 650nm >800nm.



Same trend as discussed above was noticed. During electrolysis the dark blue colour of the solution fades and after one hour time interval, the complete decolourisation of the dye solution was seen.

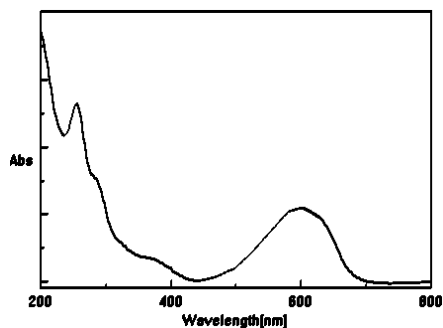


Fig.1. UV-VIS spectrum reactive blue 19

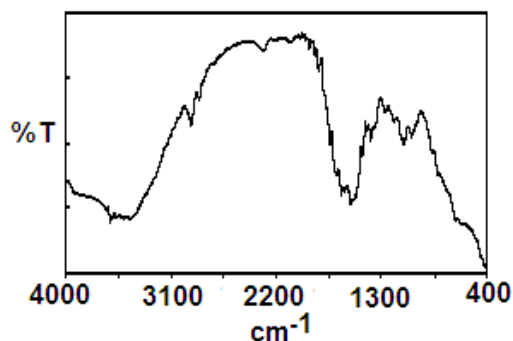


Fig.2. FTIR spectrum reactive blue 19

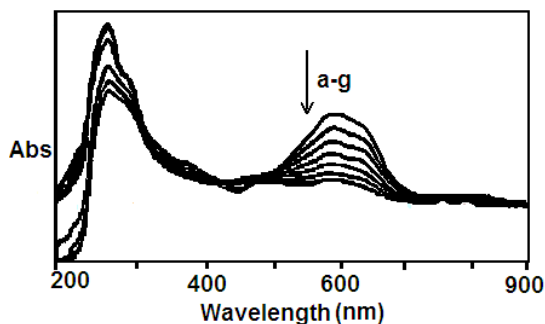


Fig.3. UV-VIS spectrum of reactive blue 19 at various applied potentials in volt 0.2, 0.3, 0.4, 0.5, 0.6, 0.7 and 0.8 respectively at 10 minutes.

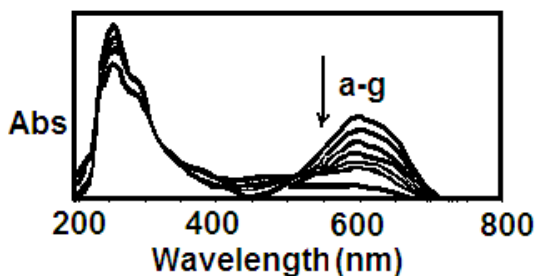


Fig.4. UV-VIS spectrum of reactive blue 19 at various time intervals in minutes at a constant applied potential of 0.8V (a) 0 (b) 10 (c) 20(d) 30 (e) 40 (f) 50 (g) 60

References:

- [1] William Kemp, Organic Spectroscopy, English Language Book Society, The Macmillan Press Ltd. Hong Kong, 1975.
- [2] Mark R. Antonio, Ming-His Chiang, Clayton W. Williams, L. Soderholm, Mat. Res. Soc. Sump. Proc. 802, 2004, DP4.5.1.
- [3] Marc De Backer, Francois X Sauvage, Journal of Electroanalytical chemistry, 602, 2007, 131.
- [4] Sonmez Arslan, Ismail Yilmaz, Transition Metal Chemistry, 32, 2007, 292.



- [10] H.W. Wang, Z.A Hu, Y.Q. Chang, Y.L. Chen, Z.Y. Zhang, et.al, Mat. Chem. Phy, 130 (2011) 672–679.
- [11] T.Y. Wei, C.H. Chen, K.H. Chang, S.Y. Lu, C.C. Hu, Chem. Mater., 21 (2009) 3228.
- [12] M.J. Deng, F.L. Huang, I.W. Sun, W.T. Tsai, J.K. Chang, Nanotechnology, 20 (2009) 175602.

1.26 PREPARATION AND CHARACTERIZATION OF ACTIVATED CARBON FROM PEANUT SHELLS BY CHEMICAL ACTIVATION METHOD

C.Kalaiselvi, M.Sivakumar, R.Subadevi*

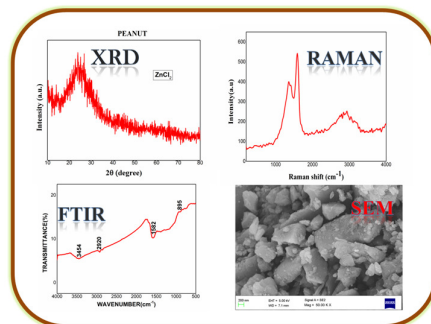
#120, Energy Materials Lab, Department of Physics, Alagappa University,
Karaikudi - 630 003, Tamil Nadu, India.

(* Corresponding Author: susimsk@yahoo.co.in; susiva73@yahoo.co.in)

ABSTRACT:

Activated carbon is a microcrystalline, non-graphitic form of carbon. The structure of activated carbon is well described as a twisted network of defective carbon layer plane, cross-linked by aliphatic bridging groups. The most commonly used activating agents are phosphoric acids, zinc chloride and salts of sodium and magnesium. These chemical agents may restrict the formation of tar during carbonization. The activated carbon was prepared from peanut shell by using $ZnCl_2$ as an activating agent via chemical activation method.[1,2] Then the as-prepared carbon was characterized by XRD, FTIR, RAMAN and SEM analyses. In the XRD pattern, we observed that the structure was collapsed and amorphous carbon was identified. FTIR analysis confirms the presence of functional groups present in the surface of activated carbon. There are two well resolved bands namely D and G were identified from the RAMAN spectrum. The SEM was used to investigate the structure and morphology of the sample, which shows the porous particles in various sizes. The activated carbon behaves as a composite material that could be added into the positive electrode material in Li-sulfur batteries to adsorb lithium polysulfide. The as-prepared peanut shells of activated carbon were developed as a conducting framework for lithium-sulfur battery in future studies.

Keywords: activated carbon; chemical activation method; Lithium sulfur battery; $ZnCl_2$.



References:

- [1] J. Yang and K.Qiu, Experimental design to optimize the preparation of activated carbons from herb residues by vacuum and traditional $ZnCl_2$ chemical activation, Ind.Eng.Chem.Res, 2011, 50, 4057-4064.
- [2] S.Zang,M.Zheng,Z.Lin,Y.Liu,B.Zhao,H.Pang,J.Cao,P.HeandY.Shi,Activated carbon with ultrahigh specific surface area synthesized from natural plant material for lithium-sulfur batteries,J.Mater.Chem.A,2014,2,15889-15896



1.27 Influence of composition on ionic conductivity of P(S-co-MMA)/PVC blend polymer electrolyte

M.Shanthi^{a,b}, M.Sivakumar^{b,*}, R.Subadevi^b

^a Department of Physics, Kamaraj College of Engg. And Tech, Virudhunagar 626001, Tamil Nadu, India.

^b #120, Energy Materials Lab, Department of Physics, Alagappa University, Karaikudi - 630 003, Tamil Nadu, India.

(* Corresponding Author: susiva73@yahoo.co.in; susimsk@yahoo.co.in)

Abstract

The tremendous increase in electronic gadgets like cell phones, laptop, ipod, notebook demands for lightweight, high energy density rechargeable batteries. Large research efforts have been devoted on development rechargeable batteries based on polymer- solid electrolytes, which fulfils such high-energy density [1]. Poly (ethylene oxide) (PEO) - based polymer electrolytes are extensively studied, and the electrolytes exhibit poor conductivity ($\approx 10^{-8}$ to 10^{-5} S/cm) at ambient temperature [2]. Apart from PEO, poly (methyl methacrylate) (PMMA) [3], poly (vinylidene fluoride) (PVdF) [4], poly (acrylonitrile) (PAN) have also been used as the polymer host material. In this work, gel polymer electrolyte system based on the Poly(styrene –co-methyl methacrylate)/ PVC, Lithium bis (trifluoro methane sulfonyl) imide(LiTFSI) salt and the plasticizer EC+PC were prepared by solvent-casting technique. Ionic conductivity of the electrolyte film has been investigated by varying the blend ratio in the polymer matrix. The structural and the complex formation have been confirmed by X-ray diffraction spectroscopic analysis. The ionic conductivity of the electrolyte was found to increase with the increase of PVC concentration and then decreased after an optimum value. The highest ionic conductivity achieved was 2.7×10^{-5} S cm⁻¹ for 25-75 weight ratio of P(S-MMA)-PVC based LiTFSI+EC+PC electrolyte system. Finally, the microstructure of the maximum ionic conductivity sample has been depicted with the help of scanning electron microscope analysis.

References

- [1] J. R. MacCallum, C.A. Vincent, Polymer Electrolyte Reviews, vols. I and II, Elsevier, New York, (1987) and (1989).
- [2] Kim HT, Kim KB, Kim SW, Park JK (2000) Electrochim.Acta 45:4001.
- [3] Bohnke O, Frand G, Rezzazzi M, Rousselot C, Truche C (1993) Solid State Ionics 66:97.
- [4] Alamgir M, Abraham KM (1993) J.Electrochem.Soc 140: L96.
- [5] Han HS, Kang HR, Kim SW, Kim HT (2002) J. Power Sources 112:461.

1.28 Effect of BaTiO₃ filler in P(VDC-co-AN) based gel polymer electrolytes employed in Lithium secondary batteries

M.Shanthi^{a,b}, M.Sivakumar^{b,*}, R.Subadevi^b

^a Department of Physics, Kamaraj College of Engg. And Tech, Virudhunagar 626001, Tamil Nadu, India.

^b #120, Energy Materials Lab, Department of Physics, Alagappa University, Karaikudi - 630 003, Tamil Nadu, India.

(* Corresponding Author: susiva73@yahoo.co.in; susimsk@yahoo.co.in)

Polymeric complexes with inorganic salts have widely been studied due to their potential importance of their application in solid state batteries, electrochromic devices and electrochemical sensors [1]. Most efforts were made to investigate lithium ion conducting polymer electrolytes based on a linear polyethylene oxide (PEO) because of its easy coordination with alkali metal ions. However, the room temperature conductivity is very low and exhibit insufficient mechanical property, which restricts the practical applications of PEO based polymer electrolytes. To overcome these problems, composite polymer electrolytes with inert ceramic fillers were explored by Weston and Steele initially [2]. The addition of inorganic fillers, such as alumina (Al₂O₃), silica (SiO₂), titania (TiO₂), to the polymer electrolyte the improves the ionic conductivity as well as EC and physical properties [3,4].



In this work, we investigated the preparation of P(VDC-co-AN) based composite polymer electrolytes composed of LiBF₄ as a salt EC as plasticizer and BaTiO₃ as a ceramic filler. This study focuses on improvement of the ionic conductivities of polymer electrolytes by the addition of BaTiO₃ nano particles. The effect of concentration of BaTiO₃ nano particles in to the polymer matrix has been studied in the view point of ionic conductivity and the results are discussed.

The ionic conductivity of the electrolyte is found to increase with the increase of BaTiO₃ concentration and then decreased after an optimum concentration (6%). The highest conductivity achieved was $5.424 \times 10^{-4} \text{ S cm}^{-1}$ at 6 wt% of BaTiO₃. The structural and the complex formation have been confirmed by X-ray diffraction and FTIR analyses. The above studies confirmed the fact that there exists a definite complex coordination between P(VdC-AN) and lithium salts and the filler BaTiO₃ particles. Finally, thermal stability of the maximum ionic conducting sample has been depicted with the help of DSC analysis.

REFERENCES

- [1] C.A. Vincent, Prog. Solid State Chem. 17(1987)145.
- [2] J.E. Weston, B.C.H. Steele, Solid State Ionics 7(1982)75.
- [3] K.M. Kim, K.S. Ryu, S.G. Kang, S.H. Chang, I.J. Chung, Macromol. Chem.. phys., 202(2001)866.
- [4] F. Croce, G.B. Appetecchi, L. Persi, B. Scrosati, Nature 394(1998)456.

1.29 Stable nanofibrous poly (aryl sulfone ether benzimidazole) membrane with high conductivity for high temperature PEM fuel cells

P. Muthuraja^{a#}, S. Prakash^{a#}, V. Sethuraman^a, P. Manisankar^{a*}

^a Polymer Materials Laboratory, Department of Industrial Chemistry, Alagappa University, Karaikudi-630006, India.

[#] These authors contributed equally to this work.

*Tel: +91 4565 228836, Fax: +91 4565 225202,

E-mail: manisankarp@alagappauniversity.ac.in

Abstract

Novel electrospun nanofiber poly (aryl sulfone ether benzimidazole) (SO₂-OPBI) membrane was synthesized for improve the proton conductivity and chemical stability. Incorporation of the flexible aryl sulfone- and ether-linkages in the polymer backbone can be improved the physico-chemical properties of membranes. We made different types of membranes, namely dense SO₂-OPBI membrane, nanofiber SO₂-OPBI and *m*-PBI membrane and evaluated their physico-chemical properties for suitability application of high temperature PEM fuel cells. Interestingly, the nanofiber membranes possessed a greatly increased proton conductivity (0.0667 S cm^{-1} at 160 °C and acid doped level of 338%), which is comparable to that of the dense membrane (0.033 S cm^{-1} at 160 °C and 221% acid doping). The nanofiber and dense membrane shows good oxidative stability under Fentons reagent.

Keywords: Fuel cells, High-Temperature, Poly(aryl-sulfone-ether benzimidazole), Proton Conductivity



1.30 Corrosion behavior of Zn/Graphene composite in aqueous electrolyte system

K.Saminathan^{a*}, M. Selvam^b, R.Sathiyamoorthi^c and P. Saha^d

^aDepartment of Chemistry, Kongunadu Arts and Science college, Coimbatore

^bCentre for NanoScience and Technology, K S Rangasamy College of Technology, Tiruchengode –637215, Tamil Nadu.

^cN.S.N College of Engineering and Technology, karur, 639004, TN,

^dDepartment of Ceramic Engineering, National Institute of Technology, Rourkela, Odisha-769008, India,

ABSTRACT

In the present study, the electrochemical corrosion behavior of zinc (Zn) and thin layer of graphene on Zn (ZnG) in different salt electrolyte such as NaCl, KCl and Na₂SO₄ are report. The phase structure and Crystallinity is investigate using X-ray diffraction, Surface morphology and purity of the sample is investigate using Scanning Electron Microscopy and Energy dispersive X-ray analysis (SEM/EDAX) and Raman spectroscopy. The electrochemical corrosion behavior of the Zn and graphene coated on Zn are also investigated using Electrochemical Impedance Spectroscopy (EIS) analysis. The tafel slop and Nyquist plot confirms that ZnG shows better corrosion resistance and lower corrosion rate in KCl solution compare to all other electrolytes which is performed in Zn.

Key words: Graphene, Electrochemical techniques, Composite materials, Corrosion Test, Surface properties, Electron microscopy

Corresponding Author E-mail: ksaminath@gmail.com

1.31 Enhancement of Discharge Capacity of Mg/MnO₂ Primary Cell with Nano α -MnO₂-Graphene as Cathode

K.Saminathan^{a*}, M. Selvam^b, R.Sathiyamoorthi^c and P. Saha^d

^aDepartment of Chemistry, Kongunadu Arts and Science college, Coimbatore

^bCentre for NanoScience and Technology, K S Rangasamy College of Technology, Tiruchengode –637215, Tamil Nadu,

^cN.S.N College of Engineering and Technology, karur, 639004, TN

^dDepartment of Ceramic Engineering, National Institute of Technology, Rourkela, Odisha-769008, India,

*Corresponding Author E-mail: ksaminath@gmail.com

ABSTRACT

In the present study, pristine \square -MnO₂ and graphene mixed with nanoparticles \square -MnO₂-based cathode were prepared and their electrochemical performances were studied in a magnesium/manganese dioxide-graphene (Mg/ \square -MnO₂-graphene) primary battery cell. The discharge measurements of the modified Mg/MnO₂ cell were analyzed using galvanostatic constant current (1, 5 and 10 mA) discharge with the cutoff voltage of 0.2 V. The discharge capacity of α -MnO₂ based cathode was 20, 46 and 73 mAhg⁻¹ respectively at 1, 5, 10 mA constant current, respectively. Similarly the discharge capacity of α -MnO₂-graphene based cathode was 68, 308 and 271 mAhg⁻¹, respectively. Moreover, the discharge capacity of cathode based on α -MnO₂-graphene increased three times compared to α -MnO₂ based electrode. The present work unveils that graphene- \square -MnO₂ based cathode is suitable for primary magnesium battery application.

KEYWORDS: Nanoparticles, Graphene, Cathode Material, Discharge Capacity, Modified Mg/MnO₂ Primary Cell.



1.32 Enhanced capacitance behaviour CuS@Cu(OH)₂ Binary nanocomposite for Supercapacitors Applications

P. Naveenkumar and G. Paruthimal Kalaignan*

Advanced Energy Technology Laboratory, Department of Industrial Chemistry, Alagappa University, Karaikudi-630 003, Tamilnadu, India.

Email id: naveenperumal@yahoo.com & pkalaignan@yahoo.com

Transition metal sulfides (e.g., CuS, NiS, CoS, and VS) have been considered as one of the most promising pseudocapacitor materials with respect to their specific capacitance and cost effectiveness [1-2]. In the recent past, CuS have been extensively investigated due to their good electronic conductivity and high energy capacitance [3-5]. In this work, we have prepared CuS@Cu(OH)₂ by one pot hydrothermal method using a mixture of solvent in 1:3 ratio of water and ethylene glycol at 180°C for 24 hours. The bare CuS was prepared without addition of the Sodium hydroxide in hydrothermal method. The final product was filtered and washed several times in water and ethanol. The washed product was dried at 60°C temperature. The phase purity of the synthesized samples was confirmed by XRD. The surface morphology of the samples was identified by SEM with EDAX and TEM. Electrical conductivity of the samples at room temperature was determined by using a conventional four-probe method on pressed pellets, formed under a pressure of 20 MPa with a diameter of 10 mm. The electrochemical performances were measured in typical three-electrode cell system consist of 1M KOH electrolyte using the as-prepared electrodes as working electrode, Platinum and Hg/HgO as counter and reference electrodes respectively. Cyclic Voltammetry was examined in the potential window of -0.5 to 1.0V at 5 to 100 mVs⁻¹, Galvanostatic Charge/Discharge tested different current rate and their cycle life, and Electrochemical Impedance Spectroscopy were carried out in 10kHz ~ 0.1 Hz using a sinusoidal signal of 5 mV at open circuit potential.

Key Words: CuS@Cu(OH)₂ and Nanocomposite.

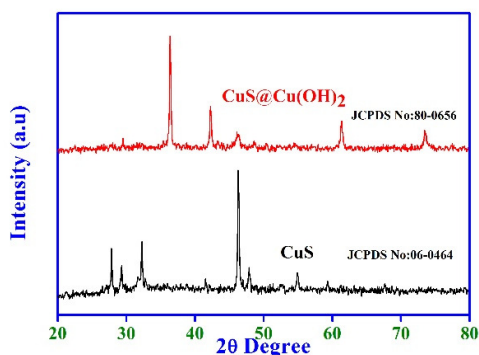


Figure 1 shows the XRD results of the synthesized CuS and CuS@Cu(OH)₂.

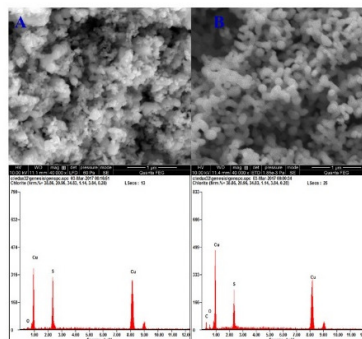


Figure 2 shows the SEM images with EDAX Spectrum of A) CuS and B) CuS@Cu(OH)₂.

References

- [1] X. Rui, H. Tan, Q. Yan, *Nanoscale* 6 (2014) 9889–9924.
- [2] Y.-W. Lee, B.-S. Kim, J. Hong, *J. Mater. Chem. A* 4 (2016) 10084–10090.
- [3] C. Feng, L. Zhang, G. Liu, *ACS Appl Mater Interfaces* 7 (2015) 15726–15734.
- [4] Y.-K. Hsu, Y.-C. Chen, Y.-G. Lin, *Electrochimica Acta* 139 (2014) 401–407.
- [5] D. Yuan, G. Huang, F. Zhang, D. Yin, L. Wang, *Electrochimica Acta* 203 (2016) 238–245.



1.33 Synthesis of Mn₂O₃ nanomaterials for high-performance asymmetric supercapacitor applications

Srinivasan Alagar, Rajesh Madhuvilakku and Shakkthivel Piraman*

Sustainable Energy and Smart Materials Research Lab, Department of Nanoscience and Technology, Science Campus, Alagappa University, Karaikudi-630 002, Tamil Nadu, India.
 Email: apsakthivel@yahoo.com

Manganese oxide (Mn₂O₃) has emerged as a new and promising pseudocapacitive material due to its prominent valance states. In the present study, cubic Mn₂O₃ nanostructures have been prepared *via* hydrothermal method employing isopropanol and non ionic surfactant. Glycerol ensures a slow rate of hydrolysis to form small size Mn₂O₃ nanostructures. The crystal structure of the Mn₂O₃ nanomaterials were conformed through X-ray diffraction and the fourier transform infrared spectroscopic (FT-IR) analysis confirmed the presence of (O-Mn-O-Mn-O) bond exhibiting functional groups. The surface of nanostructured materials and their structures were confirmed by using the scanning electron microscopy and transmission electron microscopy studies. Further, the electrochemical characteristics of the Mn₂O₃ were studied and it shows higher specific capacity with an excellent rate capability and cycleability. When the charge/discharge current density increased from 0.5 to 5 A g⁻¹ the reversible charge capacity was decreased from 540 F g⁻¹ to 135 F g⁻¹ while 100% capacity retention at a high current density of 5 A g⁻¹ even after 1000 cycles could be achieved. Furthermore, the asymmetric supercapacitor based on Mn₂O₃ exhibited a significantly higher energy density of 45.6 Wh kg⁻¹ at a power density of 187.5 W kg⁻¹ with good cyclic stability. This electrochemical result highlighted the suitability of the Mn₂O₃ nanostructure electrode material for supercapacitor applications.

Keywords: Supercapacitor, Mn₂O₃ nanoparticles, specific capacity, power density, energy density,

References

- [1] Z. Wang, F. Wang, Y. Li, J. Hu, Y. Lu and M. Xu, *Nanoscale*, 2016, **8**, 7309–7317.
- [2] S. Chen, G. Yang, Y. Jia and H. Zheng, *J. Mater. Chem. A*, 2017, **5**, 1028–1034.
- [3] W.-B. Zhang, L.-B. Kong, X.-J. Ma, Y.-C. Luo and L. Kang, *New Journal of Chemistry*, 2014, **38**, 3236.

1.34 Nanostructured Zr substituted LiNi_{1/3}Mn_{1/3}Co_{1/3}O₂ as a cathode material for high- Energy lithium-ion battery

K. Kalaiselvi^a, G. Paruthimal Kalaignan^{a,*}

^aDepartment of Industrial Chemistry, Alagappa University, Karaikudi – 630 003, India
 Corresponding author mail id : pkalaignan@yahoo.com

Lithium-ion batteries are recognized as the most promising energy storage technology for electric vehicles (EVs) and hybrid electric vehicles (HEVs) in the next decades. To meet the requirements of EVs and HEVs, Li-ion batteries need to possess the following characteristics: low cost, large energy intensity, high rate capability, long cycle life, and nontoxic Rechargeable lithium-ion batteries are widely employed for electronic gadgetry with high capacity and long cycle life. Zr substituted cathode materials were synthesized by sol–gel method. The physical and electrochemical properties of the synthesized materials were characterized by using TG/DTA, XRD, SEM, TEM, XPS, cyclic voltammetry, charge/discharge and electrochemical impedance spectroscopy techniques. The cycling behaviours of Zr substituted LiNi_{0.33}Mn_{0.33}Co_{0.33}O₂. Cathodes were evaluated with various discharge rates between 4.2 and 2.8V. The effects of doping on the structural and electrochemical properties were investigated in detail.

XRD analysis indicated that all the prepared samples were mainly belong to cubic crystal form with Fd3m space group.



SEM analysis shows that $\text{LiNi}_{0.33}\text{Mn}_{0.33}\text{Co}_{0.33-x}\text{Zr}_x\text{O}_2$ has smaller particle size and more regular morphological structure than those of $\text{LiNi}_{0.33}\text{Mn}_{0.33}\text{Co}_{0.33}\text{O}_2$. Zr substituted $\text{LiNi}_{0.33}\text{Mn}_{0.33}\text{Co}_{0.33}\text{O}_2$ cathode has improved the structural stability, high-capacity retention, better elevated temperature performance and excellent electrochemical performances of the rechargeable lithium-ion batteries. Figure 1. Shows the cyclic performances of cells in the voltage range of 2.8-4.2 V at room temperature. At first cycle, cells were charged and discharged at C/10 (0.14 mA/cm²) and at the following cycles at 1C (1.4 mA/cm²). The initial discharge capacities of 117, 110, 100 and 92mAh/g were obtained with increasing 0.5C, 1C, 5C, and 10C in Zr Substitutes $\text{LiNi}_{1/3}\text{Mn}_{1/3}\text{Co}_{1/3}\text{O}_2$. small amount of Zr substitution in has developed the structural stability, rate capability and cycling performances of the cathode materials for the rechargeable lithium-ion batteries.

Key word: Sol-gel method, XRD, SEM, Charge / discharge

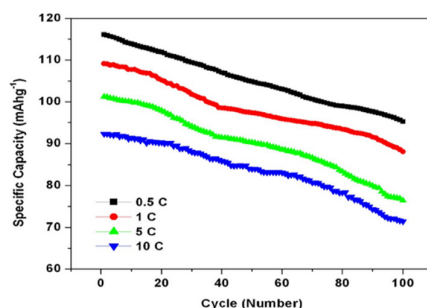


Figure1. Cyclic Performance of $\text{LiNi}_{1/3}\text{Mn}_{1/3}\text{Co}_{1/3}\text{O}_2$ cell cycled between 2.8 and 4.2 v at different discharge rates at elevated temperature

References:

- [1] Z. Lu, D. D. MacNeil, J. R. Dahn, *Electrochem. Solid-State Lett.* 2001.
- [2] W. B. Luo, J. R. Dahn, *J. Electrochem. Soc.* 2011.

1.35 Preparation and Analysis of thermoelectric thin films at different coating cycles

A. Amali Roselin^a, N. Anandhan^{a*}, R. Priyatharshinin^a, M. Karthikeyan

^a *Advanced Materials and Thin Film Laboratory, Department of Physics, Alagappa University, Karaikudi-630 003, India.*
Presenting author email: amaliroseline86@gmail.com

Abstract

In this study, we deposited Bismuth Selenide (BSO) thin films on glass substrate using sol-gel spin coating technique at different coating cycles. The structural, optical, luminescent properties and surface morphology of BSO thin films are examined using X-ray diffraction (XRD), UV-Visible spectroscopy (UV-Vis) and Photoluminescence spectroscopy (PL) and Scanning Electron Microscopy (SEM). From the X-ray diffraction analysis, the thin films are found to be a body center cubic structure with a preferential growth along the (310) and (321) plane. UV-Vis spectra revealed the decreasing percentage of transmittance from 82 to 70 while increasing the number of coating cycles. The band gap values of the prepared thin films are also found to decrease from 3.8eV to 3.5eV. Photoluminescence spectra of BSO thin films showed strong yellow emission peak at 575nm under the excitation of 405 nm due to electron-hole recombination. Surface texture of the prepared films was noticed by means of Scanning Electron Microscopy (SEM). In addition, we also described the correlation between crystallite size and optical band gap energy with different number of coating cycles of the prepared BSO thin films.

Keywords: BSO thin films, Spin coating.



Graphical representation

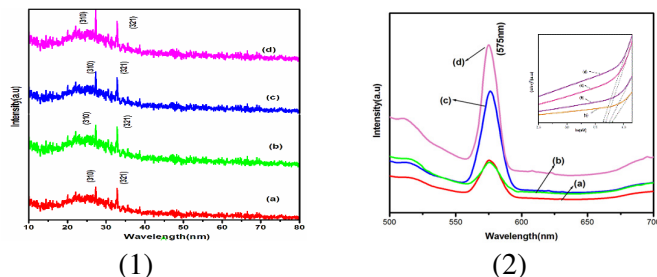


Fig (1) indicates the XRD diffraction pattern and (2) indicates the PL spectra and band gap of the prepared BSO thin films at different number of coating cycles.

References

- [1] Xiaoxing Zhu, Jianjun Xie, Debao Lin, Fang Lei, Yali Wang J.Alloys.Comp., 582 (2014) 33-36.
- [2] Gonggong Lu, KehuiQiu, YunleiBu ,XiluHou, XiqiangYuan, ICMCCCE, 308 (2015) 2830-2835.
- [3] Junfeng Li, Wentao Zhang, Xiang Yuan, KehuiQiu, J.Bio.Chem., 32 (2016) 93-99.

1.36 A case study on Sol-gel Spin coated Rare Earth Doped ZnO thin films

S. Fathima Thaslin^a, N.Anandhan^a, A.Amali Roselin^a, M. Karthikeyan^a

^aAdvanced Materials and Thin Film Laboratory, Department of Physics, Alagappa University, Karaikudi- 630 003, India.
Presenting author email: fathisareef@gmail.com

ABSTRACT

In the present work, we report the pure and Dysprosium (Dy) doped Zinc oxide ZnO thin films were grown on glass substrates using Sol-Gel spin coating at 3000rpm for 30s and annealed at 450°C. The structural, optical, luminescent and morphological properties of the prepared films were characterized by X-ray diffraction (XRD), Ultra -Visible spectroscopy (UV-Vis), Photoluminescence spectroscopy (PL) and Scanning Electron Microscopy (SEM). XRD pattern revealed that prepared films are polycrystalline with hexagonal Wurtzite structure and the film crystallites are preferentially oriented along (101), (002) and (100) plane. The PL spectra of ZnO and Dy doped films showed the peak at 384nm (violet emission) is more intense than the peaks at 432nm, 413nm (violet emission) and 500nm (blue emission). All the prepared films exhibited good optical transparency at the wavelength of above 450 nm in the visible region and the optical band gap decreasing from 3.22eV to 3.02eV with increasing doping concentration. Morphological properties of the films are also investigated using Scanning Electron Microscopy technique.

Keywords: Sol-gel spin coating method, Zinc Oxide thin film , Dysprosium doped ZnO thin film

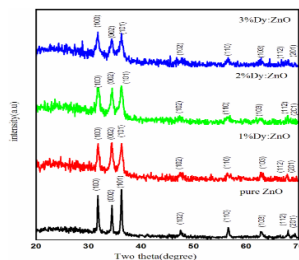


Fig.1.

Fig.1. XRD Pattern of ZnO and Dy doped Thin films;

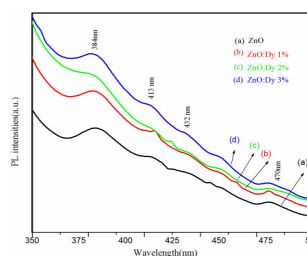


Fig.2

Fig.2. Luminescent spectra of Pure and Dy doped Thin film



References

- [1] Oranuch Yayapao, Titipun Thongtem, Anukorn Phuruangrat., J.Alloys Compd., 576,(2013) 72-79.
- [2] C. Jayachandriah, K. Siva Kumar, G. Krishnaiah, J.Alloys Compd., 623, (2015), 248-254.
- [3] J. Arul Mary, J. Judith Vijaya, M. Bououdina, Phys.B, 456 (2015), 344-354.

1.37 Synthesis of Nanostructured NiCo₂O₄ by Hydrothermal Route for Supercapacitor Applications

K. Uma Maheswari, R. Dhilip Kumar, C. Karthikeyan and S. Karuppuchamy*

*Department of Energy Science, Alagappa University, Karaikudi-630 003, Tamilnadu, India
Email: skchamy@gmail.com and skchamy@alagappauniversity.ac.in*

Abstract

Supercapacitor is an energy storage device that has attracted a much attention due to its superior characteristics such as expanded life time, higher energy density and high power density. Conducting polymer is a promising electro-active material for supercapacitor applications. However, it has less stability and durability. Nanostructured metal oxides especially transition metal oxides are also attracting as a potential candidates for the supercapacitors due to their enhanced optical, mechanical, chemical stability and electrical properties. Among the nanostructured metal oxides, NiO and Co₂O₄ reveal many polymorphs with unique properties and wide applications such as supercapacitors, photocatalysis and sensors. Recently, Scientists have developed bimetal oxides especially nickel cobalt oxide (NiCo₂O₄) for supercapacitor applications. This material has been showing excellent performance as an electro-active material for supercapacitor applications. In the present work, we synthesized nanostructured NiCo₂O₄ by hydrothermal route and subsequently physicochemical characterization was carried out. The XRD pattern revealed the formation of cubic phase NiCo₂O₄ powder. The prepared NiCo₂O₄ nanopowder was coated on nickel (Ni) foam to serve as a working electrode in electrochemical test. The electrochemical behavior of the NiCo₂O₄ powder coated electrodes was investigated using electrochemical impedance spectroscopy (EIS), cyclic voltammetry (CV) and galvanostatic charge-discharge (GCD) techniques. The performance of supercapacitor results will be reported.

Keywords: Hydrothermal, nickel cobalt oxide, nanopowder and supercapacitor.

1.38 Development of inorganic hole conductor for highly efficient perovskite solar cells

R. Dhilip Kumar^a, Vibha Saxena^b, G. Murugadoss^c, R. Thangamuthu^c and S. Karuppuchamy^{a*}

^a*Department of Energy Science, Alagappa University, Karaikudi, Tamil Nadu-630 003, India*

^b*Technical Physics Division, Bhabha Atomic Research Centre, Trombay, Mumbai-400085, India*

^c*Electrochemical Materials Science Division, CSIR-Central Electrochemical Research Institute, Karaikudi, Tamil Nadu.*

E-mail: skchamy@gmail.com and skchamy@alagappauniversity.ac.in

Abstract

The need for renewable energy is rising tremendously due to global warming issues. The energy demanding activities usually initiate the greenhouse effect and exhaust the conventional energy resources. Energy which arrives from natural resources for instance geothermal, wind, tides and sunlight are attracting due their renewable nature and eco-friendly. Today, renewable energy obtained particularly from sunlight is showing enormous interest due to its abundant availability. The different types of solar cells are available, but exclusively silicon solar cells are sold in the market. The crystalline silicon solar cell is often referred as the first generation photovoltaic technology; which produces the high efficiency approximately 24 %. Second and third generation solar cells are not able to overcome the first generation solar cell. It is necessary to produce low cost solar cells with high efficiency in order to use the rural and tribal people.



Recently, researchers are developing the perovskite solar cells due to its low cost and high efficiency. The perovskite solar cells are suffering from the stability issues. Moreover, expensive organic hole conductors are used in perovskite solar cells which prevent the practical applications. For instance, the current marketable price of high purity spiro-OMeTAD is over ten times that of Pt and Au. Therefore, alternative low cost hole conductors are required to use in perovskite solar cells. The inorganic copper based p-type semiconductors are right choice for developing perovskite solar cells with low cost. In this study, we report the perovskite solar cell using copper thiocyanate (CuSCN) as the hole conductor. CuSCN was selected due to its suitable valance band position and good conductivity. The perovskite solar cell performance was carried out using solar simulator unit and the results will be discussed.

1.39 ELECTROCHEMICAL DETERMINATION OF 3-NITRO – 1, 4-DIHYDRO-1,2,4-TRIAZOL-5-ONE USING GLASSY CARBON ELECTRODE

B. Kavitha^a, N. Senthil Kumar^b and H. Gurumallesh Prabu^c

^a Department of Chemistry, Sri Ranganathar Institute of Engineering and Technology, Coimbatore, Tamilnadu.

^b Department of Chemistry, Arignar Anna Government Arts College, Cheyyar, Tiruvannamalai, Tamilnadu.

^c Department of Industrial Chemistry, Alagappa University, Karaikudi, Tamilnadu.

ABSTRACT

In recent years identification and quantification of traces of explosives has constituted an emerging and important topic. The interest due to their relevant role in many areas concerning the security and health of the population, including environmental and toxicological effects, land mine detection and prevention of terrorist attacks [1]. A nitro compound like 3-Nitro – 1, 4-dihydro-1,2,4-triazol-5-one(NDTO) during explosion forms harmful products which are carcinogenic in nature.

Explosive like NDTO was detected by various techniques like TGA, DSC [2] and chromatography. Voltammetry is the one of the powerful to detect explosive compounds. The voltammetric behaviour of NDTO was studied using glassy carbon in different pH media (1.7 and 13.0). Among the pH studies, pH 1.0 on glassy carbon electrode showed good peak response at a potential of -0.2 V (reduction peak). Based on cyclic voltammetric studies differential pulse voltammetry (DPSV) and square wave stripping voltammetry (SWSV) response were studied for analytical purpose. In DPSV techniques, different parameters like Accumulation Potential, Initial Scan Potential, Pulse Amplitude, Potential Increment, Pulse Period, Pulse Width and Accumulation Time were carried out. In SWSV techniques, different parameters like Accumulation Potential, Initial Scan Potential, Square Wave Amplitude, Potential Increment, Frequency and Accumulation Time were carried out.

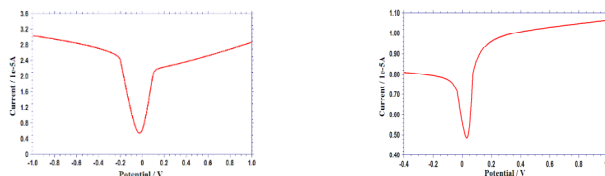
Optimized values obtained in DPSV and SWSV techniques of NDTO are given in Table 1 and the voltammograms obtained under optimized DPSV and SWSV of NDTO are given in Fig 1.

Table 1: Optimum parameters obtained in stripping voltammetry

Mode	Parameter	Range Examined	Optimum Value
DPSV	Accumulation potential (E_{acc}), V	-1.50 to +1.50	1.0
	Initial scan potential (E_{is}), V	0.50 to 0.1	0.4
	Pulse amplitude (PA), V	0.01 to 0.20	0.05
	Potential Increment (PI), V	0.001 to 0.005	0.002
	Pulse period (PP), s	0.04 to 0.20	0.08
	Pulse Width (PW), s	0.02 to 0.10	0.04
	Accumulation time (t_{acc}), s	20 to 100	20
SWSV	Accumulation potential (E_{acc}), V	-1.50 to +1.50	1.0
	Initial scan potential (E_{is}), V	0.50 to 0.1	0.4
	Square wave amplitude (SWA), V	0.01 to 0.20	0.04
	Potential Increment (PI), V	0.001 to 0.005	0.005
	Frequency (FR), Hz	2 to 10	4
	Accumulation time (t_{acc}), s	20 to 100	20



Figure 1: (a) DPSV (b) SWSV Voltammogram of NTO under optimized condition.



References

- [1] A.M. Jimenez, M.J. Naval, J. Hazard. Mater., 106A (2004) 1.
- [2] Gregory T, Long, Brittany A, Brems, Charles A, Wight, J. Phys. Chem., B 106(2002)4022.

1.40 *In-situ* generation of Pt based nanocatalysts on conducting polymer support by Galvanic Displacement Reaction route and its electro-(chemical) catalytic applications

C. Mathi and C. Sivakumar

*Electrode and Electrocatalysis Division
CSIR-Central Electrochemical Research Institute, Karaikudi-630 006
India*

E-mail: ccsivakumar@cecri.res.in

Abstract:

Conducting polymers have been employed significantly to synthesize the nanomaterial for the reason that of its low cost and easy process ability which boosted its utilization in the field of chemical or Electrocatalysis, drug delivery, sensor and so on. In addition incorporation of precious or non precious metal nanoparticles also enhances its electro-catalytic activity, sensing capability and electro transfer kinetics etc. Here in we report the *in-situ* generation of Pt based nanocatalysts on conducting polymer support namely polyaniline (PANI) by three step synthetic procedures. First, PANI has been synthesized by Chemical oxidative polymerization route. In the second step, PVP/CTAB capped Cu nanoparticles was achieved by mixing of metal precursor salt solutions with reducing agent like NaBH₄. In the third step, *in-situ* generation of PVP or CTAB capped CuPt-PANI attained by adopting galvanic displacement reaction route. Similarly Ag-poly(2,5-dimethoxyaniline) (PDMA) nanocomposites was synthesised by Rapid mixing polymerization route. AgPt-PDMA nanocomposite was succeeded by adopting galvanic displacement reaction route. The resulting PVP/CTAB capped PANI nanocomposites were subjected to examine or tested for methanol oxidation reaction in aqueous acidic medium. Ag-PDMA and AgPt-PDMA nanocomposites were examined for the chemo-selective reduction of 4-nitrophenol. The structural and surface morphology of the synthesized nanocomposites were characterized by various tools like FT-IR, XRD, SEM and TEM. The electrochemical behaviour and electrocatalytic activity of PVP/CTAB capped CuPt-PANI modified glassy carbon electrode was characterized by cyclic voltammetry (CV) and chronoamperometry (CA) methods in an aqueous 0.5 M H₂SO₄. The PVP/CTAB capped CuPt-PANI electrode showed an improved electrocatalytic performance towards the methanol oxidation. The enhanced electrocatalytic activity might be due to the uniform distribution of CuPt nanocatalysts and the synergistic effect between CuPt nanocatalysts and PANI support. Further Ag-PDMA nanocomposite was tested towards the chemical reduction of 4-nitrophenol to 4-aminophenol and the catalytic reduction process was monitored by UV-Visible spectroscopy.

Key words: CuPt-PANI and Ag-PDMA nanocomposites, FE-SEM, XRD, FT-IR, CV and UV-Visible spectroscopy.



1.41 Nanostructural modified glassy carbon electrode utilized for voltammetric determination of ibuprofen

E. Suresh^a, K. Sundaram^a, B. Kavitha^b, N. Senthil Kumar^c

^a Department of Chemistry, Karpagam University, Karpagam Academy of Higher Education, Coimbatore, Tamil Nadu,

^b Department of Chemistry, Sri Ranganathar Institute of Engineering and Technology, Coimbatore-641 110, Tamil Nadu,

^c Department of Chemistry, Arignar Anna Government Arts College, Cheyyar-604 407, Tiruvannamalai (Dt.), Tamil Nadu,

Presenting author's e-mail: unibct@yahoo.com

Abstract

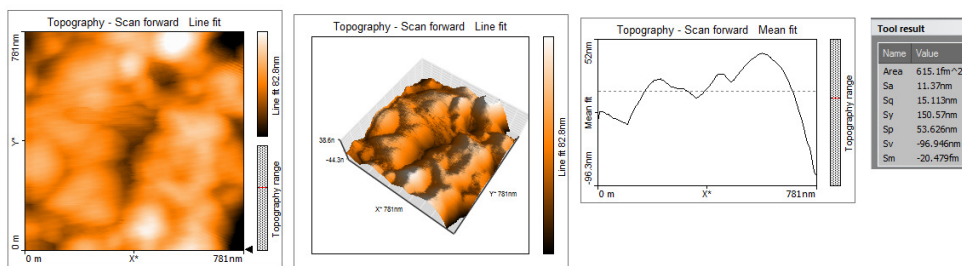
All the voltammetric measurements were carried out using polyaniline/Ag modified glassy carbon electrode as the working electrode, Ag/AgCl₃ mol L⁻¹ KCl as the reference electrode and platinum wire as an auxiliary electrode. Electroanalytical methods are simple, economical, rapid and sensitive to reach the lower limit of detection. Among the electro-analytical techniques, voltammetry coupled with pulse waveform is considered a highly sensitive technique with very low detection profiles attributed to zero background current. The effect of pH was studied at different medium such as pH 1.0 to pH 13.0. The cyclic voltammogram of 300 ppm ibuprofen in pH 1.0 on polymer film modified electrode exhibits a single well defined anodic peak in the potential range -0.5 to 1.8V. The electroanalytical parameters of the biosensors are highly dependent on their configuration and on the dimensions of the carbon electrode. The best limit of detection obtained for ibuprofen was 10 ppb and the linear range from 20 to 200 ppb on GCE configuration (Table 1). The biosensors were successfully applied for the detection of ibuprofen in several drug formulations.

The polymer/Ag film is uniformly coated on the electrode surface and forms a nanorod -like porous reticulated morphology. The compound adsorbed surface exhibits granular adsorbed nanosize rod like photographs. This surface morphology accounts for the finding that the active surface area of the composite electrode is 5 times greater than the geometric area. The polymer film is uniformly coated on the electrode surface and forms a nanorod -like porous reticulated morphology. The compound adsorbed surface exhibits granular adsorbed nanosize rod like photographs (Fig 1). This surface morphology accounts for the finding that the active surface area of the composite electrode is 5 times greater than the geometric area.

Table 1. Optimum experimental conditions in DPSV

Variable	Range studied	Optimum value
pH	1-13	1.0
Accumulation potential (V)	0.1 to 0.6	0.6
Accumulation time (Sec)	10-60	5
Initial scan potential (V)	-0.5 to 0.3	0.1
Pulse Height (PH) (mV)	25 to 150	50
Pulse width (PW) mSec	25 to 150	50
Scan Increment (SI) mV	2 to 20	4
Scan rate (SR) mV/sec	10 to 100	50
Stirring rate (rpm)	50 to 250	250
Rest period (Sec)	2 to 10	5

Fig. 1. AFM behavior of ibuprofen adsorption on PANI/Ag/GCE



1.42 MICROBIAL FUEL CELL ASSISTED DISPOSAL OF PHOSPHATE SORBED RICE HUSK BIOCHAR.

Krishnaveni, M. Jayalakshmi and A.N. Senthilkumar*

*PG & Research Department of Chemistry, Alagappa Government Arts College,
Karaikudi – 630 003, Tamil Nadu, India.*

**ansent@gmail.com*

1. Introduction

Biochar is a pyrolysis derived carbonaceous material from biomass in limited supply of oxygen. Biochar serves as an excellent sorbent material for removing environmental contaminants. The discharge of phosphate from various sources causes eutrophication and other related problems [1]. It is most essential to develop an effective technology for removing phosphate from aqueous solutions [2]. Biochar derived from rice husk (RHB) can act as a promising candidate for phosphate removal. Hence a study was planned to investigate an adsorption process using phosphate as adsorbate and RHB as adsorbent. Phosphate adsorbed RHB may pose environmental concerns and subsequently the work was extended for disposing the RHB absorbed phosphate through microbes in microbial fuel cell (MFC).

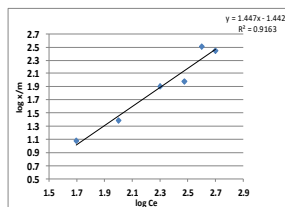
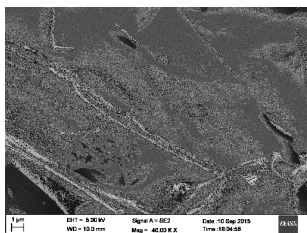
2. Experimental Techniques

Rice husks were collected from in and around rice mills of Pudukkottai block of Karaikudi town. The collected husks were dried in mild sunlight for 5 days and then massacrated into powder for slow pyrolysis process whose yield was 47 %. Surface functional group of RHB was analysed by Fourier transform infrared (FT-IR) spectrometer of Bruker Optik GmbH make. Scanning electron microscopy (SEM) was done by using Hitachi, Japan instrument to investigate the surface morphology of RHB. The phosphate absorbing capacity of RHB was assessed by the ascorbic acid method [3]. The obtained results were fitted into standard isotherms. The phosphate adsorbed RHB was disposed in soil microbial fuel cell constructed using 150 mL glass beaker. Soil (100 g) was moisturised with 50 mL of distilled water. Mild steel anode was buried at the bottom of the beaker using moisturized soil and mild steel cathode was allowed to float in the distilled water over packed soil. Soil bacteria served as MFC mediators. Two similar MFC were constructed and one out of it was packed with 5 g of RHB used for phosphate adsorption from aqueous solution of 50 ppm concentration and another one served as control. The open circuit potential offered by the two MFC's were measured using digital multimeter individually.

3. Result and Discussion

FTIR spectroscopy of RHB showed 3 important characteristics peak. A band at 3452 cm^{-1} proves the existence of hydroxyl group. The band at 1629 cm^{-1} corresponds to amide and amine functional group. A well stretched band at 1098 cm^{-1} is attributed to C-O vibrational stretching frequency of aliphatic ethers. Thus hydroxyl, amide, amine and aliphatic ethers are present in the RHB. Surface morphology presented in Figure 1 depicts macro porosity of RHB which were resulted due to volatilization of organic compounds. The experimental values obeyed with Freundlich isotherm as evidenced from Fig.2 ($R^2=0.923$). Hence RHB provides heterogeneous site for phosphate adsorption in non-uniform layer with reversibility [4]. The free energy of adsorption ($\Delta G_{ads} < -20\text{ kJ}$) calculated from equilibrium constant (K_c) values showed physical mode of phosphate adsorption on RHB. Open circuit potential discharged by MFC containing RHB lasted steadily for 24 days and then falls steeply. Control MFC offered a low potential value (around 120 mv) and delivered potential up to 15 days. Higher potential offered by MFC with RHB was due to absorbed phosphate nutrient.





4. Conclusions

Figure 1: SEM micrographs of Rice Husk Biochar.

Figure 2: Freundlich adsorption isotherm for phosphate on RHB

The study concluded that RHB effectively adsorbs phosphate from synthetic aqueous solution obeying Freundlich adsorption isotherm. The calculated free energy of adsorption supported physical mode of binding between RHB and phosphate. The adsorbed phosphate was disposed in MFC with subsequent power generation.

5. References

- [1] D.S. Bhargava, S.B. Sheldarkar, Use of TNSAC in phosphate adsorption studies and relationships- literature, experimental methodology, justification and effects of process variables, *Water Res.* 27 (1993) 303–312.
- [2] C.P. Huang, Removal of phosphate by powdered aluminum-oxide adsorption, *J. Water Pollut. Control Fed.* 49 (1977) 1811–1817.
- [3] S.R.Olsen, L.E.Sommers, Phosphorus. In: Page, A.L., Miller, R.H., Keeney, D.R. (Eds.), In: *Methods of Soil Analysis, Part 2: Chemical and Microbiological Properties.* Agronomy Monograph 9, ASA and SSSA, Madison, WI, USA.1982
- [4] Hu Tang, Weijie Zhou, Lina Zhang, Adsorption isotherms and kinetics studies of malachite green on chitin hydrogels, *J. Hazardous Materials*, 209-210 (2012) 218-225.

1.43 Studies on Synthesis, Structure and Characterization of Nd₂Mo_{2-x}In_xO₉ Oxide ion Conductor for Solid Oxide Fuel Cell Application

N.Kalaivania, M.Rajasekharb*

^{a,b*} *Advanced Energy Research Lab, PG& Research Department of chemistry, Government Arts College, Dharmapuri-636 705, South India.*

Abstract

Nd₂Mo_{2-x}In_xO₉ (0 ≤ x ≤ 0.5) oxide ion conductor powders are synthesized with Nd(NO₃)₃, In(NO₃)₃, (NH₄)₆Mo₇O₂₄, and aspartic acid (fuel) by assisted combustion method which heating at 550 °C for 6 hours. X-ray diffraction analysis indicates that the structure of Nd₂Mo_{2-x}In_xO₉. Scanning electron microscopy is used to identify the surface morphology. The particle size of the synthesized product is measured by Scherrer equation and by using a transmission electron microscope. The influence of the Indium substitution for Mo in Nd₂Mo₂O₉ of the phase transition has been investigated by DTA. The formation of Nd₂Mo_{2-x}In_xO₉ is confirmed by FTIR studies. The Arrhenius plot shows the ionic conductivity on the variation of temperature. These results indicates that assisted combustion method is a promising method to prepare nanocrystalline Nd₂Mo_{2-x}In_xO₉ oxide ion conductor for solid oxide fuel cell.

KEYWORDS: Ionic conductivity, Scanning Electron Microscopy, Transmission Electron Microscope, Thermal Analysis, X-ray diffraction.



1.44 Label Free Microfluidic Electrochemical Biosensor for Aflatoxin B1 in Rice

S. Viswanathan^{a,b*}, Cristina Delerue-Matos^b, C. Rani^c

^a Department of Industrial Chemistry, Alagappa University, Karaikudi - 630003, Tamilnadu.

^b REQUIMTE - Instituto Superior de Engenharia, Instituto Politécnico do Porto, 4200-072 Porto, Portugal.

^c Department of Chemistry, Alagappa Govt. Arts college, Karaikudi - 630003, Tamilnadu.

Contact: email: rsviswa@gmail.com

Due to the warm and favourably humid climate of southern India, the rice is one of the most important crops. The protection against crop damage caused by fusarium and Aspergillus species is essential. Aflatoxin B1 (AFB1) is considered the most toxic and is produced by both Aspergillus flavus and Aspergillus parasiticus. Aflatoxins have caused much harm to human and animal health due to their toxicity and carcinogenicity. It is estimated that about 4.5 billion people are chronically exposed to Aflatoxins. Since it is impossible to reverse its carcinogenic effects, the identification and prevention of human exposure to aflatoxins have become a major research topic in the area of food science. Therefore, effective detection of AFB1 in food products is indispensable for ensuring that the products offered meet regulatory and market requirements. We have therefore investigated to develop sensitive microfluidic electrochemical immunosensor for the detection of AFB1. In this work microfluidic channel was made from polydimethylsiloxane and this integrated with gold nanoelectrode ensembles. Aflatoxin B1-BSA conjugate immobilized onto gold electrode by self-assembled monolayer of 3-mercaptopropionic acid. The biosensor integrates a microfluidic channel with gold nanoelectrode based indirect competitive immunoassay. The AFB1 concentration can be quantitatively determined in the 2 ng/mL range. The developed sensor were found to be highly sensitive and exhibited a remarkably low limit of detection (LOD; 1 ng/mL).

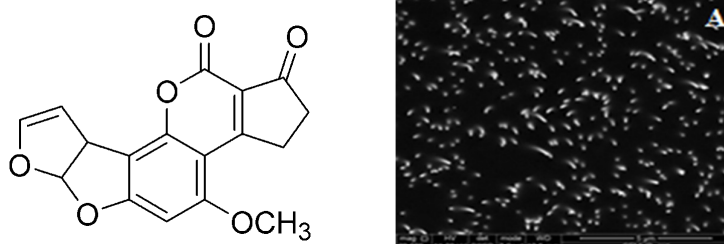


Figure 1. A. Scanning electron microscopic image of a GNEE

Keywords: Microfluidic, Biosensor, Aflatoxin B, Rice, Electrochemical

1.45 Label Free Electrochemical detection of exosomes derived from ovarian cancer cells

S. Viswanathan^{a,b*},Cristin Delerue-Matos^b, C. Rani^c

^aDepartment of Industrial Chemistry, Alagappa University, Karaikudi - 630003, Tamilnadu.

^bREQUIMTE - Instituto Superior de Engenharia, Instituto Politécnico do Porto, Rua Dr. António Bernardino de Almeida 431, 4200-072 Porto, Portugal.

^c Department of Chemistry, Alagappa Govt. Arts college, Karaikudi - 630003, Tamilnadu.

Email id: rsviswa@gmail.com

Extracellular vesicles (EVs), including exosomes, are nanoscale vesicles that carry molecular information of parental cells. Since EVs can be detected in a variety of biofluids and contain a specific set of biomarkers which are reminiscent of their parental cells, they show great promise in clinical diagnostics as EV analysis can be performed in minimally-invasive liquid biopsies. Exosomes show potential for cancer diagnostics because they transport molecular contents of the cells from which they originate.¹ Detection and molecular profiling of exosomes is technically challenging and often requires extensive sample purification and labeling. However, reliable, fast and cost-effective methods for their determination are still needed, especially if decentralized analysis is intended. Here we describe a label-free,high-throughput approach for quantitative analysis of exosomes.



We developed an electrochemical biosensor which works with ~10 μL sample volume, and can detect as low as 150 exosomes per microliter, with a linear range spanning almost four orders of magnitude. Gold nanoelectrode array is functionalized with antibodies to enable profiling of exosome surface proteins and proteins present in exosome lysates. This was achieved by immobilizing rabbit anti-human CD24 antibodies on gold nanoelectrodes array, and using monoclonal antibodies against CD24 for detection of captured exosomes. Capability of detecting exosomes in real samples (diluted serum) was shown. We report that this approach offers good sensitivity, enables portable operation when integrated with miniaturized chips and allows retrieval of exosomes for further study.

Key words: Cancer, CD24, ovarian cancer, nanoelectrodes, immunosensor.

Reference:

- [1] Im, H.; Shao, H.; Park, Y. I.; Peterson, V. M.; Castro, C. M.; Weissleder, R.; Lee, H., Label-free detection and molecular profiling of exosomes with a nano-plasmonic sensor. *Nat Biotech* **2014**, *32* (5), 490-495.

1.46 Electrochemical Biosensor for Organophosphorus Insecticides- Chlorpyrifos

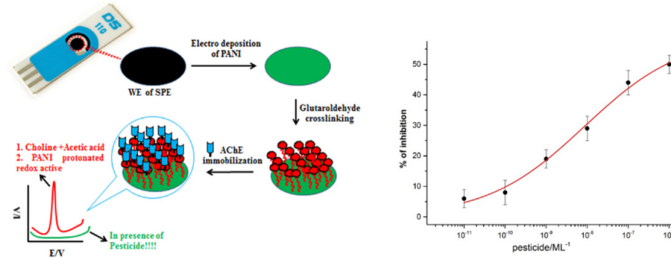
K.Divya^a, T. Ponmuthuselvi^a, C. Rani^b, P. Manisankar^a S. Viswanathan^{a*}

^a Department of Industrial Chemistry, Alagappa University, Karaikudi - 630003, Tamilnadu.

^b Department of Chemistry, Alagappa Govt. Arts college, Karaikudi - 630003, Tamilnadu.

*Contact: email: rsviswa@gmail.com

An electrochemical biosensor for the determination of pesticide chlorpyrifos, one of the common organophosphorous insecticide used in vegetable crops, is described. Thin film of polyaniline deposited on screen printed electrode was used for acetylcholinesterase (AChE) enzyme immobilization. The incorporation of PANI not only provided the conductive pathways to promote the electron transfer, but also increased the surface area of flexible three dimensional conductive supports for acetylcholinesterase enzyme. Thin PANI film on SPE –AChE acted as good sensor for enzyme by-product acetic acid. The changes of local pH in the vicinity of an electrode surface by enzymatic reaction increases the redox activity of PANI thin film on SPE. The pesticides were determined with the proposed biosensor through the enzyme inhibition mechanism. The biosensor was successfully tested in the determination of chlorpyrifos. The dynamic range for the determination of methyl chlorpyrifos was found to be in between 1.0×10^{-11} M up to 1.0×10^{-6} M with correlation coefficient 0.994. The detection limit was found to be 1×10^{-12} M.



Schematic illustration of the different steps for the biosensor construction and Calibration curve for chlorpyrifos determination.

Keywords: Biosensor, Pesticide, Chlorpyrifos, Acetylcholinesterase



1.47 Determination of Heavy metals in fish liver oil extracts using Bismuth electrode

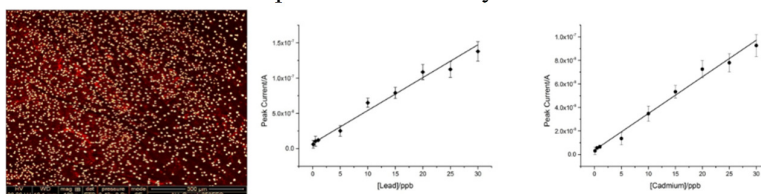
R. Logeswari^a, T.Ponmuthuselvi^a, C. Rani^b, P. Manisankar^a, S. Viswanathan^{a*}

^a Department of Industrial Chemistry, Alagappa University, Karaikudi - 630003, Tamilnadu.

^b Department of Chemistry, Alagappa Govt. Arts college, Karaikudi - 630003, Tamilnadu.

*Contact: email: rsviswa@gmail.com

The environmental pollution is a matter of great concern worldwide. Consequently contamination of food chain is getting increasingly important in view of its role in human health and nutrition. There is large number of environmental pollutants that constitute a potential danger to humanity. Heavy or toxic metals are trace metals which are detrimental to human health and having a density at least five times that of water. Once liberated into the environment through the air, drinking water, food, or countless varieties of man-made chemicals and products, heavy metals are taken into the body via inhalation, ingestion and skin absorption. In this work, we developed Bismuth micro/nanoparticles deposited glassy carbon electrode for heavy metal analysis. The Bi ME has been developed to simultaneously and sensitively determine Cd²⁺ and Pb²⁺ using the SWASV method. The characteristic peaks of Cd²⁺ and Pb²⁺ were observed at -0.746 and -0.496 V respectively, metal ion stripping characteristics with a pre-concentration deposition time of 120 s. Different concentrations of lead and Cadmium were prepared between 0.1ppb and 30 ppb. Heavy metal contamination in fish liver oil extracts sample is analyzed by modified electrode. Recovery studies shows that in fish liver oil spiked with (1ppm) Pb and (1ppm)Cd metal content present in 97% and 98% is observed. This method is rapid, sensitive and economic as compared to other analytical methods.



SEM picture of Bi deposited on glassy carbon electrode and Calibration plot of lead and cadmium under optimised conditions

Keywords: Heavy metal, voltammetry, bismuth electrode, pollution

1.48 Label-Free Detection of Myoglobin- a Cardiovascular Disease Biomarker

S. Viswanathan^{a*}, M. Sangeetha^a, C. Rani^b,

^a Department of Industrial Chemistry, Alagappa University, Karaikudi - 630003, Tamilnadu.

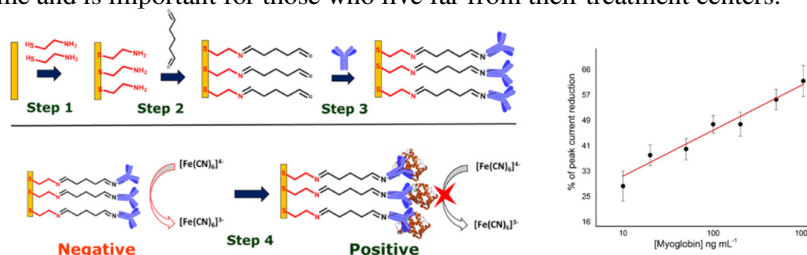
^b Department of Chemistry, Alagappa Govt. Arts college, Karaikudi - 630003, Tamilnadu.

*Contact: email: rsviswa@gmail.com

Cardiovascular diseases account for ca. 30% of adult deaths in the age group of 30-70 years, which is greater than the combined mortality rate from all types of cancer. The ability to foresee cardiac pathology is therefore of utmost concern to clinicians. Several potential cardiac biomarkers have attracted attention because of their ability to predict future cardiovascular events. Serum cardiac markers, particularly myoglobin (MB), play an important role in clinical diagnosis; an increased MB level indicates myocardial damage. Detection of elevated levels of MB has become a gold-standard for diagnosis in cases of acute myocardial infarction (AMI); MB is released in the blood within 4-5 h after an AMI episode with the expression level in plasma serum increasing up to 600 ng mL⁻¹ after AMI, over 3 to 6 times above the normal level expressed in healthy patients. Direct determination of serum MB level is very important in the early detection of cardiac problems. A simple and label-free electrochemical immunosensor based on Au-SPE for MB determination has been developed.



The construction of the proposed biosensor consists of a cysteamine self-assembled monolayer forming an organized and packed layer on the surface of a gold electrode which enabled a fast and successful modification with antibody molecules. Anti-myoglobin antibodies molecules were immobilized by glutaraldehyde cross linker. Direct determination of serum MB level is very important in the early detection of cardiac problems. Human serum samples were spiked with known amount MB and analysed for method validation. The accuracy of the MB determination was examined by comparison of the results obtained by this method with those from the ELSIA myoglobin analysis kit. The LOD value thus obtained was $5 \text{ ng} \cdot \text{mL}^{-1}$. Serum testing using proposed biosensor is simple, making it an attractive, effective alternative to conventional ELISA testing, and the possibility of developing home testing kits would further facilitate it as a diagnostic aid, enabling patients to monitor their own health at home and is important for those who live far from their treatment centers.



Schematic illustration of the different steps for the immunosensor construction and calibration plot

Keywords: Biosensor, Myoglobin, Immunosensor, Cardiovascular, Biomarker

1.49 Single Drop Micro-Extraction of Methyl Parathion and Electrochemical Determination

D. Suganthi^a, T.Ponmuthuselvi^a, C. Rani^b, P. Manisankar^a, S. Viswanathan^{a*}

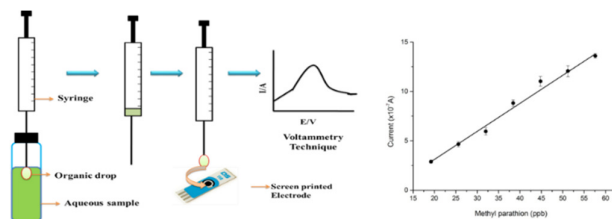
^a Department of Industrial Chemistry, Alagappa University, Karaikudi - 630003, Tamilnadu.

^b Department of Chemistry, Alagappa Govt. Arts college, Karaikudi - 630003, Tamilnadu.

*Contact: email: rviswa@gmail.com

Analytical technology is an extremely broad field which impacts on many major industrial sectors such as the pharmaceutical, healthcare, food, and agriculture industries as well as environmental monitoring. Pesticides have the insecticidal property due to which they are in great use. But human health and the surroundings are affected by these pesticides as they contain the toxic compounds. These toxic compounds are hazardous as they can accumulate in grains, vegetables, fruits, and so forth, percolate in soil, and finally lead to water contamination. Single drop micro-extraction (SDME) is based on the principle that the equilibrium ratio of the concentration of solute between the organic phase and the aqueous phase. A solvent micro drop is exposed to an aqueous sample, where the analyte is extracted into the drop. In this way, high enrichment factors are obtained owing to the high ratio of sample volume to organic phase volume. After extraction, the micro drop is retracted back into the micro syringe and injected into instruments such as GC-MS, GC, and HPLC for further analysis. In this work we developed a simple SDME procedure coupled with electrochemical technique for the trace-level determination of Methyl Parathion in aqueous samples. Under optimal extraction conditions the maximum extraction of Methyl Parathion was achieved. Screen Printed Electrode (SPE) was utilized to enhance electrochemical performance. The combination of both SDME and SPE resulted the lower detection limit, good linearity and repeatability for the detection of Methyl Parathion in water.





Keywords: Micro-Extraction, Pesticide, Methyl Parathion, Voltammetry

1.50 Structure and Electrochemical performance of $\text{LiV}_x\text{Mn}_{2-x}\text{O}_4$ ($0 \leq x \leq 0.20$) cathode materials for rechargeable lithium ion batteries

P. Mohan^a and G. Paruthimal Kalaignan^b

^aDepartment of Chemistry, Sree Sevugan Annamalai College, Devakottai-630 303.

^bAdvanced Lithium-ion Battery Research Lab, Department of Industrial Chemistry, Alagappa University, Karaikudi – 630 003, India

Email: pmohanic@gmail.com

In this work, the pristine LiMn_2O_4 and vanadium substituted $\text{LiV}_x\text{Mn}_{2-x}\text{O}_4$ ($x = 0.05, 0.10, 0.15$ and 0.20) positive electrode material were prepared by using the tartaric acid assisted sol-gel method. The structure and electrochemical properties of the prepared materials were characterized by using XRD, SEM, TEM and charge/discharge studies. The mechanisms of improving the electrochemical performances of the pristine LiMn_2O_4 and vanadium substituted $\text{LiV}_x\text{Mn}_{2-x}\text{O}_4$ cathode materials are discussed. X-ray powder diffraction analysis was changed in lattice parameters with increasing vanadium content suggesting the occupation of substituent within LiMn_2O_4 interlayer spacing. TEM and SEM analyses show that $\text{LiV}_{0.15}\text{Mn}_{1.85}\text{O}_4$ has smaller particle size and more regular morphological structure with narrow size distribution than those of LiMn_2O_4 . It is concluded that the structural stability and cycle life improvement were due to many factors like better crystallinity, smaller particle size and uniform distribution compared to LiMn_2O_4 cathode material. $\text{LiV}_{0.15}\text{Mn}_{1.85}\text{O}_4$ cathode material has improved the structural stability and excellent electrochemical performances of the rechargeable lithium-ion batteries.

Key words: Positive electrode materials, XRD, TEM, Charge/discharge

1.51 STUDIES ON PANI/ZnO NANOCOMPOSITE POLYMER ELECTROLYTE FOR PEMFC

J. Marimuthu¹, M. Rajasekhar²

Advanced Energy Research Lab, PG and Research Department Chemistry, Government Arts College, Dharmapuri-636705,

ABSTRACT

Polyaniline/ZnO Nanocomposites are synthesized by chemical oxidation polymerization method with varying amounts of Zinc Oxide (0.1g, 0.5g wt. %). The structure and properties of PANI/ZnO nanocomposites are assessed by X-Ray Diffraction (XRD), Scanning Electron Microscope (SEM) and FT-IR spectroscopy. The XRD analysis demonstrate the nanocrystalline nature of PANI and its composites. FT-IR results show broadening and shifts of peaks towards lower wave numbers in all composites suggesting better conjugation and some chemical interactions between PANI and Al particles.

KEYWORDS: Polyaniline, Nanocomposites, FT-IR, SEM, XRD and Conductivity



2. Nanoscience and Technologies

2.1 Effect of metal incorporation in tungsten oxide / zinc sulphide nanostructures

V P Mahadavan Pillai

*Department of Optoelectronics, University of Kerala, Kariavattom- 695581 Thiruvananthapuram, Kerala, India
Email: vmpillai9@gmail.com*

Incorporation of metals in semiconductors can have profound influence on their structural, morphological and optical properties. Au, Ag, Cu and Mn incorporated nanostructures of tungsten oxide and zinc sulfide nanostructured films are prepared using RF magnetron sputtering technique and effect of metal incorporation on their structural and optical properties are investigated in detail. It is observed that Ag and Au incorporation in tungsten oxide matrix promote the formation of $W_{18}O_{49}$ crystalline phase. Silver incorporation on tungsten oxide matrix enhances crystalline quality, film thickness and grain size and at same decreases the transmittance and band gap energy. The surface plasmon resonance of silver and gold nanoparticles in tungsten oxide matrix is studied in detail. Cu doping in ZnS nanostructures results in phase modification and affects its luminescence behavior. PL analysis revealed that increase in Cu incorporation results in the enhancement of self activated PL emissions with the appearance of a new green emission peak due to the recombination of a shallowly trapped electron and Cu^{2+} . Incorporation of Mn in ZnS lattice enhances the crystalline quality of ZnS films. Mn incorporated films show an intense orange emission due to the d-d transition of Mn^{2+} ions in the ZnS along with the blue and green emissions as observed in the pure ZnS film. Ag incorporated ZnS films reveal the presence of hexagonal wurtzite zinc sulfide phase. ZnS films with higher Ag incorporation exhibit surface plasmon resonance band in the 450-650 nm region. In the Au loaded ZnS films nanoflowers of triangular and leaf-like petal morphologies are achieved. A selective enhancement of Raman intensity is observed for the Au loaded nanoflowers due to the plasmon scattering at the ZnS/Au interface. Nanoflowers with higher Au loading concentration exhibit surface plasmon resonance band of Au in the 550-650 nm. The Au incorporation in ZnS lattice has changed the PL emission properties of the ZnS nanostructure drastically.

2.2 Graphene based metal chalcogenide nanocomposite catalysts foreffective degradation of organic pollutants

E. Murugan

Department of Physical Chemistry, School of Chemical Sciences, University of Madras, Guindy Campus, Chennai, 600025, TamilNadu, India

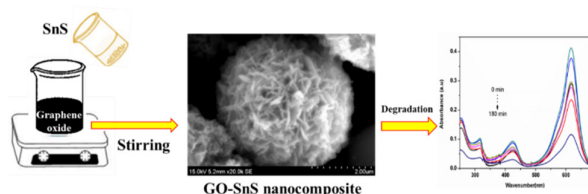
Email: dr.e.murugan@gmail.com

The activity of TiO_2 nanotubes is largely restricted to the ultraviolet region owing to the large band gap (3.0 eV for rutile phase and 3.2 eV for anatase phase), and thus contributes only 3-5% of the conversion from solar energy [1]. On the basis of the drawbacks of TiO_2 based materials, semiconducting metal sulfides have the ability to absorb light in the visible region due to their relatively narrow band gap [2]. They are considered as a promising class of materials and have been used as sun-light activated photocatalysts and efficient separators of photogenerated charges in coupled hetero structures. Among them, CdS has been mostly studied. However, CdS is far from any realistic application due to its high toxicity. By contrast, SnS gained interest as being a n-type semiconductor, nontoxic, inexpensive and chemically stable IV-VI semiconductor, with a band gap within 2.08-2.44 eV, a CdI_2 -type layered structure and it has good stability in visible light-sensitive photocatalyst. Targeting environmental and energy-related reactions, processes have been recently implemented for the synthesis of SnS of different morphologies as well as coupled with carbon-based materials namely, carbon nanotubes and graphene for elaborating hybrid nanocomposites.

Graphene exhibits a unique structure of one-atom thick and two-dimensional layers of sp^2 -bonded carbon, the surface properties of graphene can be adjusted via chemical modification, which offers tremendous opportunities for the development of functionalized graphene-based materials [3].



Such graphene-based materials show unique electronic and optical properties and good biocompatibility, which make these materials attractive for many potential applications including energy storage, catalysis, biosensors, molecular imaging and drug delivery. Recently, functionalized graphene-based semiconductor photocatalysts have attracted a lot of attention due to the ability to act as electron transfer medium, large specific surface area and high adsorption. These properties has stimulated an extensive research on the preparation, modification, and application of graphene-based semiconductor photocatalysts. Taking into consideration of all these points, in this work, graphene oxide-SnS (GO-SnS) nanocomposite catalysts were synthesized through hydrothermal method and characterized by X-ray diffraction, scanning electron microscopy, Raman spectroscopy, Fourier transform infrared spectroscopy, UV-vis spectroscopy. The catalytic potential of these photocatalysts were demonstrated through photodegradation of malachite green in the water. The effects of GO/SnS ratio and initial solution pH on the photodegradation efficiency were studied extensively. The nanocomposite based catalyst has showed excellent sunlight-excited photocatalytic activity to toxicity malachite green in the water. The photodegradation rate has found to increase dramatically on increasing with the load ratio of GO/SnS. Similarly, the variation of pH has largely influenced in the catalytic activity due the large surface-to-volume ratio and lower band gap.



References

- [1] Buddee S, Wongnawa S, Sriprang and Chaval, *Journal of Nanoparticle Research* (2014) **16**,1.
- [2] Ephirin Z, Mouloungui Z, and Virginie N *Bioinorganic Chemistry and Applications*, (2010) 1-8.
- [3] Shahriary L and Athawale A *International Journal of Renewable Energy and Environmental Engineering*, (2014) **02** 58-63.

Acknowledgements

The author acknowledge DST-SERB and DST-PURSE, New Delhi, Government of India, for providing financial assistance.

2.3 The Development of Silica Nanoparticle from Top Down & Bottom Up Approach for Using in Nanocomposites

Toemsak Srikehrin

School of Materials Science and Engineering, Faculty of Science, Mahidol University, Rama VI Rd., Rajthawee, Bangkok, Thailand 14000

The use of silica nanoparticle prepared by both bottom up (commercially available silica colloidal nanoparticle) and top down (bead milling) for the development of scratch resistant nanocomposites will be discussed. The technique for the preparation of bead milled silica particle with the control target size, ranging from 200 nm to 800 nm in organic media, will be shown. The preparation of silica-methyltriethoxy silane coating solution from silica nanoparticle will be used for the coating preparation on both transparent plastic and wood. The nanocomposite films were evaluated for their optical and scratch resistant property. The presentation will also cover the discussion on future prospect for the use of nanoparticle in the coating application.



2.4 AIE Nanodots Ensued from Pyrene Schiff Base and It's Indispensable Applications

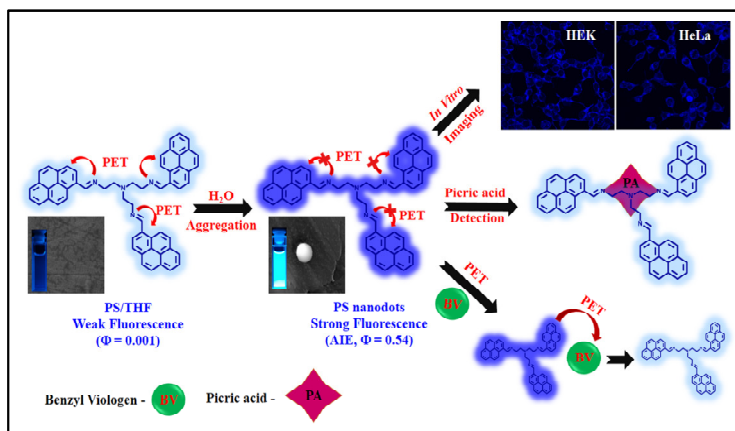
Venkatesan Srinivasan,^[a] Mariadoss Asha Jhonsi,^{[a]*} Arunkumar Kathiravan^[b]

[a] Department of Chemistry, B. S. Abdur Rahman University, Vandalur, Chennai-600 048, Tamil nadu, India.

[b] National Centre for Ultrafast Processes, University of Madras, Taramani Campus, Chennai – 600 113, Tamil Nadu, India.

E-mail: asha@bsauniv.ac.in. (Dr. M. Asha jhonsi)

Development of efficient organic aggregation-induced emission (AIE) luminescent materials is one of the hot current research topics, owing to their high demand in diverse high tech fields, such as sensing, optoelectronics and biotechnologies.¹ The AIE phenomenon stands for a photophysical process that certain nonfluorescent or weakly fluorescent luminogens in solutions can turn on strong fluorescence in the aggregated state.² Various AIE molecules were developed such as tetraphenylethene, hexaphenylsilole, distyryanthracene, tetraphenylpyrazine, etc.³ However, most of the AIE molecules were synthesized by difficult synthetic routes, herein plan to synthesize a new AIE active molecule with concise synthetic route. From the literature, the Schiff base based molecules can be synthesized by simple method and cost effective method and has also applied to many emerging fields. However, these conventional fluorophore cannot produce satisfactory results in practical application. Therefore, we need the fluorophore must have with high molar extinction coefficients, high fluorescence quantum yields (QYs), good photostability, and longer absorption and emission, are needed. Recently, pyrene is a good fluorophore, due to its good photostability, excellent photoluminescence properties for utilized in sensor and bio imaging applications. Therefore, we have synthesized pyrene based Schiff base (PS) which is well characterized by using ¹H, ¹³C NMR, FT-IR and mass analysis. In solution state, the PS molecule fluorescence is completely quenched due to photo induced electron transfer (PET). The PS molecule emission intensity is increases at THF: H₂O (10:90) aggregate states for suppression of PET. The aggregation state of PS molecule is characterized by using HR-SEM, HR-TEM, AFM and DLS measurements. From the characterization, PS molecule could exhibit spherical shape with average size is ~1 nm. Therefore the PS aggregates are expressed as AIE nanodots. The AIE nanodots have high fluorescence lifetime (4 ns) and high quantum yield (54%) with compare to commercial fluorophore. The PS based AIE nanodots were successfully used to several applications such as in-vitro bioimaging, detection of picric acid and photoinduced electron transfer studies.



References:

- [1] S. Mukherjee and A.K. Paul, *J. Fluoresc.* 2015, 25, 1461-1467.
 - [2] Y. Hong, J. W. Y. Lam, B. Z. Tang, *Chem. Soc. Rev.* 2011, 40, 5361–5388.
 - [3] Y. Dong, Z. Yang, Z. Ren and S. Yan, *Polym. Chem.*, 2015, 6, 7827-7832.
-

2.5 Green Synthesis and Characterization of Nano bound Terpolymer Resin

A.Neela¹, G.R.Priya Dharsini², V.Rama*

¹ Department of Chemistry, Rani Anna Govt. College, M.S.University Tirunelveli-12

² * Department of Chemistry, Sarah Tucker College, M.S.University Tirunelveli-12

E-mail: rama242002@gmail.com

Abstract:

Currently, plant-mediated biological synthesis of nanoparticles is gaining importance due to its simplicity and eco-friendliness. In this work, the reaction mixture is prepared by adding 1mmol solution of zinc nitrate as a source of zinc to 30 mL of *Acacia catechu* (Karungali) plant extract at 60°C (fuel) under constant stirring for ~30 min. This reaction mixture is kept in a pre-heated muffle furnace maintained at 400 ± 10 °C. ZnO NPs are formed within 3–4 min. The particle size is calculated from X-ray diffraction images of ZnO powder using Scherrer formula $D=K \lambda/\beta \cos\theta$. The absorption spectrum of the sample is measured by a UV–vis-spectrophotometer. Morphological features are studied by using Hitachi-7000 Scanning Electron Microscopy (SEM), Transmission electron microscopy (TEM, TECNAI F-30). Encapsulation of inorganic nano metal oxides (as a core) by polymers (as a shell) is also one of the most interesting research subjects, in the authors' point of view, that leads to the synthesis of nanocomposites, whose properties include properties of not only the organic polymer (e.g., optical properties, toughness, flexibility, etc.), but also the inorganic nanometaloxides (e.g., mechanical strength, thermal stability, etc.). The applied preparative method involves Green synthesis of a terpolymer resin by ultrasonic irradiation technique using monomer resorcinol (0.1 mol) and guanidine hydrochloride (0.1mol) with formaldehyde (0.2mol) in the presence of 2M HCl medium at 80°C for 15 minutes. After the completion of the reaction, terpolymer incorporated with nanometaloxide is purified by dissolution in 8% NaOH and re-precipitated by drop-wise addition of 1:1 2M HCl and then characterized by different spectral methods like FT-IR, UV-visible, ¹H NMR and ¹³C NMR to elucidate the structure of the ZnO/RGF nanocomposite.

References:

- [1] J. M. Cho et.al., "Characterization Of ZnO Nanoparticles Grown By Laser Ablation Of a Zn Target In Neat Water", *Journal Bull. Korean Chem. Soc.*, Vol. 30(7), pp. 1616-1618, **2009**.
 - [2] Gedanken, "Using sonochemistry for the fabrication of nanomaterials," *Ultrasonics Sonochemistry*, vol. 11, no. 2, pp. 47–55, **2010**.
 - [3] Gananasangeetha D. et.al., "One Pot Synthesis Of Zinc Oxide Nanoparticles via Chemical and Green Method", *Research Journal Of Material Science*, Vol. 1(7), pp. 1- 8, **2013**.
 - [4] synthesis and characterization of zinc oxide nanoparticles from *Ocimum basilicum* L. var. *purpurascens* Benth.-lamiaceae leaf extract *Mater. Lett.* 131 (**2014**), pp. 16–18.
 - [5] Rahangdale, S.S. Gurnule, W.B. *chem. Sci. Trans.* **2013**.
-



2.6 CuO Nanoparticles Catalyzed Synthesis of 1,2,3-Triazoles under Solvent-Free Condition

J. Paul Raj^a, D. Gangaprasad^a, M. Vajjiravel^a and J. Elangovan^{*b}

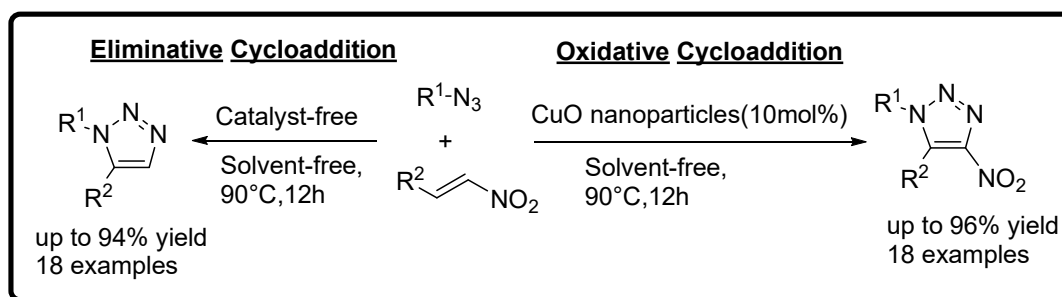
^a Department of Chemistry, B. S. Abdur Rahman Crescent University, Chennai-600048.

^b Department of Chemistry, Rajah Serfoji Government College, Thanjavur, Tamil Nadu- 613005.

*Email: elangoorganic@gmail.com

1,2,3-Triazoles have gained paramount importance for the past two decades owing to their versatile applications in various fields such as drug discovery, medicinal chemistry, supramolecules, functional coatings, material science and polymers.¹ Particularly, 1,2,3-triazoles bearing NO₂ group gain additional importance since they are the starting materials for nitrogen group substituted 1,2,3-triazoles. Apart from acting as nitrogen source, NO₂ group can be derivatized further to access diverse molecules.² In spite of the conventional Huisgen cycloaddition, major breakthrough was achieved in this area only after the discovery of copper catalyzed azide-alkyne cycloaddition (CuAAC) which amassed numerous publications encapsulating a wide spectrum of applications in various fields.³ As an alternative approach to azide-alkyne cycloaddition olefins were envisaged in the place of alkynes since olefins are easily accessible and economically viable than alkynes. This type of azide-olefin cycloaddition was pioneered by Huisgen and Labbe with organic azides and electron deficient olefins.⁴

To convert these unstable triazolines into stable aromatic triazoles, two ingenious approaches have been adopted. The first one is eliminative azide-olefin cycloaddition (EAOC) and the second approach is oxidative azide-olefin cycloaddition (OAOC). Above all, nitro-olefin is yet another potential candidate which has feebly come into limelight. When nitroalkene is subjected to cycloaddition with azides, HNO₂ gets eliminated from the resulting triazoline furnishing the required triazole. A few research groups have made laudable contributions in the EAOC of nitro-olefins in the past decade.⁵ However 1,2,3-triazoles from nitroolefins without elimination of nitro group (OAOC) has been dormant for several years. Recently, Chen et al, have reported Cu(OTf)₂ catalyzed regioselective OAOC of nitroalkenes with organic azides in DMF/AcOH in excellent yields of 78–96%.⁶ In continuation to that, we have developed an environmentally benign and economically viable tunable method to achieve oxidative and eliminative cycloaddition of nitro-olefins with organic azides simply by tweaking the reaction condition.⁷ Some of the noteworthy features of CuO nanoparticles are: The catalyst is comparatively cheaper and heterogeneous. CuO nanoparticles are less cytotoxic than the conventional Cu(I)-precursors.⁸



References:

- [1] (a) H. C. Kolb; K. B. Sharpless, *Drug Discovery Today* **2003**, 8, 1128; (b) P. Thirumurugan, D. Matosiuk, K. Jozwiak, *Chem. Rev.* **2013**, 113, 4905.
- [2] N. Ono, *The Nitro Group in Organic Synthesis*; Wiley-VCH: Weinheim, Germany, **2001**; p 159.
- [3] (a) Huisgen, R. *Angew. Chem., Int. Ed. Engl.* **1963**, 2, 565; (b) Tornøe, C. W.; Christensen, C.; Meldal, M. *J. Org. Chem.* **2002**, 67, 3057;
- [4] R. Huisgen, G. Szeimies, L. Möbius, *Chem. Ber.* **1966**, 99, 475.
- [5] (a) D. Janreddy, V. Kavala, C.-W. Kuo, W.-C. Chen, C. Ramesh, T. Kotipalli, T.-S. Kuo, M.-L. Chen, C.-H. He, C.-F. Yao, *Adv.Synth. Catal.* **2013**, 355, 2918; (b) N. Singh, S. K. Pandey, R. P. Tripathi, *Carbohydr. Res.* **2010**, 345, 1641; (c) Y.-Y. Xie, Y.-C. Wang, H.-E. Qu, X.-C. Tan, H.-S. Wang, Y.-M. Pan, *Adv. Synth. Catal.* **2014**, 356, 3347.
- [6] Y. Chen, G. Nie, Q. Zhang, S. Ma, H. Li, Q. Hu, *Org. Lett.* **2015**, 17, 1118.



References:

- [1] Jake Yeston, Robert Coontz, Jesse Smith, Caroline Ash, Science 313 (2006) 2-9.
- [2] Udaybir Singh Mann, Arvind Dhingra, Jaswinder Singh, International Journal of Advanced Technology in Engineering and Science, 2 (2014)70-74.
- [3] Anila Ajmal, Imran Majeed, Riffat Naseem Malik, Hicham Idriscand, Muhammad Amtiaz Nadeem, RSC Advances, 4 (2014) 37003-370026.

2.8 Nano scale zero valent Iron (n ZVI) - montmorillonite (MMT) composite for dye adsorption

K.Jayaraj, G. Aruna Devi and Anitha Pius*

Department of Chemistry, The Gandhigram Rural Institute – Deemed University, Gandhigram, Dindigul – 624 302. Tamil Nadu, India.

Ph: +91-451-2452371 (O); Fax: +91-451-2454466 (O)

*E-mail: jrajaregha@gmail com & dranithapius@gmail.com**

Abstract:

Quality of the water is just as important as the quantity. Waste water containing dyes are difficult to remove because of their stable nature. Various methods are currently used for the treatment of industrial waste water. Adsorption technique, which is simpler and cost effective, stands one among the alternatives introduced to remove dye. The use of montmorillonite (a natural phyllosilicate) has gained much attention in composite preparation [1]. Layered structure of montmorillonite (MMT) having exchangeable hydrated cation is the main parameter responsible for the remarkable adsorptive properties. High specific surface area and resulting high reactivity of nano scale zero valent iron (n ZVI) makes it a promising one in the composite formation [2]. In this study, n ZVI/MMT was prepared. The prepared composite was characterized using SEM with EDAX, FTIR, XRD and TGA.

The degradation efficiency of Indigo carmine dye from aqueous solution using the prepared composite has been found to be dependent on contact time and pH. Adsorption efficiency of n ZVI in MMT is 93%. Removal of dye followed pseudo second order kinetics and the analysis of adsorption of dye under different initial concentration followed Freundlich isotherm. The prepared composite using n ZVI with MMT was found to be an excellent material for the adsorption of Indigo carmine dye from aqueous solution.

Figure:

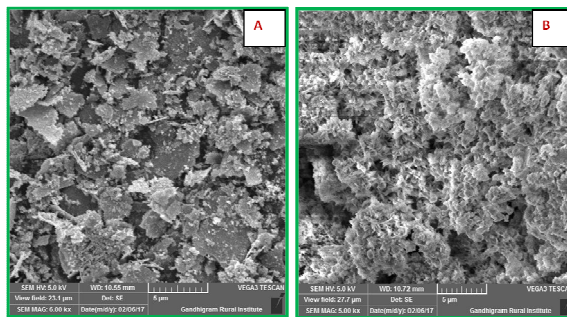


Figure 1. SEM images of (A) n ZVI and (B) n ZVI/MMT

References:

- [1] Wang. L &Wang A, Journal of Hazardous Material A,(2007),147,979-985
- [2] Kanel SR, J Nanopart Res 9(5):725-735



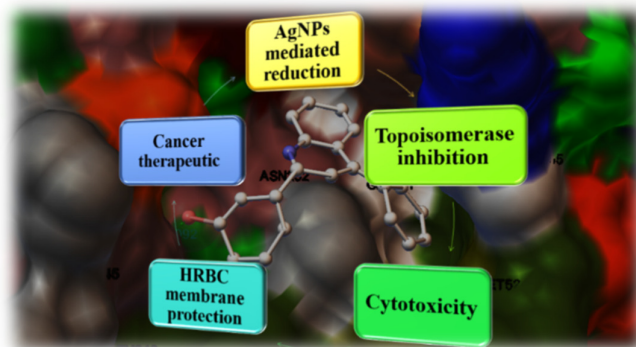
2.9 Silver nanoparticles mediated reduction of 2-nitro to 2-amino-5-(4-phenylquinolin-2-yl) phenols; molecular rationale of these small molecules as Topoisomerase-II inhibitors and anticancer therapeutics

Manikandan A^a and Sivakumar A^{*a}

^aDept. of Biotech., School of Bio-Science and Technology, VIT University, Vellore-632014, Tamil Nadu, India.

^{*}corresponding author, E-mail: siva_kumar.a@gmail.com

Substituted 2-amino-5-(4-phenylquinolin-2-yl)phenols (**5a-h**), achieved by reducing 2-nitro-5-(4-phenyl quinolin-2-yl)phenols (**4a-h**) mediated by algal route derived silver nanoparticles (AgNPs), were emerged as the inhibitors of Topoisomerase-II (Topo- II) and anti-cancer agents. Synthesized AgNPs was used as highly active catalysts for the reduction of nitroarene present in compounds (**4a-h**), giving the corresponding aryl amines (**5a-h**) with NaBH₄ in moderate to high yields. In the physio-chemical analysis/predictions and the biological activities, there was excellent superiority observed for compounds (**5a-h**) over (**4a-h**) due to excellent energy minimized in the reduction of nitroarene to aryl amines. Docking results suggested the hydrophobic interactions in Topoisomerase (PDB ID: 1A36 (Topo-I) and 4FM9 (Topo-II)) binding pocket dominated affinity of most efficiently binding ligands (**5a**, **5c**, **5f**, and **5g**; inhibitory constant (k_i) = 46.45 nM, 124.12 pM, 62.74 nM, and 216.22 nM respectively for Topo-II). In Topo-II assay, compounds **5a**, **5c**, and **5f-h** were highly active with a percentage inhibition range between 75±1.02 to 95±0.84. IC₅₀ for these compounds were <0.05 µM. Among all tested cancer cell lines (colon (HCT 116), skin (G-361), breast (MCF-7)), excellent therapeutic result were obtained for colon cancer (HCT116); **5a**, **5c** and **5f-h** were showed excellent relative activities (82.54, 92.12, 84.24, 80.19 and 75.92% and IC₅₀ 0.25 µM (**5a**), 0.075 µM (**5c**), 0.085 µM (**5f**), 0.125 µM (**5g**) and 0.50 µM (**4j**) while the standard (Doxorubicin) found with IC₅₀ 1.25 µM (78 % relative activity). SAR studies demonstrated 2-amino-5-(4-phenylquinolin-2-yl)phenols as the Topo-I&II precise inhibitors with the imminent therapeutic potentials to treat a variety of cancers.



Keywords: 2-amino-5-(4-phenylquinolin-2-yl)phenols, Topoisomerase I&II; anticancer; SAR; molecular docking; HCT-117 cell line



2.10 Design and development of a novel poly(melamine) entrapped gold nanoparticles composite for sensitive and low level detection of catechol

S. Sonadevi, R. Hema Kalyani, S. Josphine Sarah and R. Sayee Kannan *

*PG & Research Department of Chemistry, Thiagarajar College, Madurai-09.
e-mail: sayeekannanramaraj@gmail.com*

Abstract

A simple and cost effective synthesis of nanomaterials with advanced physical and chemical properties have received much attention to the researchers, and is of interest to the researchers from different disciplines. In the present work, we report a simple and one pot electrochemical synthesis of poly(melamine) entrapped gold nanoparticles (PM-AuNPs) composite. The PM-AuNPs composite was prepared by a single step electrochemical method, wherein the AuNPs and PM were simultaneously fabricated on the electrode surface. The as prepared materials were characterized by various physicochemical methods. The PM-AuNPs composite modified electrode was used as an electrocatalyst for oxidation of catechol (CC) due to its well-defined redox behaviour and enhanced electro-oxidation ability towards CC than other modified electrodes. Under optimized conditions, the differential pulse voltammetry (DPV) was used for the determination of CC. The DPV response of CC was linear over the concentration ranging from 0.5 to 175.5 μM with a detection limit of 0.011 μM . The PM-AuNPs composite modified electrode exhibits the high selectivity in the presence of range of potentially interfering compounds including dihydroxybenzene isomers. The sensor shows excellent practicality in CC containing water samples, which reveals the potential ability of PM-AuNPs composite modified electrode towards the determination of CC in real samples.

Keywords: Poly(melamine), gold nanoparticles, catechol, differential pulse voltammetry

2.11 Preparation, characterization and photocatalytic activity of MgO nanoparticles for the degradation of Rose Bengal dye

P.Vasanth Kumar ^{a,*}, V.Vasanthi ^b, K.Anitha ^a

^aDepartment of Physics, School of Physics, Madurai Kamaraj University, Madurai-21.

^bDepartment of Laser Studies, School of Physics, Madurai Kamaraj University, Madurai-21.

E-mail ID: vasanthakumar181294@gmail.com

Abstract

In the present work, the MgO nanoparticles were synthesized via a sol-gel combustion method. The prepared sample were characterized by Powder X-ray diffraction (XRD), scanning electron microscopy (SEM) analysis and UV-Vis absorption spectroscopy. Powder X- Ray Diffraction (XRD) pattern confirmed the polycrystalline nature of MgO with cubic structure and there is no secondary phase is observed. The average crystallite size (D) was found to be 20 nm. Scanning electron microscopy (SEM) image revealed the fine particles are agglomerated and formed cluster like surface morphology. The photocatalytic degradation efficiency of the prepared MgO nanoparticle was investigated by photocatalytic degradation of Rose Bengal (RB) dye under the sunlight irradiation. The prepared MgO nanoparticle is used as a absorbent to remove Rose Bengal dye from aqueous solution. Fig. 1 (a) shows the typical time-dependent UV-Vis absorption spectra of Rose Bengal solution after UV irradiation with 10 mg of MgO nanoparticles as a photo catalyst. The characteristic absorption of Rose Bengal at 550 nm decreased rapidly with addition of photocatalyst and extension of the irradiation time. The absorption peak of dye solution disappeared completely after 150 min of irradiation. Similar trend is observed (Fig. 1 (b) & 1 (c)) when the concentration of MgO nanoparticles is increased to 30 mg and 50mg. The degradation rate is found to be increased by increasing the concentration of MgO. The small crystallite size of the obtained MgO nanoparticles resulted in larger surface area with more number of reactive sites and surface hydroxyl which supported for higher degradation efficiency. Photocatalytic degradation efficiency of MgO nanoparticles for Rose Bengal dye is increased as a function of irradiation time as well as the concentration of photo-catalyst.



The 100% degradation of dye is achieved around 90 min of sunlight irradiation. The fast degradation also feasible by further increase of MgO concentration. The degradation kinetics was studied by plotting the natural logarithm of concentration ratio, $\ln(C/C_0)$, versus the irradiation time, t . The degradation rate constant is increased from 0.03 to 0.08 min^{-1} as the concentration of the photocatalyst increases. The results confirmed that the MgO nanoparticles synthesized by a sol-gel combustion method can be applied as a potential candidate for the degradation of Rose Bengal dye under irradiation of sunlight.

Key words: Mgo nanoparticles, Photocatalytic degradation, Rose Bengal dye, Sunlight.

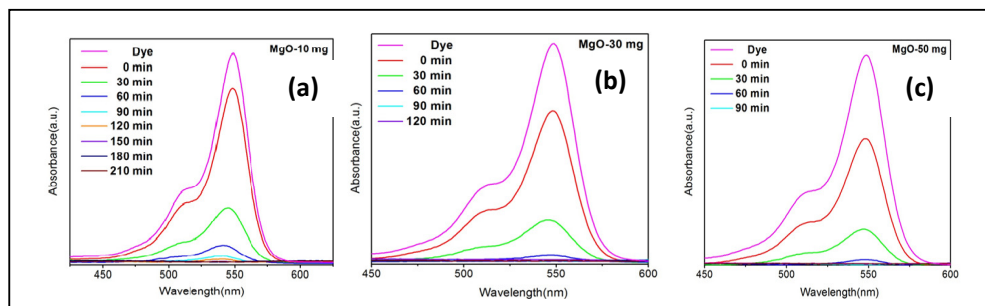


Figure 1. Time dependent UV-Vis absorption spectrum of (a) MgO - 10 mg (b) MgO - 30 mg and (c) MgO - 50 mg

References

- [1] R. Sathyamoorthy, K. Mageshwari, Sawanta S. Mali, S. Priyadharshini, and P. S. Patil, *Ceramics Int.*, 39 (2013) 323–330
- [2] S. Jorfi, G. Barzegar, M. Ahmadi, R. D. C.Soltani, N. J. Haghighifard, A. Takdastan, R. Saedi, and M. Abtahi, *Journal of Environ. Management*, 177 (2016) 111-118.
- [3] V. Vasanthi, M. Kottaisamy, K. Anitha, and V. Ramakrishnan, *Superlattices and Microstructures* 106 (2017) 174-183

2.12 Fabrication of Copper Oxide/ Poly Vinyl Alcohol nanocomposite for Electrocatalytic and Photocatalytic Applications

Karthika,^a S. Selvarajan^a, A. Suganthi^{a**}, M. Rajarajan^{b*}

^a PG & Research Department of Chemistry, Thiagarajar College, Madurai - 625009, Tamilnadu, India.

^b PG & Research Department of Chemistry, Cardamom Planters' Association College, Bodinayakanur- 626513, Tamilnadu, India.

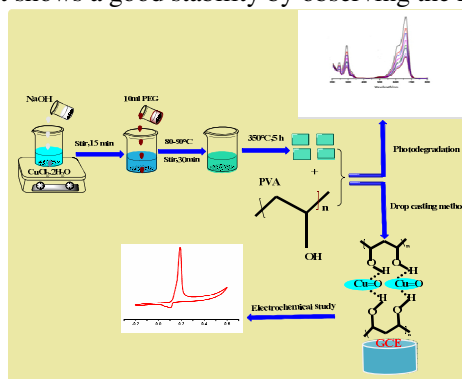
Corresponding author: suganthiphd09@gmail.com**, rajarajan_1962@yahoo.com*

Abstract

The CuO/PVA composite modified GCE prepared via simple drop casting method and the structural characterization of CuO/PVA nanocomposite was characterized by UV-vis-spectroscopy, X-ray diffraction (XRD), fourier transform infrared spectroscopy (FT-IR spectra), Scanning electron microscopy (SEM) and High resonance transmission electron microscopy (HR-TEM) technique. The CuO/PVA composite modified GCE showed excellent electrocatalytic activity towards the sensing of mercury in terms of decrease the potential and increase the cathodic peak current in comparison with different modified and unmodified electrodes. The electrocatalytic sensing of mercury based on the CuO/PVA nanocomposite modified GCE exhibited high selectivity, wide linear ranges, lower detection limit and good sensitivity. Besides, CuO/PVA/ GCE was used to analyze the mercury in real samples such as river water, tab water, laboratory water the satisfactory recovery results were obtained. On the other hand, the CuO/PVA composite played excellent catalyst towards the photo degradation of MB under visible light irradiation. The obtained results from the UV-Vis spectroscopy clearly suggested that CuO/PVA composite had high photocatalytic activity compared than CuO.



The degradation efficiency of CuO/PVA toward MB is observed about 99% within 120 min under visible irradiation and it shows a good stability by observing the reusability of the catalyst.



Reference:

- [1] Dayeon Choi and Du-Jeon Jang, Facile Fabrication of CuO/Cu₂O Composites with High Catalytic Performances, *New Journal of Chemistry*, 41 (2017) 2964-2972
- [2] Sudhir S. Arbuj Ranjit R. Hawaldar Uttamrao P. Mulik, Bina N. Wani, Dinesh P. Amalnerkar, Suresh B. Waghmode, Preparation, characterization and photocatalytic activity of TiO₂ towards methylene blue degradation, *Materials Science and Engineering B* 168 (2010) 90-94.
- [3] Nael, G. Yasri, Ashok, K. Sundramoorthy, Woo-Jin Chang and Sundaram Gunasekaran, Highly selective mercury detection at partially oxidized graphene/poly(3,4-ethylenedioxythiophene):poly(styrenesulfonate) nanocomposite film-modified electrode, *frontiers in materials* 1(2014) 1-33.
- [4] Danhong Wu, Qing Zhang, Xia Chu, Haibo Wang, Guoli Shen, Ruqin Yu, Ultrasensitive electrochemical sensor for mercury (II) based on target-induced structure-switching DNA, *Biosensors and Bioelectronics* 25 (2010) 1025-1031

2.13 Electron beam irradiated Polypyrrole nanospheres in selective determination of L-Tyrosine

D. Nathiya and J. Wilson*

*Polymer Electronics lab, Department of Bioelectronics and biosensors, Alagappa University, Karaikudi – 630004
Email: nathiyad725@gmail.com*

Research on the development of high surface area materials for the sensing of biomolecules by electrochemical method is becoming a hot area of research. Among various abundant conducting polymers Polypyrrole (PPy) plays a vital role in electrochemical sensing due to its stability, conductivity, sensitivity and better biocompatibility [1]. Further enhanced conductivity also achieved by electron beam (EB) irradiation on polymer nanomaterial which results in increased conductivity, mobility, dielectric constant, solubility, percentage of crystallinity and also decrease in d-spacing, inter-chain separation, thermal stability and T_g [2-3]. Tyr is the precursor of hormones and neurotransmitters which are responsible in causing Parkinson's disease, atherosclerosis, viral infection, autoimmune disorders, depression and tumor [4]. The deficiency of Tyr in human body could cause albinism and alkaptonuria and the more concentration results in sister chromatid exchange [5]. It acts as an antioxidant and additives in dietary, food products and to the pharmaceutical formulations [6].

In this work, we have synthesized PPy nanospheres (NSs) by oxidative polymerization method via FeCl₃ and then tend to electron beam irradiation for further modification in structural and electronic properties. The EB irradiated PPy NSs based biosensor was employed in selective determination of L-Tyrosine. The structure of the new material was characterized by Scanning Electron Microscopy (SEM), X-ray diffraction (XRD), Raman spectroscopy and the electrochemical behavior of L-Tyrosine was also studied by cyclic voltammetry (CV), Square wave voltammetry (SWV) and amperometry in phosphate buffer solution (PBS) at pH 7.0. The SWV current responses of L-Tyrosine were increased linearly in the range from 0.4 to 600 μM with a lower detection limit of 161 nM.



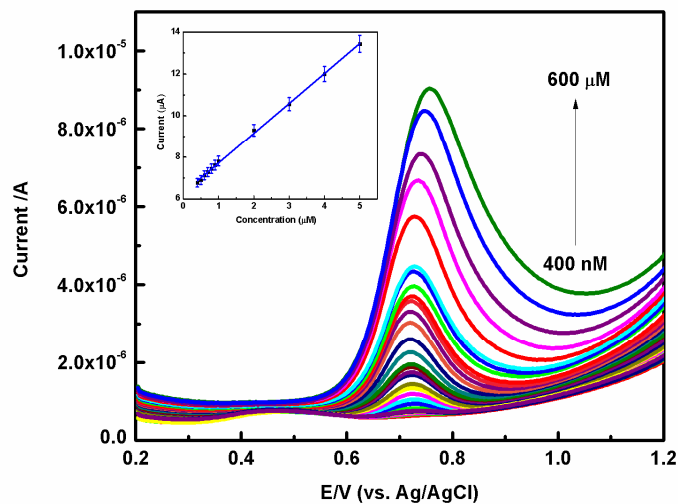


Fig. 1 SWV of L-tyrosine sensing for EB irradiated PPy modified GCE in 0.1 M PBS

References

- [1] A. Ramanavicius, A. Ramanaviciene, A. Malinauskas, *Electrochim. Acta* 51 (2006) 6025.
- [2] S. Bhadra, D. Khastgir, *Polymer Degradation and Stability* 92 (2007) 1824-1832.
- [3] [S. M. El-Sayed, H. M. Abdel Hamid, R. M. Radwan, *Radiation Physics and Chemistry* 69 (2004) 339-345.
- [4] J. Li, D. Kuang, Y. Feng, F. Zhang, Z. Xu, M. Liu, D. Wang, *Microchim Acta* 180 (2013) 49-58.
- [5] Huang, K. J.; Luo, D. F.; Xie, W. Z.; Yu, Y. S. *Colloids and Surfaces B: Biointerfaces* 61 (2008) 176-181.
- [6] Liu, X.; Luo, L.; Ding, Y.; Kang, Z.; Ye, D. *Bioelectrochemistry* 86 (2012) 38-45.



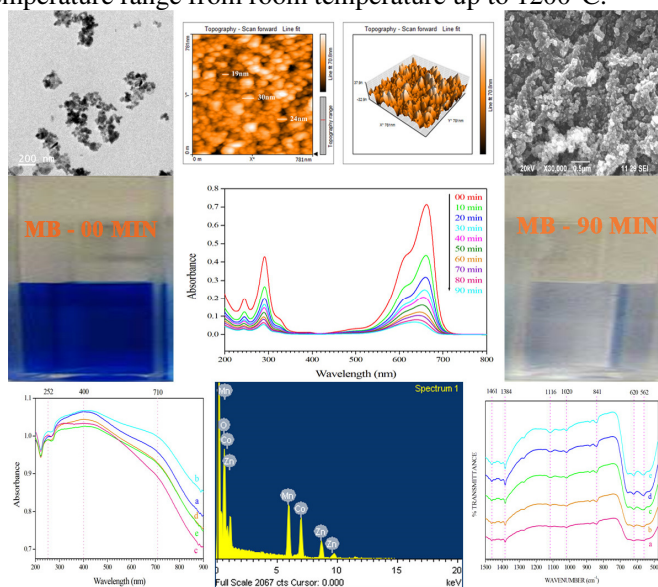
2.14 SYNTHESIS, CHARACTERIZATION AND PHOTOCATALYTIC ACTIVITIES OF Co_3O_4 - MnO_2 - ZnO TERNARY NANOPARTICLES

S. Alwin David and Dr. C.Vedhi*

Department of Chemistry, V.O Chidambaram College, Tuticorin 628008, Tamilnadu, India
E-mail: cvedhi23@gmail.com

ABSTRACT:

Nano Co_3O_4 - MnO_2 - ZnO mixed oxides were prepared by wet chemical method by mixing of equimolar solutions of cobalt chloride, manganese(II) sulfate and zinc sulfate in aqueous sodium hydroxide and refluxed at elevated temperature. The prepared mixed nano oxides were characterized by FT-IR, XRD, UV – Vis DRS, TEM, SAED, SEM, EDAX and AFM. The FTIR spectra expose the presence of M-O bonds (M = Co, Mn, Zn). From XRD studies, the size of the Co_3O_4 - MnO_2 - ZnO NPs are found to be 10.13 - 25.65nm through Scherrer's formula. The XRD patterns also reveal that the particle size is drastically increased with increasing concentration of the precursors. From UV-Vis diffuse reflectance spectra (DRS), band gap energies of the (0.1 – 0.5M) Co_3O_4 - MnO_2 - ZnO NPs are found to be in the range of 3.04 - 3.1eV. The TEM, SEM and AFM micrographs of 0.1M Co_3O_4 - MnO_2 - ZnO NPs display roughly spherical shape with size ranging from 10 - 30nm. SAED pattern confirms the crystalline nature of these nanoparticles. EDAX analysis indicates the presence of Co, Mn, Zn and O. The average surface roughness (S_a) and the root mean square roughness (S_q) of the Co_3O_4 - MnO_2 - ZnO NPs are 8.0082nm, 10.666nm respectively. From the TG analysis, a total mass loss of 12.92% can be observed in the temperature range from room temperature up to 1200°C.



The photocatalytic activity of Co_3O_4 - MnO_2 - ZnO NPs was evaluated for degradation of methylene blue (MB) under sunlight. Among the samples, 0.1M Co_3O_4 - MnO_2 - ZnO NPs with smaller particle size (10.13nm) exhibits stronger photocatalytic activity (91.98%) as compared to other NPs with larger particle size (10.65 – 25.65nm size). This can be explained as smaller particle have large surface area than that of larger particle, hence adsorbs more dye and leads to stronger interaction between MB and photocatalyst. Furthermore, the photocatalytic activity is affected by photocatalyst particle size, photocatalyst dosage, dye concentration and pH of dye solution.

KEYWORDS: Co_3O_4 - MnO_2 - ZnO NPs, Methylene blue, Photocatalyst, Photodegradation.



2.15 Synthesis and Characterization of N-doped ZnO Nanoparticles for Glucose sensor

Tamilselvan Ganesan, M. Chinnadurai and Gurunathan Karuppasamy*

*Department of Nnaoscience and Technology, Science Campus, Alagappa University,
Karaikudi- 630003. Ph: 04565-225630; E-mail: kgnathan27@rediffmail.com*

Abstract

N-doped zinc oxide powder (ZnO:N) have been realized as potential matrix for the development of the biosensor applications. Herein, we have synthesized N-doped ZnO nanoparticles through simple co-precipitation, method and correlation between the changes in property of the ZnO nanoparticles with N doping concentration has been studied. The synthesized nanoparticles were characterized by various physicochemical techniques such as XRD, FTIR, UV and FESEM. The electrochemical catalytic activities of the nanoparticles were examined by the cyclic voltammetry, impedance spectroscopy and amperometry techniques. The nitrogen doping on the ZnO nanoparticles (N-ZnO) alters its defects profile, thus improving the charge transfer characteristics and resulting in an enhanced peak oxidation current in the cyclic volt meter in comparison to that of the pure ZnO nanoparticles.

Key words: Nanoparticles, N-doped ZnO, Glucose sensor, Biosensor

2.16 Synthesis and Characterization of RGO-ZnO Nanocomposite

S. Muthumariappan and C.Vedhi*

PG & Research Department of Chemistry, V.O Chidambaram College, Tuticorin –628008, Tamilnadu, India

Abstract

A simple one-pot hydrothermal synthesis strategy has been approached to prepare the composite *viz.* reduced graphene oxide-ZnO nanoparticles (~30 nm)(RGO-ZnO).The synthesized RGO-ZnO composite has been successfully applied for glassy carbon electrode (GCE) surface modification. The RGO-ZnO composite-modified GCE is applied for sensitive and selective determination of Methyl Parathion (MP).The as-prepared composite is characterized by using Fourier Transform Infra-Red Spectroscopy(FT-IR),Scanning Electron Microscopy (SEM) along with Energy Dispersive X-ray (EDX) and elemental mapping. The atomic force microscopy (AFM) and TEM with SAED analysis confirm the presence of ZnO nanoparticles embedded over the entire surface of reduced graphene oxide.

The prepared RGO-ZnO nanocomposite was characterized using FT-IR spectroscopy and shown in Fig. 1.The reduction of oxygen containing functional groups in the GO after the thermal treatment was confirmed by FT-IR analysis. The spectrum of GO exhibits several distinct peaks related to oxygen functional groups at 3400 cm^{-1} (OH stretching vibration),1726 cm^{-1} (C=O stretching vibration), 1621 cm^{-1} (O-H bending and aromatic C=C, skeletal ring vibrations from the graphitic domain), 1380 cm^{-1} (C-OH stretching vibrations), 1240 cm^{-1} (C-O stretching vibrations of epoxy gp), and 1108 cm^{-1} (C-OH stretching vibrations, but after hydrothermal reduction the intensity of these peaks dramatically decreased in both the pure RGO and RGO-ZnO composite. The spectrum of pure ZnO shows a peak at 470 cm^{-1} corresponding to the Zn-O stretching vibration. This peak was red-shifted to 440 cm^{-1} in the RGO-ZnO composite due to interactions between the ZnO and residual epoxy and hydroxyl functional groups of the RGO.

The surface morphology was investigated by AFM studies. Higher roughness value of RGO-ZnO as shown in Fig 2 than GOES again confirms the composite formation by its better adsorption nature.



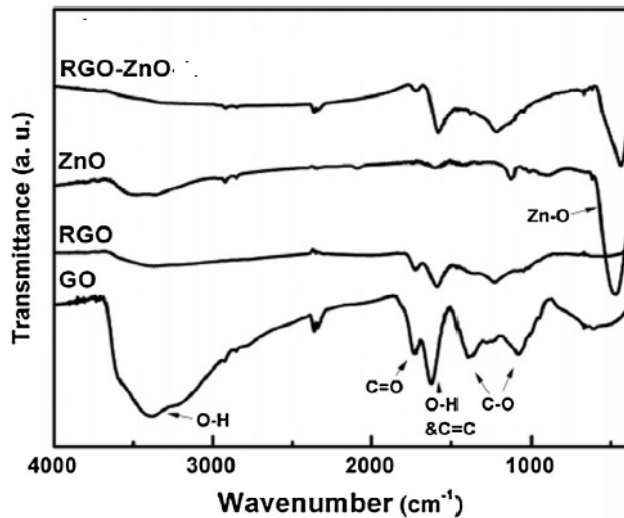


Fig 1. FTIR behaviour of nanocomposite

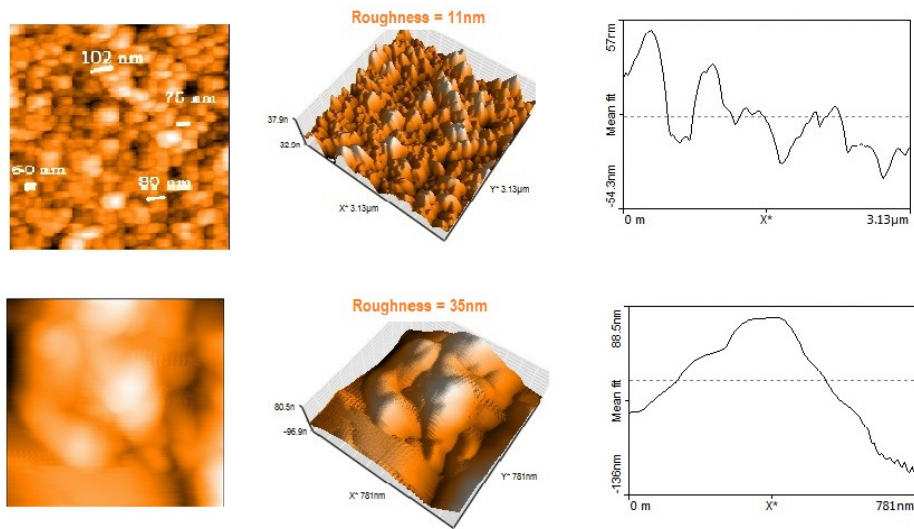


Fig 2. AFM studies of nanocomposite



2.17 A BIO-DERIVED CARBON QUANTUM DOTS FUNCTIONALIZED WITH CONDUCTING ORGANIC POLYMERS FOR ENERGY STORAGE APPLICATIONS

A. Gowrisankar¹ and T. Selvaraju^{2*}

¹Department of Chemistry, Karunya University, Coimbatore-641114

²Department of Chemistry, Bharathiar University, Coimbatore-641046

Email: veluselvaraju@gmail.com, agk.gowrisankar@gmail.com

Abstract

Carbon Quantum Dot (CQDs) is one of the most intensive research topics in the field of material science due to their extremely small size (1-10 nm), excellent dispersibility, low toxicity, good conductivity, functionality, biocompatibility and ease of preparation from different carbon based resources. All such credits help CQD to find applications in the fields of optoelectronic, energy conversion, bio-imaging, drug delivery, sensors, catalysts, etc [1]. Nowadays, CQDs based sensor and energy storage application have attracted due to their novel properties such as high photostability, biocompatibility, low toxicity. Further, chemical doping is the introduction of heteroatom such as nitrogen, boron, sulphur, and phosphorus into the CQD which enhances the chemical and physical properties.



More interestingly, the CQDs/doped CQDs exhibit significant electrical and luminescent properties. The CQDs/doped CQDs can be prepared by various methods such as hydrothermal, solvothermal and microwave irradiation.

During the past few years, CQDs have been prepared by using various precursors such as citric acid, ascorbic acid, sucrose etc. Moreover, Sugarcane bagasse is one of the agricultural waste which is developed as a carbon based material. Sugarcane bagasse is fibrous form from rod like cane and it consists of cellulose 37.65 % with carbon upto 25 %. Thus, the high percentage of carbon in sugarcane bagasse made as the potential waste for carbon resource through combustion. Therefore converting bagasse to carbon material is one of the best eco-friendly approaches. To build up high performance capacitors, various conductive polymers can be adopted to enhance the electrochemical capacitance behaviour of the electrode materials. For example, Polyaniline (PANI), Polypyrrole (PPy), Polythiophenes (PT) are extensively used in the advanced energy storage applications.

In this respect, herein, the EDLCs based SC using bio-derived CQDs from the sugarcane bagasse where the conductive polymer (i.e. polyaniline and polypyrrole) was incorporated with CQDs via normal stirring for 2 h at room temperature was developed. Finally, the samples were filtered and dried in hot air oven at 90 °C. Further, the characterization of the samples was studied by UV-Vis spectroscopy, FTIR and SEM. The prepared carbon material composites were successfully applied for the supercapacitor application using cyclic voltammetry and galvanostatic techniques.

Reference:

- [1] [1] S. Y. Lim, W. Shen, Z. Gao, *Chemical Society Reviews.*, 44(1),(2015),362–81.



2.20 Optical and conductivity properties of 2, 5 dimethoxy polyaniline / tin oxide nanocomposites

M. Senthil kumar¹ and P. Manisankar^{*2}

¹Department of Chemistry, Alagappa Chettiar College of Engineering and Technology, Karaikudi-630 003. Tamilnadu, India.

²Department of Industrial chemistry, Alagappa University, Karaikudi-630 003. Tamilnadu, India. Ph:+914565228836, Fax: +914565225202.

*Corresponding author Email: pms11@rediffmail.com, senthilshrivi@gmail.com.

Abstract

2, 5 - Dimethoxypolyaniline (DPMA) / Tin oxide nano composites, synthesized by incorporation of separately prepared Tin oxide nano particles in acid medium of 2, 5 – dimethoxyaniline (DMA) using potassium peroxodisulfate as an oxidant. The crystal structure of the Tin oxide nano particles and 2, 5 dimethoxy polyaniline / Tin oxide nano Composites at the annealed temperature of 500°C and 800°C were characterized by X-ray powder diffraction (XRD). Images of Tin oxide nano particles, DPMA and DPMA-wt% Tin oxide nano composite was observed by Scanning Electron Microscope. UV-Visible spectroscopy and Impedance spectroscopy characteristic were performed the Optical and Electrical conductivity of DPMA and DPMA -wt% Tin oxide and Tin oxide nano composites. Optical and electrical characteristic indicated that the electrical properties of PMA/ SnO₂ composites are dominated by doping SnO₂ nanocomposite.

Keywords: SnO₂ nanoparticles, DPMA-wt% SnO₂ nano composites, UV, XRD, and Impedance spectroscopy.

2.21 Development of TiO₂ Nanofiber and nanoparticle composite photo-anode for planar structure formamidinium lead iodide perovskite solar cell

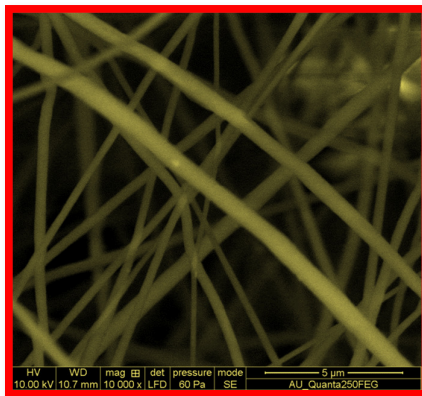
K.SAKTHI VELU, B. SUGANYA BHARATHI, P.MANISANKAR and T.STALIN*

Photo-electrochemistry lab, Department of Industrial Chemistry, Alagappa University, Karaikudi-03, Tamilnadu-India.

E-mail address: drstalin76@gmail.com, tstalinphd@rediffmail.com

Abstract:

Electrospun TiO₂ nanofiber & nanoparticle were prepared for formamidinium lead iodide perovskite solar cell. The prepared TiO₂ nanofibers and nanoparticles were characterized that the FE-



SEM, XRD pattern, FT-IR, UV-Visible spectral analysis and electrochemical impedance studies (EIS). The FE-SEM images result was observed that the formation of TiO₂ nanofiber and incorporated with the nanoparticles. The formation of composite photo-anode in anatase phase was confirmed that the XRD pattern analysis. FT-IR and UV-Visible spectra were determined the functional group of electrospun TiO₂, nanoparticle and their absorption maximum. The highest ionic conductivity with the range of 3.01 X 10⁻⁵ Scm⁻¹ at room temperature achieved by the AC impedance spectroscopy.



FE-SEM image of TiO₂ nanofiber and Nanoparticle photo-anode. The TiO₂ Nanofiber and nanoparticle composite photo-anode used in the fabrication of perovskite solar cell gave the sunlight-into-electrical energy conversion efficiency of 13.4%.

Keywords: Electrospun TiO₂ nanofibers, Nanoparticle, Photo-anode, Perovskite solar cell, Efficiency.

2.22 Facile synthesis and physical analyses of Sulfur/Carbon nanofibre composite via Solid State Reaction

P.Rajkumar, S.Sasikala, K.Diwakar, R.Subadevi*, M.Sivakumar

#120, Energy Materials Lab, Department of Physics, Alagappa University,
Karaikudi - 630 003, Tamil Nadu, India.

(* Corresponding Author: susimsk@yahoo.co.in; susiva73@yahoo.co.in)

Abstract

The increasing demands for electric vehicles and portable electronic devices require rechargeable batteries that are low cost, light weight, and long life. Among the various rechargeable batteries, Lithium-sulfur (Li-S) batteries are one of the most promising contenders that could satisfy this developing market as they possess a high specific capacity (1672 mA h g⁻¹) and energy density (2500 W h kg⁻¹), which are 3-5 times higher than those of Li-ion battery cathodes [1,2]. In addition, the elemental sulfur has the advantage of being low-cost, naturally abundant, and eco-friendly. However, several issues associated with the sulfur cathodes, namely insulating nature of sulfur, volume expansion of sulfur during discharge and dissolution polysulfides in electrolyte. In order to resolve these problems, researchers focus on finding suitable carbon/sulfur composite materials in its place of elemental sulfur to improve the utilization of sulfur and the cycle durability of the cathode. Carbon is not only represented as electrical conductor but also supplied electrochemical reaction sites for sulfur [3-5].

In the present study, sulfur - carbon nanofibre composite material was prepared by solid state reaction. The carbon nanofibers (CNFs) are excellent carbon source material for the sulfur electrode. CNF is an attractive choice as the electronic conductor for the sulfur electrode because they can provide more effective electronically conductive network than the other conductive additives, such as carbon black (CB), acetylene black (AB) and graphite [6,7]. The prepared composite was characterized for structural and morphological information using X-ray diffraction (XRD), Raman spectroscopy and Scanning electron microscopy (SEM) analyses. From the XRD analysis, the prepared S/CNF composite has been identified as orthorhombic structure (JCPDS 08-0247). Raman analysis confirms the presents of carbon phase in the S/CNF composite. SEM images describe that the sulfur particles well dispersed in the as-prepared composite. From these analyses, it is noted that the prepared composite can be a suitable candidate for Li-S battery fabrication.

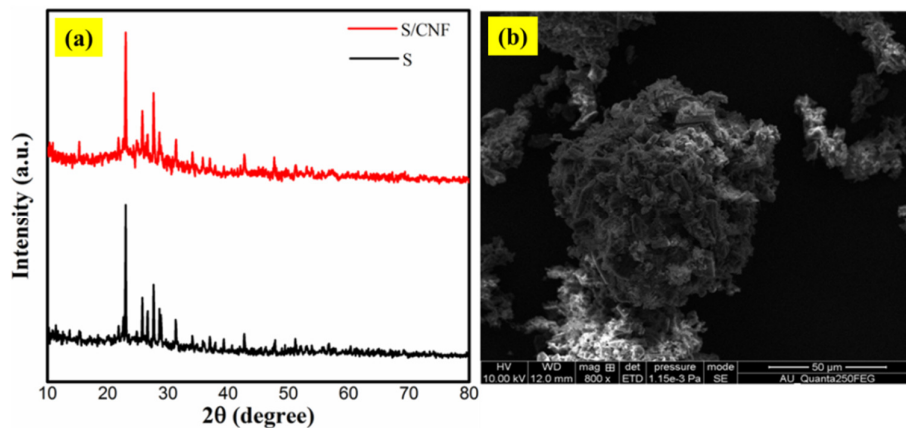


Figure 1. Fig (a) XRD patterns of pure S and S/CNF composite, (b) SEM image of S/CNF composite



Reference

- [1] P. Jamdagni, P. Khatri, J.S. Rana (2016). Green synthesis of zinc oxide nanoparticles using flower extract of *Nyctanthes arbor-tristis* and their antifungal activity. *Journal of King Saud University – Science*, doi.org/10.1016/j.jksus.2016.10.002
- [2] G. Bisht, S. Rayamajhi (2016). ZnO Nanoparticles: A Promising Anticancer Agent. *Nanobiomedicine*, 3:9, doi: 10.5772/63437 1

2.24 Antibacterial treatment of Textile Effluent by Immobilized MgO NPs in a Column Reactor

Kavitha Manoharan 1, Arumugam Ayyakannu 2*

*1*Department of Nanoscience and Technology, Alagappa University, Karaikudi – 630 003. Tamil Nadu, India.

*2**Department of Botany, Alagappa University, Karaikudi – 630 003. Tamil Nadu, India.

Corresponding Author E-Mail: sixmuga@yahoo.com

Abstract

The bactericidal effect of Metal Oxide Nanoparticles has been attributed to their small size and high surface to volume ratio, which allows them to interact closely with microbial membranes and is not merely due to the release of metal ions in solution. MgO NPs were prepared by chemical synthesis method that was used as both reducing and stabilizing agent to control the nanoparticles size. The UV-Visible spectrum showed a peak between 300 nm corresponding to the Plasmon absorbance of the MgO NPs. X-Ray Diffraction (XRD) and Scanning electron microscope (SEM) were used to analyze the crystalline structure of MgO NPs. Immobilization of MgO NPs is done by using Biopolymers that should not affect the property of the MgO NPs. Immobilized Nano metal oxides create opportunities in a wide range of sectors including environmental pollution control. Compared with suspended particles, immobilization shows many advantages, such as resistance to toxic chemicals, easy handling and reusability. The antibacterial activity of the immobilized MgO NPs was evaluated using column reactor against the textile effluent bacteria counts in wastewater. The ability of immobilized MgO NPs was tested against 6 bacterial species that are isolated and identified from the textile effluent. Initially the bacterial isolates are screened and cultivated in the nutrient media. The antibacterial activity of the MgO nanoparticles was determined using disc diffusion method in Muller Hinton agar plate in different concentrations.

Key words: Textile Effluent, *Citrus medica*, MgO NPs, Antibacterial, Immobilization, Column Reactor

2.25 One-step hydrothermal synthesis of iron oxide nanoparticles for photocatalytic and antimicrobial applications

PR. Kaleeswarran^a and A. Arumugam^{b*}

*a*Department of Nanoscience and Technology, Alagappa University, Karaikudi – 630 003. Tamil Nadu, India.

Presenting Author E-Mail: kaleeswarran@gmail.com

*b**Department of Botany, Alagappa University, Karaikudi – 630 003. Tamil Nadu, India.

Corresponding Author E-Mail: sixmuga@yahoo.com

Abstract:

Iron oxide nanoparticles (NPs) synthesis were carried out by simple one step hydrothermal method. Synthesized NPs were characterized and average crystalline size was determined by X-ray diffraction (XRD). Morphology of the synthesized Fe₃O₄ NPs was identified using Scanning Electron Microscopy (SEM). Further Fe₃O₄ NPs was characterized by FTIR and TGA.



In further investigation, synthesized metal oxide NPs used for photocatalytic degradation of Methylene Blue under visible irradiation. The feasibility of utilizing this material for antibacterial application was also studied on both Gram Positive and Gram Negative bacteria as follows Staphylococcus aureus (S. aureus), Streptococcus pneumoniae (S. pneumoniae), Bacillus Subtilis (B. subtilis) and Escherichia coli (E. coli), Klebsiella pneumoniae (K. pneumoniae), Proteus vulgaris (P. vulgaris). Finally, the study alleviates the synthesis of Fe₃O₄ which attribute the greater affinity towards the antibacterial and photocatalytic activities for industrial effluent.

Key Words: Hydrothermal method, Fe₃O₄ nanoparticles, antimicrobial activity, photocatalytic activity.

2.26 Synthesis of chitosan nanoparticles using *Penaeus semisulcatus* shells and their growth impact on *Sphaeranthus indicus* medicinal plant

C. Balalakshmi^{a*}, K. Gopinath^b, S. Abinaya^a, A. Arumugam^b, K. Gurunathan^a

^a Department of Nanoscience and Technology, Alagappa University, Karaikudi - 630 003, Tamil Nadu, India.

^b Department of Botany, Alagappa University, Karaikudi - 630 003, Tamil Nadu, India.

*Corresponding author E-mail: samyasribala@gmail.com

Abstract

Past two decades, modern world consume the downstream process of nanoscience and technology for counterpart in day to day lifestyle. In this point of nanotechnology, 'high surface to volume ratio' plays a significant role of nanomaterials when compare to bulk materials. Because, it's contains different physicochemical properties at nano scale level (1-100 nm). By this technology, predictable size and shape was key role for all other application. Intent of our research, synthesis of chitosan NPs derived from *Penaeus semisulcatus* shells. Synthesized nanomaterials were characterized by UV, FTIR, XRD and TEM analysis. In addition to that, chitosan NPs were investigated against gram positive and negative bacterial strains. In connection with different dosage of chitosan NPs (0.1, 0.3, 0.5, 0.7, and 1.0%) were treated in to *in vitro* plant tissue culture technique by rooting gel method. In this treatments were evaluate improvement for vegetative growth of *Sphaeranthus indicus* an important medicinal plant. In this easiest protocol determined the large scale industrial production of chitosan NPs and it's applied for scarce medicinal plant conservation through plant tissue culture route.

Key words: *Penaeus semisulcatus* Chitosan, Nanoparticles, *Sphaeranthus indicus*, Vegetative growth, TEM,

2.27 Biotemplate-ZnO/graphene nanocomposite for better photocatalytic performance

M.Karpuraranjith, S.Thambidurai*

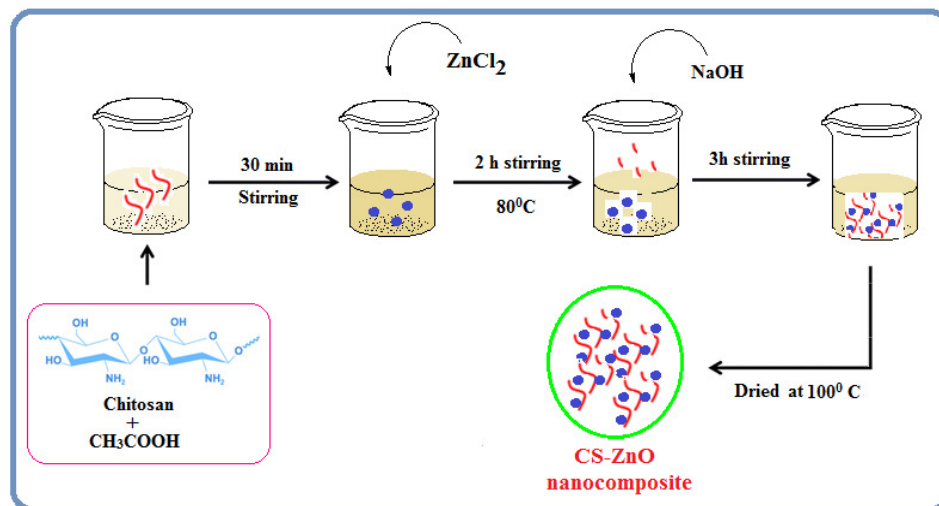
Department of Industrial Chemistry, School of Chemical Sciences, Alagappa University, Karaikudi - 630003, Tamil Nadu,
Email: ranjith3389@gmail.com

Abstract

Chitosan (biotemplate) is one of the promising natural biopolymer on earth used in wide range of applications with excellent film forming abilities, biocompatibility, non toxicity, good water permeability, metal ion adsorption, high mechanical strength, susceptible to chemical modification due to the presence of reactive hydroxyl and amino functional groups. Graphene (G) is a single layer with to dimensional structure of carbon atoms. It has extensively interesting research topic for the reason that distinctive property such as the mechanical, thermal and excellent electrical conductivity. It's promising candidate in wide range of applications for storage devices, catalysts, optoelectronic, chemical sensors, ash memory storage devices, transparent conductors and super capacitors. Zinc oxide (ZnO) is used as wide range of applications such as energy storage, gas-sensing materials and antireflecting coatings in solar cells.



Key words: Chitosan, Zinc oxide, Thermal stability, Antibacterial activity.



Schematic preparation of the CS-ZnO nanocomposite.

References

- [1] M. Dash, F. Chiellini, R.M. Ottenbrite, E. Chiellini, *Progress in Polymer Science* 36 (2011) 981–1014.
- [2] K. Pandiselvi, S.Thambidurai, *Materials Science in Semiconductor Processing* 31(2015) 573–581.
- [3] Hamed Mirzaeia, Majid Darroudi, *Ceramics International*, 43 (2017) 907-914.
- [4] L. Naamani, S. Dobretsov, *Innovative Food Science & Emerging Technologies*, 38 (2016) 231-237.
- [5] R. Jayakumar, M. Prabakaran, *Biotechnology Advances*, 29 (2011) 322-337.

2.29 One-step hydrothermal synthesis of Palladium nanoparticles and reduced graphene oxide nanocomposite for enhanced antibacterial activities

R.Rajeswari, and H.GurumallesPrabu *

*Department of Industrial Chemistry, School of Chemical Sciences
Alagappa University, Karaikudi-03, Tamilnadu, India
E-mail: hgprabu2010@gmail.com and rajiraji756@gmail.com*

Abstract

One-step approach for the synthesis of palladium (Pd NPs) nanoparticles on reduced graphene oxide (rGO) nanocomposite was prepared by hydrothermal procedure. The reduction of graphene oxide was occurred at one pot method. The synthesized Pd nanoparticles were successfully decorated on graphene oxide (GO) nanosheets. The prepared nanocomposites were characterized by X-ray diffraction spectroscopy (XRD), Fourier transform spectroscopy (FT-IR), Scanning electron microscopy (SEM), and Transmission electron microscopy (TEM). Pd-rGO nanocomposite was experimentally analyzed for its antibacterial activity, results have revealed that the prepared nanocomposite exhibited significantly improved antibacterial activities against gram positive bacteria in contrast to rGO and pure Pd nanoparticles, Minimal inhibitory concentration (MIC) was determined. Pd-rGO exhibited significant antibacterial activity at minimum concentration levels.

Keywords: Hydrothermal, Nanocomposite, Antibacterial activity.



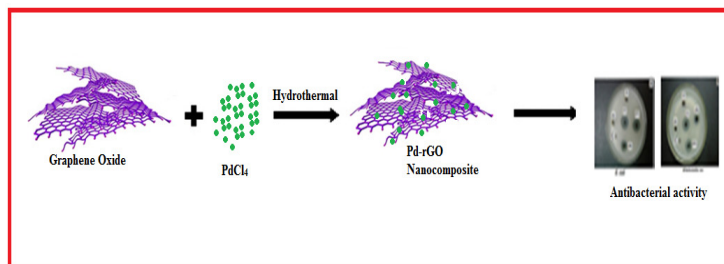


Fig. 1. Schematic preparation of Pd-rGO nanocomposite.

References

- [1] S.Pourbeyrama, A. Sharafiana, A. Tanomandb, P. Azama, Biomolecule-assisted synthesis of Ag/reduced graphene oxide nanocomposite with excellent electrocatalytic and antibacterial performance, *Materials Science and Engineering: C*, 75 (2017) 742–751.
- [2] R. Bayrami, H. Dadkhah, Green synthesis and characterization of ultrafine copper oxide reduced graphene oxide (CuO/rGO) nanocomposite, *Colloids and Surfaces A: Physicochemical and Engineering Aspects*, 529 (2017) 73–79.
- [3] X. Ji, b, Y. Song, J.Hana, L. Ge, X. Zhao, C. Xu, Y. Wang, D. Wu, H. Qiu, Preparation of a stable aqueous suspension of reduced graphene oxide by a green method for applications in biomaterials, *Journal of Colloid and Interface Science*, 497 (2017) 317–324.
- [4] M. Sookhakiana, E. Zalnehada, Y. Aliasb, Layer-by-layer electrodeposited nanowall-like palladium-reduced graphene oxide film as a highly-sensitive electrochemical non-enzymatic sensor, *Sensors and Actuators B: Chemical*, 241 (2017) 1–7.
- [5] J. Hua, Z. Zhaoa, J. Zhanga, G. Lia, P. Lia, W. Zhanga, K. Liana, Synthesis of palladium nanoparticle modified reduced graphene oxide and multi-walled carbon nanotube hybrid structures for electrochemical applications, *Applied Surface Science*, 396 (2017) 523–529.

2.30 Ionic liquid mediated green synthesis of CeO₂-ZrO₂ core metal oxide nanoparticles and its Antioxidant activity

P. Nithya^a, M. Balaji^a, S. Jegatheeswaran^a, S. Selvam^b and M. Sundrarajan^a *

^aAdvanced Green Chemistry Lab, Department of Industrial Chemistry, Alagappa University, Karaikudi- Tamil Nadu, India.

^bLaser and Sensor Application Laboratory, Engineering Building, Pusan National University, Busan - 609735, South Korea

*Corresponding author: Tel: + 91 94444 96151

E-mail: drmsgreenchemistrylab@gmail.com and nithya2291415@gmail.com

Abstract

Green synthesis of metal or metal oxide nanoparticles using plant extract is a promising alternative to traditional method of chemical synthesis. Cerium and zirconium metal oxide nanoparticles (CeO₂-ZrO₂ core metal oxide NPs) system has good oxygen storage capacity, high thermal stability, high surface area, and good redox properties. Herein, a facile and eco-friendly method for the synthesis of CeO₂-ZrO₂ core metal oxide NPs using ionic liquid (IL) mediated an ethanolic solution of *Justicia adhatoda* (JA) leaves extract. Nanoparticles (NPs) synthesized at room temperature using an ionic liquid (IL) as a mediator for the nucleation and growth process.

Preparation of CeO₂-ZrO₂ core metal oxide NPs

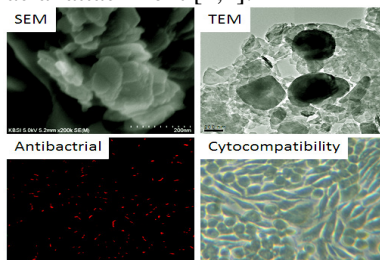
Cerium zirconium core metal oxide (CeO₂-ZrO₂) nanoparticles were prepared by greener method by cerium chloride and zirconium oxychloride used as a precursor with environment benign *Justicia adhatoda* leaves extract, and [BMIM] PF₆ (IL) is a capping agent. [CeCl₃.7H₂O] solution (0.1N), [ZrOCl₂. 8H₂O] solution (0.1N) and 1mL of [BMIM] PF₆ (IL) were added to the aqueous solution of *J. adhatoda* leaves extract under vigorous stirring for 6 hours continuously at room temperature. The resulting samples were filtered, washed with distilled water and dried at 100° C.



reaction pH (10 ± 0.5) and the mixture was stirred vigorously at room temperature for 2 h. After the stirring, the Yttrium source was added to the reaction mixture under stirring at 60 °C for 30 min.

Results and Discussion

The nanocrystalline composites were made effectively by an ionic gelation of ionic liquid of apatite phase were confirmed by FT-IR and XRD investigations. The morphology improved apatite crystal phase was uniformly incorporated by yttrium surface was displayed by SEM and TEM microscopic techniques, which was determined that the fine morphological HAp nanocrystals and Yttrium NPs have favorable interfacial attachment [1,2].



Conclusion

The Yttrium doped hydroxyapatite exhibit excellent crystallinity, antibacterial efficacy, cytocompatibility properties. It is concluded that these nanocomposites may be probable material for hard tissue regeneration applications.

References

- [1] M. Sundrarajan et al., Materials and Design 88 (2015) 1183-1190.
- [2] H. Cao et al., J. Phys. Chem.C 114 (2010) 18352–18357

2.32 NANO POLYMER BIO COMPOSITES FOR ELECTRONIC APPLICATION

Boopalan. M

*Department of Chemistry, Pachaiyappa's College for Men, Kancheepuram-631501.
Email address: boopalanm@gmail.com
Phone no : +91-9600572111*

Abstract

This Research work addresses the various issues that occur when the environmental impact of natural fibers is critically evaluated. Nano Sisal fibers (NSF) were prepared from the Sisal fiber by chemical and physical method. They were characterized by the Fourier Transformed Infra-Red Spectroscopy (FTIR), Field Emission Spectroscopy (FE-SEM) and High Resolution Transmission Electron Microscopy (HR-TEM). Epoxy polymer based composites reinforced with NSF at different loading of 1, 2, 3, 4, 5, 6, 7 and 8 wt. % were prepared by compression moulding. These NSF-composite samples were characterized by mechanical properties, thermal analysis, moisture uptake behaviour, scanning electron microscopy (SEM) and atomic force microscopy (AFM). The 7 wt. % NSF loaded composite sample revealed better properties than other wt. % of NSF.

Key words: Nano Sisal fiber, fracture behaviour, mechanical properties, HDT



Antibacterial activity result

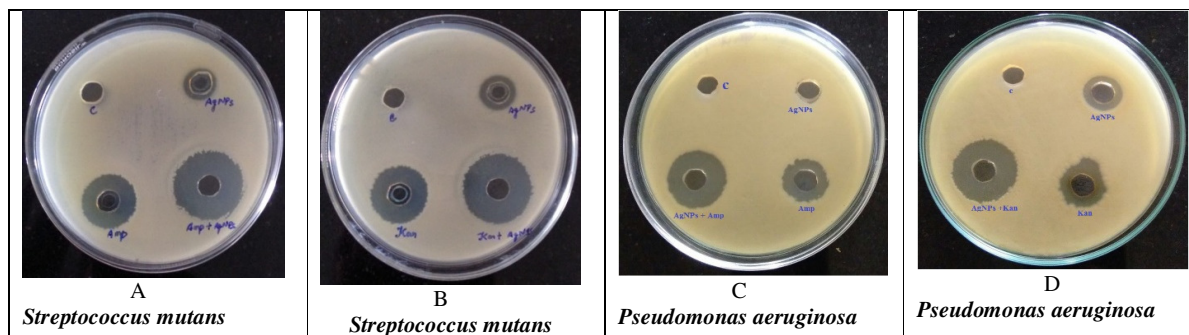


Fig.2 Antibacterial activity of AgNPs against both gram positive *Streptococcus mutans* and gram negative *Pseudomonas aeruginosa* bacteria

The pure AgNPs and conjugated with antibiotics exhibited interesting antibacterial activity against both gram positive (*Streptococcus mutans*) and gram negative *Pseudomonas aeruginosa* bacteria using well diffusion method. Control is also maintained in which no zone of inhibition is obtained. The photographs in Fig. 2 A -D clearly show the zone of inhibition for pure AgNPs, AgNPs conjugated with ampicillin and AgNPs conjugated with kanamycin. The highest zone of inhibition is observed in AgNPs conjugated with both antibiotics against both gram positive and gram negative bacteria. The least zone of inhibition is observed in pure AgNPs.

References

- [1] J. K. Salem, I. M. El-Nahhal, A. Bassam, Najri, M. Talaat, Hammad, *Chemical Physics Letters*, 664 (2016) 154.
- [2] C. Wang, D. Chen, Q. Wang, R. Tan, *Biosensors and Bioelectronics* 91 (2017) 262.



3. Sensor Technologies

3.1 Electrochemical Immunosensors –Universal Tools for Rapid Detection of Antigens and Antibodies

Hanna Radecka*, Jerzy Radecki

Polish Academy of Science Tuwima 10, 10-748 Olsztyn, Poland

*h.radecka@pan.olsztyn.pl

The naturally high selectivity and efficiency of pathogens - antibodies binding make immunosensors very promising analytical tools.

Here, we report examples of successful developing of several type of immunosensors destined for the detection of Highly-Pathogenic Avian Influenza type H5N1 virus (HPAI), markers for neurodegenerative diseases (protein S100 β , amyloid – β peptide, glycosylated albumin). The immunosensors were developed by the successive modification of gold¹⁻² as well as glassy carbon electrodes³. The whole antibody or their fragments have been applied as the sensing elements. The complex between antigens and specific antibody adsorbing on a surface of an electrode forms an insulating layer. This phenomenon, which is a base of ion – channel mimetic type of immunosensors, can be monitored by the electrochemical impedance spectroscopy (EIS) in the presence of

[Fe(CN)₆]^{3-/4-} as a redox marker. Another type of immunosensors is based on redox active layers incorporated di-pyrromethene -Cu(II)⁴⁻⁷. The changes of electrochemical parameters of redox centers upon target analyte binding are the base of analytical signal generation.

The both type of immunosensors displayed better sensitivity towards viruses as well as antibodies in the comparison to ELISA. They are also very selective. The matrices from: culture media, serum (hen and human), as well as from plum leaves have no influence on the immunosensors performance. In addition, very small analysed sample volume (10 μ l) is needed. After miniaturisation, they keep excellent analytical parameters⁸.

Therefore, immunosensors presented could be recommended for the direct electrochemical detection of viruses as well as antibodies in the natural physiological samples.

References

- [1] Wąsowicz M., Viswanathan S.; Dvornyk A.; Grzelak K.; Kłudkiewicz B.; Radecka H. *Biosensors and Bioelectronics*, 24, 2008, 284-289;
- [2] U. Jaročka, R. Sawicka, A. Góra-Sochacka, A. Sirko, W. Zagórski-Ostoja, J. Radecki, H. Radecka *Biosensors & Bioelectronics*, 2014, 55,301-306;
- [3] U. Jaročka, H. Radecka, T. Malinowski, L. Michalczyk, J. Radecki, *Electroanalysis* **2013**, 25, 433;
- [4] U. Jaročka, R. Sawicka, A. Góra-Sochacka, A. Sirko, W. Zagórski-Ostoja, W. Dehaen, J. Radecki, H. Radecka, *Analytical & Bioanalytical Chemistry*, *Anal Bioanal Chem* (2015) 407:7807-7814;
- [5] E. Mikuła; Wysłouch-Cieszyńska, A.; Zhukova, L.; Verwilst, P.; Dehaen, W.; Radecki, J.; Radecka, H. *Electrochemical biosensor for the detection of glycosylated albumin. Current Alzheimer Research* 2017, 14(3): 345-351;
- [6] Mikuła, E. Sulima, M.; Marszałek, I.; Wysłouch-Cieszyńska, A.; Verwilst, P.; Dehaen, W. Radecki, J.; Radecka, H. *Sensors* 2013, 13(9): 11586-11602
- [7] Mikuła, E.; Wysłouch-Cieszyńska, A. Zhukova, L.; Puchalska, M.; Verwilst, P.; Dehaen, W.; Radecki, J.; Radecka, H.. *Sensors* 2014, 14(6): 10650-10663
- [8] U. Jaročka, R. Sawicka, A. Góra-Sochacka, A. Sirko, W. Dehaen, J. Radecki, H. Radecka, *Sensors & Actuators B: Chemical* 228 (2016) 25-30.

Acknowledgement:

This research was supported by grant NCBiR No. PBS2/A7/14/2014, project 679/N – BELGIUM /2010 and COST Action CM1005 and National Science Centre, Poland, No 2016/21/B/ST4/03834.



3.2 Electrochemical anions recognition in water using gold electrodes modified with dipodal or di-peptide anion receptor attached to dipyrromethene- Me(II) complex

Jerzy Radecki Balvider Kaur, Piotr Gołębiewski*

Institute of Animal Reproduction and Food Research, Polish Academy of Sciences, Tuwima 10, 10-748 Olsztyn, Poland,

In recent decade, the intermolecular recognition of anions in water has been attracted the attention of numerous scientific groups involved in supramolecular chemistry.^{1, 2} The most of literature reports the recognition of anions in one organic phase. Developing systems for the recognition of anions in water medium is still a challenging task. Here, we proposed the first anion recognition study of dipyrromethene modified dipodal anion receptor or dipeptide attached to electrochemically active dipyrromethene-Cu(II) complex or dipyrromethene-Co(II) complex in highly diluted water medium (in the picomolar range). The developed systems were characterized electrochemically using cyclic voltammetry (CV) and Osteryoung square wave voltammetry (OSWV). Both of them were successfully applied for the electrochemical recognition of anions (Cl⁻, Br⁻, and SO₄²⁻) in highly diluted aqueous medium. The results obtained allowed establishing the mechanism of communication between the redox centre and receptor anion complex as well as analytical signal generation.

This work was supported by National Science Centre, Poland, in frame of grant No 2016/21/B/ST4/03834 "Redox active monolayers for exploring of anion recognitions processes in aqueous phase"

3.3 Aggregation Induced Emission of Novel Pyrene based Polyaminal Networks and Selective Sensing of a Polyaromatic Hydrocarbon, Tetracene

Thanasekaran Nandhini^a, Murugesan Shunmughanathan^a and Kasi Pitchumani^{ a,b}*

^aDepartment of Natural Products Chemistry, School of Chemistry, Madurai Kamaraj University, Madurai-21, India

^bCenter for Green Chemistry Processes, Madurai Kamaraj University, Madurai-21, India

Email id: nirmalanandini@gmail.com pit12399@yahoo.com

The pyrene moiety is one of the most useful fluorophores due to its striking efficiency for excimer formation and subsequent changes in its emission properties [1]. On our interest in polyaminal network synthesis and their potential applications, promoted as to introduce the pyrene moiety into the polyaminal networks by a simple one-pot Schiff base condensation. The resultant pyrene based polyaminal networks (PBP), which are in nanometers regime, exhibit aggregation induced emission (AIE) behavior [2-4] in the presence of suitable polar solvents. PBP is characterized and measured by FT-IR, scanning electron microscopy, solid state ¹³C and ¹⁵N CP-TOSS NMR spectroscopy and UV-Visible (UV-VIS), fluorescence spectrophotometries. It is poorly emissive in solution at an excitation wavelength of 360nm. In contrast, the polymer PBP becomes highly emissive at a wavelength of 466 nm, upon addition of water molecules due to aggregation of the pyrene units. It is also found that the nanoaggregates of PBP selectively sense the tetracene over other polyaromatic hydrocarbons and this is attributed to the inclusion of tetracene between the π-π stacking [5] of pyrene moiety.



Ammonia (NH₃) is a toxic gas, which is most commonly used by a fertilizer industry. It is released to the environment as a byproduct of a fossil fuel [3]. Ammonia can cause severe effects on human body like irritation in eyes, throat, skin and respiratory systems when exposed to concentration greater than 35 ppm for even 15 minutes [4]. The synthesized CQDs shows selective and sensitive detection of ammonia in presence of other gaseous with the detection of limit of 250 μM in aqueous medium (Fig.1f).

References:

- [1] Mazzier. D, Favaro. M, Agnoli. S, Silvestrini. S, and Moretto. A, *Chem. Commun.*, 50 (2014) 6592.
- [2] Liu.W, Li. C, Ren. Y, Sun. X, Pan W., Li. Y, Wang J. and Wang W, *J. Mater. Chem. B*, 4 (2016) 5772.
- [3] Shi. H, Shen Y., He F., Li Y., Liu A., Liu. S. and Zhang Y, *J. Mater. Chem. A*, 2 (2014) 15704.
- [4] Nikolina A. Travlou, Seredych. M, and Teresa J. Badosz, *J. Mater. Chem. A*, 3 (2015) 3821.

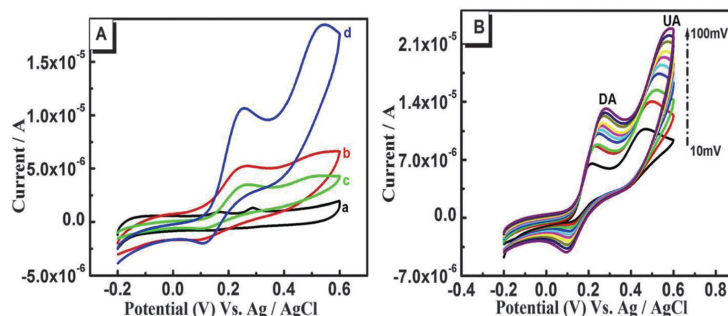
3.6 Au-Pd bimetallic nanoparticles anchored on α-Fe₂O₃ nonenzymatic catalyst for simultaneous electrochemical detection of dopamine and uric acid

R. Ramya¹ and Dr. J. Wilson^{1*}

¹Polymer Electronics Lab, Department of Bioelectronics and Biosensors, Alagappa University, Karaikudi - 630004, Tamilnadu, India.
Email:mranya155@gmail.com

ABSTRACT

We have found that magnetic α-Fe₂O₃ nanocubes exhibit an intrinsic catalytic activity toward the electrochemical sensing of dopamine (DA) and uric acid (UA). Au-Pd bimetallic nanoparticles, which act as efficient signal amplifiers, can be attached to the surface of α-Fe₂O₃ particles to further enhance the catalytic electrochemical signals. The one-step synthesized α-Fe₂O₃@Au-Pd hybrid nanostructure shows significantly well-separated oxidation peaks with enhanced peak currents of DA and UA. We then demonstrated the use of this nonenzymatic nanoelectrocatalyst for individual detection, and the linear responses of DA and UA were in the concentration ranges of 100 nM⁻¹mM and 1 μM⁻¹ mM with detection limits of 1.34 X 10⁻¹⁰ M and 1.8 X 10⁻⁶ M (S/N = 3σ/b), respectively. For simultaneous detection, the same detection ranges were retained with significantly lower detection limits of 1.38 X 10⁻¹¹ M and 597 nM, respectively. The fabricated sensor was finally applied in selectivity tests for the detection of DA and UA with satisfactory results. The practical analytical utility was illustrated by selective measurements of human urine, serum and pharmaceutical drugs without any preliminary treatment.



A) CVs obtained for DA and UA (600 mM) at the (a) bare, (b) α-Fe₂O₃, (c) Au-Pd and (d) α-Fe₂O₃@Au-Pd hybrid nanostructures modified electrodes recorded in PBS (pH 7) at a scan rate of 50 mVs⁻¹ from 0.2 to 0.6 V. (B) CVs obtained for α-Fe₂O₃@Au-Pd hybrid modified electrode at different scan rates (10–100 mV s⁻¹).



References:

- [1] J. Du, R. R. Yue, F. F. Ren, Z. Q. Yao, F. X. Jiang, P. Yang and Y. K. Du, *Biosens. Bioelectron.*, 2014, 53, 220–224.
- [2] S. Sansuk, E. Bitziou, M. B. Joseph, J. A. Covington, M. G. Boutelle, P. R. Unwin and J. V. Macpherson, *Anal. Chem.*, 2013, 85, 163–169.

3.7 SYNTHESIS AND FABRICATION OF Au-NANOPARTICLES DECORATED GO-PANI NANOCOMPOSITES AND THEIR ELECTROCHEMICAL SENSING OF HYDROQUINONE

N. RADHA ^{*a} and K. RAJESHWARI^b

^{*a} *Asst. Professor of Chemistry, Alagappa Govt. Arts College, Karaikudi – 3, Chemradha74@gmail.com*

^b *Scholar in chemistry, Alagappa Govt. Arts College, Karaikudi – 3*

ABSTRACT:

A facile electrochemical sensor for hydroquinone (HQ) and catechol (CC) determination was successfully fabricated by the modification of graphene oxide-polyaniline and Au nanoparticles composites on a glassy carbon electrode (GO-PANI-Au/GCE). A simple step synthetic procedure was adopted for the preparation of GO-PANI-Au nanocomposites. First GO-PANI nanocomposite was synthesized by chemical route. Decoration of Au nanoparticles on GO-PANI nanocomposite was done by electrochemical deposition of aqueous metal precursor salt solutions. The prepared sensor was characterized by FT-IR, Raman, XRD, scanning electron microscope (SEM), Energy dispersive X-ray analysis (EDAX) and TEM. Under optimal conditions, Cyclic voltammetry was employed to quantify individual HQ and CC within the concentration range of 10 μ M-100 μ M, respectively. The GO-PANI-Au nanocomposites modified GC electrode showed good electrocatalytic activity to hydroquinone and catechol, further the electrocatalytic response was measured using cyclic voltammetry and Amperometry-t curve techniques. Under the optimized conditions, the GO-PANI-Au modified GC sensor platform showed a linear range of 10-100 μ M for Hydroquinone (HQ) and catechol, with a detection limit of 1 μ M (S/N=3). Good reproducibility, better stability and selectivity was achieved in GO-PANI-Au nanocomposites electrode.

Key words: GO-PANI-Au nanocomposites, Raman, XRD, Sensor, Hydroquinone and Catechol



The obtained LOD was well below the guideline level of Hg(II) set by the World's Health Organization (WHO) and U.S. Environmental Protection Agency (EPA). In addition, the fabricated GR-CD/PPy composite modified SPCE selectively detected the Hg(II) in the presence of potentially interfering metal cations.

Keywords: Graphene, β -cyclodextrin, Polypyrrole, Mercury (II), Differential pulse voltammetry

3.10 Zinc oxide - multiwalled carbon nanotube-poly(vinyl chloride) film for Biocompatible glucose sensing

Palinci Nagarajan Manikandan, Habibulla Imran, Venkataraman Dharuman*

Molecular Electronics Laboratory

Department of Bioelectronics and Biosensors, Alagappa University, Karaikudi -630 003, India

Biocompatible film was fabricated using zinc oxide (ZnO), multi-walled carbon nano tubes (functionalized: f MWCNT and purified: p MWCNT), poly(vinyl chloride) (PVC) (PVC-ZnO-MWCNT) for direct glucose sensing. Biocompatibility of this composite is evaluated in presence blood proteins (bovine serum albumin and bilirubin) and bacteria *Staphylococcus aureus* and *Klebsiella pneumoniae*. Hemolysis and cell viability studies were made comparatively. It is observed that hemolysis occurs less than 1% on the PVC-ZnO-MWCNTs. Glucose sensing was made at PVC-ZnO- p MWCNT ternary composite in different solutions using cyclic voltammetry (CV), chrono amperometry (CA), flow injection analysis (FIA). The prepared composite has been further characterized by quartz crystal micro balance (QCM), Scanning Electron Microscopy (SEM), Fourier Infrared Spectroscopy (FTIR), X-ray diffraction (XRD), Raman spectroscopic and Transmission Electron Microscopic (TEM) techniques. Excellent selectivity of the glucose in presence of potential interferences. The PVC-ZnO- p MWCNT composite shows the highest Michaelis-Menten kinetic constant K_M of 21.9 mM compared to the ZnO-glucose oxidase and copper oxide-ZnO systems which exhibit 10 times lower K_M values. Blood glucose in different diabetic persons is discriminated very well without affecting the sensor performance.

Key words: Electrochemical techniques, hemolysis, antibacterial activity and biocompatibility.

3.11 Stabilization of graphene oxide film on gold electrode with Influence of volatile solvents for electrochemical sensing of acetaminophen

Habibulla Imran, Venkataraman Dharuman*

Molecular Electronics Laboratory,

Department of Bioelectronics and Biosensors, Science Block,

Alagappa University, Karaikudi – 630 004

E-mail: dharamanudhav@yahoo.com

Abstract

Graphene oxide (GO) was prepared following the modified Hummer's method and confirmed by X-RD (X-ray Diffractor), FTIR (Fourier Transform Infra-Red spectroscopy) and UV-Vis (Ultra-Violet Visible Spectroscopy). The GO was dispersed in various organic solvents such as *N,N*-dimethylformamide (DMF), *N*-methyl-2-pyrrolidone (NMP), tetrahydrofuran (THF), water, acetone, ethanol, formaldehyde, lactic acid, acetic acid, Dimethyl sulfoxide (DMSO) and glycerol by ultrasonication. It was noticed that GOs are not dispersed in benzene, chloroform and chloro benzene. The GOs in DMF, water, DMSO, NMP and formaldehyde exhibited long-term stability and used for modification of gold transducer by dropcasting. Electrochemical stability was characterized by Cyclic Voltammetry (CV) and electrochemical impedance spectroscopy (EIS) in $[\text{Fe}(\text{CN})_6]^{3-/4-}$ prepared in phosphate buffer saline (PBS). These five different GO modified gold electrodes were applied for acetaminophen sensing.



Among these, GO/DMF on gold exhibits high sensitivity in terms of increased peak currents and reversibility than the other GO/solvent modified gold electrodes. This surface is further for acetaminophen (paracetamol) sensing in PBS using cyclic voltammetry (CV). This is the first report on anchoring GO using different solvents on gold electrode and acetaminophen detection.

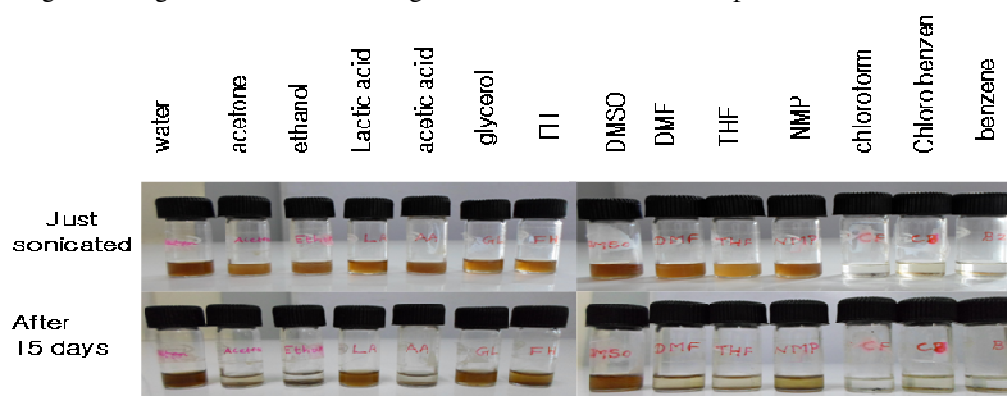


Fig. Graphene oxide dispersed in different solvents (water, acetone, ethanol, lactic acid, acetic acid, glycerol, formaldehyde, dimethylsulphoxide, dimethylformamide, tetrahydrofuran, n-methylpyrrolidone, chloroform, chloro benzene and benzene) by ultrasonication. Top: at the time of dispersed, Bottom: At 15 days after the dispersion

Key Words: Graphene, organic solvent, acetaminophen, electrochemical.

3.12 Fabrication of Co-Ni alloy nanostructures on 3D Copper foam for highly sensitive amperometric sensing of acetaminophen

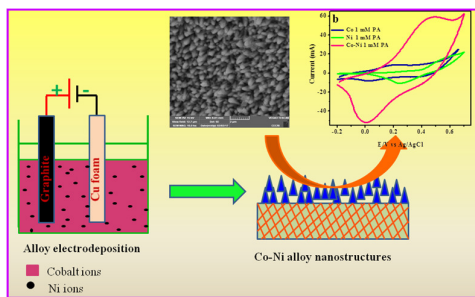
S. Premlatha*, G.N.K. Ramesh Babu

*CSIR-AcSIR Research Scholar, Electroplating and Metal Finishing Technology Division, CSIR- Central Electrochemical Research Institute, Karaikudi-630 003 (Tamilnadu) INDIA.

Abstract

In this work, electrodeposition of Co-Ni alloy nanostructures was performed on 3D copper foam and directly applied as an electrocatalyst for the electrooxidation of acetaminophen (Paracetamol) and its detection. The surface morphology and the elemental composition were investigated using SEM and EDX analysis respectively. The morphology was appeared as nano cones that are uniformly grown on the electrode surface. EDX analysis also confirmed the presence of both cobalt and nickel in the electrodeposit. The preferred orientation lies in (002) and (110) planes of cobalt and nickel respectively that confirmed the formation of alloy. Electrooxidation of acetaminophen was carried out using cyclic voltammetric method. On addition of acetaminophen, an apparent anodic oxidation current enhancement was observed with lesser overpotential than cobalt and nickel electrodes which revealed the excellent electrocatalytic activity of the material. Interference studies also revealed the good selectivity for acetaminophen even in the presence of some interfering species. The reproducibility and stability was checked for the proposed 3D Co-Ni alloy modified electrode. The analytical applicability was examined using the commercial paracetamol tablets and the recovery results were also good. The above results revealed that 3D Co-Ni modified electrode on copper foam is a suitable candidate for electrochemical detection of acetaminophen.





Schematic representation of Co-Ni nanostructures for acetaminophen sensor

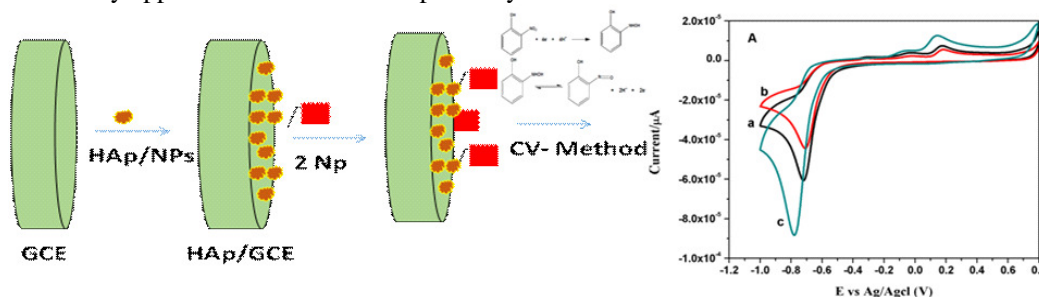
3.13 Fabrication of 2-Nitrophenol sensor based on green synthesized hydroxyapatite

N. Sudhan, C.Sekar*

*Department of Bioelectronics and Biosensors, Alagappa University, Karaikudi, Tamilnadu, India.
Sekar2025@gmail.com*

2-Nitrophenol, one of the main compounds in phenol families, is broadly applied in the manufacturing of explosives, dyes, rubber, pharmaceutical, pesticides, and various industrial applications. They affect plants and animals, and can readily accumulate in the human organs to cause carcinogenesis, mutagenesis by the nature of its toxicity [1]. Numerous diseases like methemoglobinemia, headaches, and nausea are caused by inhaling of the 2-Nitrophenol compound in even at very low concentration. 2-Np is cited in the list of pollutants by U.S Environmental Protection Agency (EPA) due to its toxicity and persistence [2]. Therefore, it is necessary to develop an effective method for determination of 2-Nitrophenol in the environment.

Hydroxyapatite is a predominant mineral for bone and teeth and it has extreme biocompatibility, ion exchangeability, and having a lot of attracting properties HA NPs have been synthesized by various methods such as solvated, hydrothermal, sol-gel, chemical precipitation and microwave methods [3]. Here we report synthesis of HA NP by using different plant extract like Eucalyptus, Ocimum basicilium, Plectranthus amboinicus, and Jusiticia Adathoda by microwave irradiation method and the detection of 2-Nitrophenol by voltammetric method. The fabricated sensor shows high electrochemical activity towards the 2-Nitrophenol in 0.1M PBS (pH 6.0).The sensor was successfully applied for in the real sample analysis.



References

- [1] Chuan Yao, etal *Electrochimica Acta* 156 (2015) 163-170.
- [2] US Environmental Protection Agency, Fed. Regist. 52 (1989) 131.
- [3] P.Kanchana, C. Sekar, *Spectrchim Acta Part A* 137(2015)58-65.



3.14 Binary liposome (DOTAP-DOPE) vesicle-gold nanoparticle for enhanced label free DNA and protein sensing

Karutha Pandian Divya, Venkataraman Dharuman*

*Molecular Electronics Lab, Department of Bioelectronics and Biosensors, Alagappa University, Karaikudi
Email: dharumanudhay@yahoo.com*

Supported binary liposome mixture of cationic liposome N-[1-(2,3-Dioleoyloxy)propyl]-N,N,N-trimethylammonium propane (DOTAP) and the zwitterionic liposome 1,2-Dioleoyl-sn-Glycero-3-Phosphoethanolamine (DOPE) were tethered on thiol monolayers in the absence and presence of gold nanoparticle to enhance sensor stability and sensitivity for label free DNA and protein sensing for the first time. Cysteamine hydrochloride (Cyst), 3-Mercaptopropionic acid (MPA), 11-Mercaptoundecanoic acid (MUDA) and 11-amino-1-undecane thiol (AUT) monolayers were used as tethers on gold surfaces. Electrochemical studies in the presence of $[\text{Fe}(\text{CN})_6]^{3-/4-}$ indicate that the presence of both DOPE and AuNP decreases the electrostatic interaction between DOTAP and MPA layer during the formation of DOPE-DOTAP-AuNP (DDA) whereas they enhance the repulsive force on the Cyst and AUT monolayers. In the thiol monolayer supported DDA, the gelation of neutral lipid DOPE by the AuNP is disfavored which in turn promotes stability of vesicle structure. The membrane protein melittin's interaction with the DDA indicates the presence of intact vesicle by showing decreased charge transfer for the MUDA and AUT in the presence of $[\text{Fe}(\text{CN})_6]^{3-/4-}$. On the contrary, the presence of the bilayer and semi circled DDA on the MPA and cysteamine layers were confirmed by the increased redox reaction. Atomic Force Microscopic (AFM) and Transmission Electron Microscopic (TEM) images support the presence of an array like semi circled DDA on the MPA and well separated DDA vesicles on the MUDA with variable sizes. Dynamic Light Scattering (DLS) and Fourier Transform Infrared spectroscopy (FTIR) suggest effective coordination between DOPE, DOTAP and AuNP. Label free DNA hybridization sensing in presence of the negatively charged $[\text{Fe}(\text{CN})_6]^{3-/4-}$ indicates the lowest DNA detection limit of 1×10^{-14} M with linearity range 1×10^{-13} to 1×10^{-9} M. Similarly, streptavidin sensing shows the lowest detection of 1 ng ml^{-1} with a linear range 100 ng to $1 \mu\text{g}$ due to the increased reactive sites and distance

Keywords: Binary liposome, Gold nanoparticle, Solid surface, DNA, Protein.

3.15 Synthesis and Fabrication of Au-Nanoparticles decorated GO-PANI Nanocomposites and their Electrochemical Sensing of Phenols

S. Michelraj, K. Rajeswari and C. Sivakumar

*Electrodeics and Electrocatalysis Division, CSIR-Central Electrochemical Research Institute
Karaikudi-630 006, India
E-mail: ccsivakumar@cecri.res.in*

ABSTRACT:

A facile electrochemical sensor for hydroquinone (HQ) and catechol (CC) determination was successfully fabricated by the modification of graphene oxide-polyaniline and Au nanoparticles composites on a glassy carbon electrode (GO-PANI-Au/GCE). A simple step synthetic procedure was adopted for the preparation of GO-PANI-Au nanocomposites. First GO-PANI nanocomposite was synthesized by chemical route. Decoration of Au nanoparticles on GO-PANI nanocomposite was done by electrochemical deposition of aqueous metal precursor salt solutions. The prepared sensor was characterized by FT-IR, Raman, XRD, scanning electron microscope (SEM), Energy dispersive X-ray analysis (EDAX) and TEM. Under optimal conditions, Cyclic voltammetry was employed to quantify individual HQ and CC within the concentration range of $10 \mu\text{M}$ - $100 \mu\text{M}$, respectively. The GO-PANI-Au nanocomposites modified GC electrode showed good electrocatalytic activity to hydroquinone and catechol, further the electrocatalytic response was measured using cyclic voltammetry and Amperometry i-t curve techniques.



Under the optimized conditions, the GO-PANI-Au modified GC sensor platform showed a linear range of 10-100 μM for Hydroquinone (HQ) and catechol, with a detection limit of 1 μM (S/N=3). Good reproducibility, better stability and selectivity were achieved in GO-PANI-Au nanocomposites electrode.

Key words: GO-PANI-Au nanocomposites, Raman, XRD, Sensor, Hydroquinone and Catechol

3.16 Electrochemical Hydrocarbon Sensing Performances of YSZ-based sensor attached with Nano-NiO

K. Mahendraprabhu¹, V. Dharuman, P. Elumalai^{2,*} and E.R. Nagarajan³

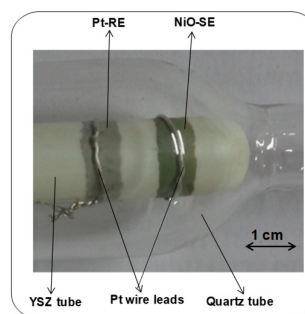
¹Department of Bioelectronics and Biosensors, Alagappa University, Karaikudi-630 003, Tamilnadu, India.

²Centre for Green Energy Technology, Pondicherry University, Pondicherry-605014, India.

³Department of Chemistry, Kalasalingam University, Krishnankoil, Srivilliputtur, Tamilnadu, India.

*Corresponding Authors. E-mail: elumalai.get@pondiuni.edu.in (P. Elumalai), dharumanudhay@yahoo.com (V. Dharuman) and kpprabhu1@gmail.com (K. Mahendraprabhu)

Automobiles have major contribution for the emissions of oxides of nitrogen and carbon along with unburnt hydrocarbons such as methane, propane and propene. So it is necessary to monitor automobile exhaust with high performance gas sensors. In the present work, The Nanostructured nickel oxide (NiO) was synthesized by urea-based hydrothermal route followed by subsequent heat treatment. The influence of nickel precursors, nickel acetate, chloride, nitrate, and sulphate was investigated on the formation of morphology of NiO nanostructures. The synthesized samples were characterized by XRD, SEM, FT-IR and Raman spectroscopy. The XRD patterns confirmed the presence of cubic NiO phase in all the heat-treated samples. It was observed that the samples obtained from nickel acetate and sulphate resulted in agglomerated shapeless grains while those obtained from nickel chloride and nitrate resulted in nanospheres made up of nanoflakes. The difference in the nucleation process seemed to be responsible for formation of varying NiO morphology. Ytria-stabilized Zirconia-based sensor was fabricated using the NiO nanospheres (which consists of nanoflakes) obtained from nickel chloride precursor. The sensor attached with the hydrothermally synthesized NiO-SE showed high sensitivity and selectivity to C_3H_8 and C_3H_6 at 750, 800 and 850 $^\circ\text{C}$ in all oxygen concentrations. The sensor shown highest sensitivity and selectivity in 21 vol % O_2 . The ΔV of the sensor varied linearly with C_3H_6 concentrations on the logarithmic scale. The sensor exhibited excellent sensing response to even very low concentration of C_3H_6 (10 ppm). The sensor retained good stability even for about 40 days. Thus, the sensor attached with the hydrothermally derived NiO-SE can be a reliable hydrocarbon sensor (C_3H_8 and C_3H_6).



Acknowledgment: Authors thank DST-SERB (SERB/F/290/2017-18, Dt. 04/05/2017 (PDF/2016/001899))



3.18 Synthesis and live cell imaging studies of rhodamine based organic nanorods: a new strategy in cation and anion sensing applications

M. Maniyazagan^a, R. Mariadasse^b, M. Nachiappan^b, J. Jeyakanthan^b, N. K. Lokanath^c, S. Naveen^c, G. Sivaraman^d, P. Muthuraja^a, P. Manisankar^a, T. Stalin^{a*}

^a Department of Industrial Chemistry, School of Chemical Sciences, Alagappa University, Karaikudi-03, Tamil Nadu, India.

^b Structural Biology and Bio-computing Lab, Department of Bioinformatics, Alagappa University, Karaikudi-04,

^c Dept. of Studies in Physics, University of Mysore, Mansangotri, Mysore-06, India.

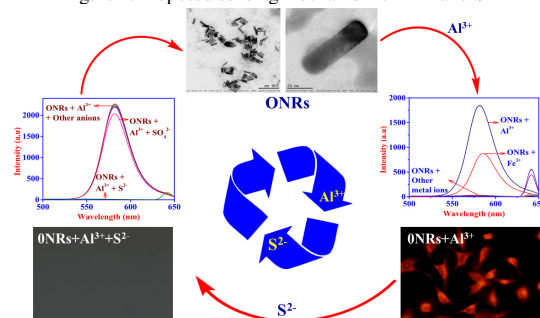
^d Institute for Stem Cell Biology and Regenerative Medicine, Bangalore-560065, India.

Email: manichemist@gmail.com

Nanorods with shape anisotropy have received much attention due to their promising applications in chemical sensors, imaging, biomedicine, electronics and catalysis [1]. Re-precipitation was first introduced by Nakanishi and co-workers as a facile method to prepare organic nanomaterials, more and strategies have been developed for constructing organic nanomaterials with different morphologies. This organic nanomaterial better performances such as multicolour emission, chemiluminescence, chemical sensor, etc.,

The rhodamine moiety has been used extensively in the field of chemosensor, particularly as a fluorescence chemodosimeter, given its fluorescence OFF–ON behavior resulting from its unique structural design and properties [2]. Here, we report a novel rhodamine-based organic nanorods with controlled size using hydrothermal method. The ONRs can serve as a fluorescent probe for rapid, sensitive and selective detection of Al^{3+} ions in aqueous solution.

Figure 1. Proposed sensing mechanism of Al^{3+} and S^{2-}



A novel highly selective rhodamine based organic nanorods (ONRs) was successfully designed and synthesized, which showed both absorption and fluorescence turn-on responses for Al^{3+} ions in aqueous solution. The ONRs possess strong fluorescence emission in aqueous solution. These spectral changes are sufficient to detection of Al^{3+} ions in the visible region of the spectrum and thus support naked eye detection. The aforesaid studies reveal that ONRs– Al^{3+} complex is highly selective and fully reversible in presence of sulphide anions. This ONRs could be used as a fast, fluorescence sensor for Al^{3+} and S^{2-} ions in aqueous solution. The visible changes the FRET based fluorescence response makes it a dual probe for naked eye detection through change in colour and fluorescence spectroscopy. The complex formed between ONRs and Al^{3+} ions is dissociable only in presence of S^{2-} ions, which makes the ONRs– Al^{3+} complex an efficient sensor for S^{2-} ions. From the extensive spectroscopic studies, it is clear that the ONRs and ONRs– Al^{3+} complex could be used as a fluorescent sensor for the detection of Al^{3+} and S^{2-} ions. This study raises the new possibility of a highly selective and sensitive ONRs having multifunctional detection, including cation and anions, using a successive fluorescence response strategy in biological systems. Besides, the fluorescence microscopic studies confirmed that the fluorescent probe ONRs could be used as an imaging probe for detection of uptake of Al^{3+} ions in HeLa cells.

References

- [1] Y. Huang, X. Duan, Q. Wei and C.M. Lieber, *Science*. 291 (2001) 630.
- [2] B. Valeur, *Molecular Fluorescence: Principles and Applications*, Wiley-VCH Verlag GmbH, New York, 2001, ch. 10.



4. Supramolecular and Photochemical Technologies

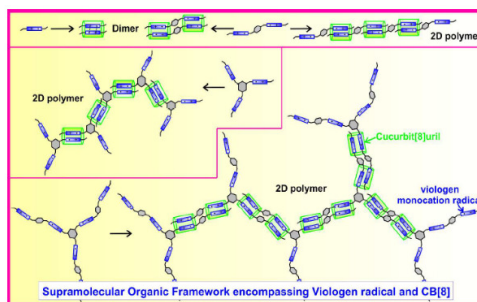
4.1 Reversible 2D Supramolecular Organic Frameworks encompassing Viologen Cation Radicals and CB[8]

Kanagaraj Madasamy, David Velayutham, Murugavel Kathiresan*

*Electro-Organic-Division, CSIR-Central Electro Chemical Research Institute, Karaikudi-630003, TamilNadu, India.
E-mail: kathiresan@cecri.res.in*

Abstract

Two dimensional reversible supramolecular organic frame work was constructed using viologen architectures and cucurbit[8]uril^[1] and their spectroscopic investigations were carried out via UV-Vis. UV-Vis study clearly indicated the intermolecular dimerization of viologen mono radical cation and their inclusion in to the hydrophobic CB[8] cavity. This argument was further confirmed by EPR spectroscopy (electron paramagnetic resonance) spectroscopy. Binding constants were measured from UV-Vis titrations using Job Plot. The binding tendency of viologen dimer and CB[8]^[2] were found to be in the range of 10^3 - 10^4 /M. Particle size measurements of the self-assembled architectures by dynamic light scattering method showed particle size in the range of several μm demonstrating larger aggregates. Zeta potential measurements proposed the instability of these particles and their tendency to form aggregates.



References

- [1] L. Zhang, T.-Y. Zhou, J. Tian, H. Wang, D.-W. Zhang, X. Zhao, Y. Liu and Z.-T. Li, *Polym. Chem.*, 2014, 5, 4715–4721.
- [2] C. Zhou, J. Tian, J.-L. Wang, D.-W. Zhang, X. Zhao, Y. Liu and Z.-T. Li, *Polym. Chem.*, 2014, 5, 341–345.

4.2 Novel Pyrimidine Tagged Silver Nanoparticle Based Fluorescent Immunoassay for the Detection of *Pseudomonas aeruginosa*

Sundaram Ellairaja^a and Vairathevar Sivasamy Vasantha^{a*}

^a*Department of Natural Products Chemistry, School of Chemistry, Madurai Kamaraj University, Madurai-625 021,
Email id: rajadhan.raja17@gmail.com*

Amidst the Pseudomonadaceae family, *Pseudomonas aeruginosa* has been pointed out as an opportunistic Gram-negative human pathogen that causes acute diseases in humans as well as animals.[1-2] The *Pseudomonas aeruginosa* pathogen is the fourth most commonly isolated nosocomial pathogen accounting for 10.1% of all hospital-acquired diseases. Several serious health issues by this pathogen are sepsis, inflammatory, fester otitis, pneumonia, and cystic fibrosis. In concern with the sensitivity, usage, time, selectivity, etc., so many analytical protocols such as polymerase chain reaction (PCR), microarrays,[3] quartz crystal microbalance resonators (QCM),[4] carbohydrate-mediated cell recognition using gold glyconanoparticles,8 products,10 diffraction-based cell detection,[5] and nanowire-based detection [6] are continually being developed in the recent decades for various pathogens.



fluorimetric technique based immunoassay offers high accuracy, speed, simplicity, and cost effectiveness. In past years, the labeling of growing pathogens with fluorescent tags during bacterial culture had played a remarkable part in fluorescent microscope based bacterial detection [7].

Scheme. 1 Simple Immunoassay assay for selective recognition of *Pseudomonas Aeruginosa*.

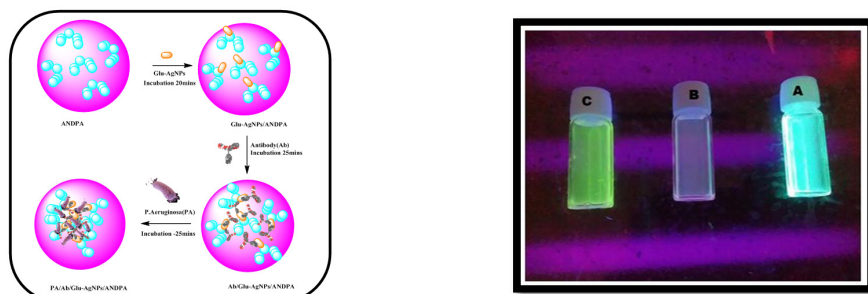


Figure. 1 Transilluminator images: Synthesized fluorophore ANDPA (A), Glu-AgNPs/ANDPA (B) and PA/Ab/ Glu-AgNPs/ANDPA(C).

Sl. No.	Agricultural Soil	This method (unknown) (CFU/mL)	Plate count Method (unknown) (CFU/mL)
1.	Test 1	275	320 (TNTC)
2.	Test 2	135	180
3.	Test 3	50	70
4.	Test 4	26	45
5.	Test 5	10	17

Table 1. Detection of *Pseudomonas aeruginosa* in soil sample using current developed fluorescence immunoassay protocol and comparison with the plate count method. [Concentration of ANDPA is 5 μ M, Glu-AgNPs: 6 % (v/v), Ab: 0.36 μ g/mL (20 μ L), soil samples (40 μ L) under different dilutions factor from 10^{-5} – 10^{-9}].

In this current work A simple pyrimidine-based fluorescent probe (R)-4-(anthracen-9-yl)-6-(naphthalen-1-yl)-1,6-dihydropyrimidine- 2-amine (ANDPA) was synthesized through the greener one pot reaction and characterized by IR, NMR, and ESI-Mass. Glucose stabilized silver nanoparticles (Glu-AgNPs) were also synthesized and characterized using UV, IR, XRD, SEM, and TEM. When ANDPA was tagged with Glu-AgNPs, the fluorescent intensity of ANDPA decreased drastically. When the monoclonal antibody (Ab) [immunoglobulin G (IgG)] of *Pseudomonas aeruginosa* (PA) was attached with ANDPA/Glu-AgNPs, the original intensity of the probe was recovered with minimal enhancement at 446 nm. On further attachment of PA with ANDPA/Glu-AgNPs/PA, the fluorescence intensity of the probe was enhanced obviously at 446 nm with red shift. This phenomenon was further supported by SEM and TEM. The linear range of detection is from 8 to 10^{-1} CFU/mL, and LOD is 1.5 CFU/mL. The immunosensor was successfully demonstrated to detect *Pseudomonas aeruginosa* in water, soil, and food products like milk, sugar cane, and orange juices.

KEYWORDS: Pyrimidine, Fluorescence, Aggregation, *Pseudomonas aeruginosa*, Nanoparticles, Immunosensor.

REFERENCES

- [1] K. J. Ryan, C. G. Ray, C. G., Eds. Sherris Medical Microbiology, 4th ed.; McGraw Hill: New York, (2004).
- [2] Y. Anzai, H. Kim, J. Y. Park, H. Wakabayashi, Int. J. Syst. Evol. Microbiol. (2000), 50 (4), 1563–1589.
- [3] K. Otto, T. J. Silhavy, Proc. Natl. Acad. Sci. U. S. A. (2002), 99, 2287–2292.
- [4] X. Zhao, L. R. Hilliard, S. J. Mechery, Y. Wang, R. P. Bagwe, S. Jin, W. A. Tan, Proc. Natl. Acad. Sci. U. S. A. (2004), 101, 15027–15032.



- [3] X.Chen,X.Tian,I.Shin,J.Yoon,*Chem.Soc.Rev.*40(2011)4783-4804
 [4] Q.Wang,Y.Xie,Y.Ding,X.Li,W.Zhu,*Chem.Comm.*46(2010)3669-3671
 [5] H.A.Benesi,J.H.Hildebrand,*J.Am.Chem.Soc.*71(1949)2703

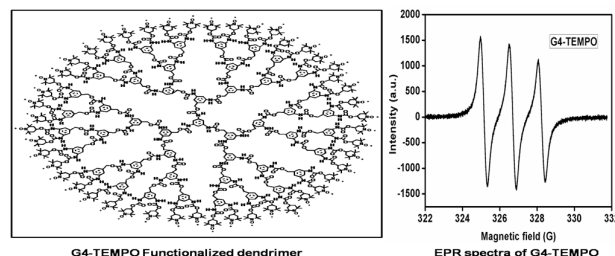
4.5 Synthesis and scavenging applications of polyurethane dendritic nitroxide radical dendrimers

B. Mohamad Ali and A. Sultan Nasar*

*Department of Polymer Science University of Madras, Guindy Campus, Chennai-600025, India
 E-mail: mohamad4r@gmail.com*

Abstract

Dendrimers are highly branched macromolecules with a carefully tailored architecture and the end groups¹. They have attracted much attention due to their unique physical and chemical properties. The low polydispersity and nanoscopic dimensions of well defined functionalized dendrimers may give rise to new properties for example, in molecular recognition, catalysis, or molecule-based electronics and optics². An increasing number of dendrimers are being functionalized with stable organic radicals or redox active groups, aiming at molecules or materials with a wide variety of functional properties³. Dendrimers are characterized by special features that make them promising candidates for a lot of applications such as MRI contrast agents⁴, NMR imaging⁵, catalytic oxidation and clinical applications⁶.



In the present work, a series of blocked isocyanate-terminated polyurethane dendrimers up to fourth generation were synthesized adopting a three step divergent method⁷. The synthesized polyurethane dendrimers were further functionalized with a stable 2, 2, 6, 6 – tetramethyl-piperidine-1-oxyl (TEMPO) free radicals. The structures of the dendrimers were confirmed by FT-IR, H¹ NMR, UV, fluorescence spectroscopy. The absolute molecular weights of the dendrimers were determined by SEC-MALLS technique. The presence of nitroxide radical units in the dendrimers was confirmed by using EPR spectroscopy at g = 2.01. All the EPR spectra showed similar three line spectral pattern and hyperfine coupling is not observed because of no spin interaction between nitroxide radical units. Nitric Oxide scavenging ability of synthesized dendrimers was determined via invitro experiments and found that the scavenging activity of dendrimers increased with increasing the number of radical units at the surface of the dendrimers.

References

- [1] Elham Abbasi, Sedigheh Fekri Aval, Abolfazl Akbarzadeh, Morteza Milani, Hamid Tayefi Nasrabadi, Sang Woo Joo, Younes Hanifehpour, Kazem Nejati-Koshki and Roghiyeh Pashaei-Asl, *Nanoscale Research Letters*, 9:247, (2014), 1-10.
 [2] A. W. Bosman, R. A. J. Janssen, and E. W. Meijer *Macromolecules*, 30, (1997), 3606-3611.
 [3] Elena Badetti, Vega Lloveras, Jose Luis Munoz-Gomez, Rosa Maria Sebastian, Anne Marie Caminade, Jean Pierre Majoral, Jaume Veciana, and Jose Vidal-Gancedo, *Macromolecules*, 47, (2014), 7717-7724.



- [4] Giancarlo Francese, Frank A. Dunand, Claudia Loosli, Andre´ E. Merbach and Silvio Decurtins Magn. Reson. Chem, 41, (2003), 81–83.
- [5] Maristella Gussoni, Fulvia Greco, Paolo Ferruti, Elisabetta Ranucci, Alessandro Ponti and Lucia Zetta New J. Chem., 32, (2008), 323–332 .
- [6] Muhammad Afzal Subhani, Maryam Beigi, and Peter Eilbrachta, Adv. Synth. Catal, 350, (2008), 2903 – 2909.
- [7] S. Veerapandian and A. Sultan Nasar RSC Adv, 5, (2015), 3799–3806.

4.6 Development of a Novel Bimetallic Au-FeNPs Decorated on g-C₃N₄ with Enhanced Photocatalytic Performance for the Degradation of Organic Dyes

Baishnisha Amanulla and Sayee Kannan Ramaraj*

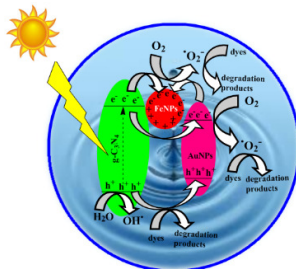
PG & Research Department of Chemistry, Thiagarajar College, Madurai-09.
e-mail: sayee kannanramaraj@gmail.com

Abstract

In this study, we report a facile synthesis approach and photocatalytic performance of a novel magnetic Au-FeNPs/g-C₃N₄ nanocomposite for the efficient degradation of organic dyes under visible irradiation. The as prepared Au-FeNPs/g-C₃N₄ nanocomposite was characterized by X-ray diffraction (XRD), Fourier transform infrared (FT-IR), UV-visible diffuse reflectance spectroscopy (DRS), Scanning electron microscopy (SEM), Transmission electron microscopy (TEM) and energy-dispersive X-ray (EDX). The photocatalytic performance of the prepared nanocomposite was evaluated for the degradation of malachite green (MG) and rhodamine B (RhB) as an organic dyes under visible light irradiation. The obtained results of Au-FeNPs/g-C₃N₄ nanocomposite shows outstanding photodegrading behavior towards MG and RhB compared to pure g-C₃N₄ and AuNPs/g-C₃N₄. Maximum degradation efficiency of 99.1% and 97.3% were achieved for the MG and RhB dyes, respectively. Furthermore, Au-FeNPs/g-C₃N₄ nanocomposite was particularly durable after five consecutive photocatalytic activity. Therefore, the present investigation focuses the synthesis of highly efficient magnetic bimetallic based nanocomposite for effective degradation of various organic contaminants in aqueous solution .

Key Words: Magnetic Au-FeNPs/g-C₃N₄, Photocatalytic degradation, malachite green and rhodamine B

Photocatalytic degradation of MG and RhB over Au-FeNPs/g-C₃N₄ under visible light irradiation.



References

- [1] N. Cheng, J. Tian, Q. Liu, C. Ge, A. H. Qusti, A. M. Asiri, A. O. Al-Youbi, X. Sun, *ACS Appl. Mater. Interfaces*, 2013, **5**, 6815-6819.
- [2] M.A. Gondal, A.A. Adeseda, S.G. Rashid, A. Hameed, M. Aslam, M.I. Iqbal Ismail, B. Umair, M. A. Dastageer, A.R. Al-Arfaj, A. U. Rehman, *J.Mol. CatalysisA: Chemical*, 2016, **423**,114-125.
- [3] Y. Feng, J. Shen, Q. Cai, H. Yang, and Q. Shen, *New J. Chem.*, 2015, **39**, 1132-1138.



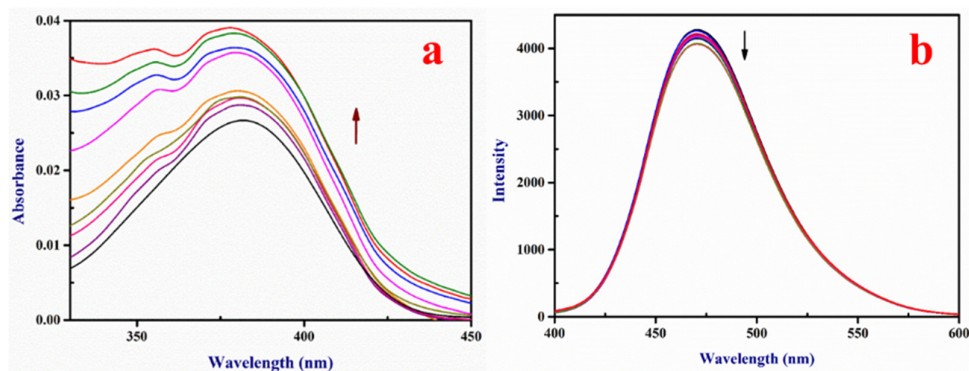


Fig. 1. The UV-Visible titration (a) and Emission titration (b) of C460 (1×10^{-6} M) in the absence and presence of *p*-SC4. (1×10^{-5} to 9×10^{-4} M)

Fluorescence spectral titration

Quenching is observed in the fluorescence intensity of C460 upon increasing the concentration of *p*-SC4 (Fig. 1b). The calculated binding constant (Eqn. 2) is $1.7 \times 10^3 \text{ M}^{-1}$, which shows an excellent binding of *p*-SC4 with C460. The quenching constant value for C460 with *p*-SC4 is $3.5 \times 10^{11} \text{ M}^{-1}\text{s}^{-1}$. This higher value of quenching constant is due to static quenching.

Conclusion

An active binding of C460 with *p*-SC4 is observed in this study. The binding constant values from both absorption and emission studies is around 10^3 M^{-1} shows efficient binding. The Job's plot emphasized the 1:1 binding of C460 with *p*-SC4. Static quenching is observed in fluorescence titration.

References

- [1] C.D. Gutsche, Calixarenes, Royal Society of Chemistry, 1989.
- [2] B. M. Ashwin, A. Vinothini, T. Stalin, P. Muthu Mareeswaran, *ChemistrySelect*, 2 (2017) 931-936.
- [3] G. Somasundaram, A. Ramalingam, *J. Lumin.*, 90 (2000) 1-5.
- [4] E. Herz, T. Marchincin, L. Connelly, D. Bonner, A. Burns, S. Switalski, U. Wiesner, *J. Fluoresc.*, 20 (2010) 67-72.
- [5] C. Saravanan, M. Senthilkumaran, B. M. Ashwin, P. Suresh, P. Muthu Mareeswaran, *J. Incl. Phenom. Macrocycl. Chem.*, (2017). doi:10.1007/s10847-017-0729-1

4.11 Investigation on molecular recognition of 4-nitro-*o*-phenylenediamine with *para*-sulfonatocalix[4]arene

C. Saravanan, G. Vigneshkumar and P. Muthu Mareeswaran*

Department of Industrial Chemistry, Alagappa University, Karaikudi.
E-mail: saravanangri92@gmail.com

1. Introduction

p-Sulfonatocalix[4]arene (*p*-SC4), is a widely studied water soluble, biocompatible promising host molecule, composed of *para*-hydroxybenzenesulfonate units linked by methylene groups, which offers flexibility, π -rich cavity and negative charge to bind with plenty of metal ions, organic cations, neutral organic molecules, dyes and bio-relevant molecules to form supramolecular complexes. Construction of supramolecular architectures involves different types of interactions like electrostatic, hydrophobic, Van der Waals, π - π , cation- π , hydrogen bonding, depends on the nature of the guest molecules [1-3]. 4-nitro-*o*-phenylenediamine (NOPD) is an aromatic amine is one of the widely-used constituent of many hair dye formulations and these have been shown to cause bacterial mutations without prior activation.



4. Conclusion

The binding constant values obtained from absorption titration is $4.3 \times 10^4 \text{ M}^{-1}$. These value show that the considerable binding occurs between NOPD and p-SC4. From the above discussion, we concluded the NOPD molecule is inserted into the p-SC4 cavity in 1:1 molar ratio. Therefore, p-SC4 is a suitable host molecule for the molecular recognition of NOPD.

Reference

- [1] C. Saravanan, M. Senthilkumar, B.C.M.A. Ashwin, P. Suresh, P. Muthu Mareeswaran, *J. Incl. Phen. Macro. Chem.* (2017) 1. DOI: 10.1007/s10847-017-0729-1;
- [2] B.C.M.A. Ashwin, A. Vinothini, T. Stalin, P. Muthu Mareeswaran, *ChemistrySelect* 2 (2017) 931.
- [3] P. Muthu Mareeswaran, B. Ethiraj, S. Veerasamy, B. Kim, S. I. Woo, R. Seenivasan, *New J. Chem.* 38 (2014) 1336.
- [4] E. Saikia, M.P. Borpuzari, B. Chetia, R. Kar, *Spectrochim. Acta Part A: Mol. Biomol. Spec.* 152 (2016) 101;
- [5] P. Li, Y. Zhu, S. He, J. Fan, Q. Hu, Y. Cao, *J. Agric. Food Chem.* 60 (2012) 3013.

4.12 Encapsulation of Triphenylpyrylium cation with p-Sulfonatocalix[4]arene

M. Senthilkumar, G. Vigneshkumar, K. Maruthanayagam, P. Muthu Mareeswaran*

Department of Industrial Chemistry, Alagappa University, Karaikudi – 630 003, India
E.mail. senthilkumaransbk@gmail.com.

Introduction

The *para*-sulfonatocalix[4]arene (p-SC4) is a water soluble macrocycle synthesized from the upper rim modification of *tert*-butylcalix[4]arene. The p-SC4 possess π - electron rich cavity (aromatic ring), negative charges (sulphanato group) and hydrophilic nature (-OH group), therefore it has the propensity to encapsulate neutral, cationic organic molecules and ions to form supramolecular complexes [1,2]. Pyrylium salt is one of the cationic organic molecules having trivalent oxygen atom. Due to the electron accepting nature of the pyrylium cation, it can be used as electron transfer agent and in catalysis. Optical and electron transfer properties of pyrylium salt is used to design sensor for amino acids, and proteins [3]. In this work, we have studied host-guest interaction of 2,4,6-triphenylpyrylium tetrafluoroborate (TPP) with p-SC4 using absorption and emission technique.

Experimental

For binding constant calculation from UV-visible titration using Benesi–Hildebrand equation [4] (Eqn. 1),

$$1/\Delta A = 1/K_a \Delta \epsilon [p\text{-SC4}] + 1/\Delta \epsilon [TPP] \quad (1)$$

Here, ΔA is the change in absorbance of the TPP on addition of p-SC4. $\Delta \epsilon$ is the difference in the molar extinction coefficient between the free TPP and p-SC4–TPP complex. The plot of $1/\Delta A$ vs. $1/[p\text{-SC4}]$ gives straight line. The free energy change, ΔG value is calculated from the binding constant value [5], K_a using the Eqn. 2,

For binding constant calculation from emission titration using modified Benesi–Hildebrand (Eqn. 2),

$$I_0/(I-I_0) = b/(a-b) \times [1/K_a[H]+1] \quad (2)$$

Where, I_0 is the luminescence intensity of the guest in the absence of host, I is the luminescence intensity of the complex in the presence of host, $[H]$ is the concentration of the host, and K_a is the binding constant for the binding of the host with guest.

Stoichiometric binding ratio between TPP and p-SC4 is calculated by using job's method.



- [3] A. M. Bonch-Bruевич, E. N. Kaliteevskaya, T. K. Razumova, A. D. Roshal and A. N. Tarnovskii, *Opt. Spectrosc.* 89 (2000) 216.
- [4] J. R. Lakowicz, in *Principles of Fluorescence Spectroscopy*, Springer US, Boston, MA, (1999) 291-319.
- [5] B. M. Ashwin, A. Vinothini, T. Stalin and P. Muthu Mareeswaran, *Chem. Select.* 2(2017) 931-936.

4.13 Morphology controlled synthesis of Carbon Quantum Dot/Cu₂O Hybrid Material for Visible Light Photocatalyst

G. Muthusankar, S. Revathi, S. Dhanalakshmi, G. Gopu*

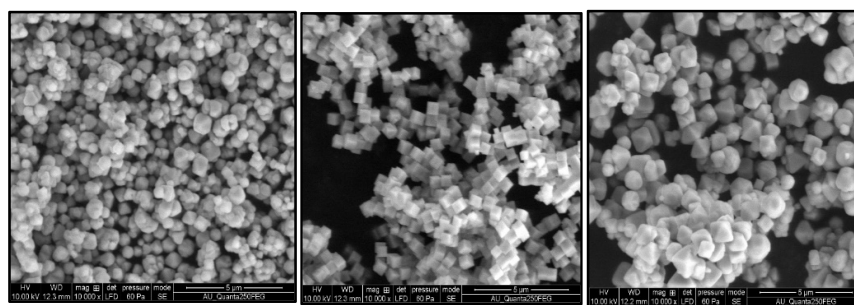
Department of Industrial Chemistry, Alagappa University, Karaikudi – 630003

Email: gmsankar.g@gmail.com

Carbon Quantum Dots (CQDs) are a new class of carbon materials with sizes less than 10 nm and have optical properties as well as high thermal and chemical stabilities, good electron conductivity, and excellent water solubility. CQDs can serve as excellent electron acceptors or electron donors, permitting electron transfer between CQDs and semiconductors and hindering the recombination of photoelectrons and holes on the semiconductors, which therefore improve the photocatalytic activity.

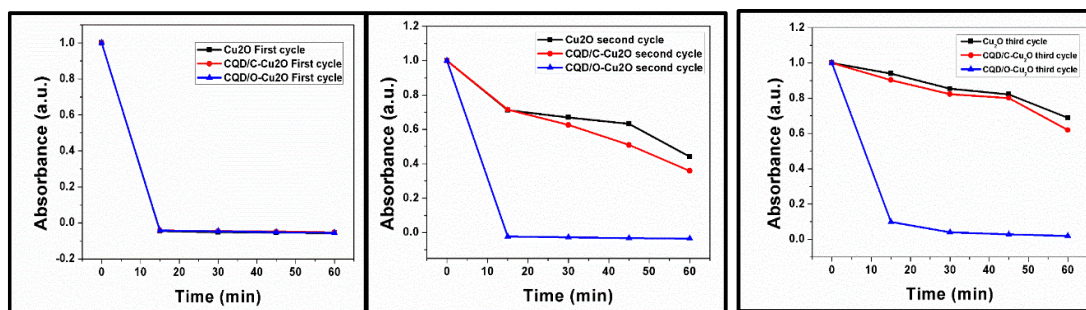
Cuprous oxide (Cu₂O) is an attractive photocatalyst because of its visible-light-driven photocatalytic behavior, abundance, low toxicity, and environmental compatibility. However, its short electron diffusion length and low hole mobility result in low photocatalytic efficiency, which hinders its wider applications. Herein we synthesized the CQDs decorated cuprous oxide (CQD/Cu₂O) nano composite for the enhanced photocatalytic activity. It is interestingly found that the introduction of CQDs control the morphology of Cu₂O and the most encouraging result is that all of the obtained CQD/Cu₂O composites exhibit better photocatalytic activities than pure Cu₂O cubes.

It is demonstrated that the excellent photocatalytic performance of CQD/Cu₂O composites can be attributed to the octahedral structure and the suppression of electron–hole recombination as a result of the introduction of CQDs. These findings demonstrate that the conjugation of CQDs is a promising method to improve the photocatalytic activities for traditional semiconductors.



Pure Cu₂O

CQD/Cu₂O composites at various morphologies at various concentration of CQDs



Comparison of Cr⁶⁺ ion reduction by pure Cu₂O, CQD/ Cube-Cu₂O and CQD/ Octahedral-Cu₂O



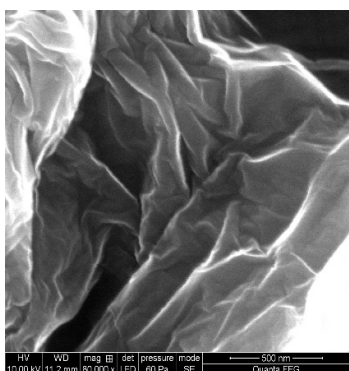
4.15 Synthesis and Characterization of Polythiophene- Graphene oxide-Zinc selenite Nanocomposite for Photocatalytic hydrogen production

S. Senthilnathan, S. Sivasakthi, Dr. K. Gurunathan*

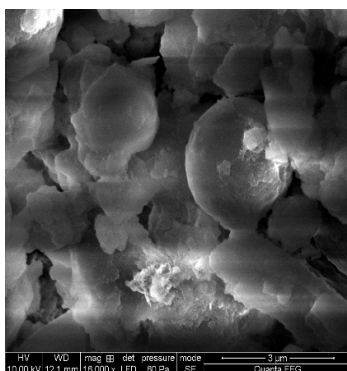
Department of Nanoscience & Technology, Science Campus, Alagappa University,
Karaikudi-630003. Ph:04565-225630; e-mail: kgnathan27@rediffmail.com

Abstract

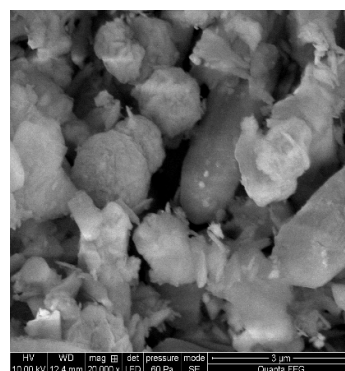
In our tentative work, reduced graphene oxide (rGO) was covalently functionalized by zinc selenite (ZnSe) and polythiophene (PTh). We report for the photocatalytic activity of the newly designed facile synthesized nanocomposite consisting of reduced graphene oxide, polythiophene and ZnSe via simple wet chemical method. In this paper, the metal oxide plays the major role of photocatalyst incorporated by reduced graphene oxide which is a good conductor. Graphene oxide (GO) sheets have highly tunable electronic properties because of their unique 2D carbon structure, which allows extensive modification with surface functionalities. Photo-driven water splitting uses semiconducting materials that have electronic structures suitable for electron and hole injection for H₂ and O₂ evolution from water decomposition, GO is an ideal material to mediate photo-generated charges for water decomposition. These properties make it become an ideal support of the photocatalyst to enhance the transfer and separation of photo-generated electrons and holes. The potential application of graphene-based photocatalysts to boost the efficiency of solar energy conversion has been explored. The present Perspective is a short report of recent research activities related to graphene-based H₂ production photocatalysts and discussion of their emerging role in photocatalytic hydrogen evolution, enhances the prospects for using ZnSe as an effective catalyst for photocatalytic degradation of organic pollutants. ZnSe is an important material in shorter wavelength applications. Advantages of the hydrothermal method are generating highly crystalline and pure products with narrow size distribution and low aggregation of ZnSe. Moreover, the rate and uniformity of nucleation, growth and aging can be controlled by adjusting the hydrothermal reaction conditions which subsequently control the morphology and crystal form of the products. Depending on the characteristics of starting monomer, different preparative methodologies have been adopted to obtain the polymeric materials. They are classified into two major methods, such as electrochemical and chemical polymerization methods. The chemical oxidative polymerization is more applicable than electrochemical method for the preparation of bulk electrode materials with controllable sizes. The polythiophene having good hole conducting property. This sufficiently small band gap, it is possible to excite an electron from the VB to the CB using both UV and visible light. The Polythiophene has comparable visible and UV light transitions possibilities of PTh along with those of metal oxides. The obtained conjugated system of modified reduced graphene oxide composite was characterized by various techniques including X-Ray diffraction spectroscopy (XRD), ultra-violet spectroscopy (UV), photoluminescence (PL), scanning electron microscopy (SEM), Fourier transform infrared spectroscopy (FTIR).



Graphene oxide



polythiophene



zinc selenide



Reference

- [1] R. Kalyani and K. Gurunathan J.Photochem. and Photobiol. A: Chemistry Volume 329, 1 October 2016, Pages 105-112
 - [2] Ji Chen, Bowen Yao, Chun Li, Gaoquan Shi CARBON 64 (2013) 225 – 229
 - [3] F. Mollaamin*, S. Gharibe, and M. Monajjemi Int. J. Phys. Sciences Vol. 6(6), pp. 1496-1500, 18 March, 2011.
 - [4] LIU RuoChen & LIU ZhengPing Chinese Sci Bull, 2009, 54: 2028-2032.
-



5. Green Chemical Technologies

5.1 Chitosan - A Natural Biopolymer: Applications in Biosorption and Pervaporation

Krishnaiah Abburi

Professor of Chemistry (Retd.), Sri Venkateswara University, Tirupati 517502 (A P)
e-mail: abburikrish@yahoo.com

Abstract

Chitin is the most abundant naturally occurring polysaccharide that contains amino sugars. This abundance, combined with the specific Chemistry of chitin and its derivative chitosan, make for the array of potential applications. Its structure resembles that of cellulose, except that the hydroxyl groups in position 2 have been replaced by acetyl amino groups. Chitosan, deacetylated product of chitin, primarily consists of repeating units of beta (1-4) 2-amino-2-deoxy-D-glucose (or D- glucosamine). Chitosan is being used extensively in agriculture, food processing, cosmetics, health and pharmaceutical industries.

We have been working for the past fifteen years on development, characterization and evaluation of potential of chitosan based biosorbents for the removal of metals and phenols from aqueous media and pervaporation membranes for dehydration of industrial solvents as it is biodegradable, biocompatible and available in abundance in nature.

Chitosan, in its natural form, is soft and has a tendency in aqueous solutions to agglomerate or to form a gel. In addition, the active binding sites are not readily available for sorption in their natural form. It is also necessary to provide physical support and increase the accessibility of the metal binding sites for process applications. A new composite chitosan biosorbents were prepared by coating chitosan, a glucosamine biopolymer, onto ceramic alumina and perlite. The composite biosorbents were characterized by high-temperature pyrolysis, porosimetry, scanning electron microscopy, and X-ray photoelectron spectroscopy. Batch isothermal equilibrium and continuous column adsorption experiments were conducted to evaluate the potential of chitosan coated alumina in removing chromium[1] and of chitosan coated perlite in removing cadmium[2] and chromium[3] from synthetic as well as field samples.

Pervaporation, in its simplest form, is an energy efficient combination of membrane permeation and evaporation. It's considered an attractive alternative to other separation methods for a variety of processes. Calcium alginate-chitosan (CA/CS) blended membranes were prepared and cross linked with maleic anhydride (MA) for the pervaporative (PV) dehydration of ethylene glycol[4] and 1,4-dioxane[5]. The structure and properties of blend membranes were studied using FTIR, XRD, TGA, and SEM. The effect of experimental parameters such as feed composition, membrane thickness, and permeate pressure on separation performance of the MA cross linked membranes were determined in terms of flux, selectivity, and pervaporation separation index.

The experimental results suggest that the developed chitosan based sorbents and membranes have potential respectively in removing metals from water and dehydration of industrial solvents.

References

- [1] V. M. Boddu, A. Krishnaiah, J. L. Talbott, E. D. Smith, *Environ. Sci. Technol.* 37(2003) 4449.
- [2] S. Hasan, A. Krishnaiah, T. K. Ghosh, and D. S. Viswanath, *Ind. Eng. Chem. Res.* 45(2006) 5066.
- [3] S. Hasan, A. Krishnaiah, T. K. Ghosh, D. S. Viswanath, V. M. Boddu and E. D Smith, *Sep. Sci. Technol.* 38(2003) 3775.
- [4] A. Subba Reddy, N. Sivakumar, M. Venkatasubbaiah, M. Suguna and A. Krishnaiah, *J. Macromol. Sci. Part A: Pure and Applied Chemistry* 46(2009) 1069.
- [5] A. Subba Reddy, S. Kalyani, N. Siva Kumar, V. M. Boddu, A. Krishnaiah, *Polymer Bulletin* 61(2008) 779.



5.2 Green Chemistry through Process Research & Development

S. Srinivasan

Fleming Laboratories Limited, Secunderabad
Corresponding email address: s.srinivasan@fleminglabs.com

The concepts of green chemistry have been promoted as an effective qualitative framework for developing more sustainable Organic syntheses.

This has been demonstrated by many theoretical and practical cases. In addition, there are several approaches and frameworks focused on demonstrating that improvements were achieved through some of Green Chemistry technologies. However, the application of these principles is not always straightforward in the development of Pharmaceutical products. We propose using systematic frameworks and emerging technologies, tools that help practitioners when deciding which principles can be applied, the levels of implementation, prospective of obtaining simultaneous improvements in all Sustainability aspects, and ways to deal with multi-objective problems.

Therefore, this contribution aims to provide a systematic combination of three different and complementary design tools for assisting designers in evaluating, developing, and improving Pharma manufacturing and Process mass index, under GC perspectives. The Quality by Design- Design of Experiments, Driving force analysis, PAT were employed for this synergistic approach.

Incorporating sustainability at early stages of process research and development. In this demonstration, Process development for Pharmaceutical products is used as a case study to illustrate this advancement. Results show how to identify process design areas for improvements, key factors, multi-criteria decision-making solutions.

Finally, conclusions were presented regarding the tools' use in more robust sustainable process in Pharmaceutical Industry.

5.3 Antimicrobial silver nanoparticles green synthesized using aqueous extracts of red seaweeds against plant pathogens: A potential source for nanopesticide formulation

T.AntonyRoseline and K. Arunkumar*

Marine Algae Research Division
Post Graduate and Research Department of Botany, Alagappa Government Arts and Science College, (Alagappa University), Karaikudi-630 003, Tamil Nadu, India

*Present Address
Department of Plant Science, School of Biological Sciences, Central University of Kerala, RSTC, Padanakkad-671 314, Kasaragod, Kerala

Abstract

Nanoparticles (NPs) are clusters of atoms in the size range of 1–100 nm. The silver (Ag) is being used as antimicrobial agent since ancient civilizations in Ayurvedic therapeutics because of its broad-spectrum and multiple modes of antimicrobial activity. The Ag ions exhibit higher toxicity to microorganism and lower toxicity to mammalian cells. Agriculture production in the world is decreasing because of emergence of plant diseases and every year millions of dollars are being spent for pest control. Pesticides of natural and artificial origin are being used in agriculture either ineffective or create environmental hazards and residual problems. But green synthesized AgNPs can be the effective alternate to chemical pesticides and usage of AgNPs as antimicrobial agents are not uncommon.

In the present study, AgNPs were green synthesized using the aqueous extracts of two agar seaweeds (*Gracilaria corticata* and *Gracilaria edulis*) and two carrageenan seaweeds (*Hypnea musciformis* and *Spyridia hypnoides*) showing antibacterial activity against *Xanthomonas axonopodis* pv. *citri* and *X. oryzae* pv. *oryzae* and antifungal activity against *Ustilaginoidea virens* (cause diseases in plants) were tested under disc diffusion assay as well as broth assay under *in vitro*. The reduction of Ag⁺ to Ag⁰ in the medium was visually observed by the color change from pale yellow to brown and the silver ion reduction bonds corresponding to the surface plasma resonance were confirmed using UV-visible spectra between 410 nm and 430 nm.



The antibacterial activity was higher than the antifungal activity and the bioactivity was increased with increasing concentration of AgNPs.

The FTIR spectra show the presence of common functional groups such as aliphatic amine, alcohols, carboxylics, ether, carboxylic acids, anhydrides, cyclic peptides etc., in the sulphated polysaccharides (agar and carrageenan) and proteins in the aqueous extracts would presumably involve in the reduction of Ag^+ to Ag^0 and stability of nanoparticles synthesized by the four red seaweeds. The XRD, SEM and AFM studies showed that spherical shape with average size of 37, 54, 53 and 49 nm AgNPs synthesized by *G.corticata*, *G.edulis*, *H. musciformis* and *S.hypnoides*, respectively. The EDX results of AgNPs reveal the strong silver signal of 84 % in *G.corticata*, 80 % in *G.edulis*, 65 % in *H.musciformis* and 50 % in *S.hypnoides* along with weak oxygen, carbon and nitrogen. The DLS data indicates the average size of 168, 315, 255 and 938 nm with PDI values of 0.311, 0.250, 0.361 and 0.151 for *G.corticata*, *G.edulis*, *H. musciformis* and *S.hypnoides*, respectively as PDI below 0.5 did not aggregate in liquid but exhibiting agglomeration. From this study, first time that the AgNPs green synthesized from four different red seaweeds showing good antimicrobial activity against plant pathogens under disc diffusion assay as well as broth assay not in aggregate but agglomerate form in the liquid.

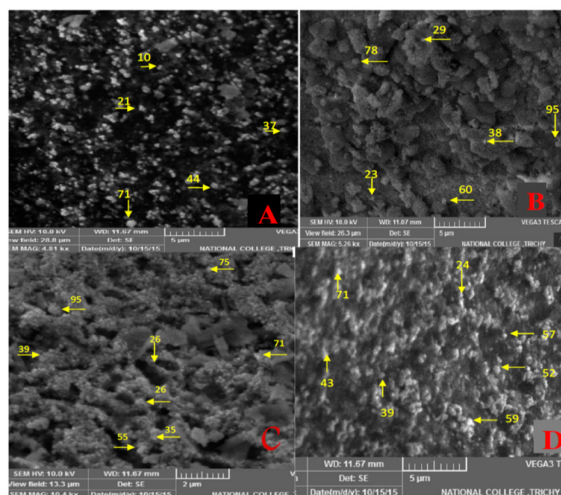
This study conclude that AgNPs green synthesized using four red seaweeds show strong antimicrobial properties against phytopathogens furthered the scope of nanopesticides formulation using seaweed based green synthesis of nanoparticles to control agricultural pathogens.

Key words: Red seaweeds, Silver nanoparticles, Antimicrobial property, Plant pathogens, Green nanopesticides



Fig. 1 Four red seaweed (two are agar yielding a-*Gracilaria corticata* and b-*Gracilaria edulis*) and two are carrageenan yielding (c-*Hypnea musciformis* and d-*Spyridia hypnoides*) collected along the coast of Puthumadam, Gulf of Mannar, India

Fig. 2 SEM image of synthesized AgNPs using algal extracts: a) *G. corticata*, b) *G. edulis*, c) *H. musciformis*, d) *S.hypnoides*



5.5 *Dodonaea viscosa* extract mediated synthesis of AuNPs and its anticancer potential against A549 NSCLC cancer cells

M. Anandan and H. Gurumallesh Prabu*

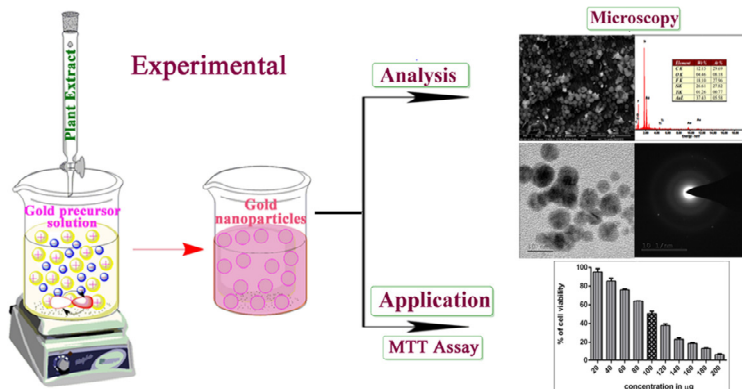
Department of Industrial Chemistry, School of Chemical Sciences, Alagappa University,
Karaikudi - 630 003, India

*Corresponding author. Tel.: +919443882946; Fax: +91 4565225202

E-mail address: hgprabu2010@gmail.com, hgprabhu@alagappauniversity.ac.in

Abstract

Gold nanoparticles (AuNPs) were prepared from the precursor solution by the reduction of gold ions using the leaf extract of *Dodonaea viscosa*. Water was used as a solvent in the extraction process.



The extract acts as both reducing (from Au^{3+} to Au^0) as well as capping agent in the reduction process. The constituents present in the extract like carbohydrates and phenolic compounds were responsible for the formation of stable AuNPs. The synthesized nanoparticles were characterized by UV-Vis, FT-IR, X-Ray diffraction (XRD) methods, Scanning Electron microscopy (SEM) coupled with EDAX and Transmission electron microscopy (TEM) with SAED patterns. Surface plasmon resonance of gold nanoparticles results in a strong absorption peak at 534 nm in the UV-Vis spectroscopy. Peak shifts in FT-IR clearly indicate the presence of the residual plant extract in the sample as a capping agent to the AuNPs. The SEM and TEM results confirmed the spherical gold particles with the average particle size of 30 nm. The presence of gold particles was also confirmed by the XRD and EDX results. The MTT assay reveals that the synthesized AuNPs was able to inhibit the growth of the A549 NSCLC cells effectively and the IC_{50} value was obtained to be of 100 $\mu\text{g}/\text{ml}$.

Keywords: *Dodonaea viscosa*, Gold nanoparticles, TEM, A549 NSCLC cells.

5.6 Green Synthesis of Some Piperidin-4-one Derivatives Using Sugar Based Deep Eutectic Solvent

^aD. Ilangeswaran and ^bK. Hemalatha

^a Department of Chemistry, Rajah Serfoji Govt. College (Autonomous), Thanjavur-613005

^b Department of Chemistry, Justice Basheer Ahmed Sayeed College for Women (Autonomous), Teynampet, Chennai - 600018

email: dhailangeswaran@gmail.com and khema243@gmail.com

Abstract

Deep eutectic solvents (DES) are emerging type of environmentally green solvents. As a new type of solvent, DES has an extremely large number of applications. Even though the problems associated with conventional volatile organic solvents are well studied, the usage of green and bio-renewable solvents still remains a never ending challenge [1].



In this sense, the advantages of using Deep Eutectic Solvents (*DES*) as reaction medium is highlighted from the fact that they are bio-degradable, non-toxic, recyclable and could be easily prepared using inexpensive raw materials [2-6]. *DES* have been studied in a variety of applications including metal deposition, metal oxide dissolutions, purification of bio-diesel, bio-transformations, different synthetic processes and metal-catalyzed organic reactions. In recent years, low melting mixtures consisting of carbohydrates, urea and inorganic salts have been introduced as new alternative sustainable solvents for organic transformations [7].

In this work we synthesized piperidin-4-one, 2,6-diphenylpiperidin-4-one and 3-methyl-2,6-diphenylpiperidin-4-one using a deep eutectic solvent (*DES*) of glucose and urea with the percentage composition of 60:40. The yields of these products were 58, 65% and 62% respectively. The products obtained were characterized by FTIR, ^{13}C and ^1H NMR spectroscopic techniques. The spectral data were compared with the reports already available for these compounds [8, 9].

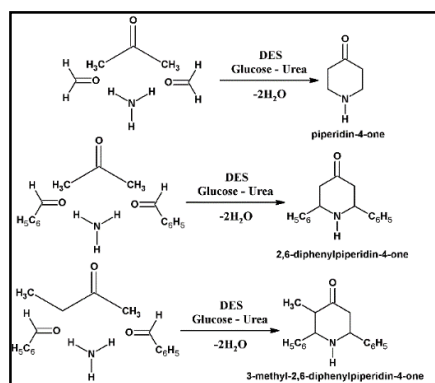


Figure 1. Reaction Scheme for the Preparation of Piperidin-4-ones

The FTIR spectra of piperidin-4-one (A), 2,6-diphenylpiperidin-4-one (B) and 3-methyl-2,6-diphenylpiperidin-4-one (C) in figure 2 revealed their formation from the following observations. In all the three spectra N-H stretching frequency of secondary amino group were noticed at 3300 cm^{-1} and the C=O stretching of carbonyl group were observed around 1700 cm^{-1} .

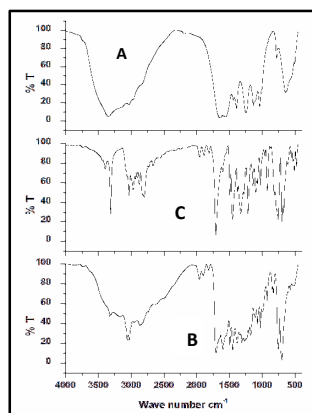


Figure 2. The FTIR spectra of piperidin-4-one (A), 2,6-diphenylpiperidin-4-one (B) and 3-methyl-2,6-diphenylpiperidin-4-one (C)

References

- [1] P. T. Anastas; Wiley-VCH: Weinheim Handbook of Green Chemistry, Vols. 4, 5, and 6, Green Solvents, Ed., Germany, (2011).
- [2] Qinghua Zhang, Karine De Oliveira Vigier, Sebastien Royer and Francois Jerome, Chem. Soc. Rev. (2012),



- [3] A. P. Abbott, R. C. Harris, k. S. Ryder, C. D'Agostino, L. F. Gladden and M. D. Mantle, *Green Chem.*, 13 (2011) 82.
- [4] D. Carriazo, M. C. Serrano, M. C. Gutiérrez, M. L. Ferrer, F. del Monte, *Chem. Soc. Rev.* 41 (2012) 4996.
- [5] C. Ruß, B. König, *Green Chem.* 14 (2012) 2969.
- [6] M. Francisco, A. van der Bruinhorst, M. C. Kroon, *Angew. Chem. Int. Ed.* 52 (2013) 3074.
- [7] D. Reinhardt, F. Ilgen, D. Kralisch, B. König and G. Kreisel, *Green Chem.*, 10 (2008) 1170.
- [8] V. Baliah, V. Gopalakrishnan, R. Jeyaraman, *Indian. J.Chem, Soc.,Sec.B*, 6B (1978) 1065.
- [9] N. Jayalakshmi and S. Nanjundan, *Int. J. Chem. Sci.:* 6(3) (2008) 1177.

5.7 Development of Newer Ethylene Glycol Based Deep Eutectic Solvents and Their Applications for the Synthesis of Some Piperidin-4-one Derivatives

^aD. Ilangeswaran, ^aP. Sukanya, ^aR. Periyanyaki, ^aR. Ranjitha and ^bP.G. Ramesh

^aDepartment of Chemistry, Rajah Serfoji Govt. College (Autonomous), Thanjavur – 613005

^bDepartment of Chemistry, Swami Dayananda College of Arts & Science, Manjakkudi, Tiruvarur-612610

Email: dhailangeswaran@gmail.com, suganyasuvathi@gmail.com, gangadevi17051993@gmail.com,

ranjitharaju@gmail.com and pgrjan2011@gmail.com

Abstract

Making a cost effective and environmentally caring solvent is of gaining importance in organic synthesis [1]. Ionic liquids (ILs) and their equivalent known as deep eutectic solvents (DESs) with desired properties were recognized as potential substitutes to be used as “green” solvents for industries [2–7]. DESs include simple eutectic mixtures made from a combination of quaternary ammonium salts, like choline chloride (ChCl), with either hydrogen bond donors like urea and glycerol, or with metal halides (complexing agent) like zinc chloride. Such eutectic mixtures have emerged as biodegradable, economical alternatives and efficient replacement for conventional solvents and molten salts. Due to their high polarity, metal halide based DESs have outstanding solvation properties and can serve as high temperature electrolytes, reusable or homogeneous catalysts, and as solvent in biodiesel applications. This indicates the wide industrial horizon in which they can play essential roles [7–14].

In this work newer ethylene glycol (EG) based DESs made from two different metal halides such as $MnCl_2$ and $ZnCl_2$ salts were prepared and characterized by measuring some of their important physical properties. These DESs were introduced to replace conventional organic solvents for synthesizing two piperidin-4-ones namely N-Phenylpiperidin-4-one and N-(p-methylphenyl)piperidin-4-one. The DESs and piperidin-4-ones were characterized by FTIR spectra. The density of EG $MnCl_2$ DES and EG $ZnCl_2$ DES were found to be 1.39 and 1.61 g cm^{-3} respectively. The conductivities of both the DES were measured as 0.015 $mS\ cm^{-1}$. The melting point of N-Phenylpiperidin-4-one and N-(p-methylphenyl)piperidin-4-one were observed to be 136 and 128 $^{\circ}C$ respectively.

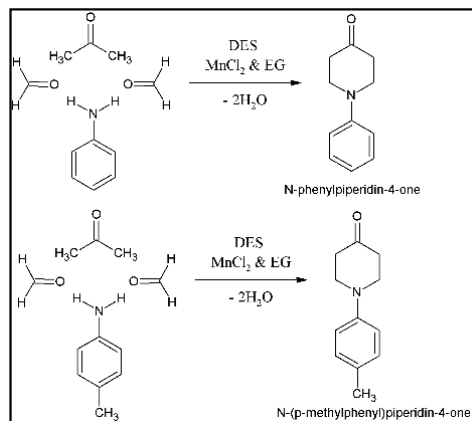


Figure 1. Reaction Scheme for Preparation of Piperidin-4-ones using the newly formed DES



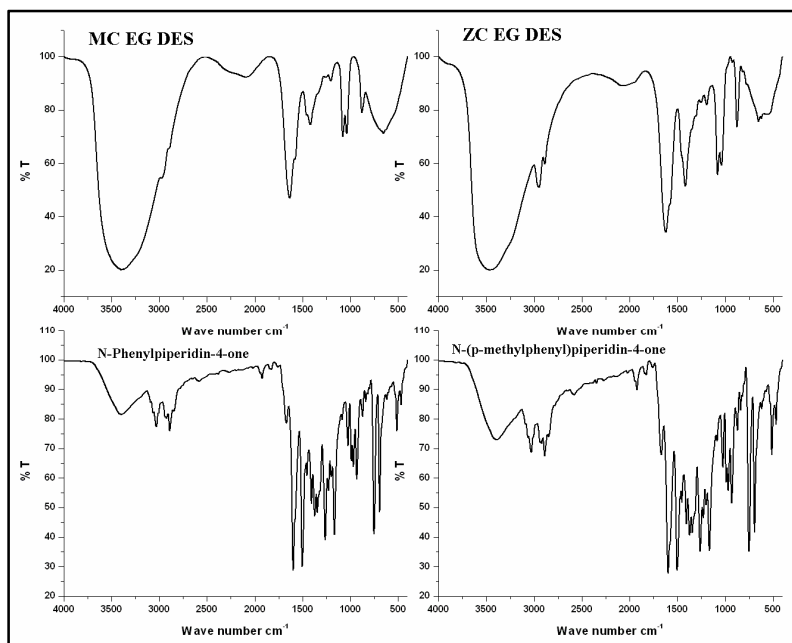


Figure 2. FTIR Spectra of DES and Piperidin-4-one Derivatives

References

- [1] M.A. Kareem, F.S. Mjalli, M.A. Hashim, I.M. AlNashef, J. Chem. Eng. Data 55 (2010) 4632.
- [2] R.D. Rogers, K.R. Seddon, J. Am. Chem. Soc. 125 (2003) 7480.
- [3] M.G. Del Popolo, G.A. Voth, J. Phys. Chem. B 108 (2004) 1744.
- [4] A.B. Pereiro, J.L. Legido, A. Rodriguez, J. Chem. Thermodyn. 39 (2007) 1168.
- [5] N.V. Plechkova, K.R. Seddon, Chem. Soc. Rev. 37 (2008) 123.
- [6] W.M. Nelson, Are ionic liquids green solvents? ACS Symposium Series, Ionic Liquids, (3) 2002, pp 30.
- [7] E.R. Parnham, R.E. Morris, Acc. Chem. Res. 40 (2007) 1005.
- [8] A.P. Abbott, G. Capper, D.L. Davies, R.K. Rasheed, V. Tambyrajah, Chem. Commun. 1 (2003) 70.
- [9] R.C. Harris, Physical Properties of Alcohol Based Deep Eutectic Solvents thesis University of Leicester, 2008.
- [10] A.P. Abbott, D. Boothby, G. Capper, D.L. Davies, R.K. Rasheed, J. Am. Chem. Soc. 126 (2004) 9142.
- [11] A.P. Abbott, G. Capper, D.L. Davies, R.K. Rasheed, Chem. Eur. J. 10 (2004) 3769.
- [12] Y. Fukaya, Y. Iizuka, K. Sekikawa, H. Ohno, Green Chem. 9 (2007) 1155.
- [13] E.R. Parnham, E.A. Drylie, P.S. Wheatley, A.M.Z. Slawin, R.E. Morris, Chem. Int. Ed. 45 (2006) 4962.
- [14] M.C. Gutiérrez, M.L. Ferrer, C.R. Mateo, F. Monte, Langmuir 25 (2009) 5509.

5.8 SYNTHESIS, CHARACTERIZATION, ANTI-MICROBIAL AND ANTI-OXIDANT SCREENING OF NOVEL SULFONAMIDE SCHIFF'S BASES

Swathi.S, Umarani.G, Abdul hasan sathali.A

*Department of Pharmaceutical chemistry, College of Pharmacy,
Madurai Medical College, Madurai-20.
pharmswathi28@gmail.com*

INTRODUCTION:

Sulfanilamide and its derivatives are responsible for a broad spectrum of biological activities. Already many of the scientists have done the anti-microbial studies for sulfanilamide derivatives, which are substituted by various molecules in the position of amino group of sulfanilamide and substitution of aryl ring. In this way we would like to substitute the various aromatic substituted aldehydes in the



position of sulfanilamide containing amino group by Schiff's base reaction and also we tried with various compounds having two primary amino groups instead of sulfanilamide for the anti-microbial and anti-oxidant studies.

OBJECTIVES:

To synthesis sulfanilamide derivatives by Schiff's base reaction by using microwave assisted method. It involves two steps,

Sulfanilamide was synthesized from aniline and acetanilide in the presence of acetic anhydride and ammonia respectively.

O-phenylene diamine was synthesized from nitrochlorobenzene and ammonia followed by hydrogenation in the presence of zinc dust powder.

Sulfanilamide and O-phenylenediamine reacts with various aromatic substituted aldehydes like salicylaldehyde, anisaldehyde, N-dimethylamino benzaldehyde and P-chlorobenzaldehyde by Schiff's base reaction method.

The synthesized novel series of sulfanilamide and O-phenylene diamine derivatives were characterized by TLC and IR spectroscopy and evaluated for anti-microbial and anti-oxidant activities.

METHODOLOGY:

SYNTHESIS OF SULFANILAMIDE DERIVATIVES:

STEP 1: Preparation of sulfanilamide from aniline and acetanilide in the presence of acetic anhydride and ammonia respectively.

STEP 2: Preparation of sulfanilamide Schiff's bases (compound A-D) by Schiff's base reaction.

SYNTHESIS OF O-PHENYLENE DIAMINE DERIVATIVES:

STEP 1: Preparation of O-phenylene diamine from nitrochlorobenzene and ammonia followed by hydrogenation in the presence of zinc dust powder.

STEP 2: Preparation of O-phenylene diamine Schiff's bases (compound E-H) by Schiff's base reaction.

DESIGN: Sulfanilamide and O-phenylene derivatives were designed by following software:

- CHEMDOODLE
- CHEMSKETCH

CHARACTERISATION:

The synthesized compounds were characterized by Infra-red spectroscopy by Pressed-pellet technique and also characterized by thin layer chromatography.

BIOLOGICAL EVALUATION:

Anti-microbial activities were evaluated by cup plate method.

Anti-oxidant activities were evaluated by hydrogen peroxide method only for compound E.



RESULT AND DISCUSSION:

ANTI-BACTERIAL AND ANTI-FUNGAL ACTIVITY

COMPOUND	CONCENTRATION (µg)	E.coli*	S.aureus*	Candida albicans	Aspergillus niger
A	10	3	8	R	R
	30	9	16	4	3
B	10	3	2	R	5
	30	6	7	8	16
C	10	5	R	3	8
	30	11	6	10	18
D	10	4	7	R	5
	30	10	18	R	11
E	10	4	R	14	6
	30	10	4	25	8
F	10	4	R	2	R
	30	11	8	7	9
G	10	5	R	R	5
	30	12	3	6	13
H	10	4	R	R	4
	30	12	7	8	11
CONTROL		R	R	R	R
STANDRAD		12	20	25	18

*All measurements in MMS

R=resistant; Control= DMSO; Standard: Ciprofloxacin, Ketoconazole

ANTI-OXIDANT ACTIVITY

S.NO	CONCENTRATION(gm/ml)	ASCORBIC ACID	TEST SOLUTION
1	10	36.4±1.45	33
2	20	45.91±0.99	47
3	30	52.17±0.87	49
4	40	79.58±1.27	65
5	50	91.23±0.97	88
	IC 50	24.23µg/ml	27.22µg/ml

CONCLUSION:

All the compounds were synthesized by Schiff's base reaction method using microwave irradiation method.

The structure of the synthesized compounds was confirmed by FT-IR spectroscopy.

The anti-microbial activity was performed and when compared to the standard, compound C, D, E, F&H produce the best anti-microbial activity against gram positive organisms.

Synthesized compound E was tested for in-vitro anti-oxidant activity by hydrogen peroxide method and the result was compared with standard Ascorbic acid.

Ultimately we would like to deliver the compound 2-(1H-benzimidazol-2-yl) phenol having Anti-bacterial and Anti-oxidant activity, in future compound E can be modified by chemical reaction when it gives potent and effective molecule.



5.10 Extraction and characterization of Carrageenan from some red algae (Fresh and Defatted algae) along the Pamban coast, Tamilnadu, India

C. Poonam¹ and *C. Pothiraj²

¹Marine Algae Research Division, Post Graduate and Research Department of Botany, Alagappa Government Arts and Science College (Alagappa University), Karaikudi-630003, Tamil Nadu, India

²Department of Botany, Government Arts College, Melur, Tamil Nadu, India.

Abstract

Increasing worldwide demand and development of new applications for carrageenan have added urgency to the search for new or additional raw material sources. Carrageenan is a biopolymer synthesized by several genera of marine red macroalgae (Rhodophyta). It is built on disaccharide-repeating unit of 3-linked D-galactose and 4-linked 3,6-anhydro-L-galactose (3,6-AG) residues, with possible occurrence of sulfate, methoxyl, and/or pyruvate substituents at various positions in the polysaccharide chain. Carrageenans represent one of the major texturising agents in the food industry. They are natural ingredients, which are used for decades in food applications. In general, carrageenan serves as a gelling, stabilising and viscosity-building agent. In order to define the seaweed carrageenan, vibrational spectroscopy can reveal detailed information concerning the properties and structure of materials at a molecular level. Techniques based on FTIR, allowed for the accurate identification of diverse phycocolloids. In the present study the carrageenan extraction characterization from fresh and defatted some red algae along the Pamban coast.

Studies carried out to breakdown the yield and FTIR spectral properties of polysaccharide from *Corallina elongata*, *Liagora mannarensis* and *Porteria hornemannii*. Carrageenan yield ranges from 16.4 to 24.2 % in fresh algae than 14.2 to 23.8% defatted algae recorded.

Spent biomass between 62.0 to 72.0% in fresh algae than 61.2-70.4% defatted algae recorded. Total carbohydrate and Sulphate was abundant in *Porteria hornemannii* and least in *Corallina elongata* having fresh algae carrageenan compared to the defatted algae carrageenan. FTIR spectra in the ranges of 800 to 850 and 930 to 1260 cm^{-1} are useful to differentiate various types of carrageenan (iota, kappa, and lambda) because vibrational bands in these regions are due to stretching vibrations of the sulfate esters and the 3,6-anhydro ring (Pelegrín *et al.*, 2011). The spectra wave number is slightly varied not highly varied from the fresh and defatted algae carrageenan compared to the standard carrageenan. FTIR spectroscopy study shows that *Corallina elongata* fresh and defatted carrageenan having both kappa and iota carrageenan and *Liagora mannarensis* and *Porteria hornemannii* fresh and defatted carrageenan having kappa, lambda and iota carrageenan. Fresh and defatted algal samples have involve the changes total sugar, reducing sugar, sulphate content, spent biomass and carrageenan yield but not change in the carrageenan types of the algal samples.

Keywords: Red algae, Carrageenan, defatted algae, Kappa, lambda, iota, FTIR

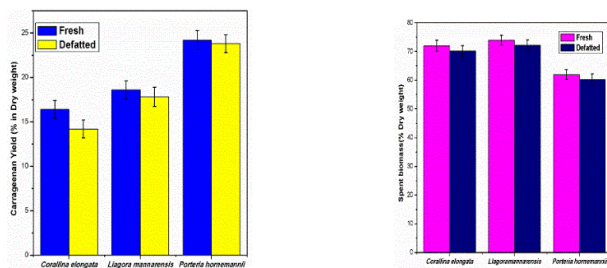


Fig.1 The carrageenan yield and spent biomass of fresh and defatted red algae collected along the coast of Pamban (Rameswaram), Gulf of mannar, India during March 2015



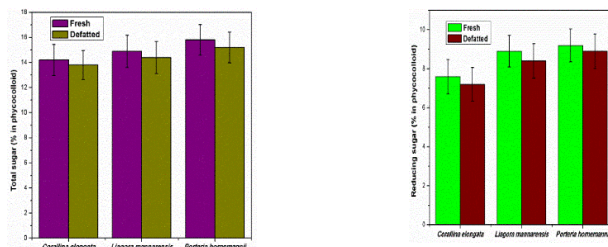


Fig.2 The total sugar and reducing sugar of fresh and defatted phycocolloids of red algae collected along the coast of Pamban (Rameswaram), Gulf of Mannar, India during March 2015

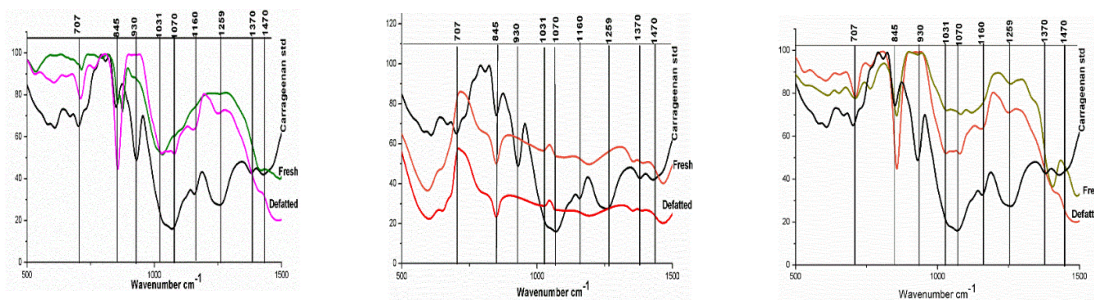


Fig.3 Comparative FTIR spectra of standard carrageenan with that of fresh and defatted carrageenan of red algae *Corallina elongata*, *Liagora mannarensis* and *Porteria hornemannii* collected along the coast of Pamban, Gulf of Mannar, India

5.11 Adsorptive removal of Orange G using activated carbon obtained from most abundant cashew nut shell and karuvelai leaves: Equilibrium, thermodynamics and kinetic studies

Govindan Ramathilagam^a, Kanakkan Ananthakumar,^{*b}

^aResearch Scholar, Department of Chemistry, Raja Doraisingam Government Arts College, Sivaganga-623 561; Email: thilaga0609@gmail.com.

^bHead, Department of Chemistry, Kamarajar Government Arts College, Surandai-627 859; Email: rakeshraahul@gmail.com

Abstract

The adsorption mechanism of organic dye, Orange G (OG) to the activated carbon powder obtained from the most abundant and inexpensive cashew nut shell powder (CNP, *Anacardium occidentale*) and karuvelai leaf powder (KVP, *Prosopis juliflora*) as the adsorbents from aqueous solutions were investigated as a function of pH, temperature, initial dye concentration and contact time. The effect of initial concentration of OG on CNP and KVP and the effect of pH variation of OG on CNP and KVP are shown in Figure 1. This shows that the percentage of dye removal increased with the decreasing initial dye concentration and pH. The increase of temperature decreases the percentage of dye removal. Experimental adsorption data were modeled by different equilibrium isotherms such as Langmuir and Freundlich adsorption isotherms. The adsorption process fitted well to pseudo-second-order kinetics and the Langmuir model. The isotherm data are in accordance with the Langmuir isotherm with a monolayer adsorption capacity of about 31.6 and 36.9 (mg/g) at 30^oC for CNP and KVP adsorbents respectively. Thermodynamic parameters such as ΔH^0 , ΔS^0 and ΔG^0 have also been evaluated. The thermodynamic studies show that the OG dye adsorption onto KLP is a spontaneous, exothermic process. The surface of the CNP and KVP before and after adsorption of OG dye was analyzed by SEM images. The SEM images are shown in Figure 2 and 3. The obvious morphological difference is evident that there is a strong adsorption of OG dye on CNP and KVP.



Though the entire surface is not seen with pores, some pores seen on the surface of the adsorbents could contribute towards the OG adsorption.

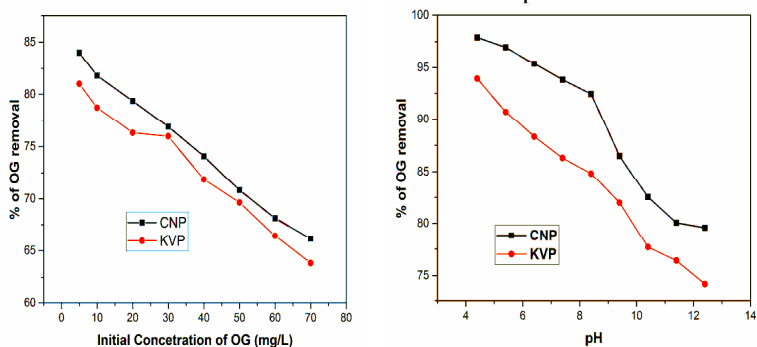


Figure 1. Effect of initial concentration of OG on CNP and KVP (left) and the effect of pH variation of OG on CNP and KVP (right).

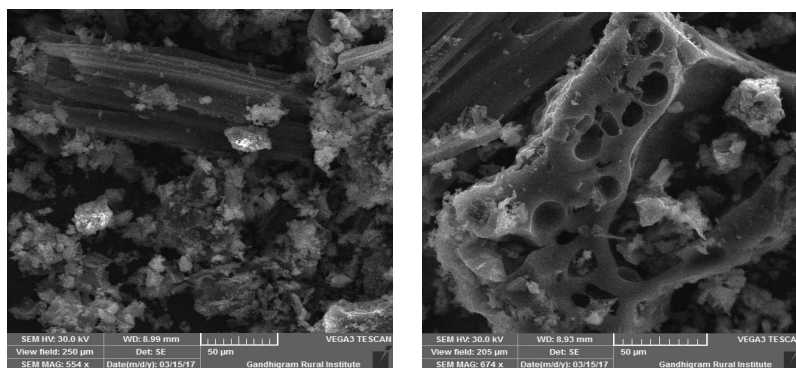


Figure 2. SEM images of before (left) and after (right) adsorption of OG dye on CNP.

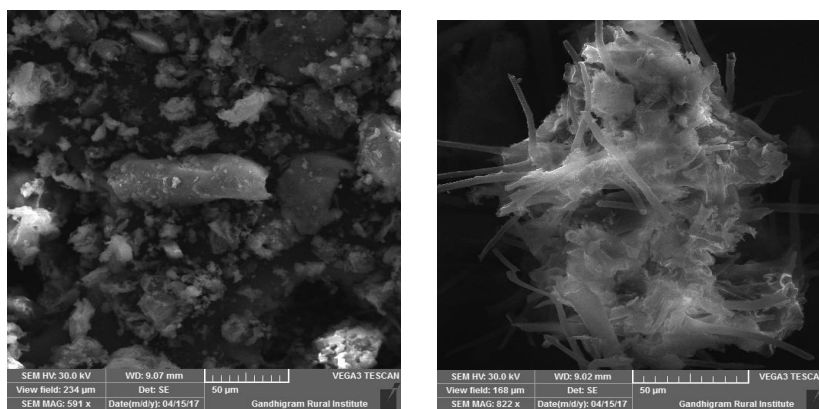


Figure 3. SEM images of before (left) and after (right) adsorption of OG dye on KVP.

References

- [1] F. Falil, F. Allam, B. Gourich, Ch. Vial, F. Audonnet, *Journal of Environmental Chemical Engineering*, 4 (2016) 2556.
- [2] M. A. Salam, S. A. Kosa, A. A. Al-Beladi, *Journal of Molecular Liquids*, (2017) In press.



5.12 GREEN SYNTHESIS OF NOVEL BENZIMIDAZOLE DERIVATIVES, CHARACTERIZATION AND SCREENING OF ANTI-INFLAMMATORY ACTIVITY.

Abdul hassan sathali.A, Umarani.G, Tamilarasi.G, Rajasekaran.K*

Department of Pharmaceutical Chemistry,
College of Pharmacy, Madurai Medical College, Madurai--625020

ABSTRACT

Green chemistry also called as sustainable chemistry and focused on the designing of products and it involves the utilization of a set of principles that reduces or eliminates the use or generation of hazardous substances in the design, manufacture and applications of chemical products. The recent trend, the synthesis of heterocyclic compounds under various conditions like solvent free, green catalyst and microwave irradiation conditions, etc., have appeared. Various benzimidazole derivatives are well known to possess pharmacological activities such as human and veterinary. The literature precedence revealed that the substitutions at the 1, 2 and 5 positions of the benzimidazole moiety are crucial for exhibiting wide range of pharmacological activities. The aim of present study is to obtain substituted benzimidazole from ortho-phenylene-diamine and different aldehydes by **micro wave irradiation methods** because other methods are lot of time consuming, hazardous and required high cost, more instrumental setups. I tried to overcome the above defects from “**Green synthesis of novel benzimidazole derivatives, characterization and screening of anti-inflammatory activity** by using microwave irradiation method.

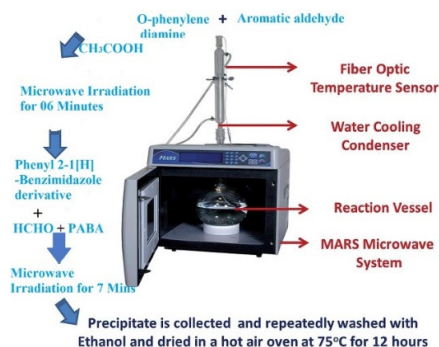


Figure: SYNTHESIS OF NOVEL BENZIMIDAZOLE DERIVATIVES BY MICROWAVE IRRADIATION METHOD

Keywords: Green synthesis, Substituted benzimidazole derivatives, Micro-wave irradiation.

5.13 GREEN SYNTHESIS OF Ce DOPED CdO NANOPARTICLES BY THE PEEL EXTRACT OF CITRUS SINENSIS AND ITS PHOTOCATALYTIC ACTIVITY

Dr. R.R. Muthuchudarkodi* and G. Murugeswari

Department of Chemistry, V.O Chidambaram College, Tuticorin –628008, Tamilnadu, INDIA

*Corresponding Author's Email:muthu.rajaram@gmail.com

ABSTRACT

The objective of this paper is to report a non-toxic, potential green synthetic method for preparing cadmium oxide nanoparticles from cadmium nitrate and ammonium ceric sulphate using *Citrus sinensis* peel extract as a stabilizing agent. The synthesised undoped and Ce doped CdO nanoparticles were characterized using UV-Visible Spectrophotometer. Photocatalytic degradation of Rhodamine B dye under UV-irradiation was also investigated.

Green synthesized nanoparticles eliminate the formation of toxic byproducts. CdO nanoparticles have wide applications as gas sensors, fuel cells, solar cells and reactivity as a catalyst [1]. *Citrus sinensis* (Sweet orange) is a tree of family Rutaceae. Sweet orange has anti-inflammatory, antiseptic, antidepressant and antimicrobial and antioxidant properties.



The UV-Vis spectrum of undoped and Ce ion doped CdO nanoparticles synthesized using *Citrus sinensis* is shown in Fig.1a and 1b. The absorption band for undoped and Ce ion doped CdO nanoparticles were observed at 274 nm and 253 nm [2]. These are effectively blue shifted when compared to the wavelength of bulk CdO which gets absorbed at 350 nm. This blue shift is attributed to the smaller size of nanoparticles and the quantum size effect. The absorption band below 400 nm is due to charge transfer transitions from O 2p to Cd 3d [3].

Fig 2a and 2b shows the decrease in absorbance values of the *Rhodamine B* dye under UV-Vis irradiation in the presence of undoped and doped cadmium oxide nanoparticles. From the absorbance spectra, it was observed that the maximum degradation efficiency of *Rhodamine B* dye within 60 min irradiation time was about 51% for undoped CdO nanoparticles and 62% for Ce ion doped CdO nanoparticles. Thus, Ce ion doped CdO nanoparticles possess much higher photocatalytic activity than undoped CdO nanoparticles.

Keywords: CdO nanoparticles, Green synthesis, *Citrus sinensis*, Photodegradation

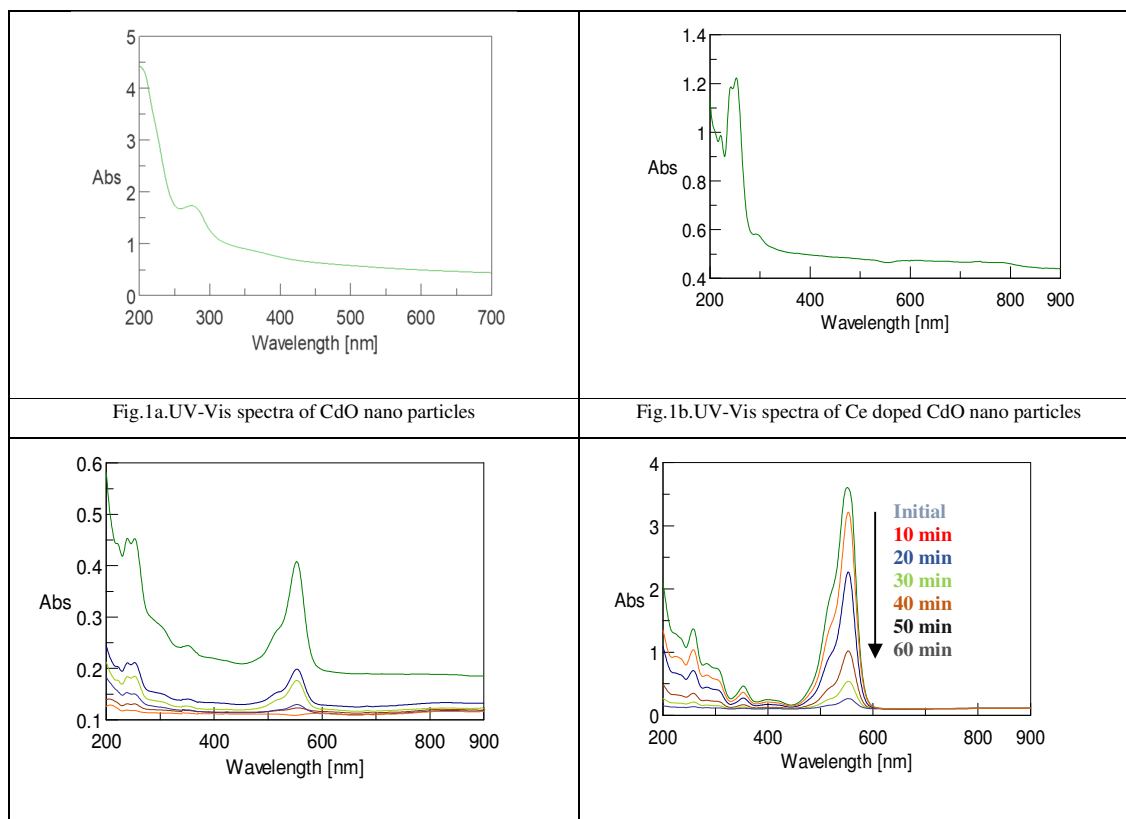


Fig.2.UV-Vis spectra of *Rhodamine B* with (a) undoped CdO nano particles (b) Ce doped CdO nano particles

REFERENCES

- [1] Z. Fan, J.G.Lu, *Journal of Nanoscience and Nanotechnology*, 5 (2005) 1561-1573
- [2] M.C. Sabu, R. Kuttan, *J Ethnopharmacol* 81(2002)155-160
- [3] D. Manoharan, K. Vishista, *Asian Journal of Chemistry*, 25 (2013)9045-9049



5.14 GREEN SYNTHESIS OF NANO-SIZE GRAPHENE AND CHARACTERIZATION

D.Carolin Jeniba Rachel and Dr. C.Vedhi*

Department of Chemistry, V.O Chidambaram College, Tuticorin –628008, Tamilnadu, INDIA

*Corresponding Author's e-mail:cvedhi23@gmail.com

Graphene is a crystalline allotrope of carbon with 2-dimensional properties. Graphene has many unusual properties. It efficiently conducts heat and electricity and is nearly transparent. Graphene shows a large and nonlinear diamagnetism greater than graphite. Graphene is a zero-gap semiconductor. The synthesis of graphene is a growing area for research due to its potentiality in the application and development of advanced technologies. Green synthesized graphene eliminates the formation of the toxic byproducts. Also to compare the nature of graphene prepared using both chemical and green method by only varying the surfactant. The prepared four samples of graphene from graphite by exfoliation method using surfactants such as soap as well as aloe vera gel with the help of magnetic stirrer and sonicator. These are then characterized using UV-Visible spectroscopy, IR spectroscopy. The surface morphology can be studied using AFM technique. The electrochemical studies are carried out by chronopotentiometry, chronoamperometry, EIS and cyclic voltammogram. From FTIR studies graphene exhibits, band at 2922.25 cm^{-1} corresponds to C-H stretching present in graphene. Then bands at 1636.97 cm^{-1} and 1439.41 cm^{-1} assigned to C=C Stretching. The peaks could be ascribed to the C=C from unoxidized sp^2 C=C bonds. And the band at 670.24 cm^{-1} is due to the presence of =CH stretching in alkene. The synthesized graphene samples as well as graphite powder were dispersed in distilled water as solvent using sonication and coated on glass substrate to form thin films. The thin films formed are used to measure surface morphology through AFM. The surface morphology of graphene shown triangular shape of flake and roughness value also presented figure 1. The capacitance of the double layer was evaluated by cyclic voltammetry technique at different scan rates in a potential interval of $\pm 50\text{ mV}$ from the potential of null current of each system, following the relationship given by the equation.

$$\Delta i = I_a - I_c \text{ vs. } (dE/dt)$$

The measurements were performed at the scan rate of 50 mVs^{-1} in the potential range between -1.0V and 1.0 V given in figure 2. For samples obtained by reduction process was chosen, to avoid the risk of oxidation of the graphene samples.

Keywords: Graphene, Green synthesis, Aloe Vera, chemical surfactant, exfoliation and electrode.

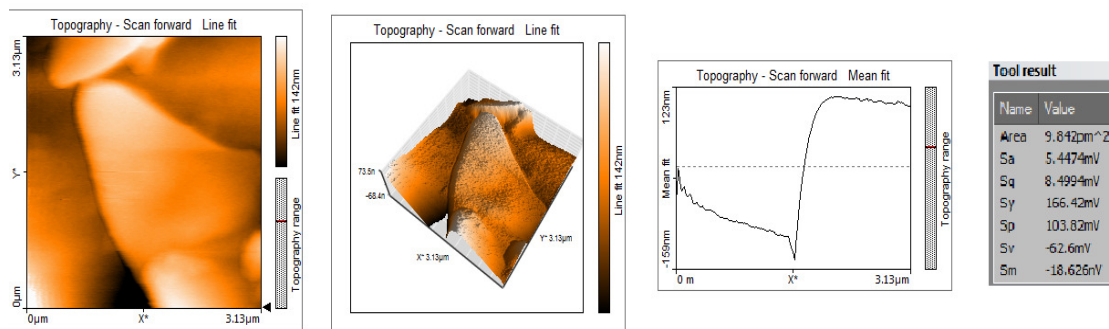


Fig 1 AFM behavior of water dispersed graphene sample



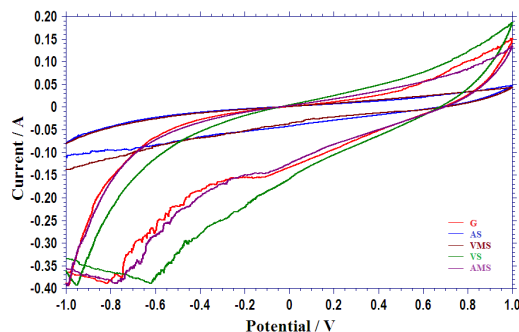


Fig 2 Cyclic voltammetric behavior of synthesized graphene samples and graphite powder

5.15 BIOSYNTHESIS OF COBALT NANOPARTICLES USING MORUS INDICA AND APPLICATION

R. Kirupakaran¹ and Dr. C. Vedhi²

¹PG & Research Department of Chemistry, Govt Arts College, Dharmapuri-636 705, Tamilnadu.

²Department of Chemistry, V.O.Chidambaram College, Thoothukudi-628008, Tamilnadu
Email: kirupasivathmika@gmail.com

ABSTRACT

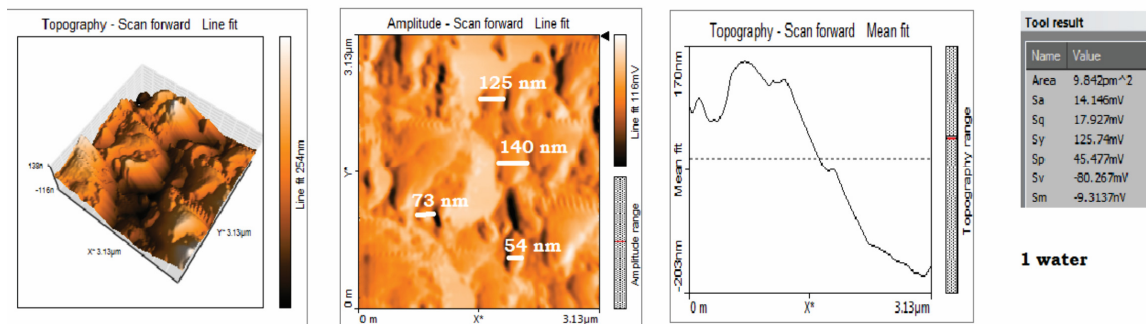
The present study an effort has been made to developed nanoparticles used to biological and industrial application. The green synthesis of cobalt nanoparticles using aqueous & methanol extract of morus indica leaves & stem has been demonstrated. The high biological activity of cobalt and its nanoparticles have an extensive range of applications. The healthy morus indica leaves and stem was collected from Echampatti village, Nallampalli in Dharmapuri district of Tamil Nadu in India. The phytochemically isolated components and the water soluble heterocyclic components such as alkaloid and flavones were principally responsible for the reduction of ions and the stabilization of the nanoparticles. The synthesized cobalt nanoparticles are characterized by UV-Visible spectroscopy, FT-IR, SEM, AFM and antibacterial activity. The phytochemical screening test displayed the presence of dynamic phyto constituent of morus indica leaves and stem aqueous & methanol extracts. The synthesized cobalt nanoparticles exhibits spherical shape with in aqueous extracts average diameter range is 54-125 nm & methanol extracts average diameter range is 92-175 nm. Green synthesized cobalt nanoparticles could be a potential antibacterial agent.

The major Absorption band appeared at 3851, 3430, 2920, 2850, 1717, 1628, 1463, 1384, 1272, 1167, 1074, 880, 720 cm^{-1} . The strong band at 3430 cm^{-1} is due to O-H stretching H-bonded Alcohols and phenol. The band at 2920 cm^{-1} is due to C-H stretching H-bonded Alkane. The band at 2850 cm^{-1} due to C-H stretching H-bonded alkane. The band at 1717 cm^{-1} due to overtones. The band at 1628 cm^{-1} due to overtones. The strong band at 1463 cm^{-1} is attributed to the C-H scissoring in methyl group. The band at 1384 cm^{-1} due to C-H stretching of methyl rock group. The band at 1272 cm^{-1} C-O stretching. The band at 1167 cm^{-1} C-O stretching of ether group. The band at 1074 cm^{-1} is due to in plane C-H stretching bending. The weak band at 880 cm^{-1} is due to C-H bend out of plane bending. The weak band at 720 cm^{-1} is due to C-H out plane bending in long chain methyl rock. The chemical constituents present in Morus Indica leaves aqueous and methanol extract such as polyphenol components and the water soluble heterocyclic components such as alkaloid, flavones imply that the Co-NPs were successfully synthesized and capped with bio-compounds present in the Morus India leaves aqueous and methanol extract by using a green method.

Atomic Force Microscope is employed to analyze the shape of the cobalt nanoparticles synthesized by green method using Morus Indica leaves aqueous extract and methanol extract fig 1



shows AMF image of cobalt nanoparticle. Majority of the particle were spherical in shape formed with diameter range 54-125 nm & 92-182 nm. These particle were well distributed with aggregation.



5.16 ECO- FRIENDLY SYNTHESIS OF ZINC OXIDE NANOPARTICLES FOR BIOMEDICAL APPLICATIONS

ArjunKumar Bojarajan, GurunathanKaruppasamy*

Department of Nanoscience and Technology, Alagappa University, Karaikudi- 630 003.
Ph :04565-225630; e-mail: kgnathan@rediffmail.com

Abstract

The present study reveals that the biosynthesis of zinc oxide nanoparticles (ZnO) was achieved by a novel, biodegradable and convenient procedure using *Gymnemasylvestre* was reducing and capping agent. ZnO nanoparticles were synthesized by using *Gymnemasylvestre* leaf extract. Synthesized ZnONPs were characterized by UV-DRS, X- ray diffraction, Transmission Electron microscopy. Furthermore, the ZnO nanoparticles were evaluated for antimicrobial activity. The UV-VIS absorbance peak was showed at 340 nm. XRD revealed the crystalline structure of the synthesized ZnO NPs with hexagonal. TEM studies of ZnO NPs were found to be spherical in shape with the average size of 20 – 50 nm. Then the applications of the synthesized ZnONps were investigated such as Antibacterial activity which shows a significant inhibition towards both gram positive and gram negative bacterial strains.

Keywords: ZnO NPs, *Gymnemasylvestre* Leaf, Bio-medical applications, Antibacterial activity

5.17 Green Synthesis of Silver Nanoparticles and their Antimicrobial Activity against Gram Positive and Negative Bacteria

Prakashkumar Nallasamy, Gurunathan Karuppasamy*

Department of Nanoscience & Technology, Science Campus, Alagappa University,
Karaikudi-630003.Ph:04565-225630; e-mail: kgnathan27@rediffmail.com

Abstract

Our research focused on the production, characterization and application of silver nanoparticles (AgNPs), which can be utilized in biomedical research and environmental cleaning applications. We used an environmentally friendly extracellular biosynthetic technique for the production of the AgNPs. The reducing agents used to produce the nanoparticles were from aqueous extracts made from the leaves of various plants. Here the plant used for Synthesis of colloidal AgNPs was done by *clitoria ternatea* leaf extract. The reduced silver nanoparticle was monitored by UV-Visible spectroscopy.



The UV-Visible spectrum showed a peak between 420 nm corresponding to the Plasmon absorbance of the AgNPs. The characterization of the AgNPs such as their size and shape was performed by Atom Force Microscopy (AFM), and Scanning Electron Microscopy (SEM) techniques which indicate the morphology. The anti-bacterial activity of AgNPs was investigated at different concentrations for Gram-negative and Gram-positive bacteria. The zone of inhibition increased with the increase in the concentration of silver nanoparticles. These studies are quite useful as it shows the utility of green nanotechnology for the synthesis of silver nanoparticles without any toxic residuals and by-products. Further, efficient antimicrobial activity of the synthesized silver nanoparticles proves the application potential of green synthesis in the area of nano-medicine.

Keywords: Biosynthesis, silver nanoparticles, *Clitoria ternatea*, cytotoxicity bacteria, antibacterial activity

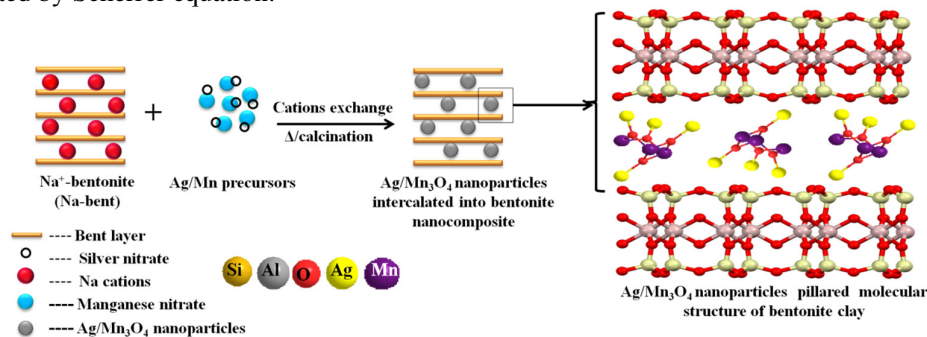
5.18 A Green approach: Silver/manganese oxide nanocomposite supported on bentonite by thermal decomposition method and their biological activities

K. Bama and M. Sundrarajan*

*Advanced Green Chemistry Lab, Department of Industrial Chemistry,
School of Chemical Sciences, Alagappa University, Karaikudi -3, Tamil Nadu, India.*

Abstract

Present study report, we have been developed and introduced the green synthesis of silver/manganese oxide/montmorillonite (Ag/Mn₃O₄/bent) nanocomposite by advanced method of thermal decomposition technique. The synthesized Ag/Mn₃O₄ nanocomposite supported on bent was characterized by XRD, FT-IR, BET, UV-DRS, and SEM techniques. Quasi-spherical sizes of Ag coated on rod shape of Mn₃O₄ nanoparticles intercalated into the bent layers were studied through SEM analysis. The major peak of XRD at 34.9° and 32.4° corresponds to the (105) and (103) lattice plane of tetragonal of Ag and BCC of Mn₃O₄ phase and average crystalline size of nanoparticles is 15 nm was calculated by Scherrer equation.



In FT-IR analysis shows Ag/Mn₃O₄/bent nanocomposite were confirm the presence of Ag and Mn₃O₄ nanoparticles peaks at 1383 cm⁻¹, 600 cm⁻¹ and 528 cm⁻¹ corresponds to the Ag/Mn₃O₄/bent nanocomposite. In SEM analysis result shows the clearly exposes the size of nanoparticles were around ca. 50 nm in excellent spherical shape. The diffuse reflectance spectra show that the value of band gap energy for Ag/Mn₃O₄/bent nanocomposite (3.2 eV) is smaller than Mn₃O₄ nanoparticles (5.3 eV). It was found that decrease in the particles size of Mn₃O₄ nanoparticles due to quantum size effect. Antibacterial activity was carried out using agar well diffusion method for human pathogenic bacteria like Gram positive *Staphylococcus aureus* and Gram negative *Escherichia coli*. These results showed that this nanocomposite has probable to be used as antibacterial materials.



References:

- [1] Sarah C. Motshekga, Suprakas S. Ray, Maurice S. Onyango, Maggie N.B. Momba, Microwave-assisted synthesis, characterization and antibacterial activity of Ag/ZnO nanoparticles supported bentonite clay, *Journal of Hazardous Materials* 262 (2013) 439-446.
- [2] Sh. Sohrabnezhad, M.J. Mehdipour Moghaddam, T. Salavatiyan, Synthesis and characterization of CuO-montmorillonite nanocomposite by thermal decomposition method and antibacterial activity of nanocomposite, *Spectrochimica Acta Part A: Molecular and Biomolecular Spectroscopy* 125 (2014) 73-78.

5.19 GREEN SYNTHESIS AND CHARACTERISATION OF MnO₂ NANOPARTICLES USING CROTON SPARSIFLORUS MORONG LEAVES EXTRACT AND THEIR ANTIBACTERIAL STUDY

N.Latha*, J.Anuradha and M.Gowri

*Department of Chemistry, Kandaswami Kandari's College, Velur - 638 182, Tamil Nadu, India.
Corresponding Author Email : lathaankl@gmail.com, Phone : +91 9487427667*

Abstract

Green synthesis of metal nanoparticles is an eco-friendly approach. At room temperature manganese dioxide (MnO₂NPs) nanoparticles were prepared by using *Crotons Sparaflorus Morong* leaves extract which serves as stabilizing and capping agent. As synthesized MnO₂NPs nanoparticles were analysed by using UV-Vis, FT-IR, SEM /EDAX and XRD techniques and antibacterial assay by disc diffusion method. UV- Vis spectroscopy showed that the peaks appeared at 235 nm - 405 nm. SEM analysis showed that synthesized MnO₂NPs were homogeneous spongy surface besides smaller granules. Elemental analysis conformed that the presence of Mn and O. XRD results clearly indicated that the surface of the MnO₂NPs were amorphous. Antibacterial study clearly revealed that as synthesized MnO₂NPs via green approach are promising antibacterial agent against the *Staphylococcus aureus* and *Pseudomonas aeruginosa* bacteria.

Key Words: Green synthesis, MnO₂NPs, Characterization, Antibacterial activity.

MnO₂NPs have been synthesized by various methods, such as microemulsion, precipitation, sonochemical and hydrothermal methods etc. MnO₂NPs have attracted considerable interest as inexpensive, non-toxic and potential applications in catalysis, alternative materials as rechargeable batteries, molecular adsorption, biosensor, drug carriers for targeted delivery, cancer treatment, gene therapy and DNA analysis, antibacterial agents, and energy storage. Nanometer-sized manganese oxides are of great significance in that their large specific surface areas and small sizes may bring some novel electrical, magnetic, and catalytic properties different from that of bulky materials. One-dimensional manganese dioxide (MnO₂) nanostructures such as nanorods, nanowires, and nanofibers have generated intense research interests over the past recent years due to their superior optical, electrical, catalytic, magnetic and electrochemical properties [1-4].

UV-Vis spectra of MnO₂NPs formed from different volume of *Crotons Sparaflorus Morong* leaves extract separately mixed with different concentration of KMnO₄ solution. UV-Vis results showed the presence of MnO₂NPs peak formed at 200- 410 nm. (Fig.1). The FT-IR spectrum of broad band at 3911 cm⁻¹, 3828 cm⁻¹ and 3810 cm⁻¹ corresponds to the hydroxyl group.



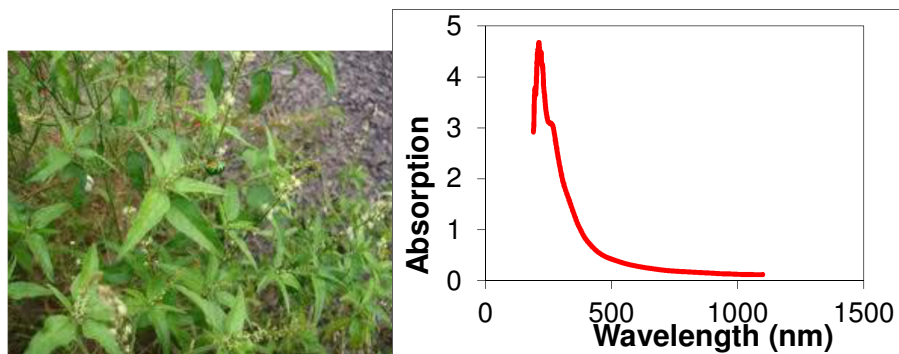


Fig.1 Picture of *Crotons Sparaflorus Morong* leaves & UV-Vis spectra of MnO₂NP's.

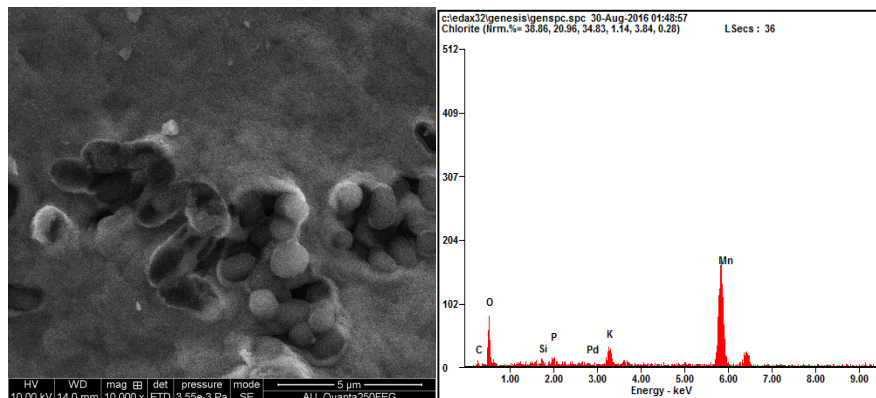


Fig.2 SEM/EDAX image of MnO₂NP's.

The peak at 3167 cm⁻¹ corresponds to OH stretching frequency of phenol. Peak observed at 2904 cm⁻¹ denotes the -CH₃ stretching vibrations. The absorption peak at 2356 cm⁻¹ is due to N-H bond. The peak at 1631 cm⁻¹ corresponds to the C=O group, which is attached to the -N=H bonded primary amines group and the peak observed at 1550 cm⁻¹ corresponds to -N-O stretching vibrations. The bands appear at 949 cm⁻¹ corresponds to the stretching bonds O-Mn-O, which is confirmed in the presence of MnO₂ nanoparticles. SEM image showed that surface of these nanoparticles were smooth, uniform and spherical shape. EDAX analysis showed the presence of Mn & O signals with at.% of Mn and O were found to be 29.03%, 49.55% respectively (Fig.2). From the XRD pattern, it was found that a peak width larger than 10° occurs as a result of the broadening of the peak appear in between 15° to 35°, which corresponds to an amorphous material. The broad peak indicated that the synthesized MnO₂NPs is lower degree of crystallization. From the antibacterial study, it was found that the zone of inhibition of bacterial growth gradually declined when the concentration of MnO₂NPs increased from 1 mg to 4 mg.

References

- [1] S. C. Pang and M. A. Anderson, *J. Mater. Res.* vol. 15, no. 10, pp.2096–2106, 2000.
- [2] S. C. Pang, M. A. Anderson, and T.W. Chapman, *J. Electrochem. Soc.* vol. 147, no.2, pp. 444–450, 2000.
- [3] S. F. Chin, S. C. Pang, and M. A. Anderson, *J. Electrochem. Soci.*, vol. 149, no. 4, pp. A379–A384, 2002.
- [4] S. F. Chin and S. C. Pang, *Mater. Chem. Phys.* vol. 124, no. 1, pp. 29–32, 2010.



5.20 Validation of Anti-inflammatory Phytochemicals from Methanolic Leaf Extract of *Crateva adansonii* DC by Using Molecular Docking Study

Subramanian Ammashi^a and Thirumalaisamy Rathinavel^{a&b}.

^aDepartment of Biochemistry, Rajah Serfoji Government College (Autonomous),
Thanjavur (Dt.) – 613 005, Tamil Nadu, India.

^bDepartment of Biotechnology, Mahendra Arts & Science College (Autonomous),
Namakkal (Dt.) -637 501, Tamil Nadu, India.

Abstract:

Crateva adansonii is a valuable anti-inflammatory plant that belongs to the family Capparacea was screened for its phytochemicals with anti-inflammatory activity. The methanol leaf extracts of the plant was prepared by soxhlet extraction method and screened for its anti-inflammatory phytochemicals by GCMS method. The phytochemicals with anti-inflammatory activity identified in methanol leaf extracts were 3,7,11,15-Tetramethyl-2-Hexadecen-1-ol, Phytol, 1,2-Benzenedicarboxylic acid Mono(2-ethylhexyl) ester and Cyclotrisiloxane Hexamethyl among eight identified major phytochemicals in methanolic leaf extract of the plant. The four anti-inflammatory phytochemicals were further evaluated its anti-inflammatory potential by docking study by FlexX software. Phytochemical 1,2-Benzenedicarboxylic acid Mono(2-ethylhexyl) ester shows maximal docking score with three enzyme (COX-1, COX-2 and 5-LOX) targets.

Keywords: *Crateva adansonii*, Phytochemicals, GCMS and FlexX

Introduction:

Inflammation is the complex biological response of vascular tissues to harmful stimuli including pathogens, irritants or damaged cells [1]. It has been implicated in a broad range of diseases, including diabetes, cancer, hypertension and atherosclerosis [2-5]. Non-steroidal anti-inflammatory drugs (NSAIDs) are one of the best-selling groups of drugs globally but it has several side effects [6]. In order to overcome the side effects of non steroidal anti-inflammatory drugs, it is necessary to develop new agents with more powerful anti-inflammatory activities from plant with fewer side effects [7]. The research into plants with anti-inflammatory agents should therefore be viewed as a fruitful and logical research strategy in the search for new anti-inflammatory drugs.

Materials and Methods

Processing and Preparation of plant material:

The leaves of *Crateva adansonii* were collected from Salem district and authenticated by Botanical Survey of India (BSI), Coimbatore. The leaves were further processed and extract was prepared in methanol solvent in Soxhlet apparatus.

GCMS Analysis

The methanolic leaf extract of the plant was screened for anti-inflammatory phytochemicals using Perkin Elmer Clarus 680 gas chromatography mass spectrometer.

Docking study

The three dimensional structures of three receptors such as COX-1 (PDBID: 4COX), COX-2 (PDBID: 1CQE) and 5-LOX (PDBID: 3O8Y) [8] and the 2D structures of four anti-inflammatory phytochemicals were drawn in ACD-Chemsketch [9] and its SMILES notation was obtained. The SMILES notation was submitted to “Online SMILES convertor and Structure file generator” [10] and converted into 3D SDF format. The developed SDF structures were docked with the predicted binding site of all three receptor binding site by using FlexX [11]. The interactions of phytochemicals with three receptors in the docked complex were analyzed by the pose-view of LeadIT [12].



Result and Discussion

GCMS Analysis

The GC-MS analysis of methanol extract of *Crateva adansonii* leaves revealed the presence of eight phytochemicals by comparing their retention times and interpretation of their mass spectra. The major and minor compounds with their retention times (RT), molecular formula (MF), molecular weights (MW) and peak area percentage are presented in Table 1 and their GCMS chromatogram was shown in Figure 1. Among the eight identified phytochemicals of methanolic leaf extract for phytochemicals possess anti-inflammatory activity namely 3,7,11,15-Tetramethyl-2-Hexadecen-1-ol, Phytol, 1,2-Benzenedicarboxylic acid Mono(2-ethylhexyl) ester and Cyclotrisiloxane Hexamethyl. It is further evaluated their anti-inflammatory potential against three anti-inflammatory enzyme targets (COX-1, COX-2 & 5-LOX) by insilico docking study.

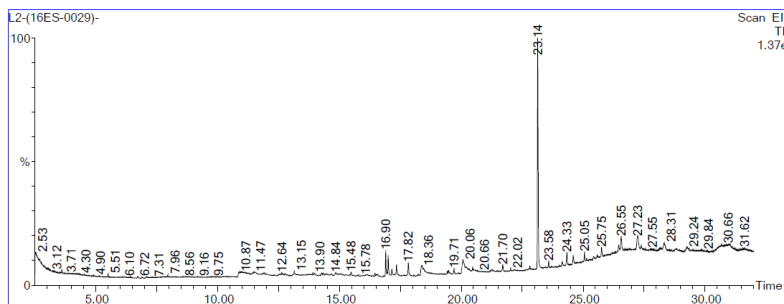


Figure 1 - GCMS Chromatogram of methanolic extract of *Crateva adansonii* leaves

Table.1: Identified of phytochemicals of methanolic leaf extracts of *Crateva adansonii* by GCMS.

S. No	RT	Name of the Compound	Peak Area %	MW	MF	Biological Activity/Uses
1.	16.999	2 Pentadecanone, 6,10,14-Trimethyl	4.406	268	C ₁₈ H ₃₆ O	Allelopathic activity, Antimicrobial activity
2.	17.344	3,7,11,15-Tetramethyl-2-Hexadecen-1-ol	2.489	296	C ₂₀ H ₄₀ O	Antimicrobial, Antinflammatory activity
3.	17.825	Tetradecanoic Acid, 10,13-Dimethyl-, Methyl Ester	3.751	270	C ₁₇ H ₃₄ O ₂	Not Reported
4.	20.075	Phytol	7.245	296	C ₂₀ H ₄₀ O	Antimicrobial, anticancer, anti-inflammatory, anti-diuretic, immunostimulatory and anti-diabetic activity
5.	23.137	1,2-Benzenedicarboxylic acid, Mono(2-ethylhexyl) ester	59.405	278	C ₁₆ H ₂₂ O ₄	Antiviral, Antimicrobial antioxidant and anti-inflammatory properties
6.	24.332	Sulfurous acid, 2-Propyl Tridecyl ester	3.622	306	C ₁₆ H ₃₄ O ₃ S	Antimicrobial, Antioxidant
7.	26.553	1,2-Bis(trimethylsilyl)Benzene	5.648	222	C ₁₂ H ₂₂ Si ₂	Not Reported
8.	27.243	Cyclotrisiloxane, Hexamethyl	8.469	222	C ₆ H ₁₈ O ₃ Si ₃	Antioxidant, Antimicrobial, Antiinflammatory activity

Docking Study

Docking score and molecular interaction results between ligand and anti-inflammatory enzyme targets were presented in Table 1. All three enzyme targets (COX-1, COX-2 & 5-LOX) shows maximal docking score (-9.2759, -8.9913 & -15.5975) respectively with phytochemical 1,2-Benzenedicarboxylic acid Mono(2-ethylhexyl) ester. Similar earlier work was reported by Atul Chopade et al., 2014 [13] on molecular docking studies of phytochemicals from the *Phyllanthus* species as potential chronic pain modulators targets such as IL1 β , TNF, PGE synthase & COX.



Table.2: Docking score of anti-inflammatory phytocompound with enzyme targets

S. No	Compound	COX-1	COX-2	5-LOX
1	3,7,11,15-Tetramethyl-2-Hexadecen-1-ol	-2.3163	2.8472	-3.0243
2	Phytol	-1.9061	3.5892	-2.4663
3	1,2-Benzenedicarboxylic acid Mono(2-ethylhexyl) ester	-9.2759	-8.9913	-15.5975
4	Cyclotrisiloxane Hexamethyl	-3.9546	-4.5422	-9.4312

Conclusion

The four anti-inflammatory phytochemicals were computationally tested for its binding efficiency with crucial targets of inflammation. The analysis of docking scores and molecular interactions of the phytochemicals with anti-inflammatory targets suggest that compounds have the ability to bind to multiple targets involved in inflammatory mechanism. It is concluded that phytochemicals from *Crateva adansonii* leaf extracts may act as a novel anti-inflammatory agent for treating various inflammatory disorders. Further research on the plant *Crateva adansonii* may be useful to isolate novel anti-inflammatory phytochemicals.

References

- [1] Denko CW. 1992, A role of Neuropeptides in inflammation. In: Whicher JT, Evans SW, editors. *Biochemistry of Inflammation*. London: Kluwer Pub. pp. 177-181.
- [2] Schmid-Schonbein, G.W. 2006, Analysis of Inflammation. *Annu. Rev. Biomed. Eng.*, 8, 93–151.
- [3] Duncan, B.B.; Schmidt, M.I.; Pankow, J.S.; Ballantyne, C.M.; Couper, D.; Vigo, A.; Hoogeveen, R.; Olsom, A.R.; Heiss, G. 2003, Low-grade systemic inflammation and the development of type 2 diabetes. *Diabetes*, 52, 1799–1805.
- [4] Kayak, B.S.; Roberts, L. 2006, Relationship between inflammatory markers, metabolic and anthropometric variables in the Caribbean type 2 diabetic patients with and without microvascular complications. *J. Inflammation (London)*, 3, 17–23.
- [5] Solinas, G. Vilcu, C.; Neels, J.G. Bandyopadhyay, G.K. Luo, J.L. Naugler, W. Grivennikov, S. Wynshaw-Boris, A. Scadeng, M.; Olefky, J.M. 2007, JNK1 in hematopoietically derived cells contributes to diet-induced inflammation and insulin resistance without affecting obesity. *Cell Metab.*, 6, 386–397.
- [6] Mizushima Y and Kobayashi M. 1968, Interaction of anti-inflammatory drugs with serum preteins, especially with some biologically active proteins. *Journal of Pharma Pharmacol.*, 20:169- 173.
- [7] Anilkumar M. 2010. Ethnomedicinal plants as anti-inflammatory and analgesic agents. *Ethnomedicine: A Source of Complementary Therapeutics*. 267-293.
- [8] Berman HM, Westbrook J, Feng Z, Gilliland G, Bhat TN, Weissig H, Shindyalov IN, Bourne PE (2000). The protein data bank, *Nucl Acids Res*, 28:235–242.
- [9] ACD/ChemSketch Freeware, version 11 (2006) Advanced Chemistry Development, Inc. Toronto, ON, Canada, www.acdlabs.com
- [10] Weininger D (1988) SMILES, a chemical language and information system. Introduction to methodology and encoding rules, *J Chem. Inf. Comput. Sci.*, 28:31–36.
- [11] Rarey M, Kramer B, Lengauer T, Klebe G (1996) A fast flexible docking method using an incremental construction algorithm, *J Mol Biol*, 261: 470-89.
- [12] Stierand K, Maab P, Rarey M (2006) Molecular Complexes at a Glance: Automated Generation of two-dimensional Complex Diagrams, *Bioinformatics*, 22: 1710-1716.
- [13] Atul R. Chopade, Fahim J. Sayyad, Yogesh V.Pore, (2015) Molecular Docking Studies of Phytochemicals from the *Phyllanthus* Species as Potential Chronic Pain Modulators, *Sci. Pharm.* 83: 243–267



5.21 Synthesis and characterization of TiO₂ Nanoparticles by *Nigrospora oryzae* for biomedical applications

S. Gowri¹ and A. Arumugam²

¹. Department of Nanoscience and Technology, Alagappa University, Karaikudi, Tamil Nadu.

². Department of Botany, Alagappa University, Karaikudi, Tamil Nadu.
Corresponding Author E-Mail: sixmuga@yahoo.com

TiO₂ NPs were synthesized using *Nigrospora oryzae* from the family of fungus by varying the different pH parameters (5,6,7,8,9). Mycosynthesized TiO₂ NPs were characterized by UV-visible spectroscopy, X-ray diffraction spectroscopy, FTIR spectroscopy, SEM and TEM analysis. UV-visible and XRD studies showed better results at pH 9 and was further characterized. SEM analysis revealed that the clustered spherical particles were formed and TEM results confined the particle size in the range of 10-20 nm. The SAED pattern indicated the high crystalline nature of TiO₂ sample. Furthermore, antimicrobial activity of Mycosynthesized TiO₂ nanoparticles examined against four bacteria and one fungus at various concentrations. The better inhibition was observed in *Staphylococcus aureus* and *Streptococcus pneumonia* whereas modulated effect against *Candida albicans*.

Keywords: SEM, TEM, *Candida albicans*, Antimicrobial activity,

5.22 Biosynthesis of Cobalt Oxide Nanoparticles and their Evaluation of Antimicrobial, Hemolytic and cytotoxicity studies

Viswanathan Karthika¹, Ayyakannu Arumugam^{2*}

¹Department of Nanoscience and Technology, Alagappa University, Karaikudi – 630 003. Tamil Nadu, India.

^{2*}Department of Botany, Alagappa University, Karaikudi – 630 003. Tamil Nadu, India.

Corresponding Author E-Mail: sixmuga@yahoo.com

Abstract

A simple one-step biological route was developed for the synthesis of magnetite (Co₃O₄) nanoparticles in *Terminalia chebula* (*T. chebula*) bark extract. The nanoparticles were characterized by XRD, FT-IR, UV-Vis, FE-SEM and HR-TEM. In the reaction system, the influence of organic anions on the morphologies of Co₃O₄ nanostructures was also investigated. The as-synthesized spherical sphere nanoparticles with a concentration of 5–100 µg/mL⁻¹ exhibited nontoxicity towards hemocompatibility in RBC cells, indicating their potential application in biology. In contrast, spheres cobalt oxide nanoparticles (diameters of 30-40 nm) produced using *T. chebula* extracts are highly stable. We suggest that the presence of organic acids (such oxalic or citric acids) plays an important role in the stabilization of cobalt nanoparticles. In the present study cobalt nanoparticles were synthesized by an ecofriendly and cost effective method using bark extract. Antibacterial activity of the synthesized nanoparticles was measured by disc diffusion method. The cobalt nanoparticles showed effective antibacterial activity against Gram positive and negative bacteria. The *In-vitro* cytotoxicity test revealed that the magnetite particles exhibited excellent biocompatibility, suggesting that they may be further explored for biomedical applications.

Keywords: Cobalt nanoparticles, *Terminalia chebula*, Antimicrobial activity, Antibiofilm, Hemocompatibility..



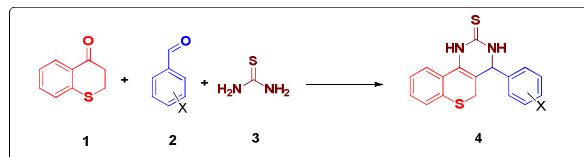
5.23 A microwave mediated solvent-free Biginelli reaction towards the synthesis of highly functionalized novel tetrahydropyrimidines

J. Shanmugapriya^a K.Rajaguru^b and S. Muthusubramanian^b

^aDepartment of Chemistry, Thiagrajar College of Engineering, Madurai

^bSchool of Chemistry, Madurai Kamaraj university, Madurai

Multi-component reactions (MCRs) establish a vastly valuable synthetic tool for the assembly of polyfunctionalized heterocyclic motifs required for drug discovery platforms. They make available convergent, atom economic and eco-friendly synthesis of high level complex molecules and empowering the assembly of three or more simple and diversely flexible building blocks in practical one-pot synthetic operations.



In the present work, three-component domino reaction of substituted-thiochroman-4-ones **1**, aromatic aldehydes **2** and thiourea **3** has been investigated under solvent-free conditions as well as in solvents such as water, dioxane, glycol and ethanol. The thiochromeno-fused pyrimidine-2-thiones **4** have been obtained in very good yield. To increase the product yield, the investigation was continued under solvent free condition with microwave programmed at 100 °C for about 5 min or the duration in which the reaction got completed and based on the optimized conditions, a library of dihydropyrimidines has been synthesized. Structural elucidation of the thiochromeno-fused pyrimidine-2-thiones was accomplished from 1D and 2D NMR spectral data.

5.24 Biofabrication of copper nanoparticle using *Enicostema axillare* extract and antibacterial and antimicrobial activity

S. Saravanan^{a*}, S. Pari^a, D. Madankumar^a, K. Praveen^a, V. Balachandran^b, G. Govindarajan^a

^aPG and Research Department of Physics, National College, Tiruchirappalli – 620 001.

^bPG & Research Department of Physics, AA Government Arts College, Musiri, Tiruchirappalli.

E-mail address: sarantry2009@gmail.com (S. SARAVANAN)

ABSTRACT:

Development of green nanotechnology is generating interest of researchers toward ecofriendly biosynthesis of nanoparticles. In this study, biosynthesis of stable copper nanoparticles were done using *Enicostema axillare* leaf extract. First we prepared leaf extract of *Enicostema axillare* in deionised water. This extract added to 5mMol of copper sulfate solution and we observed the change in color of the solution from colorless to colored solution, this indicates that there is a formation of Cu nanoparticles. These biosynthesized Cu nanoparticles were characterized with the help of UV-Vis analysis, X-ray diffraction (XRD), Fourier transform infrared spectroscopy (FTIR), Field effect scanning electron microscope (FESEM), and Energy dispersive X-ray analysis (EDAX), High resolution transmission electron microscope (HRTEM). It was observed that the *Enicostema axillare* leaf extract can reduce copper ions into copper nanoparticles within 8 to 10 min of reaction time. Thus, this method can be used for rapid and ecofriendly biosynthesis of stable copper nanoparticles. Great antimicrobial activity against bacterial cultures was displayed by these formed copper nanoparticles.

Keywords: Green synthesis, FESEM, HRTEM, Anticancer activity



5.25 Bio synthesis of copper silver nanoparticles using *Scoparia dulcis* extract and antibacterial activity

S. Saravanan^{a*}, S. Pari^a, R. G. Kanagan^a, G. Sathiskumar^a, V. Balachandran^b, N. Kathirvel^a

^aPG and Research Department of Physics, National College, Tiruchirappalli – 620 001.

^bPG & Research Department of Physics, AA Government Arts College, Musiri, Tiruchirappalli

* Corresponding author. Tel.: +919994562858

E-mail address: sarantry2009@gmail.com (S. SARAVANAN)

ABSTRACT

The present study reported green synthesis of bioactive silver nanoparticle (AgNO_3) under different temperature using the aqueous extract of sea grass *Scoparia dulcis* as a potential bioreductant. At first the reduction of AgNO_3 ions were confirmed through colour change which produces absorbance spectra UV-visible spectrophotometer. Additionally various exclusive instrumentation such as X-ray diffraction (XRD), Field effect scanning electron microscope (FESEM) analysis and Higher resolution transmission electron microscope (HRTEM) were authorized the biosynthesis and physio-chemical characterization of CuSO_4 . from Fourier transform infrared spectroscopy (FTIR) analysis and energy dispersive X-ray (EDAX). The overall results suggest that *Scoparia dulcis* is valuable bioresource to generate rapid and eco-friendly bioactive AgNPs towards cancer therapy.

Keywords: Green synthesis, FESEM, HRTEM, Anticancer activity



6. Inorganic Chemistry

6.1 The usefulness of *d-d* transitions in designing new Inorganic Pigments

Srinivasan Natarajan

Framework Solids Laboratory, Solid State and Structural Chemistry Unit, Indian Institute of Science, Bangalore 560 012, India, snatarajan@sscu.iisc.ernet.in

Crystalline inorganic oxides displaying bright colours attracted much attention from early days for application as gemstones and pigments. Ruby (Cr^{3+} doped Al_2O_3) and Emerald (Cr^{3+} doped $\text{Be}_3\text{Al}_2(\text{SiO}_3)_6$) and Azurite ($\text{Cu}_3(\text{CO}_3)_2(\text{OH})_2$), Han blue ($\text{BaCuSi}_2\text{O}_6$) and Turquoise ($\text{CuAl}_6(\text{PO}_4)_4(\text{OH})_8 \cdot 4\text{H}_2\text{O}$) for example found application as gemstones and pigments since ancient times.^[1] In addition to the naturally occurring gemstones and pigments, several man-made (synthetic) coloured solids were also developed to meet the demand. Thus, hydrated chromium oxide (Viridian), cobalt aluminate (Thénard's blue) and various cadmium sulphides (Cadmium Yellow, Cadmium Red) as well as anhydrous Fe_2O_3 (Red ochre) are some of the early synthetic pigments for green, blue, yellow and red colours respectively.^[1] Y_2BaCuO_5 , copper substituted apatites, Mn(III) substituted YInO_3 and $\text{CaTaO}_2\text{N} - \text{LaTaON}_2$ perovskites are some of the more recent pigment materials for green, blue, red-yellow colours.^[2-5] A scientific inquiry into the origin of colours of inorganic solids is essential for a rational design and synthesis of coloured materials. While there are several causes for the colour of solids, the main factor that causes colour in an inorganic oxide containing transition metal ion is the electronic transitions within the partially filled d-states arising from the ligand field effects around the transition metal ion. Octahedral and tetrahedral are the most common geometries where the colour and optical absorption spectra of all the transition metal ions have been well-documented. Transition metal ions in less symmetric geometries such as distorted octahedral and five-fold coordinated (square pyramidal and trigonal bipyramidal) geometries produce colours different from those in regular octahedral and tetrahedral geometries in materials. The present talk would address some of these issues and our efforts towards employing the *d-d* transitions of the transition metals in designing new inorganic pigments.^[6-11]

References:

- [1] P. Ball, *Bright Earth: Art and the Invention of Color*, The University of Chicago Press, Chicago, **2001**.
- [2] P.E. Kazin, M.A. Zykina, Y.V. Zubavichus, O.V. Magdysyuk, R.E. Dinnebier, and M. Jansen, *Chem. – European J.*, **2014**, *20*, 165 – 178.
- [3] J. K. Kar, R. Stevens, C. R. Bowen, *J. Alloys Compd.* **2008**, *455*, 121-129.
- [4] A. E. Smith, H. Mizoguchi, K. Delaney, N. A. Spaldin, A. W. Sleight, M. A. Subramanian, *J. Am. Chem. Soc.*, **2009**, *131*, 17084-17086.
- [5] M. Jansen, H. P. Litschert, *Nature*, **2000**, *404*, 980-982.
- [6] S. Tamilarasan, D. Sarma, S. Natarajan and J. Gopalakrishnan, *Inorg. Chem.*, **2013**, *52*, 5757 – 5763.
- [7] S. Tamilarasan, D. Sarma, M.L.P. Reddy, S. Natarajan, J. Gopalakrishnan, *RSC Advances*, **2013**, *3*, 3199 – 3202.
- [8] S. Tamilarasan, S. Laha, S. Natarajan, J. Gopalakrishnan, *J. of Mater. Chem. C*, **2015**, *3(18)*, 4794-4800.
- [9] S. Tamilarasan, S. Laha, S. Natarajan and J. Gopalakrishnan, *Eur. J. Inorg. Chem.*, **2016**, 288 – 293.
- [10] S. Laha, S. Tamilarasan, S. Natarajan and J. Gopalakrishnan, *Inorg. Chem.*, **2016**, *55*, 3508 – 3514.
- [11] S. Laha, S. Natarajan and J. Gopalakrishnan, *Eur. J. Inorg. Chem.*, **2016**, 288 – 293



6.3 DNA interaction and enhanced DNA cleavage investigation of transition metal(II) mixed ligand complexes having 2-naphthylamine derived Schiff Base

Natarajan Raman* and Ganesan Kumaravel

Department of Chemistry, VHNSN College (Autonomous), Virudhunagar-626 001
E-mail: ranchem1964@gmail.com

Abstract

Two novel Cu(II) and Zn(II) complexes having 2-naphthylamine have been synthesized and characterized by using FTIR, NMR, UV-Vis., elemental analysis and EPR techniques. The molar conductance values indicate that these complexes were electrolytes. The UV-Vis. data exhibit that the complexes adopt octahedral geometry. The X-band region EPR spectra of the Cu(II) complexes were recorded in DMSO at LNT. The quoted g factors were relative to the standard marker TCNE ($g = 2.0027$). Frozen solution EPR spectra reveal the axial features ($g_{\parallel} > g_{\perp} > 2.0023$) and suggest a $d_{x^2-y^2}$ ground state characteristic of octahedral geometry which was axially symmetric. The measure of exchange interaction between the copper centers in the polycrystalline compound can be given by the geometric parameter "G" using relation: $G = (g_{\parallel} - 2) / (g_{\perp} - 2)$. The exchange interaction may be negligible if G is greater than 4. The observed G values of the Cu(II) complex is 4.2 thereby indicating the negligibility of exchange interaction (Table 1). The f values of the Cu(II) complex is 208, indicating significant distortion from planarity. The magnetic moment observed for Cu(II) complex is 1.82 BM, which is consistent with value expected for copper(II) with the spin $S = 1/2$. The DNA binding

Complexes	g-tensor			$A \times 10^{-4} \text{ (cm}^{-1}\text{)}$			$g_{\parallel} / A_{\parallel}$	G
	g_{\parallel}	g_{\perp}	g_{iso}	A_{\parallel}	A_{\perp}	A_{iso}		
[CuL(bpy) ₂]	2.33	2.08	2.16	112	130	124	208	4.2

studies have been performed using electronic absorption titrations and fluorescence experiments. The experimental evidence reveals that the synthesized complexes interact with calf thymus DNA through intercalation with intrinsic binding constants ranging from 1.8×10^5 to 3.2×10^5 . Moreover, the synthesized complexes have the ability to cleave pBR322 DNA in dose dependent manner.

Table 1: The spin Hamiltonian parameters of the Cu(II) complex in DMSO solution at LNT

6.4 SYNTHESIS, STRUCTURAL STUDIES, CHEMICAL NUCLEASE ACTIVITY AND ANTIMICROBIAL EVALUATION OF TRIDENTATE (NOS) SCHIFF BASE LIGAND: 2-(4-(thiophen-2-yl)but-3-en-2-ylideneamino)phenol AND THEIR METAL-ORGANIC HYBRIDS

G.R.Priya Dharsini, A.Neela, T.Clarina, V.Rama*

Department of Chemistry, Sarah Tucker College, Manonmaniam Sundarnar University, Abishekapatti, Tirunelveli – 627 012, Tamil Nadu, India

E-mail : priyarengarajan.pr@gmail.com

ABSTRACT

Coordination chemistry has always been a challenge to the chemists as it has more branches now-a-days. In coordination chemistry, Schiff base ligands, play an imperative task. They are also found at key points in the advance of inorganic biochemistry. Schiff base ligands containing N, O, S donor atoms show broad biological activity and are of particular interest because of the array of ways in which they are bonded to metal ions. Thus in recent decades hefty number of reports related to synthesis of N, O and S containing heterocycles has appeared owing to a wide array of their biological activity. Coordination chemistry of Our present work thus stems from our curiosity in the synthesis, characterization, antimicrobial evaluation and DNA cleavage studies of a tridentate (NOS) donor Schiff base ligand (TBAP): 2-(4-(thiophen-2-yl)but-3-en-2-ylideneamino)phenol and its Co(II), Ni(II), Zn(II) and Cu(II) hybrid derivatives. TBAP was prepared by the condensation of the ketone 4-(thiophen-2-yl)but-3-en-2-one (TB) with 2-aminophenol (AP).



Possible geometry of the hybrid derivatives and the chelating atoms were investigated on the source of elemental analysis, magnetic moment, molar conductivity, infrared, EPR, NMR, electronic and mass spectral studies. The results were consistent with a three coordination environment around the metal ion. Synthesized compounds were screened for *in vitro* antimicrobial activity against bacteria *Escherichia coli*, *Pseudomonas aeruginosa*, *Klebsiella pneumonia*, *Staphylococcus aureus* and *Staphylococcus saprophyticus*, and fungi *Candida albicans*. Hybrid derivatives showed improved antibacterial and antifungal activity compared with the ligand 2-(4-(thiophen-2-yl)but-3-en-2-ylideneamino)phenol TBAP. DNA cleavage experiments done by means of gel electrophoresis with corresponding hybrid derivatives in the presence of H₂O₂ showed pronounced discernible DNA cleavage.

Key words: Antimicrobial, DNA cleavage, elemental analysis, Schiff base, tridentate, thiophene.

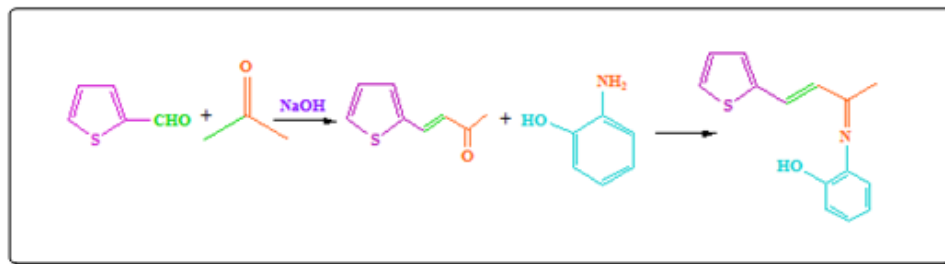


Figure 1: Reaction Scheme for the synthesis of the ligand 2-(4-(thiophen-2-yl)but-3-en-2-ylideneamino)phenol

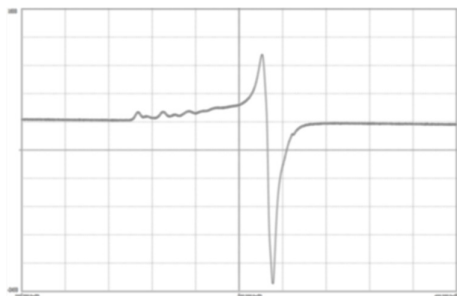
Compounds/ Molecular formula	Mol. Wt.	Yield %	Colour	Elemental analysis calculated/found%				
				C	H	N	S	Metal
TBAP C ₁₄ H ₁₃ NOS	243.32	89	Yellow	69.11 68.97	5.39 5.42	5.76 5.64	13.18 13.02	-
[Cu(TBAP)] C ₁₄ H ₁₄ CuNO ₂ S	323.88	87	Dark green	51.92 51.96	4.36 4.25	4.32 4.21	9.90 9.74	19.62 19.51
[Co(TBAP)] C ₁₄ H ₁₄ Cl ₂ CoNO ₂ S	390.17	84	Reddish brown	43.10 43.15	3.62 3.58	3.59 3.63	8.22 8.17	15.10 14.98
[Ni(TBAP)] C ₁₄ H ₁₄ Cl ₂ NiNO ₂ S	389.93	86	Grassy green	43.12 43.04	3.62 3.64	3.59 3.51	8.22 8.14	15.05 14.94
[Zn(TBAP)] C ₁₄ H ₁₄ ZnNO ₂ S	325.72	84	Dirty white	51.62 51.53	4.33 4.26	4.30 4.27	9.84 9.80	20.08 19.93

Table 1: Physical and elemental analysis data of the ligand (TBAP) and its complexes

References

- [1] A.K. Sharma, S. Chandra, *Spectrochim Acta Part A*, 103 (2013) 96.
- [2] A.O. Abdelhamid, *J Heterocycl Chem*, 46 (2009) 680.
- [3] X.M. Wu, X.S. Wu, J.Y. Xu, *J Chin Pharm Univers.*, 27 (1996) 641.
- [4] A.D. Burnett, A.M. Caplen, R.H. Davis, J. Clader, *J Med Chem.*, 37 (1994) 1733.
- [5] R. Robson, *Inorg Nucl Chem Lett.*, 6 (1970) 125.





ESR spectral data of the vanadyl complex [A_{\parallel} ($175 \times 10^{-4} \text{ cm}^{-1}$) $>$ A_{\perp} ($71 \times 10^{-4} \text{ cm}^{-1}$), g_{\perp} (1.97) $>$ g_{\parallel} (1.93)] indicates that the complex is square pyramidal geometry characteristic for the oxovanadium (IV) chelates. The *in vitro* biological screening effects of the investigated compounds were tested against bacteria: *Escherichia coli*, *Staphylococcus aureus*, *Salmonella typhi*, *Bacillus subtilis* and *Klebsiella pneumonia*. The minimum inhibitory concentration values against the growth organisms of the ligands and their complexes indicates that most of the metal chelates shows higher antibacterial activity than the free ligands.

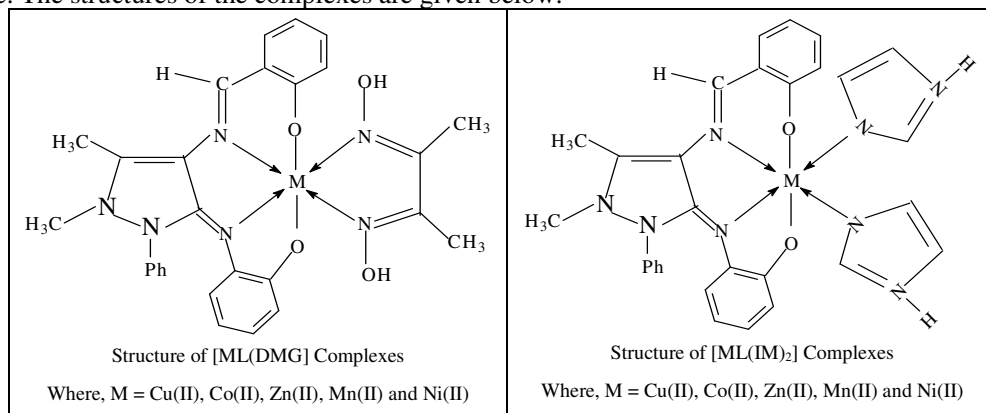
6.6 Synthesis, spectral, redox and antimicrobial activities of mixed ligand complexes derived from salicylidene-4-iminoantipyrinyl-2-iminophenol

A.Kulandaisamy*, A.Palanimurugan and S.Valarmathi

Department of Chemistry, Raja Doraisingam Government Arts College, Sivagangai – 630561.

*kulandai.kvn@gmail.com

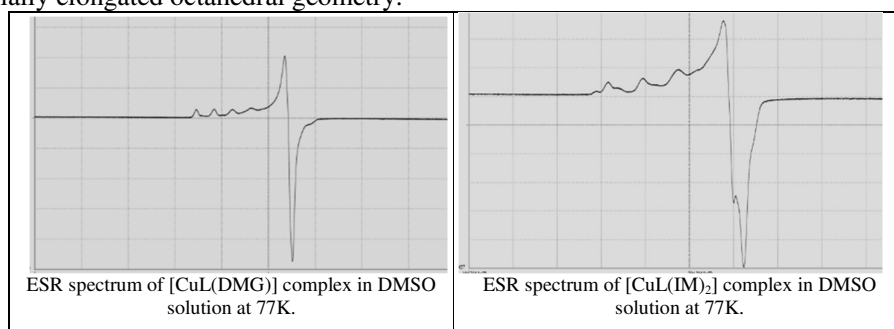
Neutral complexes of Cu(II), Ni(II), Co(II), Mn(II) and Zn(II) have been prepared using a Schiff base derived from salicylidene-4-iminoantipyrinyl-2-iminophenol and dimethylglyoxime/imidazole. The structural feature of the chelates has been confirmed by micro analytical data, IR, UV-Vis., ^1H NMR and ESR spectral techniques. Electronic absorption and IR spectra of the complexes indicate an octahedral geometry around the central metal ion. The monomeric nature of the complexes is confirmed from their magnetic susceptibility. Low conductance data of the chelates support their non-electrolytic nature. The structures of the complexes are given below:



The [CuL(DMG)] complex in MeCN solution shows a quasi reversible peak for the couple: copper(II) \rightarrow copper(III) at $E_{p_a} = +0.48 \text{ V}$ with a direct cathodic peak for copper(III) \rightarrow copper(II) at $E_{p_c} = +0.26 \text{ V}$. Further, it exhibits two peaks characteristic for copper(II) \rightarrow copper(I) ($E_{p_c} = -0.26 \text{ V}$) and copper(I) \rightarrow copper(0) ($E_{p_c} = -0.89 \text{ V}$) reduction in the cathodic region.



The corresponding oxidation peaks are observed in the anodic side, copper(0) → copper(I) at -0.64 V and copper(I) → copper(II) at -0.09 V. The cyclic voltammogram of the [CuL(IM)₂] complex in MeCN solution shows two quasi reversible peak for the couple: Cu(II)/Cu(III) at E_p_a = +0.63 V with a direct cathodic peak at E_p_c = +0.58 V and Cu(II)/Cu(I) at E_p_a = -0.71V with a direct cathodic peak at E_p_c = -0.75 V. The [CoL(IM)₂] complex in MeCN solution exhibits a quasi reversible peak at E_p_a = 0.43 V and E_p_c = 0.32 V are attributable to the Co(II)/Co(III) couple. In the negative region, it shows quasi reversible peaks at E_p_a = -0.39 V and E_p_c = -0.57 V for the couple Co(II)/Co(I). The [NiL(DMG)] complex in DMSO solution exhibits a quasi reversible peak at E_p_a = 0.55 V and E_p_c = 0.41 V are attributable to the Ni(II)/Ni(III) couple. In the negative region, it shows quasi reversible peaks at E_p_a = -0.52 V and E_p_c = -0.68 V for the couple Ni(II)/Ni(I). The ESR spectra of the copper complexes were recorded in DMSO solution and the spin Hamiltonian parameters for the copper complexes are calculated from the spectra. The observed order (A_{||} > A_⊥ ; g_{||} > g_⊥) indicates that the complexes are akin to axially elongated octahedral geometry.



The exchange parameters of copper complexes [G = 4.85 – 4.92], indicating that the exchange coupling effects are not operative in the copper complex, only the local tetragonal axes are aligned parallel or slightly misaligned and consistent with dx²-y² ground state and with elongated axial symmetry. The orbital reduction factors for the present copper complexes, K_{||} < K_⊥, demonstrating that the complexes having considerable in-plane π-bonding while the out of plane π-bonding is absent. Antibacterial activities of the compounds were tested *in vitro* against two Gram-positive (*Staphylococcus aureus* and *Bacillus subtilis*) and three Gram-negative (*Klebsiella pneumoniae*, *Escherichia coli* and *Salmonella typhi*) bacteria by the disc diffusion method.

The MIC values of Schiff base, DMG and their metal complexes (mg/l) are given in Table 1

Compound	<i>Escherichia coli</i>	<i>Salmonella typhi</i>	<i>Klebsiella pneumonia</i>	<i>Staphylococcus aureus</i>	<i>Bacillus subtilis</i>
DMG	55	50	45	45	50
L	48	43	59	34	36
[Cu L (DMG)]	23	25	34	39	44
[Ni L (DMG)]	26	29	29	29	44
[Co L (DMG)]	23	25	34	34	39
[Mn L (DMG)]	18	18	29	29	24
[Zn L (DMG)]	13	13	19	14	19
[Cu L (IM) ₂]	38	40	39	28	28
[Ni L (IM) ₂]	33	35	32	36	36
[Co L (IM) ₂]	32	34	26	31	38
[Mn L (IM) ₂]	40	45	35	34	39
[Zn L (IM) ₂]	24	23	29	24	29

The Lower MIC values of metal chelates suggested that metal chelates are higher antibacterial activities than free ligands.



6.7 Thin-Layer Chromatographic Separation and Identification of certain Inorganic toxic anions in soil, ground water and sewage sludge samples from Fireworks and Safety Matches manufacturing areas in Sivakasi, Virudhunagar District, Tamil Nadu, India

S.Thangadurai and B.Karthik prabu

Post Graduate Studies and Research Department of Chemistry
Raja Doraisingam Government Arts College, Sivagangai – 630 561
Tamil Nadu, India.
E-mail: drstdurai@gmail.com

Fireworks displays are an important source of pollution that generate substantial quantities of chemicals such as heavy metals, PAHs and oxyanions on a regional or national scale within a short and specific period of time. Examples of such events are New Year's Eve and 4th of July celebrations in the US, and the Lantern Festival in Asian countries. During the burning or explosion process, fireworks generate large amounts of smoke, usually in plumes, that is dispersed into the atmosphere. Burning of crackers and sparkles during Diwali in India is a very strong source of pollution which contributes significantly to the environment.

Sivakasi is a small town located in Tamil Nadu State with a population of about 235,000 in 2011. Sivakasi is called "A town of three industries" because it is known for its production of fireworks, safety match sticks, and printing industry. There are around 450 factories with 40,000 direct and about 1 lakh indirect labors, which include commuters and workers in affiliated business, scattered in and around Sivakasi. Fireworks in Sivakasi also produce Military Weapons training items. They are used for training in armed forces. Some airports are using Sivakasi rocket to scare away birds to avoid bird hits of aircrafts. It is known that this small town produces about 90 % of global demand of fireworks products. The prevailing dry and hot weather throughout the year favors the presence of these industries in the region.

In this study, our aim was to assess the perchlorate and chlorate contamination in soil, ground water and sewage sludge samples from fireworks and safety matches manufacturing areas in Sivakasi. Thin-layer chromatographic (TLC) behaviour of ten anions on plain silica gel G UV₂₅₄ and sprayed with citric acid reagent (CAR) solution has been investigated. The effect of CAR concentration on the mobility of anions has been examined. Methanol:n-butanol:methylamine (60:20:20) was the most effective solvent system for differential migration anions which is present in the collected samples. Better results in terms of clarity of detection and compactness of spots were found with acetone: DMSO (50:50), HCOOH: acetone (40:60), HCOOH: acetone:DMSO:H₂SO₄ (25:40:30:5), HCOOH:acetone (50:50) and HCOOH:acetone (30:70). The effect of anion loading on R_f values has been investigated.

In order to separate the inorganic anions *viz.* perchlorate (ClO₄⁻), phosphate (PO₄³⁻), sulphate (SO₄²⁻), nitrate (NO₃⁻), chloride (Cl⁻), fluoride (F⁻), nitrite (NO₂⁻), sulphite (SO₃²⁻), thio sulphate (S₂O₃²⁻) and cyanide (CN⁻) silica gel G UV₂₅₄ was used as an adsorbent. Thirteen Solvent systems were proposed for the separation and identification of certain inorganic toxic anions and visualization of these anions were performed by both short long wavelength UV (254 nm & 356 nm) and also sprayed with saturated solutions of silver nitrate in methanol, 1% of aqueous solutions of potassium ferro cyanide and CAR.

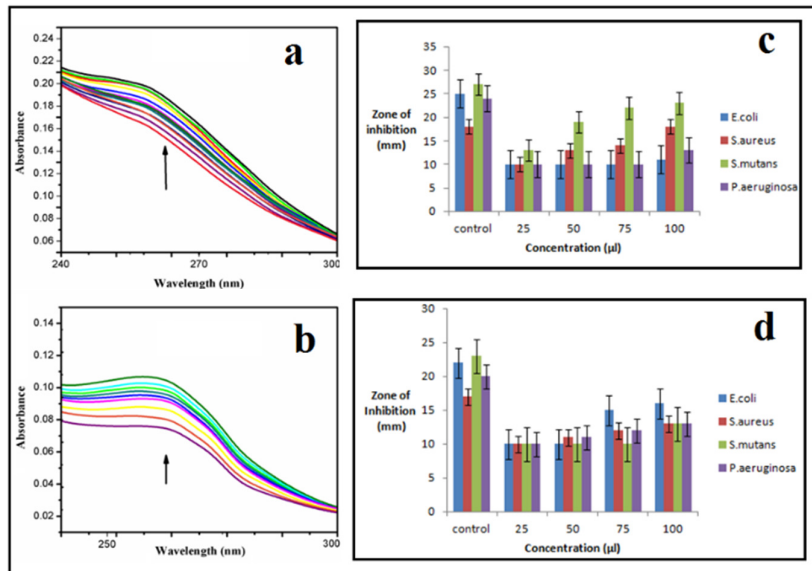
The samples collected from the industries were subjected to separate and to identify the possible toxic inorganic anions using solvent system methanol: n-butanol: methylamine (60:20:20), it was sprayed with CAR pink colour was appeared, in this system only eight anions could be separated and detected *viz.* ClO₄⁻, R_f=0.95; ClO₃⁻, R_f=0.86; PO₄³⁻, R_f=0.47; SO₃⁻, R_f=0.53; NO₃⁻, R_f=0.84; Cl⁻, R_f=0.55; F⁻, R_f=0.88 and NO₂⁻, R_f=0.40. The R_f values in various solvents and the colours developed at each stage for certain inorganic toxic anions were noted. There were no separations in the solvent systems ammonium hydroxide: acetone (30:70 & 50:50). Whereas, in the case of solvent system methanol: n-butanol: dichloromethane (60:25:15) SO₄²⁻ and S₂O₃²⁻ were separated, in the solvent system acetonitrile: methylamine (90:10) the anion NO₂⁻ alone separated.

Preliminary evaluations of TLC of KClO₃ and NaClO₄ were done on Silica Gel G UV₂₅₄ plates. Using isopropyl alcohol-1.5 N NH₄OH (95:5) R_f values were 0.85 for ClO₃⁻ and 0.90 for ClO₄⁻. Plates were over sprayed with methylene blue in ethanol for ClO₄⁻ followed by diphenyl amine (DPA) in H₂SO₄ for ClO₃⁻.



Figure 1. Absorption spectra of complexes $\text{Co}_2(\text{oxpn})(\text{acac})_2$ (a) and $\text{Co}_2(\text{oxpn})(\text{pdc})_2$ (b) in 5 mM Tris-HCl/50 mM NaCl buffer upon addition of DNA. The arrow shows the absorbance changes upon increasing the DNA concentration. Antibacterial activity $\text{Co}_2(\text{oxpn})(\text{acac})_2$ (c) and $\text{Co}_2(\text{oxpn})(\text{pdc})_2$ (d)

References:



- [1] S. Torelli, C. Belle, L. Gautier-Luneau, J.L. Pierre, Inorg. Chem. 39 (2000) 3526.
- [2] D.M. Boghaei and M. Gharagozluo. Spec. chim Acta Part A: Molecular and Biomolecular Spectroscopy 61 (2005) 3061.



7. Miscellaneous

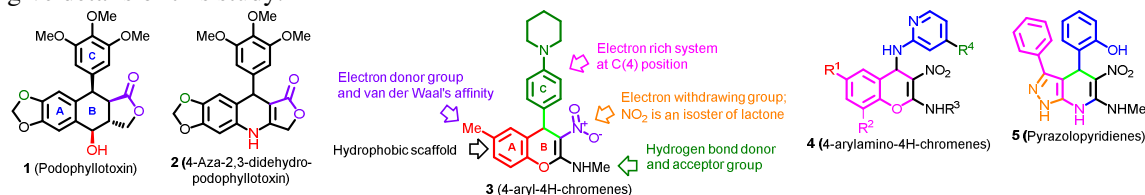
7.1 PODOPHYLLOTOXIN MIMICS: SYNTHESIS AND BIOLOGICAL ACTIVITY

H. Surya Prakash Rao

Department of Chemistry, Pondicherry University, Pondicherry – 605 014. India

ABSTRACT

In recent years synthesis and biological evaluation of diversity oriented scaffolds have been in practice in drug discovery regimen. Among the naturally occurring anticancer agents, podophyllotoxin (POD) **1** (Figure 1),¹ a lignin isolated from rhizomes of *Podophyllum peltatum*, *Podophyllum hexandrum* and *Sinopodophyllum hexandrum* gained importance owing to its promising activity against human papilloma virus (HPV) and some types of cancer.² POD and its sibling lignins destabilize the polymerization of tubulins and also suppress cellular nucleoside transport both of which lead to cellular necrosis.³ However, POD exhibits acute toxic side effects which prevent its generic use. Presently it is used for treatments of genital warts (*Condylomata acuminata*) as an ingredient in topical application.⁴ It is difficult to isolate POD in pure form or synthesize in industrial scale. Therefore, the necessity exists for the development of an easy, reliable industrial-scale synthesis of its mimics which have equal to or better pharmacological properties. In recent years mimics of POD like **2** (Figure) which possess its pharmacophore features have appeared.⁵ Unlike POD its surrogate proved to be a better anti-cancer drug candidate.⁶ It has almost equal potency, lower toxicity and extremely easy to synthesize in large quantities. Moreover, it is possible to synthesize a combinatorial library of analogs of **2** to enable discovery of better drugs.⁷ We have been interested to synthesize mimics of POD **1** for over a decade.⁸ We have introduced 4-aryl-4H-chromenes **3** as anti-cancer agents. It has several pharmacophore features of **1** as shown in Figure. In continuation of this work we have synthesized several 4H-chromenes **4** and pyrazolopyridines **5** and got their biological activity evaluated. In the seminar we will give details of this study.⁹



Reference

- [1] Bhanot, A.; Sharma, R.; Noolvi, M. *Int. J. Phytomedicine*. **2011**, *3*, 9-26.
- [2] Kelly, M. G.; Hartwell, J. L. *J. Natl. Cancer Inst.* **1954**, *14*, 967-1010. (b) Imbert, T. F. Discovery of Podophyllotoxins. *Biochimie*. **1998**, *80*, 207-222. (c) Liu, Y. Q.; Tian, J.; Qian, K.; Zhao, X. B.; Morris-Natschke, S. L.; Yang, L.; Nan, X.; Tian, X.; Lee, K. H.. *Med Res Rev*. **2015**, *35*, 1-62.
- [3] Loike, J. D.; Horwitz, S. B. *Biochemistry*, **1976**, *15*, 5435-5437.
- [4] Sundharam, J. A. *Indian J Dermatol Venereol Leprol*. **1990**, *56*, 10-14.
- [5] You, Y. *Curr Pharm Des*. **2005**, *11*, 1695-717.
- [6] Magedov, I. V.; Manpadi, M.; Slambrouck, S. V.; Steelant, W. F.; Rozhkova, E.; Przheval'skii, N. M.; Rogelj, S.; Kornienko, A. *J. Med. Chem*. **2007**, *50*, 5183-5192.
- [7] Magedov, I. V.; Frolova, L.; Manpadi, M.; Bhoga, U. D.; Tang, H.; Evdokimov, N. M.; George, O.; Georgiou, K. H.; Renner, K. H.; Getlic, M.; Kinnibrugh, T. L.; Fernandes, M. A.; van Slambrouck, S.; Steelant, W. F. A.; Shuster, C. B.; Rogelj, S.; van Otterlo, V. L. A.; Kornienko, A. *J. Med. Chem*. **2011**, *12*, 4234-4246.
- [8] Rao, H. S. P.; Tangeti, V. S.; Adigopula, L. N. *Res. Chem. Intermed*. **2016**, *42*, 7285-7303 (b) Parthiban, A.; Kumaravel, M.; Muthukumaran, J.; Rukkumani, R.; Krishna, R.; Rao, H. S. P. *Med. Chem. Res*. **2016**, *25*, 1308-1315 (c) Parthiban, A.; Kumaravel, M.; Muthukumaran, J.; Rukkumani, R.; Krishna, R.; Rao, H. S. P. *Med. Chem. Res*. **2015**, *24*, 1226-1240 Rao, H.S.P.; Adigopula, L.N.; Ramadas, K.. *ACS. Comb. Sci*. **2017**, *19*, 279-285.



7.3 METAL CATALYSED COUPLING REACTIONS IN MODIFYING HETEROCYCLES



S. Muthusubramanian

CSIR Emeritus Scientist, School of Chemistry, Madurai Kamaraj University, Madurai 625 021
muthumanian2001@yahoo.com

Metal catalyzed carbon-carbon and carbon-heteroatom cross coupling reactions find applications in the field of drug discovery, agrochemicals, material science, supramolecular chemistry and also in natural product synthesis. In our laboratory, we have successfully employed such coupling reactions to construct or modify the heterocyclic skeletons. Some of the reactions that have been achieved in this directions are: (1) Copper catalyzed domino $sp-sp^2$ decarboxylative cross coupling employing 2-iodotrifluoroacetanilide and aryl propiolic acid leading to 2-arylindoles (2) Nickel catalyzed approach towards the synthesis of diversely substituted 6-aza-tetrahydroquinazolines from pyridopyrimidine-2-thione and organoboronic acids by non-basic desulfitative C-C cross coupling strategy and a similar Liebeskind-Srogl reaction to get substituted fused thiazoles (3) Copper (II) catalyzed C-S cross coupling of thiazolidine-2-thiones with organoboronic acids towards the synthesis ofazole sulfides (4) Copper(I) catalyzed cascade intramolecular nucleophilic attack on N-sulfonylketenimine followed by rearrangement resulting in substituted 8,9-dihydro-5H-imidazo[1,2-a]-[1,4]diazepin-7(6H)-ones (5) Palladium-catalyzed decarboxylative Suzuki coupling of azaindole-2-carboxylic acid towards 2-aryl-1-(phenylsulfonyl)-1H-pyrrolo[2,3-b]pyridines (6) Palladium catalyzed C-H activation/ortho-arylation of heteroaryl-N-oxides through a decarboxylative coupling of heteroaryl carboxylic acids and (7) Silver catalyzed acylation of pyridine-N-oxides by α -oxocarboxylic acid.

The mechanistic features and the main applications related to the above reactions will be discussed in this lecture.

7.4 Efficient and safer synthesis of value-added organic molecules adopting continuous flow technologies

Balamurugan Ramalingam

Institute of Chemical and Engineering Sciences (ICES), 8, Biomedical Grove, #07-01, Singapore 138665
e-mail: balamurugan_ramalingam@ices.a-star.edu.sg

The interest in developing flow based technologies for organic synthesis has recently increased due to its several advantages such as low mass transfer limitations, efficient heat transfer, uniform reaction conditions throughout the reaction, fast optimization of reaction and catalyst parameters, easy scale-up, etc. Moreover, recently Food and Drug Administration (FDA) revised its manufacturing regulations for the first time in 25 years. The agency is now insisting the pharmaceutical industries to adopt the latest and precise manufacturing techniques for the preparation of drugs and active pharmaceutical ingredients (APIs). We are constantly developing new technologies for the synthesis of functional molecules by integrating green and sustainability principles.

In the presentation, the execution of the synthesis of selected synthetically valuable organic transformations adopting flow methodologies will be discussed in detail. The case studies include modified asymmetric Strecker synthesis of amino acids¹ using highly toxic cyanides, alkylation of amines² and lithiation³ of pharmaceutically important amides.

References.

- [1] Balamurugan, R.; Seayad, A. M.; Yoshinana, K; Nagata, T.; Chai, C. L.L.; Garland, M. *Org. Lett* **2010**, 12, 264-267; *Adv. Syn. Catal.* **2010**, 352, 2153-2158; *Chem. Eur. J* **2012**, 18, 5693.



- [2] Balamurugan, R.; Seayad, A. M.; Pei Shan, S.; Tuan, T. D. *ChemCatChem* **2014**, 6, 808-814; *ACS Catal.* **2015**, 5, 4082.
- [3] Feng, R.; Ramchandani, S.; Ramalingam, B.; Tan, B.; Li, C.; Teoh, S. K.; Boodhoo, K.; Sharratt, P. *Org. Process. Res. Dev.* Accepted.

7.5 Crystal Structure of Glutaminyl-tRNA synthetase from *Thermus thermophilus* HB8 and its complexes

Nachiappan Mutharasappan¹, Vitul Jain², Amit Sharma², Yogavel Manickam² and Jeyakanthan Jeyaraman^{1*}

¹ Structural Biology and Biocomputing Laboratory, Department of Bioinformatics, Alagappa University, Karaikudi - 630 103, ²Structural Parasitology Lab, International Centre for Genetic Engineering and Biotechnology, Aruna Asaf Ali Marg, New Delhi - 110 067.

Coresspondance E-mail: jjkanthan@gmail.com

Aminoacyl-tRNA synthetase (aaRS) are a major ensemble in protein translation and are vital in interpretation of genetic code. aaRS catalyses the esterification of a specific amino acid to one of its attuned cognate tRNAs to form an aminoacyl tRNA. Several members of this family have been characterized over the past years. The gene for the Glutaminyl-tRNA synthetase (GlnRS), a class I enzyme from the extreme thermophile, *Thermus thermophilus* HB8 has been cloned and sequenced. As the enzyme is from a hyperthermophile, its known to be stable at very high temperatures and it can be used as a model to study the general characteristics of enzymes. Sequence analysis revealed an open reading frame that codes for a protein of 548 amino acid residues (63469 Da). Codon usage in the Glutaminyl-tRNA synthetase (*Tt*GlnRS) is similar to the characteristic usage in the genes for proteins from bacteria of the genus *Thermus*, and the G+C content is as 66%. The amino acid sequence of Glutaminyl-tRNA synthetase (*Tt*GlnRS), from *thermophilus* shows high similarity with other bacterial Glutaminyl-tRNA synthetase sequences (25-50% identity). By expression of the *thermophilus* GlnRS gene in *Escherichia coli*, the thermostable enzyme was overproduced and purified to homogeneity by heat treatment followed by a single chromatography step. The protein obtained is remarkably thermostable and the crystals of the enzyme were obtained (from 0.2M Ammonium sulfate, 0.1M Sodium cacodylate trihydrate pH 6.5, 30% w/v Polyethylene glycol 8,000 solutions) by vapour diffusion techniques. Crystal structure has been solved by molecular replacement method and refined at 2.5 Å resolution. In addition, the structure complex of *Tt*GlnRS with ATP shows that substrate binding is important for construction of catalytically important active site and showing that this is a general feature of class I synthetase. Biochemical assays such as Thermal shift assay, Aminoacylation assay and Isothermal Titration Calorimetry has proved that L-Gln and ATP mediates the formation of Gln-AMP product which has higher affinity and strong binding with *Tt*GlnRS.

Keywords: aminoacyl-tRNA synthetases; glutamine; ATP; X-ray crystallography; enzyme specificity.



7.6 Wastewater Treatment for Removal of Solvents - Degradation of Octanol using Hydrodynamic Cavitation

Pravin B. Patil^a, Jyotsnarani Jena^a, Vinay M. Bhandari^{a*}, Laxmi Gayatri Sorokhaibam^b

^aChemical Engineering and Process Development Division
CSIR-National Chemical Laboratory
Pune-411 008, India.

^bDepartment of Chemistry, Visvesvaraya National Institute of Technology
Nagpur, India-440010

ABSTRACT

Hydrodynamic cavitation for the degradation of organic solvents was investigated in detail using two different cavitating devices- orifice and a newer form of cavitating device that employs vortex flow-vortex diode, process developed by CSIR-National Chemical Laboratory, Pune. Process intensification in the form of aeration was also investigated apart from addition of external oxidising agent such as hydrogen peroxide. Degradation of an organic solvent, n- octanol in terms of reduction in total organic carbon (TOC) was studied on a pilot plant scale having capacity of 1m³/h . Initial concentration of 50 ppm was employed for the wastewater treatment studies and effect of pressure was studied at two different pressure drops viz. 0.5 and 2 bar for vortex diode and at 2 and 5 bar for orifice. The results revealed that efficiency of solvent removal varies substantially with the change in physical operating conditions and nature of the cavitating device. It was found that up to only 15% degradation could be achieved for n-octanol using vortex diode which could be further enhanced to 35% using process intensification in the form of aeration. For orifice, the degradation was close to 35% and showed no effect of aeration. It was observed that lower pressure drop is more favourable for degradation (0.5 bar for vortex diode and 2 bar for orifice). In both the cases, there was no enhancement in the degradation due to addition of oxidising agent- hydrogen peroxide (100 ppm). Vortex diode that works on the principle of vortex generation for cavitation, was found to be superior over conventional cavitating device-orifice requiring significantly lower pressure drop than orifice for comparable extent of degradation. The results of this study provide newer insights into solvent removal using hydrodynamic cavitation and would have bearing on the treatment of solvent containing wastewaters.

Keywords: Vortex diode, Effluent treatment, Pollution, Wastewater, Industry

7.7 Coagulation-Flocculation treatment of dyes removal through chemical and natural coagulants

Sweety Badalia¹, Laxmi Gayatri Sorokhaibam^{1*}, Vinay M. Bhandari²

¹Department of Chemistry, Visvesvaraya National Institute of Technology Nagpur(VNIT), Maharashtra-440010

²Chemical Engineering & Process Development Division, CSIR-National Chemical Laboratory Pune-411008

*Corresponding author: laxmigayatri1@gmail.com, Phone: 0712-2801778, 9420407446 (mobile)

Abstract

Dye effluents contribute to high chemical oxygen demand (COD), suspended solids, conductivity, color, acidity, hazards to ecosystem [1]etc. Most of the dyes are persistent and non-biodegradable[2] in nature and because of their stability, there is a great hindrance in the removal process. Coagulation process can alone contribute to 80-90 % color removal[3] and suspended solids from textile effluents, and can reduce the cost of treatment in tertiary process of effluent treatment[4]. The performance of chemical coagulants, Polyaluminum Chloride (PAC), FeCl₃, and three new natural plant based coagulants (*Brassica nigra*, *Citrullus lanatus*, and *Ipomea batatus*) were investigated on different dyes(Congo Red, Brilliant Green, Aniline Blue, Reactive Red 120) under the influence of parameters like coagulant dose(Fig. 1), pH range, dye concentration etc. The surface characteristic of the sludge has been analyzed through SEM (Scanning electron microscopy) and the biocoagulants were characterized using FTIR.



The best coagulant performance is obtained by comparing the optimum coagulant dosage, settling time, rate of settling, the removal efficiency of color and reduction in dye concentration. The chemical coagulants (PAC and FeCl₃) could effectively remove up to 98-99% with a broad range of pH, while biocoagulants were effective in the range of 75-91 % for reduction in color and concentration. *Ipomoea batatas* (Fig. 2) was observed to be the best biocoagulant for congo red and aniline blue with 86% and 91% reduction respectively. The use of biocoagulants provides a greener approach and scope for development of various formulations that may enhance the coagulation process.

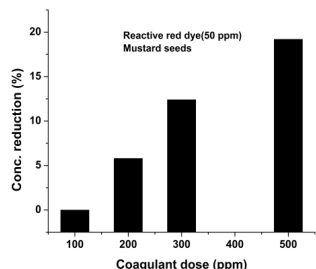
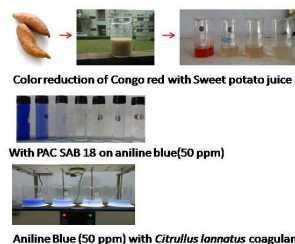


Fig. 1 Effect of Coagulant (*Brassica nigra*) dose on



Fig. 2 Coagulation of dyes with chemical coagulants and biocoagulants



Reactive Red dye (50 ppm)

Keywords: Biocoagulants, Wastewater Treatment, Textile, Pollution control

References:

- [1] Robinson, T., McMullan, G., Marchant, R., and Nigam, P. (2001) Remediation of dyes in textile effluent: a critical review on current treatment technologies with a proposed alternative. *Bioresour. Technol.*, **77** (3), 247–255.
- [2] Akbari, A., Remigy, J.C., and Aptel, P. (2002) Treatment of textile dye effluent using a polyamide-based nanofiltration membrane. *Chem. Eng. Process. Process Intensif.*, **41** (7), 601–609.
- [3] Chen, T., Gao, B., and Yue, Q. (2010) Effect of dosing method and pH on color removal performance and floc aggregation of polyferric chloride–polyamine dual-coagulant in synthetic dyeing wastewater treatment. *Colloids Surfaces A Physicochem. Eng. Asp.*, **355** (1), 121–129.
- [4] Chethana, M., Sorokhaibam, L.G., Bhandari, V.M., et al. (2016) Green Approach to Dye Wastewater Treatment Using Biocoagulants. *ACS Sustain. Chem. Eng.*, **4** (5), 2495–2507.

7.8 Biologically important of curcumin derivatives: DFT calculations and molecular docking studies

Govindharasu Banuppriya^a and Vediappen Padmini^{a*}

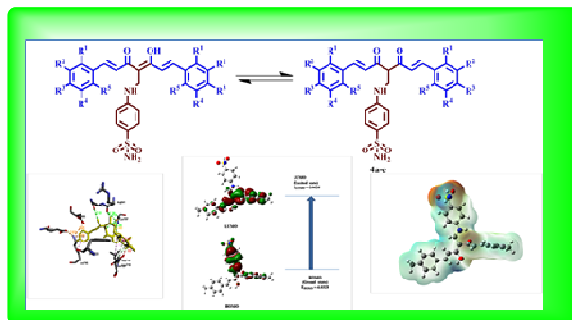
Department of Organic Chemistry, School of Chemistry, Madurai Kamaraj University, Madurai-625 021, Tamil Nadu, India.

Corresponding author E-mail: padimini_tamilenthi@yahoo.co.in

Abstract

Curcumin (diferuloylmethane) is an active ingredient of turmeric; isolated from the root of rhizome *Curcuma longa* Linn. Curcumin has extensive biological applications [1-3]. Especially, curcumin has significant cytotoxic activity and apoptosis induction upon a variety of cancer cell lines [4]. Not only curcumin, the synthesis of new curcuminoids is very interesting and important research. The variation on curcumin has been done in the active methylene groups/replacing β-Di-ketone bridge to enhance the biological activity than the natural curcumin. Based on the above ideas, the research is decided to develop the new pharmacophore that the introduction of sulfanilamide unit in active methylene of curcumin. Hence, curcumin- Sulfonamide hybrid has been synthesized, studied for their *in vitro* antioxidant, anti-inflammatory and cytotoxic activities. The compounds showed very good cytotoxic activities. Thus, the synthesized compounds were docked with EGFR TK. On Continuation, DFT calculations were studies and also analyzed for the synthesized curcumin derivatives.





Reference:

- [1] Youssefa, K. M., El-Sherbenya, M. A., El-Shafiea, F. S., Faraga, H. A., Al-Deeba, O. A., Awadallah, S. *Arch.Pharm.Pharm.Med. Chem.* 337 (2004) 42-54.
- [2] Sribalan, R., Kirubavathi, M., Banupriya, G. Padmini, V. *Bioorg.Med. Chem. Lett.* 25 (2015) 4282-4286.
- [3] Adams, B. K., Ferstl, E. M., Davis, M. C., Herold, M, Kurtkaya, S, Camalier, R. F, Hollingshead, M. G, Kaur, G, Sausville, E. A., Rickles, F. R, Snyder, J. P, Liotta, D. C., Shoji, M. *Bioorg. Med.Chem.* 12 (2004) 3871-3883
- [4] Kuttan R., Bhanumathy, P., Nirmala, K., George, M. C. *Cancer let.* 29 (1985) 197-202.

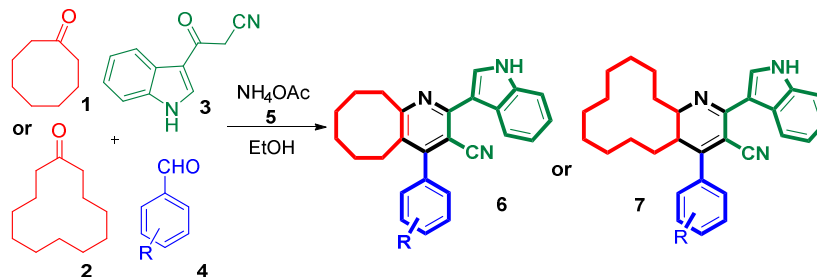
7.9 A facile one-pot four-component domino protocol for the synthesis of novel cycloocta/cyclododeca–pyridine-3-carbonitrile–indole hybrids

Muthumani Muthu and Raju Ranjith Kumar*

Department of Organic Chemistry, School of Chemistry, Madurai Kamaraj University, Madurai 625 021

E-mail: raju.ranjithkumar@gmail.com

Indole derivatives are versatile compounds well known for their broad range of biological activities.¹ Pyridine derivatives constitute one of the most privileged scaffolds that exhibit antitumor, antibiotic, antiinflammatory, antidepressant, antimalarial, anti-HIV, antimicrobial, antibacterial and insecticidal activities.²⁻⁸ Further the cycloalkano fused pyridine derivatives such as the 4-arylcycloocta[*b*]pyridine form the core of antipsychotic drug blonanserin, which has been approved for the treatment of schizophrenia in Japan and Korea.⁹ The biological significances of indoles and cycloalkano fused pyridine systems prompted us to investigate feasibility to construct hybrid heterocycles comprising these units. Accordingly the one-pot four-component reaction of cycloalkanones **1** or **2**, 3-(1*H*-indol-3-yl)-3-oxopropanenitrile **3**, aromatic aldehydes **4** and ammonium acetate **5** led to the formation of novel cycloalkano fused pyridine-3-carbonitrile indole hybrids **6** or **7** in good yields. The reaction presumably occurred through a domino Knoevenagel–Michael–Cyclization sequence of reactions resulting in the formation of two new C–C and C–N bonds in a single transformation.



References.

- [1] Sharma. V.; Kumar. P.; Pathak. D.; *J. Heterocyclic Chem.*, 2010, 47, 491.
- [2] (a) Stockwell, B.R. *Nature*, **2004**, 432, 846. (b) Dolle, R. E. *J. Comb. Chem.*, **2003**, 5, 693.
- [3] Sirisha, K.; Achaiah, G.; Reddy, V. M. *Arch. Pharm. Chem. Life Sci.*, **2010**, 343, 342.
- [4] Briede, J.; Stivrina, M.; Vigante, B.; Stoldere, D.; Duburs, G. *Cell. Biochem. Funct.*, **2008**, 26, 238.
- [5] Jim, H.; Barker, M. J. *Eur. Pat. Appl. EP0119774 A1.*, **1984**.
- [6] Nasr, M. N.; Gineinah, M. M. *Arch. Pharm. Med. Chem.*, **2002**, 335, 289.
- [7] Nizamuddin, M. G.; Manoj, K. *Boll. Chim. Farm.*, **2001**, 140, 311.
- [8] (a) G. C. Rovnyak, R. C. Millonig, J. Schwartz, V. Shu, *J. Med. Chem.*, **1982**, 25, 1482. (b) G. A. Morales, J. R. Garlich, J. Su, X. Peng, J. Newblom, K. Weber, D. L. Durden, *J. Med. Chem.*, **2013**, 56, 1922. (c) J. J. Kaminski, A. M. Doweiko, *J. Med. Chem.*, **1997**, 40, 427. (d) D. Cheng, S. Valente, S. Castellano, G. Sbardella, R. Di Santo, R. Costi, M. T. Bedford, A. Mai, *J. Med. Chem.*, **2011**, 54, 4928.
- [9] (a) Oka, M.; Noda, Y.; Ochi, Y.; Furikawa, K.; Une, T.; Kurumiya, S.; Hino, K.; Karasawa, T. *J. Pharmacol. Exp. Ther.*, **1993**, 264, 158; (b) Heading, C. E. *Idrugs.*, **1998**, 1, 813.

7.10 Computational Study on Molecular-based Non-linear Optical property of Wittig based Schiff-Base ligands

Bathula Rajasekhar and Toka Swu

Department of Chemistry, Pondicherry University, Pondicherry-605014
E-mail: tokaswu@gmail.com

Abstract

Materials displaying nonlinear optical (NLO) properties have potential applications in emerging optoelectronic and photonic technologies [1]. Molecular-based NLO materials such as organic compounds, polymers and coordination complexes [2] which possesses metal ion and organic ligand have drawn considerable focus compared to the atomic-based materials such as LiNbO_3 , KH_2PO_4 (KDP), gallium arsenide (GaAs), α -quartz (SiO_2) and β -barium borate (BBO) [3].

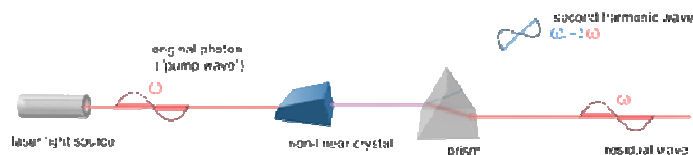


Image copied from <http://www.cristal-laser.com/en/nlo-applications.html>

In this regard, we have designed (Figure-1) several Cis and Trans conformation Wittig based Schiff-Base ligands from various aldehydes and aromatic, non-romantic amines. These ligands were optimized and further studied their Non-Linear Optical property using GAUSSIAN 09 programme. For both Optimization & Frequency independent Hyperpolarizability calculations, we used DFT based B3LYP method and 6-31G* basis set. From the result we summarized that, i) Non-Linear Optical property of Schiff-Base ligands sensitive to the HOMO-LUMO gap (from Figure-2), ii) Trans isomer Wittig based Schiff-Based ligands exhibited higher β (First Hyperpolarizability) values compared to cis isomers, iii) For Ligand-13 & 14 from each category of Schiff-Base ligands (N = 1-10) showed higher β value compared to others, iii) both cis & trans conformation Wittig based Schiff-Base ligands which are derived from fused aromatic rings contained aldehydes and lone pair rich nitrogen atoms consisted aromatic amines showed higher β values compare to others, iv) N = 5 both cis & trans conformation Wittig based Schiff-Base ligands have shown higher β value compare to other (Figure-3).



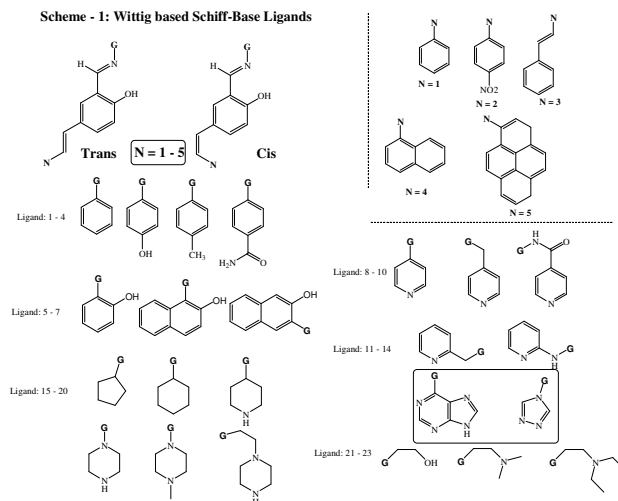


Figure-1: Library of Wittig based Schiff-Base ligands

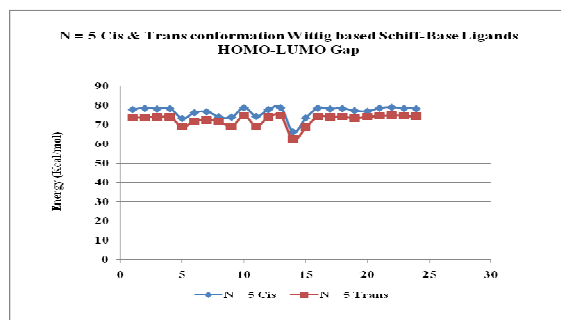


Figure-2: HOMO-LUMO gap of N = 5 Cis & Trans conformation Wittig based Schiff-Base ligands

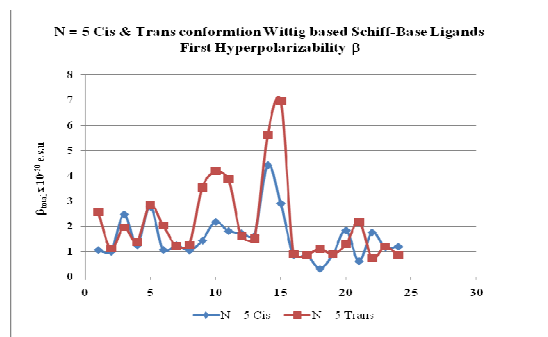


Figure-3: First Hyperpolarizability of N = 5 Cis & Trans conformation Wittig based Schiff-Base ligands

References:

- [1] (a). Chemla, D. S., Zyss, J., *Nonlinear Optical Properties of Organic Molecules and Crystals*, Orlando, FL: *Academic Press*. **1987**, Vols. 1 and 2. (b). Brkdas, J. L., Adant, C., Tackx, P., *Chem. Rev.* **1994**, 94, 243. (c). Long, N. J., *Angew. Chem. Int. Ed. Engl.* **1995**, 34, 21. (e). Delaire, J. A.; Nakatani, K. *Chem. Rev.* **2000**, 100, 1817. (f). Verbiest, T.; Houbrechts, S.; Kauranen, M.; Clays, K.; Persoons, A.J. *Mater. Chem.* **1997**, 7, 2175. (g). S.R. Marder, B. Kippelen, A.K.Y. Jen and N. Peyghambarian *Nature*. 388 (1997) 845. (h). Y. Shi, C. Zhang, J.H. Bechtel, L.R. Dalton, B.H. Robinson and W.H. Steier *Science*. **2000**, 1, 19, 288. (i). F. Kajzar, K.S. Lee and A. K. Y. Jen, *Adv. Polym. Sci.* **2003**, 1, 161. (j). V. Krishnakumar and R. Nagalakshmi, *Physica B*. 403, **2008**, 1863.



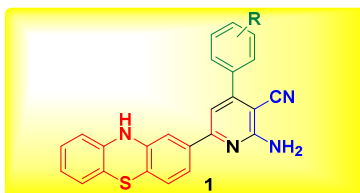
7.12 One pot synthesis of 2-amino-4-arylpyridine-3-carbonitrile tethered phenothiazines

Somi Santharam Roja and Raju Ranjith Kumar*

Department of Organic Chemistry, School of Chemistry, Madurai Kamaraj University,
Madurai-625021, Tamil Nadu
E-mail: raju_ranjithkumar@gmail.com

Pyridines are one of the most privileged nitrogen heterocycles omnipresent in numerous natural and synthetic compounds of bio-importance.¹ Pyridine derivatives have been recognized as potential synthons for the development of new drugs for the treatment of Parkinson's disease, hypoxia, asthma, kidney disease, epilepsy, cancer and Creutzfeldt–Jakob diseases.² On the other hand, phenothiazines form the core of several antipsychotic drugs used to treat schizophrenia and other psychotic disorders. In addition, phenothiazine drugs like prochlorperazine and chlorpromazine have been used for treating nausea and vomiting. Apart from the biological activities, pyridines and phenothiazines find applications in material science as dyes and potential precursors for constructing OLED's.

In view of the myriad applications of pyridines and phenothiazines in diverse areas, we envisaged to construct hybrids including both the units. Consequently in the present work the syntheses of novel 2-amino-4-aryl-6-(10*H*-phenothiazin-3-yl)-pyridine-3-carbonitriles **1** have been achieved through a one-pot four-component domino strategy employing 1-(10*H*-phenothiazin-3-yl)ethan-1-one, aromatic aldehyde, malononitrile and ammonium acetate.



- [1] Roth, H. J.; Kleemann, A. *Drug Synthesis*, in *Pharmaceutical Chemistry*, John Wiley and Sons, New York, 1988, vol. 1; (b) Michael, J. P. *Nat. Prod. Rep.* **2005**, 22, 627.
[2] Reddy, T. R. K.; Mutter, R.; Heal, W.; Guo, K.; Gillet, V. J.; Pratt, S.; Chen, B. *J. Med. Chem.* **2006**, 49, 607

7.13 SYNTHESIS, SPECTROSCOPIC AND DFT STUDIES OF 4-(5-CHLOROTHIOPHEN-2-YL)-1,2,3-SELENADIAZOLE

Sankari S* & Saranya K

*E.Mail-ggbsankam@gmail.com

Associate Professor, Dept. of Chemistry, Sri Sarada College for Women, Salem-16
Research Scholar, Dept. of Chemistry, Sri Sarada College for Women, Salem-16

Abstract

In the present study, 4-(5-Chlorothiophen-2-yl)-1,2,3-selenadiazole (CTS) has been investigated both experimentally and theoretically. In experimental study, the compound was synthesized and characterized by FTIR, FT-Raman, ¹H and ¹³C NMR spectral studies. In theoretical study, the geometric parameters of the title compound in the ground state have been calculated using the density functional method with 6-311G++ (d, p) as basis set.

The atom numbering of the optimized structure is given in Fig.1. The calculated optimized geometrical parameters obtained in this study for the title compound are compared with the experimental values



The FTIR spectra of glucose and fructose with malonic acid were given in the above figure (A) revealed that OH groups of both hydrogen bond donors as well as the malonic acid were interacted by means of intermolecular hydrogen bonding. This is due to the broad band appeared around 3440 cm^{-1} of O-H stretching vibrations. In addition to that the carbonyl group of both glucose and fructose were also involved in hydrogen bonding as the C=O stretching frequencies are noticed a broad band at 1717 cm^{-1} .

Similarly the FTIR spectra of glucose and fructose with ZnCl_2 were given in the above figure (B) showed that OH groups of both hydrogen bond donors were involved in intermolecular hydrogen bonding as the O-H stretching absorptions were observed as a broad band near 3430 cm^{-1} . Further the carbonyl group of both glucose and fructose were also involved in hydrogen bonding as the C=O stretching frequencies are noticed a broad band at 1705 cm^{-1} .

To sum up, four sugars based deep eutectic solvents were successfully synthesized in this study and further their applications are to be studied.

References

- [1] P. Wasserscheid, T. Welton, *Ionic Liquids in Synthesis*, Wiley-VCH, Weinheim, (2003).
- [2] M.A. Kareem, F.S. Mjalli, M.A. Hashim, I.M. Al Nashef, *J. Chemical and Eng. Data* 55 (2010) 4632.
- [3] J. Sun, M. Forsyth, D.R. MacFarlane, *The Journal of Physical Chemistry. B* 102 (1998) 8858.
- [4] S. Zhang, Y. Chen, R.X.F. Ren, Y. Zhang, J. Zhang, X. Zhang, *J. Chemical and Eng. Data* 50 (2005) 230.
- [5] M.A. Navarra, J. Manzi, L. Lombardo, S. Panero, B. Scrosati, *Chem. Sus. Chem.* 4 (2011) 125.
- [6] M. Hayyan, F.S. Mjalli, M.A. Hashim, I.M. Alnashef, X.M. Tan, *J. Electronanal. Chem.* 657 (2011) 150.
- [7] P.D. de María, Z. Maugeri, *Current Opinion in Chemical Biology* 15 (2011) 220.
- [8] N.V. Plechkova, K.R. Seddon, *Chemical Society Reviews* 37 (2008) 123.
- [9] D.V. Wagle, H. Zhao, G.A. Bakar, *Acc. Chem. Res.* 47 (2014) 2299.
- [10] M. Hayyan, F.S. Mjalli, M.A. Hashim, I.M. Alnashef, *J. Mol. Liq.* 181(2013) 44.
- [11] Y.S. Hu, Z.X. Wang, X.J. Huang, L.Q. Chen, *Solid State Ionics* 175 (2004) 277.
- [12] E.R. Cooper, C.D. Andrews, P.S. Wheatly, et al., *Nature* 430 (2004) 1012.
- [13] Y.T. Dai, J. van Spronsen, G.J. Witkamp, R. Verpoorte, Y.H. Choi, *Anal. Chim. Acta* 766 (2013) 61.

7.17 The stereodivergent formation of substituted tetrahydro-2H-pyran by memory of chirality

R. Chithiravel^a and S. Muthusubramanian^b

^a*Department of Chemistry, Raja Serfoji Arts College, Thanjavur 613 005*

^b*School of Chemistry, Madurai Kamaraj University, Madurai 625 021*

Presenting author's email: jai09vel@yahoo.co.in

The term “memory of chirality” (MOC) defines a fact that the chiral sp^3 carbon center is sustained in the product, even when the reaction progresses through a carbenium ion, singlet mono- or biradical, or carbanion intermediates during the reaction [1]. This phenomenon is commonly used for the synthesis of enantiopure molecules [2]. MOC arises due to the generation of long lived conformers, which originate their chirality from the existence of a stereogenic component [1,3].

In this presentation, the synthesis 2,4,6-triaryl-tetrahydro-2H-pyrans by the cyclization of 1,3,5-triarylpentane-1,5-diols has been described. The diols could be easily obtained from 1,3,5-triaryl-1,5-diketones by reduction with sodium borohydride in methanol at room temperature [4]. The triaryldiketones have been prepared by a recently reported method [5]. The reduction normally led to a mixture of diastereomeric diols. The crude mixture of the diastereomeric diols has been subjected to cyclisation employing p-toluenesulphonic acid in DMF. As the starting diols were employed as mixtures of isomers, a mixture of diastereomeric tetrahydro-2H-pyrans could be anticipated.



Still, as the reaction involves acid, initial carbocation formation at C-1 or C-5 may destroy the stereochemical identity of the different starting diols and hence the number of isomeric tetrahydro-2*H*-pyran formed may be less than that of the initial diols.

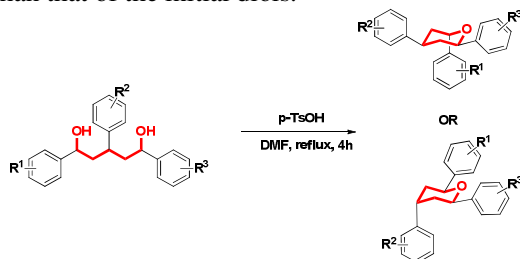


Figure 1. Major products in the cyclisation of 1,3,5-triaryl-1,5-diols

Nevertheless, the cyclisation has yielded a mixture of products in many cases and it is again very difficult to separate them in each case. However, with great effort, the major isomer has been separated in all the cases. Interestingly, it is not the same pyran with a given stereochemistry has been obtained as the major isomer in all the cases. The major isomer isolated in each case has been characterized unambiguously, which is not the most stable all equatorial isomer. This clearly shows that an initial pure carbocation formation may not be case in the mechanism and the memory of chirality effect may have a dominant say during the cyclisation step. The cyclodehydration process may involve two consecutive steps; initial protonation of one of the hydroxy groups in the 1,5-diol leading to the carbocation intermediate followed by the cyclization resulting in 2,4,6-triaryl-tetrahydro-2*H*-pyran. It is not clear why a particular diastereomer is preferred in one case and a different one in the other.

References

- [1] (a) H. Zhao, D. C. Hsu, P. R. Carlier, *Synthesis*, 1, 2005, 1. (b) J. Yang, H. Ha, *J. Bull. Korean Chem. Soc.*, 37, 2016, 423.
- [2] T. Yoshimura, T. Kinoshita, H. Yoshioka, T. Kawabata, *Org. Lett.*, 15, 2013, 864.
- [3] F. Foschi, A. Tagliabue, V. Mihali, T. Pilati, I. Pecnikaj, M. Penso, *Org. Lett.*, 15, 2013, 3686.
- [4] A. Thiruvalluvar, R. Chithiravel, S. Muthusubramanian, R. J. Butcher, *Acta Crystallogr. Sect. E*: E70, 2014, o123.
- [5] R. Chithiravel, K. Rajaguru, S. Muthusubramanian, N. Bhuvanesh, *RSC Adv.*, 5, 2015, 86414.

7.18 TEMPO-Promoted Oxidative Azide–Olefin Cycloaddition for the Synthesis of 1,2,3-Triazoles in Water

D. Gangaprasad^a, J. Paul Raj^a, K. Karthikeyan^a and J. Elangovan^{*b}

^a Department of Chemistry, B. S. Abdur Rahman Crescent University, Chennai-600048.

^b Department of Chemistry, Rajah Serfoji Government College, Thanjavur, Tamil Nadu- 613005.

*Email: elangoorganic@gmail.com

1,2,3-Triazole is an important motif present in a large number of functionalized molecules endowed with versatile applications in various fields such as medicinal chemistry, biology, material science and polymers.¹ In spite of the conventional Huisgen cycloaddition, CuAAC is prominent owing to its remarkable selectivity and functional-group tolerance. Given that it is selective to 1,4-disubstituted triazoles, CuAAC is restricted to terminal alkynes only. In continuation, ruthenium-catalyzed azide–alkyne cycloaddition (RuAAC) was developed, and it promotes the complementary 1,5-disubstitution on the triazole and is also compatible with internal alkynes.²

To convert these unstable triazolines into stable aromatic triazoles, two ingenious approaches have been adopted. The first one is eliminative azide–olefin cycloaddition (EAOC) in which an olefin bearing a leaving group such as a nitro, alkoxy, sulfone, acetate group, undergoes cycloaddition with various azides, and the resulting triazolines undergo concomitant elimination to furnish the required 1,2,3-triazoles.³



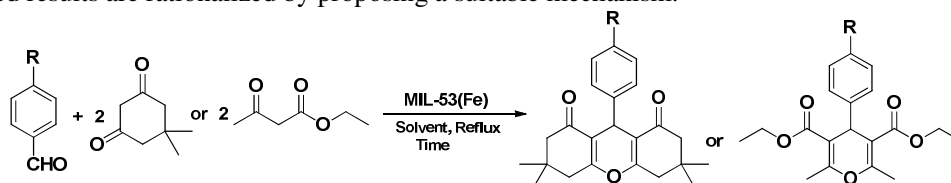
7.21 MIL-53(Fe) as an Efficient Heterogeneous Catalyst for the Synthesis and Characterization of Substituted Xanthenes and Pyrans

Ganesapandian Latha, Nainamalai Devarajan, and Palaniswamy Suresh*

*Supramolecular and Catalysis Lab, Department of Natural Products Chemistry
School of Chemistry, Madurai Kamaraj University, Madurai – 625 021.
E-mail: lathasaravanan1984@gmail.com,
E-mail: ghemistry@gmail.com

Metal Organic Frameworks (MOFs) explored as a versatile and sustainable catalyst for numerous organic transformations. Transition Metals based MOFs has employed for various applications such as imaging, controlled drug delivery, artificial kidney application, gas sorption, and biosensing, *etc.* Iron MOFs are getting more attraction and used in various applications such as isomerization, condensation reactions, asymmetric oxidations and aerobic oxidation reactions. MIL-53(Fe) is an iron(III) containing MOF built from chains of Fe (III) octahedra and 1,4-benzenedicarboxylic acid, has been chosen as the target catalyst due to its stability, low cost and non-toxic nature. Recently, MOFs are found to be a potential alternative catalyst in multicomponent reactions. Xanthene derivatives are important classes of heterocyclic compounds used as leucodyes in laser technology and pH sensitive fluorescent materials for the visualization of biomolecules. Similarly, pyran derivatives occupied an important area in natural chemistry, especially in plant life and shown significant pharmacological and ecological activity.

In the present work, MIL-53(Fe) MOF is used as a solid Lewis acidic catalyst for the synthesis of substituted xanthenes and pyrans under mild conditions. The coordinatively unsaturated metal sites present in MIL-53(Fe) MOF catalyze this reaction with catalytic amount of the catalyst. A series of substituted xanthene and pyran products are synthesized with good to excellent yield. The major advantage of the present catalyst is eliminating the stoichiometric amount of metal salts and avoids homogeneous catalysts. The catalyst is reused for several cycles without losing in catalytic activity. The observed results are rationalized by proposing a suitable mechanism.



References:

- [1] R. Cano, D. J. Ramón, M. Yus, *Synlett*, 2011, 14, 2017–2020
- [2] G. Harichandran, S. D. Amalraj, P. Shanmugam, *J. Mol. Catal. A: Chem.*, 2001, 176, 151–163
- [3] R. J. Sarma, J. B. Baruah, *Dyes Pigments*, 2005, 64, 91–92

7.22 Effect of diluents on extraction of chromium (VI) from aqueous solution Using Pickering Emulsion liquid membrane

P. Murugan*, T. V. Nihal, S. Bhuvaneshwari

*Department of Chemical Engineering, National Institute of Technology Calicut,
Kozhikode – 673 601, Kerala, India
muruga.tech86@gmail.com

Abstract

Emulsion liquid membrane (ELM) is an alternate to the existing separation processes, showing many advantages in terms of efficiency, energy consumption and operational costs. The choice of the diluent is shown to affect the rate of metal extraction. In this research the possibility of replacing the synthetic diluent kerosene was investigated.



Amphiphilic Silica Nanowires Surfactant were used to prepare the Pickering emulsion liquid membrane (PELM) system, in which the internal water and oil emulsion can simply demulsified by centrifugation. The percentage removal of chromium (VI) from aqueous solution by Pickering emulsion liquid membrane was investigated experimentally for various diluents (oils) such as coconut, sunflower, neem, pungai and mahua oils respectively. It was found that the percentage removal of chromium (VI) using mahua oil was high as 99.74%.

Keywords: Pickering emulsion liquid membrane, Amphiphilic Silica Nanowires Surfactant, Diluent, Chromium (VI) extraction.

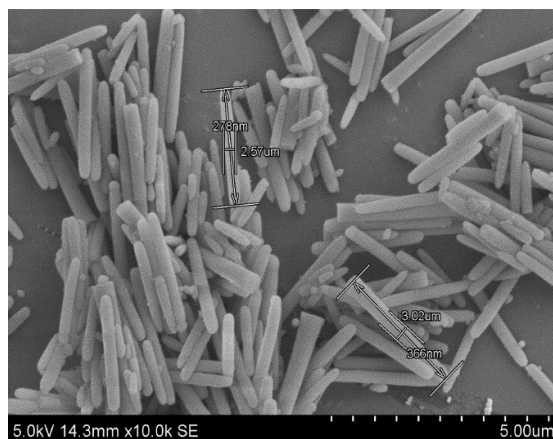


Figure 1. SEM Image of the prepared Amphiphilic silica nanowires surfactant with 35% precursor (ethanol)

References

- [1] R. K Goyal, N. S Jayakumar, M. A Hashim, Chromium removal by emulsion liquid membrane using [BMIM] + [NTf₂]- as stabilizer and TOMAC as extractant *Desalination* 278 (2011) 50-56.
- [2] V. Eyupoglu, O. Tutkun, The extraction of Cr (VI) by a flat sheet supported liquid membrane using alamine 336 as a carrier *Arabian journal science and engineering* 36 (2011) 529-539.
- [3] A. Choudhury, S. Sengupta, C. Bhattacharjee, S. Datta , Extraction of hexavalent chromium from aqueous stream by emulsion liquid membrane (ELM) *Separation science and technology* 45 (2010) 178-185.
- [4] S. Alpaydin, A. O. Saf, S. Bozkurt, A. Sirit, Kinetic study on removal of toxic metal Cr(VI) through a bulk liquid membrane containing p-tert-butylcalix [4]arene derivative *Desalination* 275 (2011) 166–171.
- [5] G. Muthuraman, T. T Teng, C. P Leh, I. Norli, Use of bulk liquid membrane for the removal of chromium (VI) from aqueous acidic solution with tri-n-butyl phosphate as a carrier *Desalination* 249 (2009) 884–890.
- [6] M. Jaishankar, T. Tseten, N. Anbalagan, B. B Mathew, K. N Beeregowda, Toxicity, mechanism and health effects of some heavy metals, *Interdisciplinary toxicology* 7 (2014) 60–72.
- [7] N. Othman, N. F. M Noah, K. W Poh, O. Z Yi, High performance of chromium recovery from aqueous waste solution using mixture of palm-oil in emulsion liquid membrane *Procedia Engineering* 148 (2016) 765 – 773.
- [8] L. Laki, A. Kargari, Extraction of silver ions from aqueous solutions by emulsion liquid membrane *journal of membrane science* 2 (2016) 33-40.
- [9] Z. Fang, X. Liu, M. Zhang, J. Sun, Mao, J. Lu, S. Rohani, A neural network approach to Simulating the dynamic extraction process of L-phenylalanine from sodium chloride aqueous Solutions by emulsion liquid membrane *Chemical Engineering research and design* 105 (2016) 188–199.
- [10] S. Bjorkegren, R. F Karimi, A. Martinelli, N. S Jayakumar, M. A Hashim, a new emulsion liquid Membrane based on a palm oil for the extraction of heavy metals *Membranes* 5 (2015) 168-179.



- [11] S. Nosrati, N.S Jayakumar, M. A Hashim, Extraction performance of chromium (VI) with emulsion liquid membrane by cyanex 923 as carrier using response surface methodology *Desalination* 266 (2011) 286–290.
- [12] P. K Parhi, Supported liquid membrane principle and its practices: a short review *Journal of Chemistry* (2013) 1-11.
- [13] A. Kuijk, A. V Blaaderen, A. Imhof, Synthesis of monodisperse, rodlike silica colloids with tunable aspect ratio *Journal of American Chemical Society* 133 (2011) 2346–2349.
- [14] J. He, B. Yu, M. J Hourwitz, Y. Liu, M. T Perez, J. Yang, Z. Nie, Wet-chemical synthesis of amphiphilic rodlike silica particles and their molecular mimetic assembly in selective solvents *Angewandte Chemie International Edition* 51 (2012) 3628–3633.
- [15] H. Yan, B. Zhao, Y. Long, L. Zheng, Chen-Ho Tung, K. Song, New Pickering emulsions stabilized by silica nanowires *Colloids and Surfaces A: Physicochemical and Engineering Aspects* 482 (2015) 639–646.

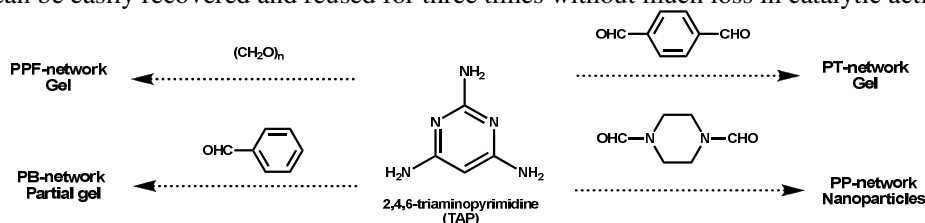
7.23 Triaminopyrimidine derived Polymeric Network Gels: Synthesis, Influence of Molar Ratio of Reactants and its Catalytic Applications

Murugesan Shunmughanathan^a, Pillaiyar Puthiaraj^a, Kasi Pitchumani^{a,b}

^aDepartment of Natural Products Chemistry, School of Chemistry, Madurai Kamaraj University, Madurai-21, Tamilnadu, India

^bCentre for Green Chemistry Processes, School of Chemistry, Madurai Kamaraj University, Madurai-21, Tamilnadu, India
E-mail: m.shunmughanathan@gmail.com, pit12399@yahoo.com

Microporous organic polymers (MOPs) are an important class of porous materials, which are constructed from monomers as organic building blocks and have shown great potential in a variety of applications such as gas storage and separation, catalysis, and chemical sensing[1]. Over the past decade the organic sol-gel processes have a great attention towards synthesis of microporous organic networks[2-4] and dynamic covalent imine gels[5,6]. The synthesis of porous polyaminal networks derived from melamine *via* Schiff base condensation of melamine and aldehydes has grown tremendously due to their broad applications in gas storage & separation, catalysis and sensors etc. Initially tetraphenyladamantane based polyaminals[7] have been synthesised *via* condensation of 2,4,6-triaminopyrimidine (TAP) and bulky tetraaldehydes but no other reports have been developed so far using TAP for synthesis of polyaminal networks. Hence we carried out the Schiff base condensation of TAP and mono- and di-aldehydes in aprotic polar solvents like DMF and DMSO, which leads to porous polyaminal network gels. The gelation conditions are studied using various parameters such as solvent, concentration of the sols, temperature and molar ratio of the reactants. We observed that the molar ratio of the reactants highly influence the gelation and also controls the opaque to transparent gel transformation. Our careful experiments clearly revealed that the molar ratio of the reactants only strongly influences the transparency of the gel rather than solvents, concentration of the reactants and temperature. The polyaminal network gels are well characterised using FT-IR, Powder XRD, thermogravimetric analysis, solid state ¹³C & ¹⁵N CP-TOSS NMR spectra, pore and surface area analysis, and electron microscopic studies. In addition, the polyaminal networks (PT-1.5 xerogel) acts as heterogeneous catalyst for Knoevenagel condensation of arylaldehydes and ethylcyanoacetate. The catalyst can be easily recovered and reused for three times without much loss in catalytic activity.



Scheme. Organic sol-gel synthesis of 2,4,6-triaminopyrimidine-based polymeric networks



Figure. a) Inversion test of polymer gel derived from TAP and TPA in 1:1 and 1:1.5 molar ratio (from left to right) respectively; b) Transparency of PT- gel (upper) and PPF-gel (lower); c) inversion test of PPF-3-gel derived from TAP and Paraformaldehyde.

References

- [1] Guoliang Liu, Yangxin Wang, Chaojun Shen, Zhanfeng Ju and Daqiang Yuan, *J. Mater. Chem. A*, 3 (2015) 3051–3058.
- [2] Su-Young Moon, Jae-Sung Bae, Eunkyung Jeon, Ji-Woong Park, *Angew. Chem. Int. Ed.* 49 (2010) 9504.
- [3] Su-Young Moon, Hye-Rim Mo, Min-Kyoon Ahn, Jae-Sung Bae, Eunkyung Jeon, Ji-Woong Park, *J. Polym. Sci., Part A: Polym. Chem.* 51 (2013) 1758.
- [4] Su-Young Moon, Eunkyung Jeon, Jae-Sung Bae, Minseon Byeon, Ji-Woong Park, *Polym. Chem.* 5 (2014) 1124.
- [5] Weijun Luo, Yixuan Zhu, Jianyong Zhang, Jiajun He, Zhenguo Chi, Philip W. Miller, Liuping Chen, Cheng-Yong Su, *Chem. Commun.* 50 (2014) 11942.
- [6] Haoliang Liu, Juan Feng, Jianyong Zhang, Philip W. Miller, Liuping Chen, Cheng-Yong Su, *Chem. Sci.* 6 (2015) 2292.
- [7] Guiyang Li, Biao Zhang, Jun Yan, and Zhonggang Wang, *Macromolecules* 47 (2014) 6664.

7.24 One-pot synthesis of β -enaminones from β -nitrostyrenes, β -dicarbonyl compounds and amines using organic polyaminal networks (OPN) as heterogeneous catalysts

Natarajan Madankumar^a, Murugesan Shunmughanathan^a and Kasi Pitchumani^{*a,b}

^aDepartment of Natural Products Chemistry, School of Chemistry, Madurai Kamaraj University, Madurai-625 021, Tamilnadu, India.

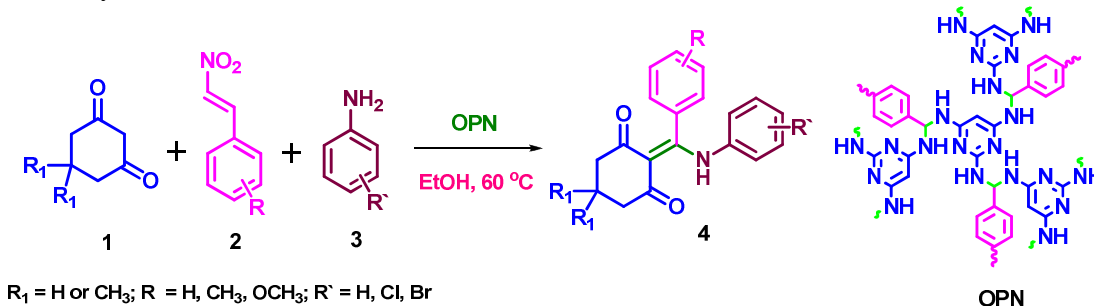
^bCentre for Green Chemistry Processes, School of Chemistry, Madurai Kamaraj University, Madurai-625 021, Tamilnadu, India.

E-mail: madhankmr6@gmail.com; pit12399@yahoo.com

Multicomponent reactions play a significant role in the field of organic synthesis in recent years due to their simple procedure, shorter reaction times, minimum waste production, one-pot technique and high degree of atom economy[1]. The skeleton of enamino diketone is a basic structural feature found in a numerous essential pharmaceutical and agro-chemical molecules, having antimicrobial, antibacterial, anti-inflammatory, antiaggregant, antiischemic, antileukemia[2] and other types of physiological activities. β -Enaminones are also known as effective and ecologically relevant herbicides and safe plant protection agents[3]. Additionally, some compounds with the enamino diketone skeleton have great potential for complexation with different metals such as Pd, Ni, and Cu, and the products have different biological activities[4]. In recent times porous organic polymers (POPs) have attracted increasing research interest because of their extensive potential to accommodate various reactive functional groups in the framework and these materials are explored in several frontline areas of energy and environmental research, including gas storage and their selective separation from the mixture of gases, heterogeneous catalysis, sensors, optoelectronic devices etc[5]. These materials have advantages, such as low density, cheap and easy synthesis, tenability, high stability to thermal treatment with water and most of the organic solvents, high thermal stability and permanent porosity[6].



In the present work, synthesis of β -enaminones from trans- β -nitrostyrenes, β -dicarbonyl compounds and amines is described *via* one-pot reaction using polyaminal networks as heterogeneous catalysts at 60 °C in EtOH as solvent. The reaction conditions are well optimized and the resulting products are confirmed by ESI-Mass and NMR techniques. The proposed system has the advantages of simple procedure, milder reaction conditions, shorter reaction times, cost effectiveness, good yields and reusability. The heterogeneous catalyst is prepared from simple starting materials, 2,4,6-triaminopyrimidine and terephthalaldehyde using DMF as solvent at 150 °C in the autoclave for three days. Then it is washed thoroughly with various solvents and dried well. The dried material is well characterized by FT-IR, solid state ^{15}N & ^{13}C CP-TOSS NMR, Powder XRD, TGA, BET, SEM and TEM analysis.



Scheme: One-pot synthesis of β -enaminones using OPN as heterogeneous catalyst.

References

- [1] I. A. Azath, P. Puthiaraj and K. Pitchumani, *ACS Sustainable Chem. Eng.* 1 (2013) 174–179.
- [2] E. Badzisz, E. Brzezinska, U. Krajewska, M. Rozalski, *Eur. J. Med. Chem.* 38 (2003) 597-603.
- [3] W. Ye, Y. Li, L. Zhou, J. Liu, C. Wang, *Green Chem.* 17 (2015) 188-192.
- [4] E. Budzisz, B. K. Keppler, G. Giester, M. Wozniczka, A. Kufelnicki, B. Nawrot, *Eur. J. Inorg. Chem.* (2004) 4412-4419.
- [5] P. Puthiaraj, K. Pitchumani, *Chem. Eur. J.* 20 (2014) 8761 – 8770.
- [6] P. Puthiaraj, K. Pitchumani, *Green Chem.* 16 (2014) 4223-4233.

7.25 TEMPO-Promoted organo catalyzed synthesis of 2-nitro-3- arylimidazo [1,2-a]pyridines under solvent free conditions.

M. Vadivelu^a, S. Sugirtha^a, K. Karthikeyan^{a*}

^aDepartment of Chemistry, B. S. Abdur Rahman Crescent University, Vandalur, Chennai-600 048, Tamil Nadu, India
Email: karthiclri@gmail.com.

Imidazopyridine, an important class of nitrogen containing heterocycles, shows a wide range of biological activities such as antitumor, antiparasitic, antiviral, antimicrobial, fungicidal, anti-inflammatory, hypnotic, etc.¹ These derivatives are also GABA and benzodiazepine receptor agonists, β -amyloid formation inhibitors, and cardiotoxic agents.² In addition, this motif is the core structure of some marketed drugs such as necopidem, saripidem, zolimidine, olprinone, zolpidem, and alpidem.³ Furthermore, a few of them exhibit excited-state intramolecular proton transfer.⁴ Different strategies have been reported to synthesize imidazo[1,2 a]pyridine scaffolds which include condensation reactions,⁵ oxidative coupling reactions and three-component coupling,⁵ intramolecular amino oxygenation/ C–H amination⁶ and coupling between 2-aminopyridine and nitroalkenes. However, looking inside the synthetic strategies, it was observed that most of the methods have used binucleophilic 2-aminopyridine as starting material and the initial nucleophilic addition mostly proceeds by exocyclic amino group resulting 3-nitro/carboxylic ester/keto/ amino/sulfonyl functionalized imidazopyridine moieties. The pharmacological activity of imidazopyridine derivatives is shown to be dependent on the nature of substituents at different positions.



There is continuous effort toward the development of new methods for the synthesis of this class of compounds with a variety of substituents at the 2 and 3 positions. Nitroimidazopyridines are important derivatives and are generally used as a key intermediate to synthesize polyfused imidazopyridine derivatives. Recently nitroalkenes have been used as a coupling partner with 2-aminopyridines for the synthesis of 3-nitroimidazopyridines.⁷ However, there is no such method for the synthesis of the 2-nitroimidazopyridines. Therefore, we became interested in whether we can change the substituent selectivity on the imidazo[1,2-a]pyridine moiety by the reaction between 2-aminopyridine and nitroalkene under suitable reaction conditions. Here, we have demonstrated an efficient and regioselective protocol for the synthesis of novel 2-nitro-3- arylimidazo [1,2-a]pyridines *via* TEMPO catalyst under mild and solvent free conditions.

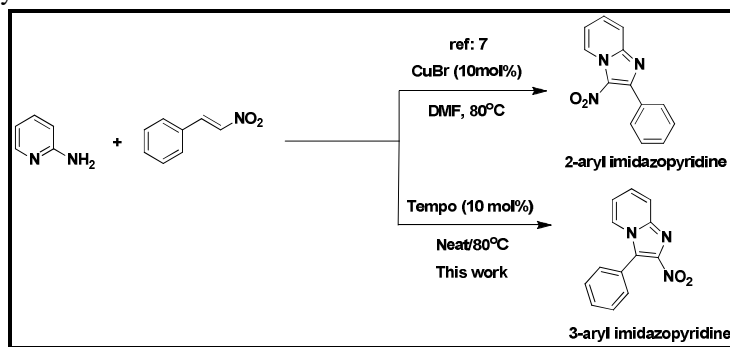


Figure: 1 Synthesis of 2-nitro-3- arylimidazo [1,2-a]pyridines

References:

- [1] Lhassani, M.; Chavignon, O.; Chezal, J. M.; Teulade, J. C.; Chapat, J. P.; Snoeck, R.; Andrei, G.; Balzarini, J.; Clercq, E. D.; Gueiffier, A. *Eur. J. Med. Chem.* 1999, 34, 271.
- [2] Humphries, A. C.; Gancia, E.; Gilligan, M. T.; Goodacre, S.; Hallett, D.; Marchant, K. J.; Thomas, S. *R. Bioorg. Med. Chem. Lett.* 2006, 16, 1518.
- [3] Mizushige, K.; Ueda, T.; Yukiiri, K.; Suzuki, H. *Cardiovasc. Drugs Rev.* 2002, 20, 163.
- [4] Stasyuk, A. J.; Banasiewicz, M.; Cyranski, M. K.; Gryko, D. T. *J. Org. Chem.* 2012, 77, 5552.
- [5] X. Xiao, Y. Xie, S. Bai, Y. Deng, H. Jiang and W. Zeng, *Org. Lett.*, 2015, 17, 3998.
- [6] H. Wang, Y. Wang, C. Peng, J. Zhang and Q. Zhu, *J. Am. Chem. Soc.*, 2010, 132, 13217.
- [7] Ru-Long Yan,* Hao Yan, Chao Ma, Zhi-Yong Ren, Xi-Ai Gao, Guo-Sheng Huang,* and Yong-Min Liang, *J. Org. Chem.* 2012, 77, 2024–2028.



7.26 Synthesis of new polyurethane bearing azomethine moieties for sequestration of Ni(II) and Cd(II) from wastewater: Parameter optimization, Equilibrium, Kinetics and Thermodynamic predictions

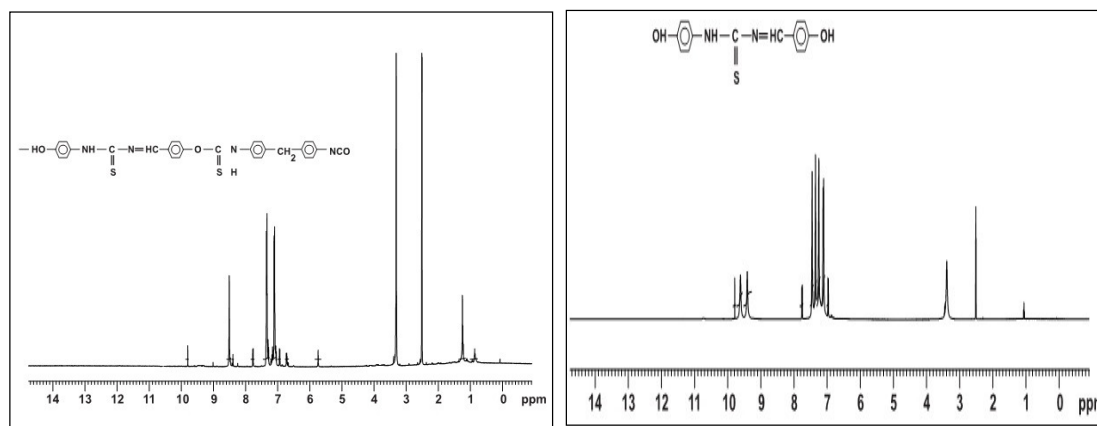
Manickam Sornalatha¹, Rangaraj Arunkumar¹, Kuzhandaivel Hemalatha¹, Selvaraj Dinesh Kirupha¹,
Lingam Ravikumar^{2*}

¹ Department of Chemistry, Coimbatore Institute of Technology, Coimbatore-14.

² Department of Chemistry, CBM College, Bharathiar University, Coimbatore-42.
Swarnalatha313@gmail.com

Abstract

New polyurethane synthesized using two-stage polycondensation technique with dihydroxyphenylthiourea monomer and methylenediisocyanate in DMF medium. The synthesized ¹H-NMR of N-(4-hydroxybenzal)N'(4-hydroxyphenyl)thiourea monomer and Polyurethane polymer were characterized using nuclear magnetic resonance (NMR).



¹H-NMR spectrum of Monomer and polymer PU

The –NH proton is observed at $\delta=9.78$ ppm, while that of –OH proton appeared at $\delta=9.40$ ppm. The –N=CH– proton is shown at $\delta=7.76$ ppm and signals at $\delta=7.45$ - 6.96 ppm are accounted for eight aromatic protons. The –OH proton of monomer appeared at $\delta=9.40$ ppm, is not seen in the ¹H-NMR of polymer PU indicating the formation of urethane link. The signal at $\delta=9.8$ ppm is due to the –NH protons. The –N=CH– proton is accounted for the signal at $\delta=8.5$ ppm. Signals at $\delta=7.7$ - 7.2 ppm are due to the aromatic hydrogen of the diol and diisocyanate monomers. Hydrogen of the urethane links appears at $\delta=7.11$ ppm. The –CH₂– protons present between the phenyl rings appeared at $\delta=1.23$ ppm.

From the FTIR spectrum of polymer PU, the –NH stretching frequency of the urethane link is observed at 3306 cm^{-1} . Since the –CH=N– stretching frequency and the C=O non bonded urethane stretching frequencies falls in the same region a peak with a shoulder at 1644 cm^{-1} is accounted for both. The H–N–C=O amide II band is observed at 1510 cm^{-1} . From the TGA thermogram of PU, Due to the hydrogen bonding of the urethanes, the polymer has good thermal stability. PU is stable upto 330°C and beyond this the polymers undergoes single stage decomposition. From the TGA analysis it can conclude that PU is thermally stable and could be used above 300°C . The surface of the polymer was found to be porous and non-homogeneous in nature. The synthesized polymer was subjected as adsorbent for the removal of Ni(II) and Cd(II) ions using batch mode adsorption studies. The process parameters such as solution pH, initial metal ion concentration, contact time and adsorbent dose were optimized. Using optimized parameters, adsorption isotherm studies and kinetic studies were carried out. These results indicated that the reaction is spontaneous, feasible in nature following redlich isotherm model with pseudo-second order kinetic model (Table 1).



Kinetic models	Parameter	Ni(II)	Cd(II)
Pseudo-first-order equation	k_{ad} (min^{-1})	0.0474	0.0568
	q_e, cal (mg/g)	84.33	104.15
	R^2	0.9943	0.9916
Pseudo-second-order equation	k ($\text{g mg}^{-1} \text{min}^{-1}$)	6.14×10^{-4}	5.85×10^{-4}
	q_e, cal (mg/g)	105.26	104.16
	h ($\text{mg.g}^{-1} \text{min}^{-1}$)	6.81	6.35
	$q_e, expt.$ (mg/g)	98.56	96
	R^2	0.9966	0.9947
Intra-particle diffusion	K_p ($\text{mg/g. min}^{1/2}$)	6.9921	7.0958
	C	27.034	24.407
	R^2	0.9027	0.8961
Elovich kinetic equation	α (mg/g.min)	48.59	67.73
	β (g/mg)	0.0452	0.0445
	R^2	0.9652	0.9596

Table -1 kinetic parameters and constants of Ni(II) and Cd(II) removal with PU polymer

The obtained experimental results were plotted using MATLAB 7.0 software to find out the adsorption capacity (q_e) and isotherm constants. The stability of the polymer in the metal ion solution were tested with different elutants and found out that the polymer was stable upto five cycles. The thermodynamic studies show that the reaction is exothermic. The adsorption capacity (q_e) were found to be 480 mg/g for Ni(II) and 458 mg/g for Cd(II) ions under solution pH 6, with 50 mL of metal ion solution (20 mg/L) in 60 minutes.

7.27 Investigation on the Development of Newer Glycerol Based Deep Eutectic Solvents and Their Applications for the Synthesis of Some Piperidin-4-one Compounds

^aD. Ilangeswaran, ^aR. Suganya, ^aG. Vaitheshwari, ^aK. Ramasundaram and ^bI. Gnanasundaram

^aDepartment of Chemistry, Rajah Serfoji Govt. College (Autonomous), Thanjavur – 613005

^bDepartment of Chemistry, AVVM Shri Pushpam College, Poondi, Thanjavur District

Email: dhailangeswaran@gmail.com, jayasahana26@gmail.com, sundar861@gmail.com and igsundaram@yahoo.com

Abstract

Developing a cheaper and eco friendly solvent is of gaining importance in organic synthesis [1]. Ionic liquids (ILs) and their equivalent known as deep eutectic solvents (DESs) with desired properties were recognized as potential substitutes to be used as “green” solvents for industries [2–7]. DESs include simple eutectic mixtures made from a combination of quaternary ammonium salts, like choline chloride (ChCl), with either hydrogen bond donors like urea and glycerol, or with metal halides (complexing agent) like zinc chloride. Such eutectic mixtures have emerged as biodegradable, economical alternatives and efficient replacement for conventional solvents and molten salts. Due to their high polarity, metal halide based DESs have outstanding solvation properties and can serve as high temperature electrolytes, reusable or homogeneous catalysts, and as solvent in biodiesel applications. This indicates the wide industrial horizon in which they can play essential roles [7–14].

In this work newer glycerol (G) based DESs made from two different metal halides such as MnCl_2 and ZnCl_2 salts were prepared and characterized by measuring some of their important physical properties. The DESs obtained from MnCl_2 and ZnCl_2 with glycerol were introduced to replace conventional organic solvents for synthesizing two piperidin-4-ones namely 1-Phenylpiperidin-4-one and 1,2,6-triphenylpiperidin-4-one. The DESs and piperidin-4-ones were characterized by FTIR spectra. The density of G - MnCl_2 DES and G - ZnCl_2 DES were found to be 1.30 and 1.62 g cm^{-3} respectively. The conductivities of these DES were measured as 0.047 and 0.009 mS cm^{-1} respectively. The melting point of 1-Phenylpiperidin-4-one and 1,2,6-triphenylpiperidin-4-one were observed to be 90 and 118 °C respectively.



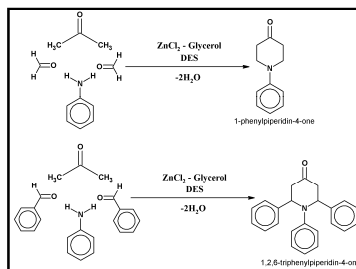


Figure 1. Reaction Scheme for Preparation of Piperidin-4-ones using the newly formed DES

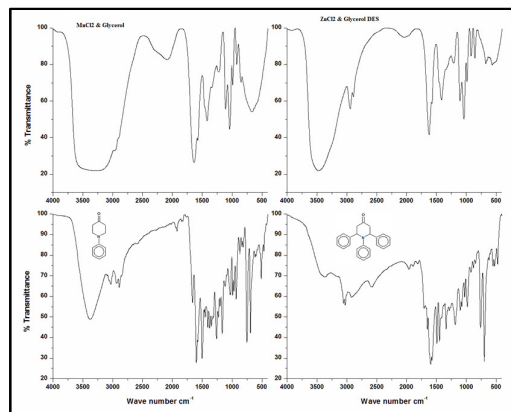


Figure 2. FTIR Spectra of DES and Piperidin-4-one Derivatives

References

- [1] M.A. Kareem, F.S. Mjalli, M.A. Hashim, I.M. AlNashef, *J. Chem. Eng. Data* 55 (2010) 4632.
- [2] R.D. Rogers, K.R. Seddon, *J. Am. Chem. Soc.* 125 (2003) 7480.
- [3] M.G. Del Popolo, G.A. Voth, *J. Phys. Chem. B* 108 (2004) 1744.
- [4] A.B. Pereiro, J.L. Legido, A. Rodriguez, *J. Chem. Thermodyn.* 39 (2007) 1168.
- [5] N.V. Plechkova, K.R. Seddon, *Chem. Soc. Rev.* 37 (2008) 123.
- [6] W.M. Nelson, Are ionic liquids green solvents? *ACS Symposium Series, Ionic Liquids*, (3) 2002, pp. 30.
- [7] E.R. Parnham, R.E. Morris, *Acc. Chem. Res.* 40 (2007) 1005.
- [8] A.P. Abbott, G. Capper, D.L. Davies, R.K. Rasheed, V. Tambyrajah, *Chem. Commun.* 1 (2003) 70.
- [9] R.C. Harris, *Physical Properties of Alcohol Based Deep Eutectic Solvents* thesis University of Leicester, 2008.
- [10] A.P. Abbott, D. Boothby, G. Capper, D.L. Davies, R.K. Rasheed, *J. Am. Chem. Soc.* 126 (2004) 9142.
- [11] A.P. Abbott, G. Capper, D.L. Davies, R.K. Rasheed, *Chem. Eur. J.* 10 (2004) 3769.
- [12] Y. Fukaya, Y. Iizuka, K. Sekikawa, H. Ohno, *Green Chem.* 9 (2007) 1155.
- [13] E.R. Parnham, E.A. Drylie, P.S. Wheatley, A.M.Z. Slawin, R.E. Morris, *Chem. Int. Ed.* 45 (2006) 4962.
- [14] M.C. Gutiérrez, M.L. Ferrer, C.R. Mateo, F. Monte, *Langmuir* 25 (2009) 5509.



7.28 QUALITY ASSESSMENT OF IRRIGATION WATER IN MAJOR RICE GROWING AREAS OF KILVELUR TALUK IN NAGAPATTINAM DISTRICT, TAMIL NADU – INDIA

^aA.Vincentraj, ^bS.Kalyanasundharam, ^cA.Arokiyaraj, ^dS. Leo Arokiaraj and ^eD.Sathya

^{a&b}PG and Research Department of Chemistry, Poompuhar College (Autonomous), Melaiyur-609 107, Nagapattinam, Tamilnadu, India.sksundharam61@gmail.com

^cPG and Research Department of Chemistry, A.V.C.College (Autonomous), Mannampandal-609 305, Nagapattinam, Tamil Nadu, India.arochemmyl@gmail.com

^{d & e} Department of Chemistry, Kalaimahal College of Arts and Science, Sembanar koil-609 309, Nagapattinam, Tamil Nadu, India.

Abstract

This research article is to assess the irrigation water quality of major rice growing area of Kilvelur Taluk of Nagapattinam District in Tamil Nadu and the influence of basic physico-chemical parameters on soil fertility. The water quality index SAR, RSC, Geo-chemical types, classification, suitability of water for irrigation purpose.

Introduction

A total Number of 30 Bore Well irrigation water samples were collected, which covers 10 revenue villages in Kilvelur Taluk by collecting 3 samples from each Revenue village. Most of the farmers utilize ground water for irrigation. All the physico - chemical parameters like pH, EC, Ca, Na, K, SO₄, Cl, Mg, CO₃, and HCO₃ are determined by standard methods and by using standard instruments. Then the irrigation water quality results are compared with standard values Recommended by World Health Organization (WHO), Bureau of Indian Standards (BIS) and Indian Council of Medical Research (ICMR). The proposed work is very essential not only for crop production but also to maintain soil fertility, to maintain hazardous free environment and to enhance the living standard and in turn to uplift our Agriculturist. Cultivation of alternate crop systems are suggested to those farmers lands which are affected by saline water in the coastal area. The concentration and composition of dissolved salts in water decides its suitability for irrigation, degradation of ground water quality of the aquifers causing sea water interference into the coastal aquifers [1].

Study Area

The study area is Kilvelur Taluk of Nagapattinam district coastal region in the southern Tamilnadu State located in the coastal region of Bay of Bengal 10.6664667 Latitude and 79.79605229 Longitude. This taluk is spread over in 27,445 hectares of Agriculture land.

Materials and Methods

Irrigation water samples were collected randomly in a systematic manner covering Kilvelur Taluk of Nagapattinam district. A total 30 samples were collected from bore wells in clean plastic cans of 1 liter capacity. The bottles are tagged individually for sufficient information similar to date, location, deepness of well. The results of the average mean value of irrigation water quality parameters are shown in Table 1. The percentage of irrigation water quality parameters are shown in Table 2. Irrigation water status of kilvelur taluk are shown in Fig 1 to 4. Water samples analyzed by standard methods [2-6].

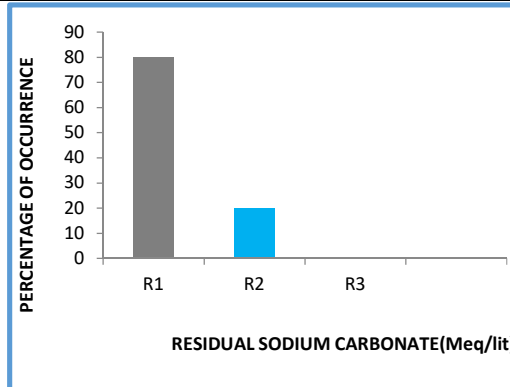
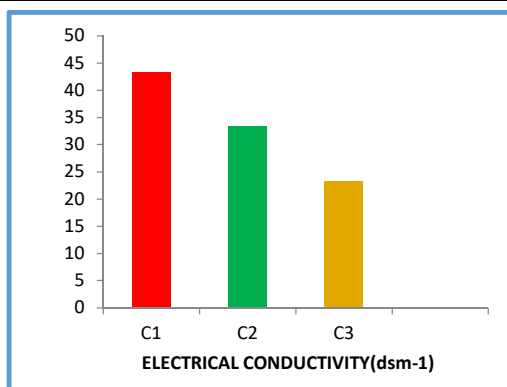
Sl. No	NAME OF THE TALUK	pH	EC(ds m ⁻¹)	ANIONS (meq/lit)					CATIONS (meq/lit)					RSC	SAR	Type	Class
				C	H	Cl	S	T	C	M	N	K	T				
1	KILVELUR TALUK	7.56	1.46	0.7	6.26	7.50	0.38	14.4	3.58	4.5	5.8	0.24	14.3	1.26	2.96	C1S1 R1	NaHCO ₃

Table 1: Average mean value of irrigation water quality parameters of kilvelur taluk in Nagapattinam district.



Table 2: Percentage of irrigation water quality parameters of kilvelur taluk in Nagapattinam district.

SLNo	NAME OF THE TALUK	NaHCO ₃	MgHCO ₃	CaHCO ₃	NaCl	MgCl ₂	CaCl ₂	C1	C2	C3	S1	S2	S3	R1	R2	R3
1	KILVELUR TALUK	43.3	6.6	6.6	30.0	13.3	-	43.3	33.3	23.3	100	-	-	80.0	20.0	-



IRRIGATION WATER STATUS OF KILVELUR TALUK

Figure.1 Electrical Conductivity Rating

Figure.2 Residual Sodium Carbonate Rating

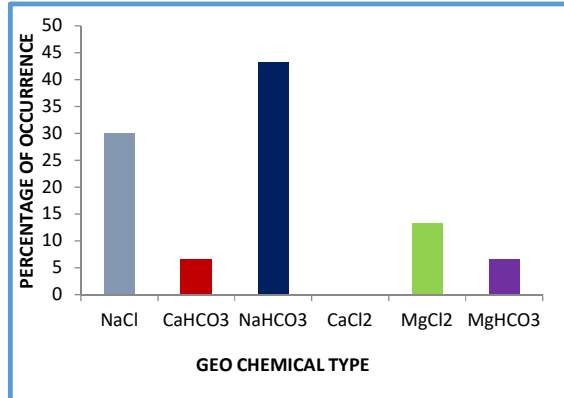
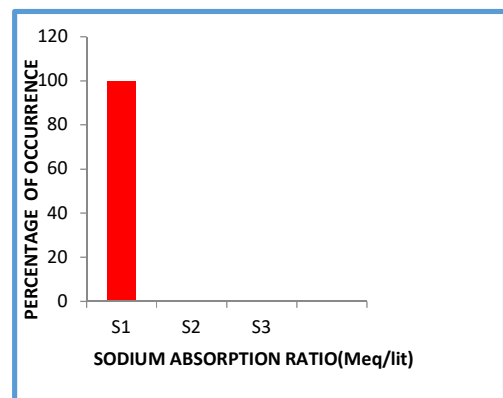
Figure.3 Sodium Absorption Ratio Rating

Figure.4 Geo Chemical Type Rating

Result and Discussion

Assess the 30 irrigation water samples collected from 10 revenue villages in Kilvelur taluk by collecting 3 water samples per village revealed that water analysis parameter in Kilvelur taluk, water samples with mean status of the C₁ S₁ R₁ classification (table.1 and fig.1 to 4).

The irrigation water status of Kilvelur taluk is given in Table 1 and 2, fig.1 to 4. Based on the electrical conductivity classification, 43.3% of villages covers under C₁ classification, 33.3 % of villages covers under C₂ classification, and C₃ classification is 23.3 %. In Kilvelur taluk, 43.3 % of villages cover under C₁ classification due to basin area. Based on Sodium Absorption Ratio classification, 100 % of villages cover under S₁ classification. S₂ and S₃ classifications are not found. In 100 % villages covers S₁ classification due to non-saline water. Based on Residual Sodium Carbonate classification, 80 % villages cover under R₁ classification, 20.0 % for R₂ and R₃ classification are not



found.



Conclusion

The present study assess the water quality status of Kilvelur taluk exposed that they have become an significant trouble (Yield limiting factor) in Kilvelur taluk.Hence the suggestion for different type of water for better yield. Sodium and chloride such water could be improved by gypsum application. Chemical amendments are aimed at to introduce favorable cationic ratios. If water contains high sodium and magnesium bicarbonates, gypsum can be added to irrigation water. Soils irrigated with poor quality water are low in fertility particularly nitrogen. Nitrogen response in good when is applied along with manure, under saline and alkaline soils, should be avoided due to nitrogen loss.

References

- [1] B. Chandrasekaran, S Anbazhagan (2007),Variability of soil–water quality due to Tsunami-2004 in the coastal belt of Nagapattinam district, Tamilnadu.
- [2] APHA standard methods for examination of water and waste,American Public Health Association,Washington D.C.(1998).
- [3] Manual on water and waste water analysis,NEERI Publications(1998).
- [4] D.R Khanna. Ecology and pollution of Ganga River,Ashish Publishing House,Delhi,1(1993).
- [5] Korfali and jurdi.Int.J.Environmental and pollution, 19,271(2003).
- [6] Manual on water and waste water analysis,NEERI Publications(1998).

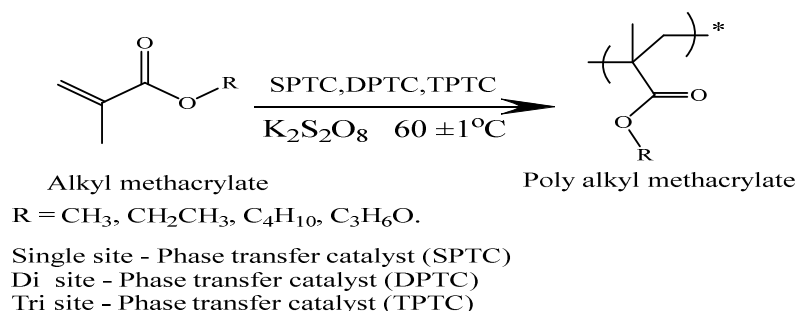
7.29 Performance of phase transfer catalysts on radical polymerization of alkyl methacrylate (RMA) in two phase system- a kinetic study.

Elumalai Marimuthu, VajjiravelMurugesan*

*Department of chemistry, B S Abdur Rahman Crescent University, Vandalur, Chennai-600 048, India. *E-mail: chemvel@rediffmail.com; 7hillsame@gmail.com*

Heterogeneous chemical reactions between two reacting species located in immiscible phases are often inhibited due to the encounter problem. Conventional techniques to avoid this mutual insolubility problem rely on the use of the rapid agitation and the use of cosolvent.The rapid agitation may have an accelerating effect by increasing the interfacial contact.The cosolvent might resolve the mutual insolubility problem. They are certain disadvantages such as the problem of promoting competing hydrolysis pathways and the difficulties in their purification and removal. A plausible technique now widely known as “phase transfer catalysis” (PTC) developed for overcoming the encounter problem due to the mutual insolubility of solvent. PTC deal with the transfer of reactant anions from an aqueous into an organic phase, where the reaction take place to obtained acceleration of the rate high under mild reaction conditions (1-2). The rate of polymerization (R_p) of alkyl methacrylate under different phase transfer catalyst (PTC) can be influenced by the nature of active site of the catalyst (3-4). Three PTC (Single-site PTC, Di-site PTC and Tri-site PTC) were used for the polymerizations of alkyl methacrylate in two phase system at $60 \pm 1^\circ\text{C}$ under inert condition. An increasing trend on the R_p of catalyst and alkylmethacrylate is $\text{TPTC} > \text{DPTC} > \text{SPTC}$ and $\text{GMA} > \text{BMA} > \text{EMA} > \text{MMA}$. The role of polymerization reactions parameters such as monomer, catalyst, initiator and temperature, solvent polarity on the rate of polymerization of alkyl methacrylate was investigated using different PTCs. Based on the kinetic studies, a plausible mechanism has been proposed and its significance was discussed. The obtained polymer was confirmed by spectral analysis.





Keywords: kinetics, active-sited phase transfer catalyst, rate of polymerization, alkyl methacrylate.

References

- [1] Y. Sasson, Handbook of Phase Transfer Catalysis, New York, USA, 1997.
- [2] R.A. Jones, Quaternary Ammonium Salts Academic Press, New York, 2001.
- [3] Reactors, kinetics, and catalysis 44,3,1998
- [4] International Journal of Industrial Chemistry, 2016, 441-448.
- [5] Journal Polymer Research, 2008, 15(1), 27-36.
- [6] catalysis reviews,45,3&4,369-395,2003

7.30 LIMESTONE: HETEROGENEOUS AND AN EFFICIENT REUSABLE CATALYST FOR SYNTHESIS OF TETRAHYDROBENZO[b] PYRAN AND ITS DERIVATIVES

T.Clarina, S.Amsaveni, V.Rama*

Department of Chemistry

Sarah Tucker College, Manonmaniam Sundarnar University, Abishekapatti, Tirunelveli – 627 012, Tamil Nadu, India

E-mail address: rama242002@gmail.com

Benzo[b]pyran is a polycyclic organic compound that results from the fusion of a benzene ring to a heterocyclic pyran ring. It is one of the privileged scaffolds with a medicinal pharmacophore such as antivasular, antimicrobial, antioxidant, anticoagulant, estrogenic, anti-helminthic, anticancer^[1], anti-HIV, anti-inflammatory^[2], analgesic, herbicidal^[3] and anticonvulsant. Tetrahydrobenzo[b]pyran derivatives were synthesized by simple condensation of three components such as aldehyde (1 mmol), malononitrile (1 mmol) and cyclic dimedone (1 mmol) in ethanol (5 mL) at room temperature in the presence of Limestone as base heterogeneous catalyst. Limestone is an organic sedimentary rock composed primarily of calcium carbonate and mainly found in clear, warm and shallow marine water. It is formed due to the accumulation of shell, coral, algal and fecal debris. Limestone from Sayamalai village of Tirunelveli district was formed by direct precipitation of calcium carbonate from marine water and it is utilized as a source of heterogeneous base catalyst for the synthesis of Tetrahydrobenzo[b]pyran derivatives. It is a simple and easy work-up, low cost, green process, inexpensive catalyst, short reaction times and excellent yields of the products are the advantages of this procedure.

To find the optimized conditions, the reaction of benzaldehyde (1.0 mmol), dimedone (1.0 mmol), malononitrile (1.0 mmol) in ethanolic medium as a model reaction in the presence of different amount of limestone is examined and variables affecting the reaction yields are studied (Table:1). We found limestone to give the excellent yield at room temperature compared to reflux conditions. Among the various solvents such as DMF, DMSO, ACN, Ethanol and Water, we found in presence of ethanol it gives good yield under ambient conditions. The necessity to use the catalyst was realized by the observation that no product was detected when the reaction was carried out in the absence of any solvent either at room temperature or at 80°C



Table 1: Catalytic Performance of Limestone under various conditions:

Entry	Catalyst	Solvent	Yield (%) ^b
1.	Limestone	Water	62
2.	Limestone	DMSO	54
3.	Limestone	Ethanol	98
4.	Limestone	Acetonitrile	28
5.	Limestone	DMF	51
6.	Limestone	-	16
^c 7.	Limestone	Ethanol	71,98
^d 8.	Limestone	Ethanol	69,98
^e 9.	Limestone	Ethanol	71,98

aldehyde (1.0 mmol), Dimedone (1.0 mmol), malononitrile (1.0 mmol), catalyst (10 mg), Ethanol (5 mL), RT. ^b Isolated yield. ^c Yield when the reaction carried at room temperature and 60°C respectively. ^d Yield of the reaction carried with 5 mg and 10 mg of catalyst respectively. ^e Yield when the reaction carried with solvent 2.5 mL and 5 mL respectively.

We have also investigated the effect of different amount of catalyst upon the reaction. By increasing of the catalyst loading to 20 mg the reaction has no significant effect on reaction rate and isolated yield of product. After optimizing the reaction conditions, we next examined the nature of substituents on the aromatic ring.

Table 2: Synthesis of substituted Tetrahydrobenzo[*b*]pyrans using Limestone catalyst:

Entry	RCHO	Time (min)	Yield (%)	Melting Point
1	C ₆ H ₅	12	98	228 – 230 °c
2	4-Cl –C ₆ H ₄	15	89	216 °c
3	4-OH –C ₆ H ₄	15	90	214 °c
4	4-NO ₂ –C ₆ H ₄	20	92	172- 174 °c
5	3,4-OCH ₃ -C ₆ H ₄	20	92	158 – 160 °c

^A aldehyde (1.0 mmol), dimedone(1.0 mmol), malanonitrile (1.0 mmol), catalyst (10 mg),Ethanol (5 mL), Room temperature. ^bIsolated yield.

This cyclocondensation reaction was then investigated with different aldehydes. Replacement of benzaldehyde by using electron withdrawing and electron donating group containing aldehyde also gives an excellent yield.

We also examined the reusability of Limestone by studying the catalytic activity of the recycled Limestone for the synthesis of tetrahydrobenzo[*b*]pyrans. After separation of the product by filtration, the filtrate containing the Limestone was rinsed with ether and further vacuumed to dryness at 90 °C for 2 h to remove any moisture. The recovered Limestone was reused directly for the next run. It was found that the Limestone can be used for the reactions for up to five runs without any appreciable loss of efficiency.

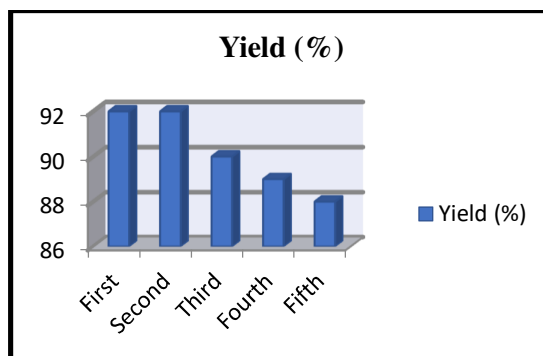


Figure: 1. Reusability of catalyst

This catalyst has a good catalytic effect for the preparation of tetrahydrobenzo[*b*] pyrans derivatives in an excellent yield compared to the previous reported works. In summary, our workup is a simple work-up procedure in a very short time and produces good yields. This make our methodology a valid contribution to the synthesis of tetrahydrobenzo[*b*] pyrans.



References:

- [1] M. M. Heravi, M. Tajbakhsh, A. N. Ahmadi, B. Mohajerani, *Monatsh Chem* 137 (2006) 175.
- [2] D. P. Sahu, S. Ponnala, *Synthetic Communication* 36 (2006) 2189.
- [3] A. B. Allouma, K. Bougrin, M. Soufiaoui, *Synthetic Communication* 44 (2003) 5935.
- [4] H. Kiyani, F. Ghorbani, *Journal of Saudi Chemical Society* 18 (2014) 689.

7.31 EFFECT OF MECHANICAL AND MECHANOCHEMICAL SHEAR TREATMENTS ON CELLULOSE IN SOLID STATE

R. Lavanya and N. Natchimuthu*

Department of Rubber and Plastics Technology, MIT Campus, Anna University, Chennai-600 044

E-mail: lavanchem1989@gmail.com

Abstract

Cellulose is one of promising material for the development of many organic materials in a sustainable manner as the biomass required for it is available in plenty and also renewable [1]. The scientific reasons for limited utility of cellulose can be easily traced to its highly crystalline and intractable nature of its structure. Cellulose molecules are linear and aggregated through van der Waals forces and strong intra and intermolecular hydrogen bonding [2]. The hydrophilic behaviour of cellulose is due to the location of hydroxyl groups in the glucopyranose rings. Most organic solvents do not dissolve cellulose due to its highly crystalline nature because of hydrogen bonding. Solid state chemical modifications on cellulose could be considered as a viable means of modifying its chemical and surface features thereby breaking the hydroxyl group between the hydrogen bonds and enabling dissolution in cellulose without degrading its basic structure [3].

In our study, mechanochemical treatment was performed on cellulose with the objective of modifying its morphology, reducing crystallinity and enabling better dissolution. Cellulose, treated with N, N'-dimethylacetamide/lithium chloride (DMAc/LiCl), was subjected to shear using rubber as a carrier and shear transfer medium. When cellulose is subjected to mechanochemical treatment, significant changes were observed in decrease in crystallinity and surface morphology of cellulose. When mechanical shear was used in the absence of DMAc/LiCl treatment, changes in crystalline index, morphology and dissolution has not shown any major change compared to that of original untreated cellulose. The morphology of regenerated cellulose has shown in Figure 1.

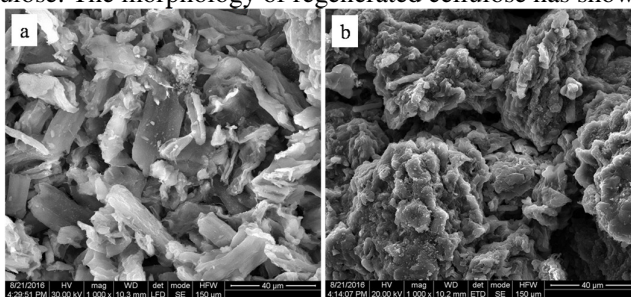


Figure 1: SEM micrographs of (a) mechanical treatment of Cellulose and (b) mechanochemical treatment of cellulose

References

- [1] Gandini, A 'Polymers from Renewable Resources: A Challenge for the Future of Macromolecular Materials', *Macromolecules* (2008) vol. 41, no. 24, pp. 9491-9504.
- [2] Gardner, KH & Blackwell, J 'The structure of native cellulose', *Biopolymers* (1974) vol. 13, no. 10, pp. 1975-2001.



- [3] Zhang, W, Liang, M & Lu, C 'Morphological and structural development of hardwood cellulose during mechanochemical pretreatment in solid state through pan-milling', Cellulose (2007) vol. 14, pp. 447-456.

7.32 Synthesis of CPT releasing Poly (ϵ -caprolactone-co-citrate) by using Deep Eutectic Solvents

Periyakaruppan Pradeepkumar^a, Mariappan Rajan*

^a*Biomaterials in Medicinal Chemistry Laboratory, Department of Natural Products Chemistry, School of Chemistry, Madurai Kamaraj University, Madurai – 625021, Tamil Nadu, India.*
ppv634@gmail.com

Abstract

Currently, Deep Eutectic Solvents (DESs) frequently used for the designing of biomedical application. Attributable to DES is a good biocompatibility, biodegradability and non-toxic nature. In the present study, we demonstrated that a development toward destination of innovative properties of DES were designed and used for polycondensation process for drug delivery application. The polycondensation optimized in the excess of hydroxyl group of DES. In the resulting Polycondensation, the presence of these salts Choline chloride and Citric acid in the ratio of 1:2. Herein, we have successfully synthesised Poly (ϵ -caprolactone-co-citrate). Camptothecin (CPT) encapsulated Poly (ϵ -caprolactone-co-citrate) were prepared by nano precipitation technique. Optimization of DES and after polycondensation of DES was characterized by UV, FT-IR spectroscopy. Then FT-IR, XRD, Raman spectra, TGA, and SEM were considered as the confirmation of carrier and CPT loaded carrier. *In-vitro* and *in-vivo* studied CPT loaded Poly (ϵ -caprolactone-co-citrate) potency of the drug delivery system. The Poly (ϵ -caprolactone-co-citrate) in DES carrier for the sustainable delivery of anti-cancer drug.

Keywords: Biocompatibility, Camptothecin (CPT), ϵ -caprolactone, Drug delivery, Deep Eutectic Solvent.

1. Introduction

The frequently solvents has been used for variety of application by Deep eutectic solvents (DESs). Even though, the developments observed with ionic liquids (ILs) in before 21st century [1]. The lot of application are using DESs. However, the limited applicability of ILs. DESs are composed of two or more compounds that are capable of self-association, often through hydrogen bond interaction to form DESs. This DESs strong interaction is responsible for the decrease of the melting point lower than individual compounds.

2. Experimental section

2.1. Synthesis of DESs

DESs was synthesised according to the methods described previously literature [2]. Briefly, a synthesis of choline chloride and citric acid salts mixture were synthesized. At different molar ratios of choline chloride and citric acid from (1:1, 1:2 and 1:3) at 28^oC for 1 hr until clear, transparent homogeneous liquids obtained.

3. Characterization of DESs

3.1. FT-IR analysis

FT-IR spectra of samples was observed from KBr samples pellets within the range of 400-4000 cm⁻¹ on a FT-IR spectroscopy (Spectrum GX-I, Perkin Elmer, Waltham, MA, USA).

4. Result and discussion

4.1. FT-IR

FT-IR spectra bands corresponding to the Choline chloride, citric acid, DES-I (1:1), DES-II (1:2) were presented in (Fig. 1). The DESs system between pure Choline chloride, citric acid can be consider based on the FT-IR spectrum of DES-I (1:1), DES-II (1:2) represented in (Fig. 1C, D).



7.33 Summer affects calcification to organic matter production in coralline red alga *Amphiroa fragilissima* occurring along the Thondi coast (Palk Bay, Indian)

J.Archanadevi and K.Arunkumar*

Department of Botany, Alagappa Government Arts College, Karaikudi-630003, Tamil Nadu, India

*Central University of Kerala, Riverside Transit Campus, Padanakkad-671 314, Kasaragod, Kerala, India

Abstract

Marine calcareous algae (CA) are unique subset of seaweeds (marine macroalgae) which incorporate calcium carbonate into their thalli. As a quite diverse group, calcification has evolved independently in the three major classes of seaweeds: *Rhodophyceae*, *Chlorophyceae* and *Phaeophyceae* commonly called as red, green and brown, respectively. CA dominate biotic communities in many subtidal, intertidal and tide pool environments worldwide. This marine algae deposit crystals of calcium carbonate (CaCO_3) in the cytozol or cell walls and significant contributors to the coastal calcium carbonate (CaCO_3) deposition. In marine ecosystems, rising atmospheric CO_2 results increase in the dissolved inorganic carbons (CO_3 , HCO_3 and H_2CO_3) cause ocean acidification (OA) which affect the primary production as well as carbon mineralization of CA. Thus CA is most sensitive calcifiers to OA. Studies on the effect of OA on calcification process in calcareous macroalgae are recently increased because of the extended contribution of CA on reef building.

In this study, carbon mineralization by marine calcareous alga commonly called coralline red alga *Amphiroa fragilissima*(Fig. 1) in varying seawater and soil chemistry occurring along the Coast of Thondi(Palk Bay, Indian) was made. Calcium and magnesium content of seawater and soil were analyzed on monthly basis. The pH, CO_2 , alkalinity and salinity of seawater and calcium carbonate content of soil were recorded(Fig. 2). The monthly variations in the pH, calcium and magnesium were not significant whereas high significant ($P > 0.01$) in the CO_2 , total alkalinity and salinity of seawater was observed. High significant difference in soil calcium carbonate and calcium ($P > 0.01$) was observed but magnesium show insignificant difference.

Carbon sequestration parameters such as biomass (dry weight), morphological volume, ash, total mineral, calcium and magnesium showed high significant ($P > 0.01$) difference among various seasons. The alga accumulated maximum biomass, ash content, calcium, magnesium and total biomineral during monsoon season whereas maximum morphological volume recorded in summer season and minimum morphological volume recorded in the monsoon season. Maximum organic matter and organic carbon was recorded in summer season and minimum in monsoon season whereas inorganic carbon was maximum in monsoon season and minimum in summer season(Fig. 3). These results show the diversion of carbon towards organic carbon accumulation in summer which affects calcification by inorganic carbon accumulation favoured in monsoon. Carbonate crystals such as calcite, aragonite and dolomite recorded by FTIR and XRD indicate the presence of high Mg-calcite, magnesium calcite, calcite and hydrocerussite correlated with high magnesium in the seawater of Thondi coast during monsoon favour calcification reflected by high magnesium calcite(Fig. 4). Significant correlation between calcium and magnesium on total mineral and ash content recorded in *Amphiroa fragilissima* further supported the calcification by seawater of monsoon season. This study concludes that soil carbonate and seawater chemistry during monsoon season support inorganic carbon sequestration whereas summer favoured organic matter accumulation hence the extended summer affect the calcification of calcareous alga *Amphiroa fragilissima* occurring along the Thondi coast.

Key words: Calcareous algae, calcification, carbonate crystal, carbon accumulation, Magnesium calcite

Fig.1 *Amphiroa fragilissima* collected along the Thondi (Palk bay) coast



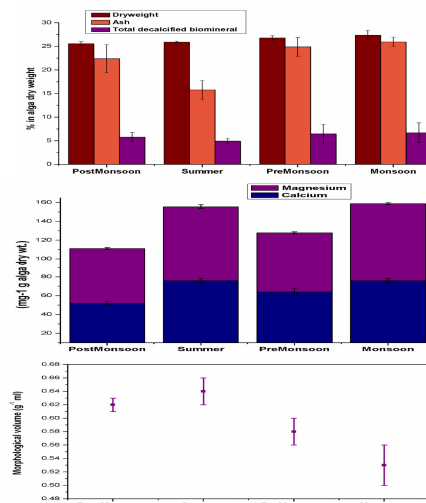


Fig.4 XRD characterization of *Amphiroa fragilissima* collected at various seasons along the Thondi (Palk bay) coast in the month January 2014 to December 2014

7.34 Advanced Linear Integral Isoconversional Methods for Estimating Activation Energy: Thermal Degradation of Polypropylene

Stephen Joel K^a, Vimalathithan PK^b, Vijayakumar CT^c

^aAssistant Professor, Department of Chemistry, Kamaraj College of Engineering and Technology, S.P.G.C. Nagar, K. Vellakulam – 625 701, India

^bAssistant Professor, Department of Mechanical Engineering, Kamaraj College of Engineering and Technology, S.P.G.C. Nagar, K. Vellakulam – 625 701, India

^cProfessor, Department of Polymer Technology, Kamaraj College of Engineering and Technology, S.P.G.C. Nagar, K. Vellakulam – 625 701, India
contactstephenjoel@gmail.com

It becomes essential to study the thermal stability, heat resistance, life time of polymeric materials for their direct practical applications and also its degradation kinetics and degradation mechanism for recycling processes such as cracking of huge quantity of plastic wastes which creates various environmental safety issues. From thermogravimetric analysis (TGA) data, the kinetic triplets, activation energy for degradation (E), pre-exponential factor (A) and reaction model ($f(\alpha)$) can be estimated. There are two approaches in estimating the E, model fitting and model free methods. Model fitting methods are based on compensation effect which can produce absurd results when compared to model free methods. The model free kinetics follows the isoconversional principle[1] which assumes E is only a function of temperature for a specific conversion (α).

Friedman (FRD) method is the most common method used to estimate E. The method follows the procedure of taking natural logarithm on either side of the general non-isothermal solid state transformation.

$$\frac{d\alpha}{f(\alpha)} = \frac{A}{\beta} e^{\frac{-E}{RT}} dT$$

Flynn-Wall-Ozawa (FWO) proposed an integral approach which used the temperature integral proposed by Doyle and using a linear approach estimated E from the following relation.

$$\ln \beta_i = \ln \left(\frac{AE}{Rg(x)} \right) - 1.0518 \frac{E}{RT_i} - 5.330$$



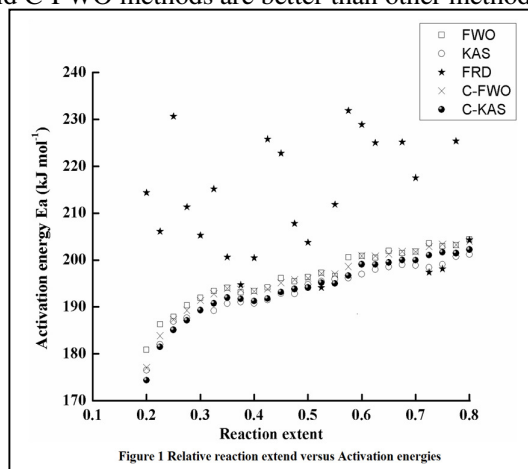
Another method that has been commonly used was proposed by Kissinger-Akahira-Sunose (KAS) which used the temperature integral developed by Coats-Redfern. However, both these methods are slightly unreliable due to the systematic errors. In order to rectify that problem, Farjas[2] has proposed an iterative approach to estimate E. A term $\bar{X} = E/RT$ has been introduced, where, \bar{T} is the average temperature over the conversion. The following are the new Corrected FWO (C-FWO) and Corrected KAS (C-KAS) relations.

$$\ln \beta_i - \ln \xi_{FWO} = \ln \left(\frac{AE}{Rg(x)} \right) - 1.0518 \frac{E}{RT_i} - 5.330$$

$$\ln \frac{\beta_i}{T_i^2} - \ln \xi_{KAS} = \ln \frac{AR}{g(\alpha)E} - \frac{E}{RT_i}$$

where ξ_{FWO} and ξ_{KAS} are the iterating terms which are the parameters of \bar{X} .

The results were validated for the thermal degradation of polypropylene under four different heating rates viz. 10, 15, 20 and 25 °C/min. From the results it is evident that the E estimated using FRD, FWO and KAS methods shows abnormality at higher values of conversion whereas C-FWO and C-KAS shows very smooth pattern which is shown in Figure1. From this it can be concluded that the E estimated using C-KAS and C-FWO methods are better than other methods.



References

- [1] S. Vyazovkin, A. K. Burnham, J. M. Criado, L. A. Pérez-Maqueda, C. Popescu, N. Sbirrazzuoli, ICTAC Kinetics Committee recommendations for performing kinetic computations on thermal analysis data, *Thermochim. Acta* 520 (2011) 1-19.
- [2] J. Farjas, P. Roura, Isoconversional analysis of solid state transformations. A critical review. Part I. Single step transformations with constant activation energy, *J. Therm. Anal. Calorim.* 105 (2011) 757-766.



7.35 Aza-Baylis–Hillman Reaction of salicyl *N*-tosylimines with *N*-substituted maleimides under solvent free condition.

S.Sugirdha^{a,b}, M.Vadivelu^a and Dr.K.Karthikeyan^{a*}

^a Department of Chemistry, B.S.Abdur Rahman Crescent University, Vandalur, Chennai-600 048

^b Department of Metallurgical and Material Science Engineering, Indian Institute of Technology Madras, Chennai-600036
Email: karthicri@gmail.com

Heterocycles are of great value in the design and discovery of new biologically active compounds. The development of efficient processes to construct heterocycles, using metal-free catalysts has been drawing much attention over the past decades.¹ Spirocyclic systems containing one carbon atom common to two rings are structurally interesting. Especially among them, the spirocyclic benzofurans have attracted considerable attention due to their useful pharmaceutical activities.² Baylis-Hillman reaction is one of the most atom economical and important carbon-carbon bond forming reactions. It has made great progress recently due to the considerable reduction of reaction time, wide range of the substrates employed and its asymmetric version as compared to the classical reaction.^{3,4} Recently, the Baylis-Hillman reaction of salicylaldehydes or salicyl *N*-tosylimines with various α,β -unsaturated compounds has been well studied and formation of different kinds of heterocycles were reported. In the continuation of our works in Baylis-Hillman reactions using maleimides.^{5,6} We planned to study the Aza-Baylis-Hillman reactions of salicyl *N*-tosylimines with maleimide in the presence of DABCO as catalyst under solvent free condition.

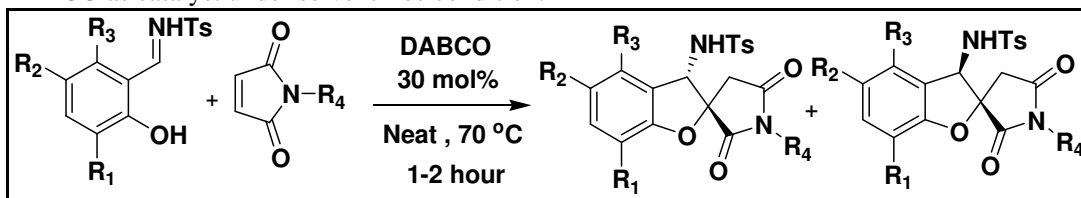


Figure 1: Synthesis of spirobenzofurans

The use of maleimide as activated olefin in aza-Baylis-Hillman reaction was limited.

The noteworthy advantages of our protocol are tolerates structurally diverse substrates, reaction proceeds under solvent free green condition, provides diastereoselectivity upto 80-90%.

Keywords: Aza-Baylis-Hillman reaction, Salicyl *N*-tosylimines, Maleimide, DABCO, Spirobenzofuran

References:

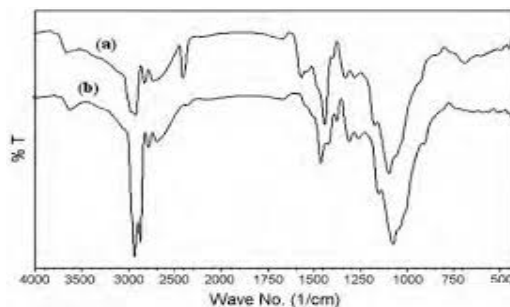
- [1] Dalko, P. I.; Moisan, L. *Angew. Chem., Int. Ed.* **2004**, 43, 5138.
- [2] Usegilo, M.; Castellano, P. M.; Operto, M. A.; Torres, R.; Kaufman, T. S. *Bioorg. Med. Chem. Lett.* **2006**, 16, 5097.
- [3] Price, K. E.; Broadwater, S. J.; Walker, B. J.; McQuade, D. T. *J. Org. Chem.* **2005**, 70, 3980.
- [4] Krafft, M. E.; Haxell, T. F. N.; Seibert, K. A.; Abboud, K. A. *J. Am. Chem. Soc.* **2006**, 128, 4174.
- [5] Karthikeyan, K.; Perumal, P. T. *Synlett.* **2009**, 2366
- [6] K.Karthikeyan, N.Saranya, A.Kalaivani, P.T.Perumal, *Synlett.* **2010**, 2751



SEM images confirmed the adsorption of As(v) onto prepared chitin through morphological observation. The adsorption capacity is comparable to results published by other authors, suggesting that the prepared modified biosorbent has potential in remediation of contaminated waters.

Keywords: As(v) removal, Adsorption, Bisorption, Chitin, Kinetics, Water/Waste water

Figure



References

- [1] Catheriene Hui Niu, Bohumil Volesky, Daniel Cleiman; Water Research, 2007, 41, 2473- 2478.
- [2] Jaafarzadeh N, Mengelizadeh N, Takdastan A, Farsani MH, Niknam N, Aalipour M; .Int J Env Health Eng 2015;4:7.

7.38 REMOVAL OF BASIC DYE FROM AQUEOUS SOLUTION USING ACID ACTIVATED CARBONS DEVELOPED FROM THE VARIOUS TREE BARK: ADSORPTION EQUILIBRIUM AND KINETICS

R.Pagutharivalan¹ and N. Kannan²

¹Department of Chemistry, H.H.The Rajah's College (Autonomous), PUDUKKOTTAI- 622 001.Tamil Nadu, INDIA.

² Centre for Research and Post graduate Studies in Chemistry, Ayya Nadar Janaki Ammal College (Autonomous) SIVAKASI – 626 124, Tamil Nadu, INDIA.
paguthuchem@gmail.com

Abstract

Removal of Rhodamine B in aqueous solution on the various tree bark carbons such as Eucalyptus Globules Bark Carbon (EGBC) Emblica officinalis bark carbon (EOBC) have been studied. The effect of various experimental parameters has been investigated using a Batch Adsorption technique (BAT) to obtain information on treating effluents from the dye industry. The extent of dye removal increased with decrease in the initial concentration of the dye and increased with increase in contact time, amount of adsorbent used and the initial pH of the dye solution. Adsorption data were modeled using the Freundlich and Langmuir adsorption isotherms and first order kinetic equations. The kinetics of adsorption was found to be first order with regard to intra-particle diffusion as the rate determining step. The adsorption capacity of dye has been compared with Commercial activated carbon (CAC). The results indicate that EOBC is one of the best adsorbent that can be used in wastewater treatment for the removal of colors and dyes. It is also reported to have been confirmed by SEM photos and FT-IR spectra, before and after adsorption.

Keywords: Adsorption of Rhodamine B, Batch Adsorption technique, Eucalyptus Globules Bark Carbon, Emblica officinalis bark carbon adsorption isotherms, Kinetics of adsorption.



7.39 REMOVAL OF RHODAMINE B FROM AQUEOUS SOLUTION BY ADSORPTION USING ACID ACTIVATED ADSORBENTS.

A. Sivakumar¹ G.Ramachandran² R. Pagutharivalan* and N. Kannan[#]

1 *PG Department of chemistry H.H The Rajah's college (Autonomous), Pudukkottai-(dt), Tamil Nadu. 2 Dr.Ambethkar Govt. Arts College Viyasarpadi, Chennai-23

Centre for Research and Post Graduate Studies in Chemistry, Ayya Nadar Janaki Ammal College Sivakasi, Tamil Nadu.

Abstract

Adsorption behavior of Rhodamine B dye by the activated *Azadirachta Indica Bark Carbon* (AIBC) prepared from Acacia Arabic tree bark by nitric acid treatment method and Commercial activated carbon (CAC) have been carried out with an aim to obtain data for treating industrial effluents from textile, leather and dye manufacturing industries. The effect of various process parameters like initial concentration, contact time, dosage, initial pH and particle size are investigated by the following batch adsorption technique at $30 \pm 1^\circ\text{C}$. Adsorption data are modeled with adsorption isotherms, the first order kinetics equations proposed by Natarajan-Khalaf, Lagerghan, Bhattacharya-Venkobachar and intra-particle diffusion as one of the rate determining steps. The adsorption capacity of AABC is compared with CAC. The result of the study revealed that AABC is a suitable adsorbent for the removal of dye and the color from aqueous solution. It is also reported to have been confirmed by SEM photos and FT-IR spectra, before and after adsorption.

Keywords: Adsorption, Rhodamine B dye, low cost adsorbents, adsorption isotherms, *Azadirachta Indica Bark Carbon*, water and land pollution, kinetics of adsorptions.

7.40 STUDIES ON REMOVAL OF MALACHITE GREEN FROM AQUEOUS SOLUTION BY ADSORPTION ONTO ACID ACTIVATED CARBONS – KINETIC AND EQUILIBRIUM STUDY

R.Arunkumar¹, K.Sarathkumar², R.Saravanan³, R.Pagutharivalan* & N.Kannan[#]

*Department of Chemistry, H.H.The Rajah's College (Autonomous), PUDUKKOTTAI-622 001.Tamil Nadu, INDIA.

#Centre for Research and Post graduate Studies in Chemistry, Ayya Nadar Janaki Ammal College (Autonomous)SIVAKASI – 626 124, Tamil Nadu, INDIA.

Abstract

Removal of Malachite Green (MG) in aqueous solution on activated *Acacia Arabic Bark Carbon* (AABC) prepared from Acacia Arabic tree bark by nitric acid treatment method and Commercial activated carbon (CAC) has been studied. The effect of various experimental parameters has been investigated using a Batch Adsorption technique (BAT) to obtain information on treating effluents from the dye industry. The extent of dye removal increased with decrease in the initial concentration of the dye and increased with increase in contact time, amount of adsorbent used and the initial pH of the dye solution. Adsorption data were modeled using the Freundlich and Langmuir adsorption isotherms and first order kinetic equations. The kinetics of adsorption was found to be first order with regard to intra-particle diffusion as the rate determining step. The adsorption capacity of dye has been compared with CAC. The results indicate that AABC is one of the best adsorbent that can be used in wastewater treatment for the removal of colors and dyes.

Keywords: Adsorption of Malachite Green, Batch Adsorption technique, *Acacia Arabic Bark Carbon*, adsorption isotherms, Kinetics of adsorption.



7.41 ADSORPTION OF ACIDIC DYE FROM AQUEOUS SOLUTION USING LOW COST ADSORBENTS - A COMPARATIVE STUDY

R.Saravanan¹, R.Arunkumar², K.Sarathkumar³, R.Pagutharivalan* & N.Kannan#

*Department of Chemistry, H.H.The Rajah's College (Autonomous), PUDUKKOTTAI-622 001.Tamil Nadu, INDIA.
#Centre for Research and Post graduate Studies in Chemistry, Ayya Nadar Janaki Ammal College (Autonomous), SIVAKASI – 626 124, Tamil Nadu, INDIA.

Abstract

Studies on the removal of Acid Violet (AV) dye by adsorption on acid activated carbon like Acacia Arabic Bark Carbon (AABC) has been made and the results have been compared with that of commercial activated Carbon (CAC). Effect of various experimental parameters has been investigated using batch adsorption technique at room temperature (30±1 °C). The percentage removal of AV increases with decrease in the initial concentration of AV, initial pH and particle size of adsorbent and increases with increase in the contact time and dose of adsorbent. Adsorption data were modeled with the Freundlich and Langmuir adsorption isotherms and various first order kinetic equations at 30±1 °C. The kinetic of adsorption is found to be first order with intra particle diffusion as one of the rate determining steps. The mechanism of adsorption for AV on to various carbons were investigated by using the experimental results and confirmed by FT-IR and SEM images. The adsorbent material AABC is employed as low cost adsorbent as an alternative material to CAC for the removal of AV.

Key words :Acid Violet Bark Carbons, Freundlich and Langmuir isotherms, Kinetics of adsorption, Intra particle diffusion, Wastewater treatment.

7.42 A COMPARATIVE STUDY ON REMOVAL OF CRYSTAL VIOLET FROM AQUEOUS MEDIUM WITH ACTIVATED LOW COST ADSORBENTS

K.Sarathkumar¹, R.Arunkumar², R.Saravanan³, R.Pagutharivalan* & N.Kannan#

*Department of Chemistry, H.H.The Rajah's College (Autonomous), PUDUKKOTTAI-622 001.Tamil Nadu, INDIA.
#Centre for Research and Post graduate Studies in Chemistry, Ayya Nadar Janaki Ammal College (Autonomous), SIVAKASI – 626 124, Tamil Nadu, INDIA.

Abstract

Removal of Crystal Violet (CV) in aqueous solution on Acacia Arabic Bark Carbon (AABC) prepared from Acacia Arabic tree bark by nitric acid treatment method has been studied. The effect of various experimental parameters has been investigated using a Batch Adsorption technique (BAT) to obtain information on treating effluents from the dye industry. The extent of dye removal increased with decrease in the initial concentration and initial pH of the dye solution and increased with increase in contact time, amount of adsorbent used and the particle size of the adsorbents. Adsorption data were modeled using the Freundlich and Langmuir adsorption isotherms and first order kinetic equations. The kinetics of adsorption was found to be first order with regard to intra-particle diffusion as the rate determining step. The adsorption capacity of dye has been compared with that of commercial activated Carbon (CAC). The results indicate that AABC is one of the best adsorbent that can be used in wastewater treatment for the removal of colors and dyes.

Keywords: Adsorption of Crystal Violet, Batch Adsorption technique, Acacia Arabic Bark Carbon, adsorption isotherms, Kinetics of adsorption.



7.43 REMOVAL OF ACIDIC DYE FROM AQUEOUS SOLUTION BY ADSORPTION USING LOW COST ACID ACTIVATED ADSORBENTS

R.Muthlakshmi¹, M.Muthumani², R.Pagutharivalan* & N.Kannan #

¹⁻²*Department of Chemistry, H.H.The Rajah's College (Autonomous), PUDUKKOTTAI-622 001.Tamil Nadu, INDIA.
#Centre for Research and Post graduate Studies in Chemistry, Ayya Nadar Janaki Ammal College (Autonomous), SIVAKASI
– 626 124, Tamil Nadu, INDIA.

Abstract

Adsorption behavior of Aniline Blue dye (Acidic dye) on to various low cost activated carbons like, *Cassia Arabic Bark Carbon (CABC)*, *Azadirachta Indica Bark Carbon (AIBC)* and *Commercial Activated Carbon (CAC)* have been carried out with an aim to obtain data for treating industrial effluents from textile, leather and dye manufacturing industries. The effect of various process parameters has been investigated by the following batch adsorption technique at $30 \pm 1^\circ\text{C}$. Adsorption data are modeled with adsorption isotherms, the first order kinetics equations proposed by Natarajan-Khalaf, Lagerghan, Bhattacharya-Venkobachar and intra-particle diffusion an one of the rate determining steps. It is also reported to have been confirmed by SEM photos and FT-IR spectra, before and after adsorption.

Keywords: Adsorption, Aniline Blue dye, low cost adsorbents, adsorptions isotherms, water and land pollution, kinetics of adsorptions.

7.44 ADSORPTION OF CHROMOTOPE DYE FROM AQUEOUS SOLUTION ONTO ACID ACTIVATED LOW COST ADSORBENTS

M.Muthumani¹, R.Muthlakshmi², R.Pagutharivalan* & N.Kannan #

¹⁻²*Department of Chemistry, H.H.The Rajah's College (Autonomous), PUDUKKOTTAI-622 001.Tamil Nadu, INDIA.
#Centre for Research and Post graduate Studies in Chemistry, Ayya Nadar Janaki Ammal College (Autonomous), SIVAKASI
– 626 124, Tamil Nadu, INDIA.

Abstract

Adsorption behaviour of Chromotrope (CH) onto various low cost activated carbons like, *Eucalyptus Globules Bark Carbon (EGBC)*, *Azadirachta Indica Bark Carbon (AIBC)* and *Commercial Activated Carbon (CAC)* have been carried out with an aim to obtain data for treating industrial effluents from textile, leather and dye manufacturing industries. The effect of various process parameters has been investigated by the following batch adsorption technique at $30 \pm 1^\circ\text{C}$. Adsorption data are modeled with adsorption isotherms, the first order kinetics equations proposed by Natarajan-Khalaf, Lagerghan, Bhattacharya-Venkobachar and intra-particle diffusion an one of the rate determining steps. It is also reported to have been confirmed by SEM photos and FT-IR spectra, before and after adsorption.

Key words: Adsorption, Chromotrope, low cost activated carbons and commercial activated carbon – adsorption isotherms - first order kinetic equations.



7.45 Convenient ytterbium triflate catalyzed one-pot multicomponent synthesis of spiro[indoline-3,4'-pyrano[2,3-c]pyrazole]

Aishwarya Venkateswaran¹, Muthuraja Perumal¹, Prakash Sengodu¹, and Manisankar Paramasivam^{1*}

¹ Department of Industrial Chemistry, Alagappa University, Karaikudi-630006, India.

*Email: manisankarp@alagappauniversity.ac.in

Abstract

We have synthesized a set of multi-substituted spiro[indoline-3,4'-pyrano[2,3-c]pyrazole] from 5-chloroisatin, substituted phenyl hydrazines, 2-chloroacetonitrile/2-bromoacetonitrile/2-hydroxy-1,4-naphthaquinone and ethyl acetoacetate in the presence of ytterbium triflate as catalyst in one-pot four component method at room temperature. Green synthetic methodology was adopted for the using green solvent ethanol, low temperature and easy work up which resulted in higher atom economy. The synthesized compounds were confirmed by FT-IR, 1D and 2D NMR spectroscopic techniques.

Key words; Multicomponent synthesis, Spiro-Indole, Lewis acid catalyst, atom-economy, Green synthesis

7.46 Environmentally Benign Copper Triflate Mediated One Pot Multicomponent Synthesis of Benzo[g]chromenes Possessing Potent Anticancer Activity

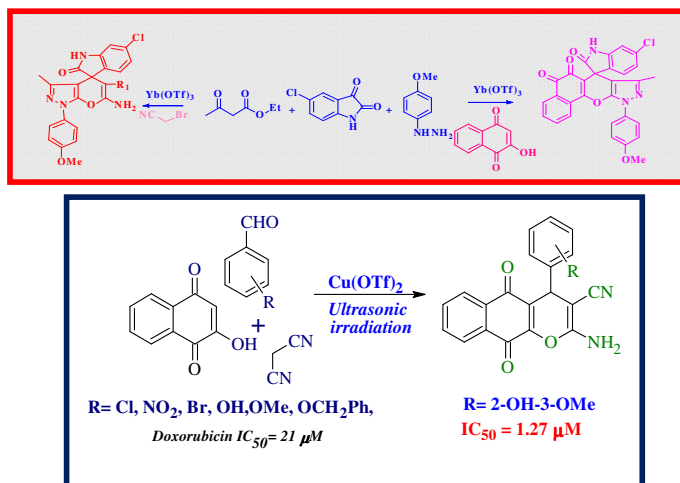
D.Umamaheswari², D.Nandhini², P. Muthuraja¹, S. Prakash¹, S.Chitra², P. Manisankar^{1*}

¹ Department of Industrial Chemistry, Alagappa University, Karaikudi-630006, India.

²Department of Organic Chemistry, Alagappa Government College, Karaikudi-630006, India.

*Email: manisankarp@alagappauniversity.ac.in

Graphical abstract



Abstract

An efficient one pot multi component synthesis of highly functionalized 5,10-dihydro-4H-benzo[g]chromenes-3-caronitrile derivatives from 2-hydroxy-1,4-naphthoquinone, aromatic aldehyde and malonitrile in the presence of Cu(OTf)₂ catalyst and eco friendly PEG solvent was carried out under ultrasonication. The reaction was completed within 10 minutes and resulted in good yield. The synthesized compounds were tested for their in-vitro anticancer activity against cervical cancer cell line (HeLa). Nine out of ten compounds showed potent antitumor activity better than that of doxorubicin. The compound 4h displayed highest activity among the test compounds and doxorubicin with IC₅₀ equal to 1.27 μM.

Keywords: benzo[g]chromene, anticancer activity, ultrasonication, multicomponent one pot synthesis



7.47 Bi-polymer based ZnO hybrid composite for better optical and thermal properties

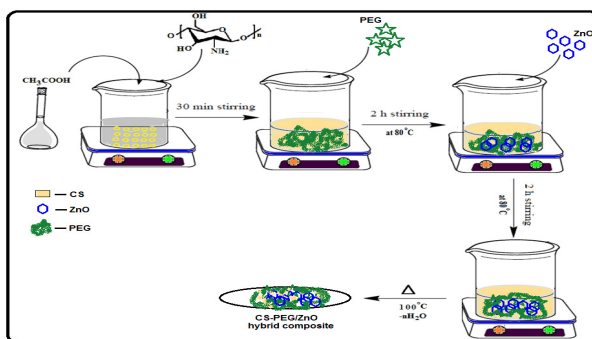
S.Rajaboopathi, S.Thambidurai*

*Department of industrial chemistry, school of chemical sciences,
Alagappa university, Karaikudi - 630003, Tamil nadu, India.
Email:siva.raja2389@gmail.com*

Abstract

In the present study, bi-polymer based ZnO composite can be synthesized by simple chemical precipitation method, chitosan was taken as a biosurfactant and polyethylene glycol was as a stabilizer. The functional groups of resultant component from chitosan, PEG and metal oxide were characterized and confirmed by FTIR and UV-Visible spectroscopy. The crystallite size was confirmed by X-ray diffraction analysis (XRD). The optical activity of the composites was tested by using absorbance and transmittance spectra. The ZnO particle intercalated on chitosan-PEG composite thermal characteristics was analyzed by TG-DTA, the enhanced thermal stability of ZnO based intercalated CS-PEG has higher stability than chitosan. The results demonstrate that ZnO intercalated chitosan-PEG matrix has reinforced effect compared to among the other three components. Therefore, ZnO intercalated bi-polymer based matrix may be promising materials for optically active sensors applications.

Key words: Chitosan, Zinc oxide, PEG, thermal stability, optical property



References:

- [1] L. Al-Naamani, S. Dobretsov, J. Dutta, J. Grant Burgess, Chemosphere. 168 (2017) 408-417.
- [2] P. Nagarajan, V. Rajagopalan, Advanced Materials. 9 (2008) 035004-035012.
- [3] A. G. Yavuz, A. Uygun, H. K. Uygun, Carbohydrate Research. 346 (2011) 2063-2069.
- [4] S. Azizi, A. Mansor, B. Ahamed, F. Namvar, Materials Letters, 116 (2014) 275-277.
- [5] J. B.Cui, Zinc oxide nanowire, Materials Characterizations, 64 (2012) 43-52.

7.48 Synthesis and characterization of new ionic liquid crystals exhibiting chiral mesophases

R.Mangaiyarjkarasi and S.Umadevi *

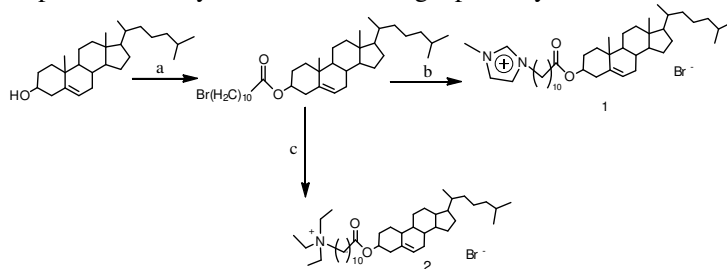
*Department of Industrial Chemistry, Alagappa University, Karaikudi -3, Tamil Nadu, India.
E-mail: mangairajkumarchem@gmail.com and umadevilc@gmail.com*

Ionic liquid crystal (ILCs) are fascinating candidates for a wide variety of applications in areas such as sensors, energy storage devices, luminescent material for displays, anisotropic hole transport layer, optoelectronic devices and so forth because of their unique features such as high solubility in polar solvents, strong interfacial dipoles from the ionic moieties, possibility of ionic and electronic migration under an applied electric field, and strong molecular aggregation behaviour due to the electrostatic interactions[1]. ILCs form mesophases through various non-covalent interactions and may exhibit properties such as macroscopic orientation, ionic conductivity, and the transportation of charges in liquid crystalline phases [2].



Up to date several ILCs exhibiting different mesophase structures namely, hexagonal, cubic, SmA (lamellar) phases have been reported and their ionic conductivity properties have been investigated in detail.[3,4,5] However, ILCs which exhibit chiral mesophases are limited in number.

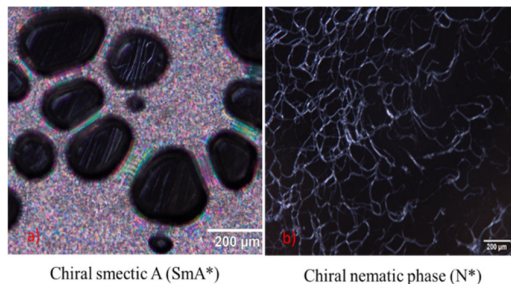
Herein, we describe the synthesis and characterization of two new calamitic (rod-like) ILCs consists of a chiral cholesterol moiety and a terminal imidazolium cation and a triethylammonium cation. These compounds were synthesized following a pathway shown in scheme 1



Reagents and conditions: a) 11-bromoundecanoic acid, 4-dimethylaminopyridine, N,N' -disopropylcarbodiimide, dichloromethane, room temperature; (b) 1-methylimidazole, toluene, 80 °C; (c) triethylamine, toluene, 80 °C.

Scheme 1: Synthetic path way for the calamitic ionic liquid crystal **1** and **2**

These new ILCs are chemically characterized through infrared (IR), nuclear magnetic resonance spectroscopy (NMR) techniques and mesophase behaviour was studied using polarizing optical microscopy (POM), differential scanning calorimetry (DSC) and X-ray diffraction studies (XRD). Compound **1** displayed a high temperature chiral nematic phase (N^*) and a low temperature chiral smectic A (SmA^*) phase where as compound **2** exhibited a chiral smectic A phase.



Chiral smectic A (SmA^*)

Chiral nematic phase (N^*)

References

- [1] K. Binnemans, *Chem. Rev.* **105** (2005) 4148.
- [2] K. V. Axenov, *Materials.* **4** (2011) 206.
- [3] M. Yoshio, T. Mukai, H. Ohno, T. Kato, *J. Am. Chem. Soc.* **9** (2004) 995.
- [4] T. Ichikawa, M. Yoshio, T. Mukai, H. Ohno, T. Kato, *J. Am. Chem. Soc.* **125** (2007) 10663.
- [5] J. Sakuda, M. Yoshio, T. Ichikawa, H. Ohno, T. Kato, *New. J. Chem.* **39** (2015) 4471.



7.50 SYNTHESIS, CHARACTERIZATION OF BENZIMIDAZOLE (WITH ISOINDOLINE) DERIVATIVES BY LEUCKART REACTION AND THEIR ANTIMICROBIAL ACTIVITY

Ashokkumar.N, Umarani.G, Abdul Hassan sathali.A,

*Department of pharmaceutical chemistry, College of Pharmacy, Madurai Medical College, Madurai.
ashokkumarpharmacist333@gmail.com*

INTRODUCTION:

A series of benzimidazole (with isoindoline) derivatives were synthesized and evaluated for their antimicrobial activities. The structures of synthesized compounds were confirmed on the basis of their spectral data. Many of benzimidazole derivatives were found variety of pharmacological activities especially compounds bearing isoindoline derivatives showed better antimicrobial activity than those bearing the oxygen atom. Therefore in the present review the chemistry of different derivatives of substituted benzimidazole and some of the important methodology (leuckart reaction) used for the synthesis has been reported.

OBJECTIVES:

To synthesis benzimidazole (with isoindoline) derivatives by leuckart reaction with microwave irradiation. It involves three steps,

Synthesis of (1, 3-dioxo-1, 3-dihydro-2 H-isoindol-2-yl) alkyl acid.

synthesis of 2-(1H-benzimidazol-2-yl alkyl)-1H-isoindole-1,3(2H)-dione

Synthesis of 2-{(1-(4-diaryl)-1H benzimidazol-2yl)-1H isoindole-1, 3(2H) Dione.

METHODOLOGY:

STEP 1: SYNTHESIS OF 2-GLYCYL ISOINDOLE-1,3 DIONE:

Preparation of 2-glycyl isoindole-1, 3 Dione from phthalic anhydride and glycine.

Synthesis of (1, 3-dioxo-1, 3-dihydro-2H-isoindol-2-yl) acetic acid from 2-benzofuran-1, 3-dione react with amino acetic acid.

STEP 2: Synthesis of 2-methyl benzimidazolyl-isoindole-1,3-dione

Orthophenylene diamine react with (1, 3-dioxo-1, 3-dihydro-2H isoindole-2-yl) acetic acid.

Synthesis of 2-(1-H-benzimidazol-2yl methyl)-1H-isoindole-1, 3(2H)-Dione

(1, 3-dioxo-1, 3-dihydro-2H isoindole-2-yl) acetic acid react with benzene 1, 3-diamine reflux for 2hours with removal of water molecule.

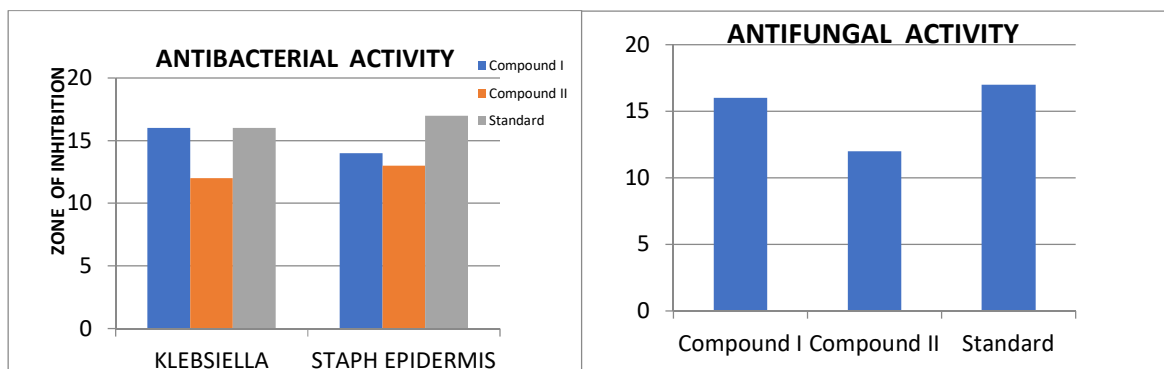
STEP 3: Synthesis of 2-{(1-benzhdryl-1H-benzo(d)imidazol-2-yl)methyl}isoindoline 1,3-dione.

Benzophenone react with 2-(1H-BENZIMIDAZOL-2YL METHYL)-1H-isoindole-1, 3(2H)-Dione and formic acid by leuckart reaction with help of microwave irradiation and removal of water and carbon dioxide.

COMPOUND-2:

Synthesis of 2-{(1phenylethyl-1H-benzo(d)imidazol-2-yl)methyl}isoindoline 1,3-dione
Acetophenone react with 2-(1H-BENZIMIDAZOL-2YL METHYL)-1H-isoindole-1,3(2H)-dione and formic acid by leuckart reaction with help of microwave irradiation and removal of water and carbon dioxide.





CONCLUSION:

The synthesis benzimidazole with isoindoline derivatives leuckart reaction is done by micro wave irradiation.

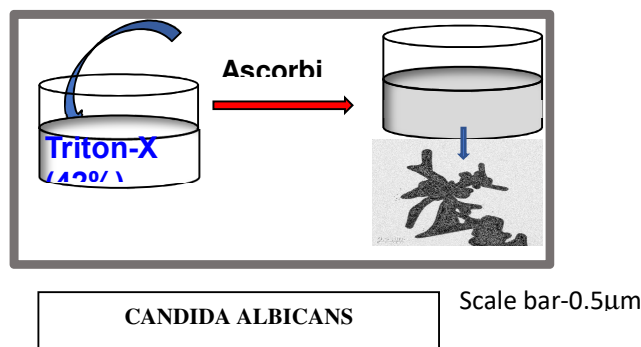
The antimicrobial activity was performed against klebsiella pneumonia, staphylococcus epidermis, and candida albicans. The zone of inhibition was performed by cup-plate method.

7.51 SILVER MICROPARTICLES STABILIZED IN A LYOTROPIC LIQUID CRYSTAL MEDIUM

K. Mohana, PR. Meyyathal and S. Umadevi*

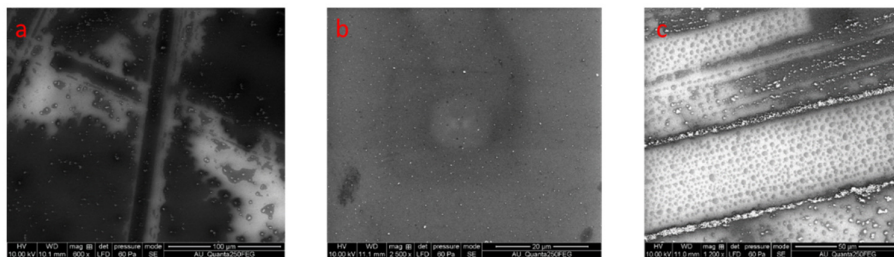
*Department of Industrial Chemistry, Alagappa University, Karaikudi, Tamilnadu, India.
E-mail: umadevilc@gmail.com and mohanakaruppiah16@gmail.com*

Herein, we describe a simple facile method for the synthesis of silver microparticles in a hexagonal mesophase of a lyotropic liquid crystal (LLC) medium at room temperature. LLC are interesting class of LC compounds which are formed by mixing an amphiphilic compound, generally a surfactant and water at a particular concentration. These phases display remarkable properties such as long range order and mobility at the nanoscale level which offer potential platform for the controlled syntheses and organization of nano materials. A binary mixture of water (58 wt%) and non-ionic surfactant triton X-100 (42 wt%) exhibits a hexagonal phase at room temperature. Silver particles were prepared in this medium by reducing different concentration of silver nitrate (10mM, 50mM, 100mM) using a mild reducing agent ascorbic acid (20mM) without the aid of any external stabilizing agents.



The LC template acted as a directing agent for the growth of microparticles. In addition, the template also provided necessary stabilization for the formed particles by preventing them from aggregation. The silver particles were characterized using UV-Vis spectroscopy, transmission electron microscopy and scanning electron microscopy. The above described method of micro particle synthesis is simple, one pot preparation and more importantly a green approach since it does not involve any organic solvents or hazardous chemicals.





SEM images of silver nano particles in hexagonal phase a) 10mM of AgNO₃ b) 50mM of AgNO₃ c) 100mM of AgNO₃

Reference :

- [1] S. Saliba, C. Mingotaud, M.L. Kahn and J. Marty, *Nanoscale*5(2013) 6641.
- [2] S.Umadevi, H.C. Lee, V.Ganesh, X.Feng and T.Hegmann, *Liq crystal*.41(2014)265

7.52 Fabrication of Graphene Oxide/ β -Cyclodextrin Composite and their application in the removal of Direct Red 7 dye

G.Sumathi and H. Gurumallesh Prabu*

Department of Industrial Chemistry, School of Chemical Sciences, Alagappa University, Karaikudi -630 003, India
*E-Mail: hgprabu2010@gmail.com Tel.: +919443882946; Fax: +91 4565225202

Abstract

The aromatic structure of the dyes makes them highly toxic, non-biodegradable. It is essential to remove dyes to permissible levels before being discharged to water bodies. Among different technologies, adsorption is considered as globally accepted method due to its wide range of applicability and economically feasibility. Recently, Graphene Oxide has been used as an adsorbent for water treatment. Cyclodextrin, the cyclic fermentation product of starch, capable of specific interactions with several molecules, play an important role in wastewater treatment. In this study, Grapheneoxide/ β -Cyclodextrin composite was prepared by hydrothermal method and used as an adsorbent for the removal of Direct Red 7 dye. Fabrication was achieved through two steps. (1) synthesis of graphene oxide by hummer's method (2) loading of β -Cyclodextrin. Characterization was performed by Fourier transmission infrared spectroscopy, X-ray diffraction, Scanning and transmission electron microscopy. FTIR studies showed the O-H stretching vibration adsorption band at 3450 cm⁻¹, C=C stretching mode at 1600cm⁻¹, bands at 1735 cm⁻¹ and 1379 cm⁻¹ as stretching vibrations peaks of carboxyl and carbonyl groups. The bands of epoxy groups were obtained at 1065 cm⁻¹. Equilibrium experiments were also performed, studying the effect of contact time and temperature. The results showed that the kinetic data followed a pseudo-second order model and equilibrium data were well fitted by Langmuir model.

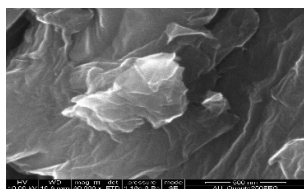


Figure 1. SEM IMAGE -GO

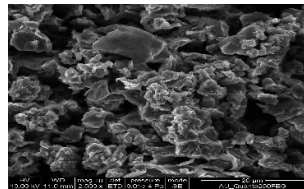


Figure 2. SEM IMAGE -GO/CD Composite

Key words: Graphene Oxide, Cyclodextrin, Direct red 7, waste water, Adsorption.



7.53 SYNTHESIS OF CARBONATE DOPED TiO₂ SUBMICROSPHERES FOR FABRICATION OF PHOTOVOLTAIC SOLAR CELL.

E. Murugan^{a,b,*}, S. Govindaraju^a

^aDepartment of Material Science, School of Chemical Sciences, University of Madras, Guindy Campus, Chennai – 600 025, India.

^bDepartment of Physical Chemistry, School of Chemical Sciences, University of Madras, Guindy Campus, Chennai – 600 025, India.

E-mail: murugan_e68@yahoo.com, dr.e.murugan@gmail.com

ABSTRACT

The present investigation reports a simple and effective strategy to synthesize TiO₂ microspheres via solvothermal method. Further, the prepared TiO₂ microspheres were doped with carbonate and studied for fabrication of dye sensitized solar cells (DSSC). The structural properties of TiO₂ and carbonate doped TiO₂ were studied using XRD. The XRD data suggest that doping of carbonate results in the reduction of particle size and also leads to phase transformation from anatase to the more stable rutile. Also, the purity of the samples in addition to the phase transformation due to the incorporation of carbonate was confirmed with Raman spectroscopy. The optical properties were determined using DRS-UV-Vis spectroscopy. Further, the morphological studies performed using SEM/EDAX and FESEM shows the TiO₂ microspheres are mesoporous in nature and carbonate doped TiO₂ sub microspheres are observed to have reduced size with uniform distribution of particles. Hence, the fabrication of carbonate doped TiO₂ sub microspheres has wide scope for conversion of light energy to electrical energy and employed for real time applications in environment and industry.

7.54 PHOTOCATALYTIC DEGRADATION OF METHYLENE BLUE DYE USING TiO₂ NANOMATERIALS

K. Santhi^a, S. Karuppuchamy^b and C. Rani^{a,*}

^aDepartment of Chemistry, Alagappa Govt. Arts College, Karaikudi, Tamil Nadu-630 003, India

^bDepartment of Energy Science, Alagappa University, Karaikudi, Tamil Nadu-630 003, India

E-mail: viswanathanrani@gmail.com

Abstract

TiO₂ nanomaterial was prepared by solution growth technique and subsequently characterization was carried out using advanced techniques. The photocatalytic activity of TiO₂ nanomaterial was studied by degrading methylene blue dye.

Introduction

Photocatalytic degradation processes using nanomaterials have been attracted as an alternative method for degradation of organic pollutants in wastewater. Among the nanophotocatalyst, TiO₂ is one of the most attractive and promising candidates for several industrial applications due to its several intriguing properties. The present work deals with the preparation and characterization of TiO₂ nanomaterials using simple solution growth technique and photocatalytic activity of the TiO₂ nanomaterial was also studied.

Experimental setup

1 g of titanium isopropoxide was dissolved in a mixture of 50 ml ethanol and 50 ml distilled water and stirred for 1 hour using magnetic stirrer to get clear solution. Then 0.1 g PEG was added into the above precursor solution and then stirred for 1 hour to get white colour precipitate. It was then washed with distilled water for 5 to 6 times to remove impurities. The precipitate was dried in hot air oven to get white colour precipitate. The dried precipitate was calcined at 300°C and 400°C for 2 hours. The photocatalytic activity of TiO₂ nanomaterial was studied. Photocatalytic degradation experiment was carried out in the 200 ml capacity photo-reactor (UV Photo Reactor System HEBER model: HP-SL254) and decomposition of methylene blue dye was recorded using UV-vis spectrophotometer.



Results and Discussion

Fig. 1 shows the X-ray diffraction pattern of the prepared samples and it shows the formation of anatase TiO₂ nanomaterial. The average crystallite size of TiO₂ sample (heat-treated at 400oC) is 17.19 nm. The photocatalytic activity of TiO₂ nanomaterial (0.1 g) was studied using decomposition of methylene blue dye (10 mg/l). The higher colour removal efficiency (75.5 %) was achieved using 400oC calcined photocatalyst within 180 min. Fig. 2 shows the UV-Vis spectra of methylene blue dye (665 nm) in the presence of 400oC calcined sample under UV light.

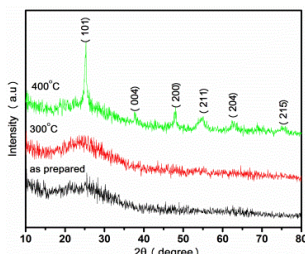


Fig. 1. XRD patterns of TiO₂ samples as-prepared and calcined at 300oC and 400oC for 2 h

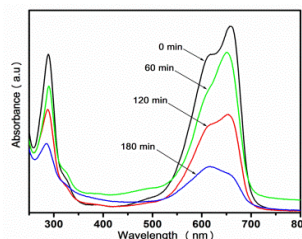


Fig. 2. UV-visible spectra of methylene blue in presence of 400°C calcined sample TiO₂ under UV light irradiation

Conclusions

Photocatalytic activity of synthesized TiO₂ nanomaterials was studied by decomposition of the methylene blue dye under UV light irradiation. The maximum colour removal efficiency of 75.5 % was achieved within 180 minutes with the addition of 0.1g sample calcined at 400oC photocatalyst.

References

- [1] K. Santhi, P. Manikandan, C. Rani, and S. Karuppuchamy, *Applied Nanoscience*, 5 (2015) 373-378.

7.55 Bifunctional Biological Active Antibiofilm and Osteoblast Adhesion Efficacy from MWCNT/PPy/Pd nanocomposite

Murugesan Balaji, Sonamuthu Jegatheeswaran, Pandiyan Nithya, and Mahalingam Sundrarajan*

Advanced Green Chemistry Lab, Department of Industrial Chemistry, School of Chemical Sciences, Alagappa University, Karaikudi - 630 003, Tamil Nadu, India.

Email: panchamuruges@gmail.com; drmsgreenchemistrylab@gmail.com

Abstract

Multifunctional biologically active materials have approached for antibiofilm, anticancer and osteoblast adhesion activities with significant biomedical applications, owing to this MWCNT modified with polypyrrole (PPy) matrix with the incorporation of palladium nanoparticles (NPs). The synthesized composite displays a tube-shaped morphology with highly dispersed crystalline Pd NPs, which are established through XRD, SEM, TEM and SAED studies. An amine linkage at 400.3 eV and an imine linkage at 398.8 eV in XPS spectra evidenced the interaction of PPy with Pd and MWCNT. Polymer stretching frequencies in FTIR and Raman spectroscopy proves successful formation of PPy and the Pd-N (1609 cm⁻¹) interaction. In the stability aspect, it is up to 58.73 % mass withstood at 800 °C in TGA analysis. The composite exhibits an efficient Anti-biofilm against a set of bacterial stain with planktonic cell growth. In vitro cytotoxicity of Vero line assesses the composites toxicity up to 100µg. The outcome of cell adhesions showed that human osteosarcoma cells (HOS) can adhere and to develop on the MWCNT/PPy/Pd composites. Furthermore, the proliferation of cells on MWCNT/PPy/Pd composites was also proved the biocompatibility of the composites against HOS cells. These results suggest that Pd-doped MWCNT/PPy composites are promising materials for biomedical applications.



Conformation Analysis

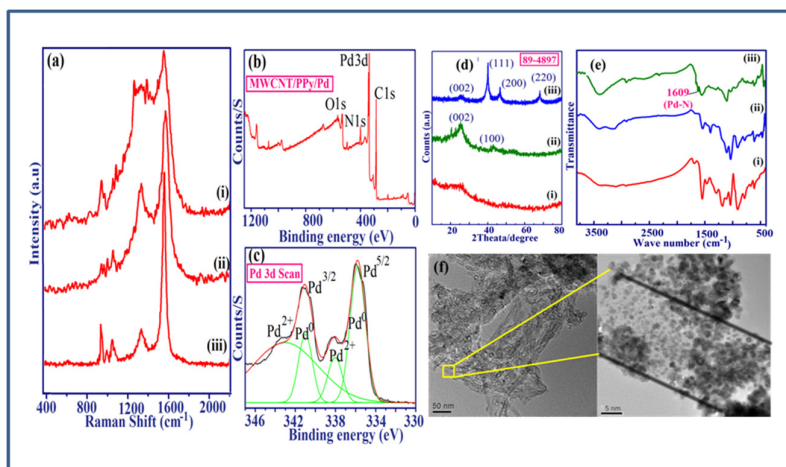


Figure 1. (a) Raman Spectral of PPy(i), MWCNT/PPy (ii), MWCNT/PPy/Pd (iii); (b) XPS spectra of MWCNT/PPy/Pd; (c) XPS of Pd scan in MWCNT/PPy/Pd composite; (d) XRD pattern; (e) FTIR spectra of PPy(i), MWCNT/PPy(ii), and MWCNT/PPy/Pd(iii); TEM images of MWCNT/PPy/Pd at 50nm (b) and 5nm

References

- [1] S. Koyal, R.V. Ramanujan, Doxorubicin loaded PVA coated iron oxide nanoparticles for targeted drug delivery, Mater. Sci. Eng. C. 30 (2010) 484–490.
- [2] H. Yang, S. Y. Fung, M. Liu, Programming the Cellular Uptake of Physiologically Stable Peptide–Gold Nanoparticle Hybrids with Single Amino Acids, Angew. Chem. 50 (2011) 9643–46
- [3] D. A. Gewirtz, M. L. Bristol, J. C. Yalowich, Toxicity issues in cancer drug development, Curr. Opin. Invest. Drugs. 11 (2010) 612–614.
- [4] J. Z. Du, X. J. Du, C. Q. Mao, J. Wang, Tailor-made dual pH-sensitive polymer-doxorubicin nanoparticles for efficient anticancer drug delivery, Am. Chem. Soc. 133 [2011] 17560–17563.

7.56 Silica-coated Magnetic Nanoparticles Supported Heteropoly Acid composites catalyzed an efficient conversion of nitrile from aldehyde

A. Sangili^a, S. Jegatheeswaran, S. Ambika, K. Bama, M. Balaji, P. Nithiya, R. Sumathi, M. Abdul Kadir^b and M. Sundrarajan^{a*}

^aAdvanced Green Chemistry Lab, Department of Industrial Chemistry, School of Chemical Sciences, Alagappa University, Karaikudi -3, Tamil Nadu, India.

^bDepartment of chemistry M.S.S. Wakf Board College, K.K. Nagar, Madurai, Tamil Nadu, India.

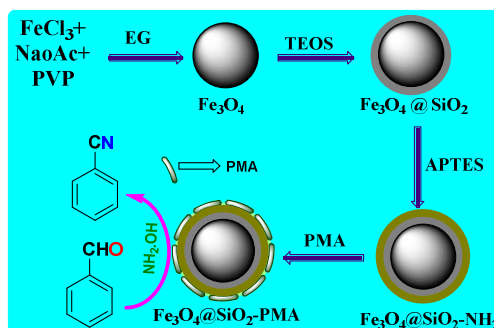
*Corresponding author: Tel: +91 94444 96151

E-mail address: drmsgreenchemistrylab@gmail.com and sangili10492@gmail.com

Abstract

An efficient synthesis of silica coated magnetite nanoparticles (Fe₃O₄ @ SiO₂) supported phosphomolybdic acid (Fe₃O₄ @ SiO₂-NH₂-PMA MNPs) was prepared by hydrothermal method. The preparation of Fe₃O₄ @ SiO₂-NH₂-PMA MNPs with aminopropyltrimethoxysilane (APTS) linker supported surface modified onto the heteropoly acid of PMA. The synthesized magnetic nanocomposites was fully characterized by X-ray diffraction (XRD), Fourier transform infrared spectroscopy (FT-IR), Scanning electron microscopy with Energy-dispersive X-ray spectroscopy (SEM with EDX), and Ultra-violet diffuse reflectance mode spectroscopy (UV-DRS)



Figure 1. Scheme, synthesis of Fe₃O₄ @ SiO₂-NH₂-PMA MNPs and application

All elements and functional groups were presented in the FT-IR and element analysis. The spherical shape and size between around 250 to 280 nm of synthesized magnetic nanocomposite were confirmed by SEM analysis, and which indicates the successful immobilization of Fe₃O₄ @ SiO₂-NH₂-PMA MNPs were confirmed by UV-Vis spectroscopy.

Fe₃O₄ @ SiO₂-NH₂-PMA MNPs catalysts have been applied for an efficient and selective conversion one-pot synthesis of nitrile directly from aldehyde compounds. The present investigation describes the synthesis of nitriles from aldehyde and hydroxylamine hydrochloride in the presence of magnetic nanocomposite catalyst in DMF under reflux condition. The catalyst could be reused by recycling, which avoids the necessity for a traditional filtration process.

Reference

- [1] M. Zhu, G. Diao, *J. Phys. Chem. C*, 115 (2011) 24743–24749.
- [2] M. Esmailpour, J. Javidi, F. N. Dodeji. *RSC Adv.*, 5 (2015) 308-315.

7.57 Alignment of liquid crystal on a flexible polymer substrate

B. Sivaranjini^a, V. Ganesh^b and S. Umadevi^{a,*}

^aDepartment of Industrial Chemistry, Alagappa University, Karaikudi-630 002

^bElectrodics and Electrocatalysis Division (EEC), Central Electrochemical Research Institute (CSIR-CECRI), Karaikudi-630 006

E-mail: sivaranjini93alu@gmail.com, ganelectro@gmail.com and umadevilc@gmail.com

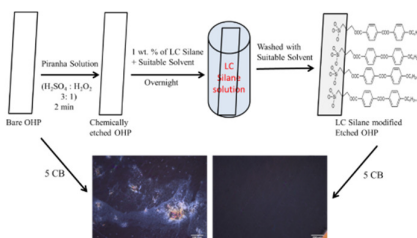
Liquid Crystals (LCs) are self-assembled soft material with a huge potential for application in a wide variety of field such as sensing, biomedical, photonics, optoelectronics, electronic conductors, photovoltaics etc. apart from their significant use in display technology. [1,2] For majority of these LC applications, a pre-oriented well aligned sample of LC on a suitable substrate is highly crucial. The conventional methods existing so far for the alignment of LCs are effective in orienting the mesophase such as nematic, smectic only and are not efficient over a long period of time. Therefore, there is a significant need for formulating simple strategies for effective alignment of these materials on different substrates. An alignment layer made of molecules with a similar shape, i.e., LC molecules itself will provide necessary shape and symmetry compatibility for the bulk LC sample to be aligned. In view of this, we are forming the self-assembled monolayers (SAMs) of tailor-made LC molecules on various substrates and investigating the alignment abilities of these films to orient the bulk LC sample.

Herein, we present the preparation of SAM of a rod-like thermotropic LC compound on a flexible, transparent overhead projector (OHP) substrate and characterization of the modified substrate through Infrared (IR), Contact Angle (CA) and Atomic Force Microscopy (AFM) studies. Further, our preliminary results on versatility of these LC crystal modified substrates for the alignment of bulk LC sample are also presented



Scheme: Graphical representation of methodology followed for the surface functionalization of OHP sheet with a LC molecule and polarizing optical microscopy images depicting alignment of a room temperature LC, 5CB on a bare (left) and modified (right) OHP

Keywords: self-assemble monolayer, liquid crystals, polymer substrate



References

- [1] M. Bremer, P. Kirsch, M. Klasen-Memmer, K. Tarumi, *Angew. Chem. Int. Ed.*, 2013, **52**, 8880, and references therein
- [2] A. M. Lowe, N. L. Abbott, *Chem. Mater.*, 2012, **24**, 746; *Liq. Cryst.*, 2013, **1**, 29.

7.58 *In silico* docking studies of anti-diabetic and breast cancer activity by N'-(1-benzylpiperidin-4-ylidene)-2-cyanoacetohydrazide

K.Tharini,* S.Umamatheswari and K.Sundaresan

Dept of Chemistry, Govt Arts College, Trichy-22

Abstract

In this study, to predict the activity of our synthesized compounds N'-(1-benzylpiperidin-4-ylidene)-2-cyanoacetohydrazide using *in silico* approaches by molecular docking. Molecular docking was utilized to prove that similar compounds can bind to receptor protein treatment of breast cancer using *in silico* approach. In our present study, *in silico* molecular docking studies were carried out using BIOVIA Discovery Studio (DS) 2017 software. The standard drug N'-(1-benzylpiperidin-4-ylidene)-2-cyanoacetohydrazide Tamoxifen, Glibenclamide and N'-(1-benzylpiperidin-4-ylidene)-2-cyanoacetohydrazide were drawn in chemdraw software, subsequently energy minimized and saved in SDF file format for docking studies.

Computational ligand-target docking approach was used to analyze structural complexes of the 2YAT and 11R3 with Tamoxifen, Glibenclamide and N'-(1-benzylpiperidin-4-ylidene)-2-cyanoacetohydrazide (ligands) in order to understand the structural basis of this target proteins. Possible binding modes between the ligands and this target proteins were studied by CDOCKER (CHARMm-based DOCKER) protocol incorporated within DS. The algorithm offers full ligand flexibility and employs CHARMm force fields. Ligand binding affinity was calculated using CDOCKER energy, CDOCKER Interaction energy, Hydrogen bonds, binding energies, protein energy and ligand protein complex energy. The CDOCKER energy mentioned in negative values. More negative value energy indicated as higher binding affinity of the ligands with target protein.

In this study, the N'-(1-benzylpiperidin-4-ylidene)-2-cyanoacetohydrazide forms non-bonding interaction with active site of human estrogen receptor protein. This N'-(1-benzylpiperidin-4-ylidene)-2-cyanoacetohydrazide forms van der Waals interactions with amino acids Leu (346, 428, 384, 387, 525, 391), Met (388, 528), Phe 404, Ala 350, Gly 521 and Ile 424 in active site. The residue Glu 423 forms electrostatic interaction with synthesis N'-(1-benzylpiperidin-4-ylidene)-2-cyanoacetohydrazide (Figure 2A and B) The CDOCKER energy of N'-(1-benzylpiperidin-4-ylidene)-2-cyanoacetohydrazide in this protein is -27.8982 Kcal/Mole⁻¹. CDOCKER energy is a total calculation of electrostatic and van der Waals interaction of the N'-(1-benzylpiperidin-4-ylidene)-2-cyanoacetohydrazide in 2YAT.

The two aromatic ring in the N'-(1-benzylpiperidin-4-ylidene)-2-cyanoacetohydrazide forms more van der Waals interactions with hydrophobic residues.



7.60 *In silico* Docking studies of α -amylase inhibitory activity of Glycoalkaloids

Jannathul Firdhouse M^{*1}, Nirmala Devie T², Hajara Banu TM³, Christina Susan I⁴, and Saxthi Vinmathi K⁵

^{1,2}Department of Chemistry, ^{3,4&5}Department of Zoology, Lady Doak College Madurai-625002

*Corresponding author: kfirdhouse@gmail.com

Abstract

Alpha amylase (α -amylase), is an enzyme which catalyses the hydrolysis of starch to maltose and plays a pivotal role in *Diabetes mellitus* (DM). The inhibition of α -amylase may control the post-prandial hyperglycemia *via* retarding the digestion of starch in type-2 DM. The phytoconstituents present in the traditionally used therapeutic plants were screened for α -amylase through *insilico* docking analysis. Out of 11 compounds, nine were chosen as ligands based on the Lipinski rule of five. The selected ligands were docked with α -amylase complexed with acarbose (PDB ID: 3BC9) using Argus lab and One-click docking software. The docking scores obtained for protein-ligand interaction were compared with the standard drug (Metformin). The best docking pose energy results reveals that the compounds *viz.* Ellagic acid, Girinimbine, Koenidine, Magnoflorine and Vicine show better docking score than Metformin.

Key words: *Diabetes mellitus*; alpha amylase; receptor; ligand

Introduction

Diabetes mellitus (DM) is a metabolic disorder, characterized by persist hyperglycemic conditions with disturbance of carbohydrate, fat and protein metabolism due to inadequacy in insulin secretion by the beta cells of pancreas or insulin action. There are three types of diabetes mellitus *viz.* Type-1 (Insulin dependent DM), Type-2 (Insulin independent DM) and gestational DM (seen in pregnant women). According to the Indian Diabetic Federation, more than 100 million are likely to be victims of DM by 2030 [1,2]. In the present work, *in silico* docking studies for the phytoconstituents present in antidiabetic plants with the receptor (α -amylase) was carried out by Argus lab and one click docking software's. The binding energy of the docked structures was compared to that of the standard drugs (Metformin).

Materials and Methods

The crystal structure of protein receptor 3BC9 used in this study was retrieved from RCSB Protein Data Bank (<http://www.rcsb.org/pdb>). The PDB files were energy minimized using Argus Lab. Hydrogen was added and the protein was prepared as PDBQT in Argus Lab and was used further for docking studies. Ligands are selected compounds from traditional plants were: *s*-methyl cysteine sulfoxide, Diphenyl amine, Allin, 4-Hydroxyisoleucine, Vicine, Mahanine, Mahanimbine, Girinimbine, Koenidine, Magnoflorine, Betalamic acid, Rutin, Ellagic acid and Mahanimbine. The ID of the ligands was obtained from PubChem database. The docking was done with One-click docking software, which is online docking software. Optimization of the ligands was carried out in Argus Lab 4.0.

Results and Discussion

The docking scores of the selected ligands and standard drug, metformin with the receptor, alpha amylase were given in table 1. After obtaining the results of docking scores for the ligands, the score is compared with the docking score of Metformin, to check for better results of the compound for its anti-diabetic activity. The docking poses were obtained according to their docking parameters and corresponding binding pockets. The best docking pose energy results reveals that the compounds *viz.* Ellagic acid, Girinimbine, koenidine, Magnoflorine and vicine show better docking score than metformin (figure 1). The binding energy for the remaining compounds, alliin, betalamic acid, *S*-methyl cysteine sulfoxide and Diphenyl amine were similar to that of metformin (Table 1). The significant constituents in curry leaves, Heart leaf moonseed and bitter guard exhibit good docking score compared to all the other compounds.

The good docking score is from, the better docked poses of the ligand with the alpha amylase receptor.



studied by quantum chemical calculations using density functional theory (DFT) method with the B3LYP hybrid functional and 6-311+G(d,p) basis set. The energy value of the both structure reveals

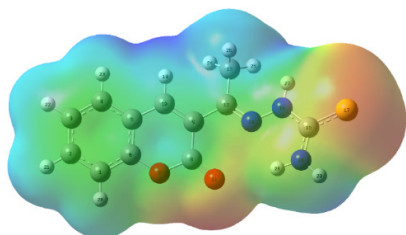


Fig 1: Molecular electrostatic potential surfaces of trans structure of CTC

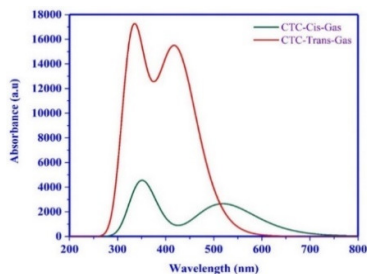


Fig 2: Electronic absorption spectra of cis and trans-CTC in gas and water phase

the trans structure of the molecule is the convenient structure than cis structure. The calculated NLO properties confirm that the NLO properties of trans structure of CTC is higher than the cis structure, and the chemical hardness of the trans structure is lower than the cis structure that shows that the reactivity and charge transfer of trans-CTC is higher than cis-CTC. The MEP maps of trans and cis structures of CTC illustrate that there are some possible region for electrophilic and nucleophilic reactivity. The calculated thermodynamic parameters are increasing with enhancing temperature. The vibrational frequencies of the two configurations of CTC demonstrate that both structures of CTC have practically comparable modes of vibrations, but the trans conformation of CTC is better in agreement with the experiment.

7.62 Structure and Electrochemical performance of $\text{LiV}_x\text{Mn}_{2-x}\text{O}_4$ ($0 \leq x \leq 0.20$) cathode materials for rechargeable lithium ion batteries

P. Mohan^a and G. Paruthimal Kalaignan^b

^aDepartment of Chemistry, Sree Sevugan Annamalai College, Devakottai-630 303.

^bAdvanced Lithium-ion Battery Research Lab, Department of Industrial Chemistry, Alagappa University, Karaikudi – 630 003, India
Email: pmohanic@gmail.com

In this work, the pristine LiMn_2O_4 and vanadium substituted $\text{LiV}_x\text{Mn}_{2-x}\text{O}_4$ ($x = 0.05, 0.10, 0.15$ and 0.20) positive electrode material were prepared by using the tartaric acid assisted sol-gel method. The structure and electrochemical properties of the prepared materials were characterized by using XRD, SEM, TEM and charge/discharge studies. The mechanisms of improving the electrochemical performances of the pristine LiMn_2O_4 and vanadium substituted $\text{LiV}_x\text{Mn}_{2-x}\text{O}_4$ cathode materials are discussed. X-ray powder diffraction analysis was changed in lattice parameters with increasing vanadium content suggesting the occupation of substituent within LiMn_2O_4 interlayer spacing. TEM and SEM analyses show that $\text{LiV}_{0.15}\text{Mn}_{1.85}\text{O}_4$ has smaller particle size and more regular morphological structure with narrow size distribution than those of LiMn_2O_4 . It is concluded that the structural stability and cycle life improvement were due to many factors like better crystallinity, smaller particle size and uniform distribution compared to LiMn_2O_4 cathode material. $\text{LiV}_{0.15}\text{Mn}_{1.85}\text{O}_4$ cathode material has improved the structural stability and excellent electrochemical performances of the rechargeable lithium-ion batteries.

Key words: Positive electrode materials, XRD, TEM, Charge/discharge



7.63 Synthesis of highly solar active $\text{Fe}_2(\text{MO}_4)_3$ nanocatalyst for the degradation of Rhodamine B

S.Tamilarasi^a, K.Balakrishnan^a, I.Muthuvel^b, B.Muralidharan^c

^aDepartment of Chemistry, A.V.V.M. Sri Pushpam College, Poondi, Thanjavur, Tamilnadu-613503, India.

^bDepartment of Chemistry, M.R.G College Mannarkudi.

^cBirla Institute of Technology & Science, Pilani, Dubai.

Corresponding author email: balki63@gmail.com and profmuthuvelchem@yahoo.com

ABSTRACT

The hetero-Fenton catalyst $\text{Fe}_2(\text{MO}_4)_3$ was prepared by simple co-precipitation method and it was characterized using X-ray diffraction (XRD), Fourier transform infrared spectroscopy (FTIR), UV-Vis diffuse reflectance spectroscopy (UV-Vis-DRS) Scanning electron microscopy (SEM) Energy dispersive X-ray spectroscopy (EDS), techniques. $\text{Fe}_2(\text{MO}_4)_3$ was used for Hetero-Fenton photocatalyst for the degradation of Rhodamine B under solar light. The effect various operational parameters like catalyst concentration, H_2O_2 dosage, initial pH initial solution concentration, reusability on photodegradation were investigated and the optimum conditions are reported.

Keywords: Heterogenous photo – Fenton, co- precipitation, Rhodamine B, solar light

7.64 Multistep synthesis of Newer 3'-(2-methoxyphenyl)-1'H-spiro[piperidine-4,2'-quinazolin]-4'(3'H)-one derivatives and their biological evaluation

V.Veeramani^a, P. Sathyaseelan^b, P.Muthuraja^c, P.Manisankar^{c*}

^aSynthetic Organic Chemistry, Syngene international private limited, Biocon, Bangalore,

^bDepartment of Chemistry, Bishop Heber College, Trichy

^cDepartment of Industrial Chemistry, Alagappa University, Karaikudi – 630 003 Tamilnadu India.

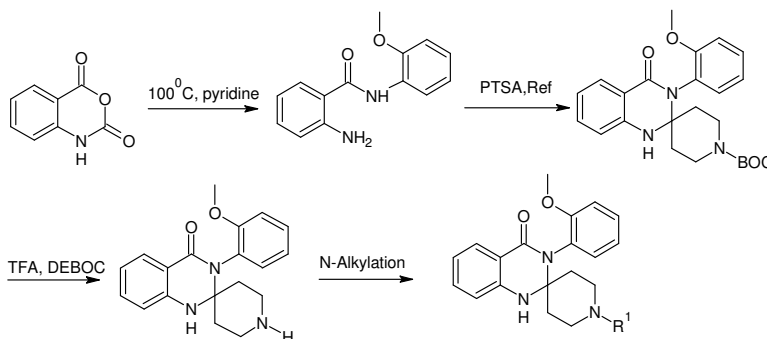
Phone: +91 4565 228836; Fax: +91 4565 225202

*Corresponding Author E-mail: pms11@rediffmail.com, pmuthuraja.chem@gmail.com

Abstract

In present study, ten new scaffolds of 3'-(2-methoxyphenyl)-1'H-spiro [piperidine-4, 2'-quinazolin]-4'(3'H)-one functionalized with different aryl/alkyl halides were synthesized and computationally evaluated using cheminformatics tools. Newer Spiro piperidine derivatives obeyed Lipinski's rule of five with good biological activity. Three targets among ten showed lesser drug likeness and drug score values compared to other Spiro piperidine derivatives using OSIRIS property explorer. Except these three derivatives, all other synthesized targets act as drugs.

Keywords: Spiro piperidine derivatives, cheminformatics tools, OSIRIS Property Explorer



7.65 Understanding the fundamental concepts on Electrochemiluminescence (ECL) and its significance in applied aspects

S. SenthilKumar

*Electrodeics and Electrocatalysis Division, CSIR-Central Electrochemical Research Institute, Karaikudi-630006, TamilNadu
E-mail: senthilmugam@gmail.com*

Electrochemiluminescence (ECL) also called as Electrogenerated chemiluminescence, is a highly sensitive process in which electrochemically generated reactive intermediates combines to undergo high-energetic electron-transfer reactions to form excited states, which emit light without applying any external source of light. Although this phenomenon of light emission was observed during electrolysis in late 1920, the first detailed ECL studies were reported by Hercules and Bard et al. in the mid-1960. Generally, Generation of ECL emission always follows primarily via two reaction mechanisms such as (1) annihilation and (2) co-reactants. Each of these mechanisms offers different advantages and relies on different pathways to generate the excited state at electrode interface that ultimately emits light. In annihilation mechanism, the reduced and oxidized species are both generated in the vicinity of the electrode surface by wide range potential sweep. The co-reactant ECL is usually generated by the reaction between the luminophore species and an additionally added assistant reagent (co-reactant) by one directional potential scanning (either anode or cathode direction). The use of co-reactant can produce more intense ECL emission than annihilation reaction. ECL with co-reactant produces highly intense signals in both aqueous and non-aqueous solutions because it needs a narrow potential window to generate stable reactive intermediates for annihilation between oxidized and reduced species. All commercially available ECL analytical instruments are based on this pathway. According to the generated intermediates and the polarity of the applied potential, the corresponding ‘‘co-reactant ECL’’ can be classified as ‘‘oxidative-reduction’’ and ‘‘reductive-oxidation’’ –ECL. The energy required to generate an excited molecule can be calculated using enthalpy factor (ΔH). The required energy to obtain an excited state molecule should be equal or greater than 2.1 eV.

$$\Delta H = \Delta G + T\Delta S = (E_{R^+/R}^0 - E_{R^-/R}^0) - 0.1 \text{ eV}$$

Using this kind of unique ECL technique offers a grand avenue to understanding the fundamental properties like physicochemical and electrical properties of organic molecules, semiconducting nanostructured materials, quantum dots, metal clusters etc. Also, this ECL emission could be used in the estimation of biologically important molecules especially at the single molecular level by either selective quenching or enhancing ECL signal.

7.66 Probing the significance of cooperative and fluxional effects in clusters and phospholipids through Ab-initio molecular dynamical simulations

Sailaja Krishnamurthy

CSIR-Central Electrochemical Research Institute, Karaikudi - 630 006

Abstract

Finite temperature behavior or response of material and biological systems has been successfully explored by classical molecular dynamics methodology in the past as well as present. On the other hand, application of ab initio molecular dynamics methodology to catalytically relevant systems is computationally expensive and to biological systems is unthinkable. The present talk discusses application of ab initio based molecular dynamical simulations to some of the practically relevant materials such as nano sized catalysts and bio molecules. The ensuing surprises; contradictions and limitations are discussed in bearing with the experimental information available/experimental results. The talk ends with the scope of application of ab initio molecular dynamical simulations towards futuristic materials.



AUTHOR INDEX

Abdul hasansathali A		Balaji M	22,72,203	Ganesh V	204
	116,123,198	Balaji R	206	Gangaprasad D	51,164
Abdul Kadir M	5	Balakrishnan K	210	Gnanasundaram I	175
Abinaya S	69	Balalakshmi C	69	Gomathi A	5
Adaikalam Shylaja	94	Balamurugan Ramalingam	150	Gopi S	7
Aishwarya Venkateswaran	194	Balvider Kaur	78	Gopi Kalaiyarasan	94
Alwin David S	59	Bama K	128,203	Gopinath K	69
Amala Jothi Grace G	5	Bathula Rajasekhar	155	Gopinath A	160
Amali Roselin A	34,35	Bharatraj Kasi	21	Gopu G	105, 208
Ambika S	203	Bhuvaneshwari S	15,168	Gopukumar Sukumaran	1
Amit Sharma	151	Boomi P	22,75	Gopukumar S	7
Amsaveni S	180	Boopalan. M	74	Govidarajan G	135
Anandan M	113	Carolyn Jeniba Rachel D	125	Govindan Ramathilagam	121
Anandha Raj J	22	Chinnadurai M	60	Govindaraju S	201
Anandhan N	34,35	Chithiravel R	163	Govindharasu Banuppriya	
Anitha K	55	Chitra C	146		153
Anitha Pius	52,53	Chitra S	194	Gowri M	129
Antony Rajam J	5	Christina Susan I	207	Gowri S	134
Antony Roseline T	110	Clarina T	139,180	Gowrisankar A	62
Anuradha J	129	Cristina Delerue-Matos	42	Gurumallesh Prabu H	
Anuradha K	26	David Aradilla	1		37,71,75,113,200
Archanadevi J	185	David Velayutham	92	Gurunathan K	69,79,107
ArjunKumar Bojarajan	27	Dhanalakshmi S	105	Gurunathan Karuppasamy	
Arokiyaraj A	177	Dharuman V	89		60,127
Arumugam A	68,69,134	Dhilip Kumar R	36	Habibulla Imran	85
Arumugam Ayyakannu	68	Divya K	43	Hajara Banu TM	207
Aruna Devi G	53	Diwakar K	66	Hanna Radecka	77
Arunkumar K	110,185	Durainatarajan P	12	Heiner A J	79
Arunkumar R	191,192	Duraisamy Chellappa	95	HemaKalyani R	55
Arunkumar Kathiravan	49	Elangovan J	51,164	Hemalatha K	113
Ashokkumar N	198	Elumalai P	89	Herculin Arun Baby A	100
Ashwin B M	100	Elumalai Marimuthu	179	Ilangeswaran D	
Authidevi P	18,19	Fathima Thaslin S	35		113,115,162,175
Ayyakannu Arumugam	134	Ganesan Jeyashree	95	Imran Hussian S	16
Baishnisha Amanulla	97	Ganesan Kumaravel	138,139	James Joseph	94
Balachandran V	135,136	Ganesapandian Latha	168	Jannathul Firdhouse M	207

Jayalakshmi M	40	Karutha Pandian Divya	88	3,30,43,44,45,65,84, 90,91, 194,210	
Jayamani A	145	Kasi Pitchumani	78,170,171		
Jayaraj K	53	Kasi Viswanathan	84	Maniyazagan M	91
Jegatheeswaran S		Kasturibai S	23	Mariadass R	91
	22,72,73,203	Kathiresen M	7	Mariadoss Asha Jhonsi	49
Jekapar Nisha Y	84	Kathirvel N	136	Mariappan Rajan	183
Jerzy Radecki	77,78	Kavitha B	37,39	Marimuthu J	46
Jessica Fernando	63	Kavitha G	17	Maruthanayagam K	103
Jeyakanthan J	22,75,91	Kavitha M	67	Mathi C	38
Jeyakanthan Jeyaraman	151	Kavitha N	146	Michelraj S	88
Joseph Sahaya Anand T	1	Kavitha Manoharan	68	Mohamad Ali B	96
Joseph Sahayarayan J	22	Kilirani F	208	Mohana K	199
JosphineSarahand S	55	kirupagaran R	126	Mohana P	46,209
Jyotsnarani Jena	152	Klankermayer J	189	Muralidharan B	210
Kalaiselvam S	16	Krishnaiah Abburi	109	Murugadoss G	36
Kalaiselvi C	28	Krishnan M	208	Murugan E	47,201
Kalaiselvi K	33	Krishnaveni D	40	Murugan P	168
Kalaiselvi M	141	Kulandaisamy A	141,142	Murugan Karthik	161
Kalaivani N	41	Kulangiappar K	14	Murugavel Kathiresan	2,92
Kalyanasundharam S	177	Kuzhandavel Hemalatha	174	Murugesan S	112
Kanagan R G	136	Latha N	129	Murugesan Balaji	202
Kanagaraj Madasamy	92	Lavanya R	182	Murugesan Kanagaraj	166
Kanagavel D	18, 25	Laxmi Gayatri Sorokhaibam		Murugesan Shunmughanathan	78,170,171
Kanakkan Ananthakumar	121		152	Murugeswari G	123
Kanmani K	9	Leitner W	189	Muthlakshmi R	193
Kannan N	190,191,192,193	Leo Arokiaraj S	177	Muthu Mareeswaran P	
Karkuzhali R	208	Liauw M	189		100,101,103
Karpagavinayagam P	17,25	Libni G	167	Muthuchudarkodi R R	123
Karpuraranjith M	69	Lingam Ravikumar	174	Muthukumaran P	64
Karthick S	208	Logeswari R	44	Muthumani M	193
Karthik R	27	Lokanath N K	91	Muthumani Muthu	154,157
Karthik prabu B	144	Madankumar D	135	Muthumariappan S	60
Karthika	56	Mahadavan Pillai V P	47	Muthuraja P	
Karthikeyan K	164,172,188	Mahalingam Sundrarajan	202		30,84,91,194,210
Karthikeyan M	34,35	Mahendraprabhu K	89	MuthurajaPerumal	194
Karthikeyan C	36	Mangaiyarjkarasi R	195	Muthusankar G	105
Karunakaran M	75	Manickam Sornalatha	174	Muthusubramanian S	
Karuppuchamy S	36,201	Manikandan A	54		135,150,163
Karuppuraja M	112	Manisankar P		Muthuvel I	210

Nachiappan M	91	Pothiraj C	120	Ramesh S	12
Nachiappan Mutharasappan		PR. Kaleeswarran	68	Ramesh Babu G N K	86
	151	PR. Meyyathal	199	Ramesh Prabhu M	10
Nagarajan E R	89	Prabakaran M	12	Ramuthai S	75
Nagarajan		Prakash S	30,84,194	Ramya R	82
Sankaranarayanan		Prakash Periakaruppan	24, 99	Ramya Arumugam	99
	119	Prakash Sengodu	194	Rangaraj Arunkumar	174
Nainamalai Devarajan	168	Prakashkumar Nallasamy	127	Rani T	25
Nandhini D	194	Praveen K	135	Rani C	42,43,44,45,201
Natarajan Madankumar	171	Pravin B. Patil	152	Rani Rosaline D	98,99
Natarajan Raman	138,139	Premlatha S	86	Ranjitha R	115
Natchimuthu N	182	Priya Dharsini G R	50,139	Rathinavel Mariammal	157
Nathiya D	57	Priyatharshinin R	34	Ravikumar Raman	1
Navamani P	197	Radha N	83	Revathi S	105
Naveen S	91	Raja G	189	Revathi T	70
Naveenkumar P	32	Rajaboopathi S	195	Saha P	31
Neela A	50,139	Rajagopal V	7	Sailaja Krishnamurty	211
Nihal T V	168	Rajaguru K	135	SakthiVelu K	65
Nirmala Devie T	207	Rajarajan M	8,56,98,99	Saminathan K	31
Nithya P	72,203	Rajasekaran.K	123	Sangeetha M	44
Pagutharivalan R		Rajasekhar M	41,46	Sangeetha P	206
	190,191,192,193	Rajendiran Nagappan	81	Sangeetha S	14,135,136
Palanimurugan A	141,142	Rajendran Kalimuthu	81	Sangili A	203
Palaniswamy Suresh		Rajesh Madhuvilakku	33	Sankar C	206
	161,166,168	Rajeshwari K	83	Sankari S	158
Palinci Nagarajan		Rajeshwari V	63	Santhi K	201
Manikandan	85	Rajeswari A	52	Saranya K	158
Pandiyan Nithya	202	Rajeswari K	88	Sarathkumar K	191,192
Pari S	135,136	Rajeswari R	71	Saravanakumar S	189
Paruthimal Kalaigan G		Rajkumar P	66	Saravanan C	101
	23,32,33,46,209	Raju Ranjith Kumar		Saravanan R	191,192
Paul Raj J	51,164		94,154,157,158	Sarjuna K	162
Periasamy V	12	Raju T	9	Sasikala S	66
Periyakaruppan		Rama V	180	Sasikumar R	10
Pradeepkumar	183	Rama V	50, 139	Sathish Kumar Ponnaiah	24
Periyamayaki R	115	Ramachandran G	191	Sathiskumar G	136
PillaiyarPuthiaraj	170	Ramasamy Raja V	98,99	Sathiyamoorthi R	31
Piotr Gołębiewski	78	Ramasundaram K	175	Sathya D	177
Ponmuthuselvi T	43,44,45	Ramesh P G	115	Sathyaseelan P	210
Poonam C	120				

Saxthi Vinmathi K	207	Stalin T	65,91,106	Umadevi S	195,199,204
Sayee Kannan R	55,84,97	Stephen Joel K	186	Umamaheswari D	94
Sekar C	87	Stephysahayam S	208	Uma Maheswari K	36
SelvaKumar K	10	Subadevi R	28,29 66	Umamatheswari S	205
Selvam M	31	Subramanian Ammashi	131	Umarani G	116,123,198
Selvam S	22,72,73	Sudhan N	87	Vadivelu M	172,188
Selvamani V	7	Suganthi A	8,56,98,99	Vairathevar Sivasamy	
Selvaraj Dinesh Kirupha	174	Suganthi D	45	Vasantha	92
Selvarajan S	8,56	Suganthy N	67	Vaitheshwari G	175
Selvaraju T	62	Suganya R	175	Vajjiravel M	51
Sengottuvelan N	145,146	Suganya Bharathi B	65,106	Vajjiravel Murugesan	21,179
Senthil kumar A N	40	Sugapriya C	26	Valarmathi S	142
Senthil Kumar M	65	Sugirdha S	172,188	Valarselvan S	3
Senthil Kumar N	37,39	Sukanya P	115	Vasantha Kumar P	55
SenthilKumar S	211	Sultan Nasar A	96,160,167	Vasanthi V	55
Senthil kumaran M	103	Sumathi R	73,203	Vedhi C	5,16,17,18,19, 25,59,60,125,126
Senthilnathan S	107	Sumathi G	200	Vediappen Padmini	153
Sethupathi M	145	Sundarababu Baskaran	149	Veeramani V	210
Sethuraman V	30,90	sundaram K	39	Velammal M	84
Shakkthivel Piraman	33	Sundaram Ellairaja	92	Velayutham D	7,9
Shanmugam V M V	9	Sundaresan K	205	Velmanirajan K	26
Shanmugapriya J	135	Sundrarajan M	22,72,73,128	Venkataraman Dharuman	
Shanthi M	29	Suresh E	39		85,88
Sivakumar M	28,29,66	Surya Prakash Rao H	148	Venkatesan Srinivasan	49
Sivakumar A	54,191	Suryanarayanan V	7	Vibha Saxena	36
Sivakumar C	88	Swathi S	116	Vidhyeswari D	15
Sivalingam Gopi	2	SweetyBadalia	152	Vignesh kumar G	101,103
Sivaraman G	91	Tamilarasi G	123	Vijayabarathi T	14
Sivaranjini B	204	Tamilarasi S	210	Vijayakumar CT	186
Sivasakthi S	107	Tamilselvan Ganesan	60	Vijayanand N	189
Somi Santharam Roja	158	Thambidurai S	27,69,70,195	Vimala A	16
Sonadevi S	55	Thanasekaran Nandhini	78	Vimalathithan PK	186
Sonamuthu Jegatheeswaran		Thangadurai S	144	Vinay M. Bhandari	152
	202	Thangamuthu R	36	Vincentraj A	177
Sreeja V	18,19	Tharini K	205,206	Viswanathan S	42,43,44,45
Srinivasan N	197	Thirumalaisamy Rathinavel		Viswanathan Karthika	134
Srinivasan S	110		131	Vitul Jain	151
Srinivasan Alagar	33	ToemsakSrikkhirin	48	Wilson J	57, 64, 82
Srinivasan Natarajan	137	TokaSwu	155	Yogavel Manickam	151



ISBN 978-81-928690-7-0



9 788192 869070 >

₹ 1000 US \$ 30